The Chemistry of Gold with Unsaturated Organics: Coordination, Activation and Catalysis

Nicky Savjani

A thesis submitted in part fulfilment of the requirements for the degree of Doctor of Philosophy.

School of Chemistry,
University of East Anglia, Norwich.

December 2012

Supervised by Prof. Manfred Bochmann.

Statement of Original Work

The research described in this thesis has been conducted by the author, Mr Nicky Savjani, and is, to the best of his knowledge, original. Where other people's work has been referred to, this has been cited by corresponding references. Any materials used that were not synthesised by the author have also been detailed as such in the Experimental section in Chapter 6.

Nicky Savjani

Abstract

The aim was to understand gold's reactivity with unsaturated organic bonds. We focused on the role of supporting ligands, activating agents and the organic substrates employed in such reactions.

Gold tetrafluorophthalimidates have been isolated, with coordination found to be surprisingly strong; no $[N(CO)_2C_6F_4]^-$ displacement with σ- and π-donors were observed. $B(C_6F_5)_3$ and norbornene addition to $[(Ph_3P)Au\{N(CO)_2C_6F_4\}]$ leads to a $[Au(nbe)_3]^+$ cation paired with a new, non-coordinating phthalimido-diborate anion.

Aryl-N substituents of $[(Ph_3P)Au\{nacnac\}]$ influences its differing solid state structures; examples of κ^1- and (the first example of) asymmetric κ^2-coordination was observed. In solution these complexes show intricate fluxional behaviour. Attempts at oxidation to synthesise a gold(III)-oxo complex were unsuccessful.

In situ generated Au^+ cations can selectively activate benzylic C-H and C-C bonds of methylarenes and dimesitylmethane under mild conditions. Mechanistic and kinetic studies with hexamethylbenzene have identified a C-H activation step of and the formation of a benzyl cation intermediate.

Zwitterionic and heterobimetallic gold(I) complexes containing a (*o*-sulfophenyl)-diphenylphosphine ligand were formed, with the supporting Cl^- and R_2S ligands on gold(I) found to be non-labile, resulting in the complexes being catalytically inert.

The incorporation of anions to $[(C_6F_5)_4Au_2Ag_2]_n$ clusters gave structural and photoluminescent data, which evidently show that the emission colours of these powders are dependent on the extent of aurophilic bonding between cluster units.

Dechlorination of $[(C_6F_5)_2AuCl]_2$ in the presence of olefins were prone to reductive elimination to yield 'naked' gold(I)-(η^2)olefin complexes. Repeating the reaction with benzene, toluene and xylenes appeared to give the unstable and unidentified gold(I)-arene analogues. ^{1}H NMR monitoring of gold(III)-catalysed hydroarylation reactions revealed that silver salts do not act as a simple chloride scavengers, but identification of the gold species in solution was unsuccessful.

In addition, a family of highly electrophilic fluorosulfonium and fluorobismuthium compounds were synthesised. These complexes decomposed at room temperature by intermolecular fluorination of the aryl substituents.

Acknowledgements

I would like to gratefully and sincerely thank Professor Manfred Bochmann for his guidance, understanding and most importantly his tolerance (*re*: the 'Pin the 'Stache on the Bochmann' game I produced during the Christmas party) during my PhD at UEA, I would not be graduating if it weren't for your continued support. I would also like to thank Dr. Simon Lancaster and Dr. Anna Fuller for their assistance and advice in adapting to life in the lab.

To all those in the Bochmann and Lancaster research groups, past and present, thank you for the laughs, drunken nights, paintball stories and the injuries from Jungle Speed. At this time I must apologise to Dragoş Roşca, as over the past 18 months he has been helpless from the torrent of pranks bestowed upon him (with 'a little' help from others): molecular sieve showers, forced face-painting and finding mini-Manfreds in every nook and cranny of his work area being just a few agonies he has suffered through. For the collection and refinements of the X-ray data within this thesis, I have to express my gratitude to Dr David Hughes, Dr Mark Schormann and the researchers at the EPSRC National Crystallography Service in Southampton for their expertise, time and support.

My start at UEA was very difficult for me due to numerous reasons, so I thank the people who welcomed me in; in particular Jamie Leeder and Stephanie Ryan for including me in your lives so willingly and helping me make Norwich feel like home. Due to the need to run away from the lab as often as possible, I frequently enjoyed the games of football and poker. So to the guys who have watched while I humiliate myself on the pitch and to those at Pokersoc and NPC who willingly let me bet ridiculous amounts of money on flips, cheers for the distractions.

I wish to thank my family: my parents, brother and sister-in-law, for their continuing love and support over the years. I also would like to congratulate Neil and Hiral for introducing my gorgeous little niece Sena Savjani to the world (even if she cries hysterically every time she sees me!). Finally, I would like to thank my girlfriend Tessa who has withstood the tantrums, understood my constant dedication

to writing my thesis, endured the lessons on relativistic effects and has taken my mind of it all when it was needed.

Thank you all.

List of Abbreviations

<	less than
≤	less than or equal to
>	more than
≥	more than or equal to
°	degrees
°C	degrees Celsius
Å	Ångström
Anal.	analytically
approx.	approximately
BAr^F_3	tris(pentafluorophenyl)borane
BDE	bond-dissociation enthalpy
br.	broad
ca.	*circa*
Calcd.	calculated
cod	cyclooctadiene
d	doublet
dipp	(2,6-di-*iso*-propyl)phenyl
DMF	dimethylformamide
dmh	the anion of 5,5-dimethylhydantoin
dmpe	1,2-bis(dimethylphosphino)ethane
e.g.	for example
ene	a simple organic molecule containing a C=C bond
EPR	electron paramagnetic resonance
Et	ethyl
et al.	*et alii*
etc.	*et cetera*
g	grams
h	hours
HOMO	highest occupied molecular orbital
i.e.	*id est.*

IMes	*N*,*N'*-bis(2,4,6-trimethylphenyl)imidazol-2-ylidene
^{i}Pr	*iso*-propyl
IPr	*N*,*N'*-bis(2,6-diisopropylphenyl)imidazol-2-ylidene
IR	infra-red
J	coupling constant
K	Kelvin
k_{expt}	rate constant of experimental reaction
KIE	kinetic isotope effect
L	litre *or* monodentate ligand
LLCT	ligand-to-ligand charge transfer
LUMO	lowest unoccupied molecular orbital
M	Molarity
m	multiplet *or* metre
m-	*meta*-
Me	methyl
MHz	megahertz
min	minutes
MMLCT	metal-metal to ligand charge transfer
MO	molecular orbital
mol	moles
nacnac	*β*-diketiminate anion
^{n}Bu	*n*-butyl
nbe	norbornene
NHC	*N*-heterocyclic carbene
NIS	*N*-iodosuccinimide
NMR	nuclear magnetic resonance
NXS	*N*-halosuccinimide
o-	*ortho*-
OAc	acetate anion
OAc^{F}	trifluoroacetate anion
OPiv	pivalate anion
OTf	triflate anion
p-	*para*-

Ph	phenyl
phth	phthalimido anion
$phth^F$	tetrafluorophthalimido anion
por	a porphyrinate ligand
ppm	Parts-per-million
Py	pyridine
q	quartet
r.t.	room temperature
s	seconds *or* singlet
suc	the anion of succinimide
t	time *or* triplet
T	temperature
THF	tetrahydrofuran
UV-vis	ultraviolet-visible
v	very
vs.	versus
X	halide
yne	a simple organic molecule containing a C≡C bond
δ	chemical shift
Δ	change *or* heated
ε	extinction coefficient
η	*eta*; signifying hapticity
μ-	bridging-
λ_{max}	wavelength of maximum absorption or emission

Table of Contents

1 - Introduction to the Chemistry of Gold with Unsaturated Organics

1.1 Background

Extensive uses of gold can be traced back to the times of the Persians and Egyptians from 3,000 BC, with evidence of gold being a prized asset to the Palaeolithic man as far back 40,000 BC. The colour, lustre and non-tarnish properties make the metal an attractive material for use in jewellery and ornaments. Until the turn of the 20th century, the chemistry of gold was regarded as an art in the recovery and conversion of gold metal into all possible forms of ornamental, monetary, anticorrosive or electrical usage, with the compounds $HAuCl_4$, or the anions $[Au(CN)_2]^-$ and $[Au(CN)_4]^-$ having importance as intermediates in the recovery of the metal.[1]

The comparison of the atomic and molecular properties of the group 11 metals provides an understanding of the unique reactivity that gold exhibits. The outer shell configuration of Au(0) is [Xe] $6s^1 4f^{18} 5d^{10}$; similar to the coinage metals copper ([Ar] $4s^1 3d^{10}$) and silver ([Kr] $5s^1 4d^{10}$); the filled *d*-subshells are a particularly stable arrangement of electrons. Gold in oxidation state +I ([Xe] $6s^0 4f^{14} 5d^{10}$) is a more stable configuration than in its +III state ([Xe] $6s^0 4f^{18} 5d^8$), as a consequence of the stabilisation imparted by the fully-filled 5*d* subshell.[1]

Table 1. Atomic properties of group 11 metals.[2]

Element	Ionisation energies /kJ mol-1			Electron affinity /eV	Electronegativity /Pauling scale
	1st	2nd	3rd		
Cu	772.6	2029	3684	1.235	1.90
Ag	757.6	2148	3483	1.302	1.93
Au	922.5	2020	2900	2.309	2.54

Gold possesses the highest 1st and lowest 3rd ionisation enthalpies of the coinage metals (Table 1).[3-5] It is because of the latter fact, a more developed field is observed for complexes of gold in oxidation state +3 (and higher) when compared to copper and silver, as they are thermodynamically and kinetically more stable.[6] The chemistry of gold(II) ([Xe] $6s^0 4f^{18} 5d^9$) is limited, as disproportionation of two

Au(II) ions to Au(I) and Au(III) is favoured.[6-8] Nonetheless, a small number of Au(II) complexes are known.[6,9-11] Gold has the unusual property of being the most electronegative transition metal at 2.54 on the Pauling scale, comparable to carbon (2.55) and an iodine (2.66), suggesting gold could be stable in the oxidation state –I, which have been confirmed experimentally, as examples are available in this oxidation state (*e.g.* CsAu).[6]

Au^+ and Au^{3+} cations in aqueous acidic solution are unstable, as indicated by the redox potentials of these ions, compared to other group 11 metals and with its neighbours platinum and mercury (Table 2).[2] It is due to its high reduction potential that gold is considered a 'noble metal'.

Table 2. The reduction potential for the standard reduction potentials of selected elements in respect to the standard hydrogen electrode.

Reaction	E^0 **/ V**
$Cu^+ + e^- \rightleftharpoons Cu^0$	0.521
$Ag^+ + e^- \rightleftharpoons Ag^0$	0.800
$Au^+ + e^- \rightleftharpoons Au^0$	1.692
$2Hg^{2+} + 2e^- \rightleftharpoons 2Hg^+$	0.920
$Au^{3+} + 2e^- \rightleftharpoons Au^+$	1.401
$Au^{3+} \rightleftharpoons 3Au^+ + 2Au^0$	-0.470
$Pt^{2+} + 2e^- \rightleftharpoons Pt^0$	1.180

1.1.1 Coordination Chemistry and Geometry

1.1.1.1 In Oxidation State +I

The chemistry of gold(I) complexes is by far the most developed, dominated by linear two-coordinate species to form neutral [L→Au-X], anionic $[X\text{-}Au\text{-}X]^-$ or cationic ($[L\rightarrow Au\leftarrow L]^+$) complexes.[12,13] The combination of large ionic radius (= high polarisability) and low oxidation state means that Au(I) centres are very soft Lewis acids.[14] A large database of gold bonding to soft Lewis bases is available, which include coordination to carbon-, phosphorus- and sulfur-donor ligands, as well as with halides.[6] In comparison, fewer examples of gold complexes coordinated to nitrogen- and oxygen- donating ligands have been isolated, with the vast majority of Au(I)-N and Au(I)-O complexes containing a gold centre supported by soft donor ligands.[6,10]

1.1.1.2 In Oxidation State +III

Because of the facile reduction of gold(III) complexes to the more stable gold(I) compounds, the chemistry of gold(III) is comparatively less well developed.[1,6,10] Gold(III) has a d^8 electron configuration, therefore gold complexes exist in a square planar geometry and display chemistry that resembles in many ways that of the isoelectronic Pt(II).[6] Au(III) centres are harder Lewis acids than Au(I), as shown by the presence of many examples of $[Au(N\hat{}O)_2]^+$ chelates, where N and O donors are preferred even over chloride-coordination.

1.2 Relativistic Properties

Some of the unusual properties of gold observed in experimental chemistry have been attributed to the 'Relativistic Effects'. This term refers to the properties intrinsic to certain heavy elements in the Periodic Table, as a consequence of Einstein's theory of special relativity.[15-17]

On the atomic scale, the theory of relativity dictates the orbital size of the electron subshells, as the number of protons in the nucleus of an element directly affects the angular momentum of the electrons in the *s*- and *p*- orbitals, which in turn affects the electron mass (relativistic mass, m_r) and ultimately the Bohr radii of the orbitals. This applies especially to the elements platinum and mercury and is particularly pronounced for gold. The theory behind this relativistic effect has been reviewed on a regular basis.[3,5,13,18-22] The relativistic effects in gold have three major consequences:

The first is the contraction of the *s* and *p* orbitals. The contraction is observed with all elements, but for the lighter elements this effect is negligible. The orbital contraction is most pronounced for gold, as the filled 4*f* and 5*d* orbitals poorly shield the vacant 6*s* and 6*p* orbitals, compounded with a large nuclear charge (Figure 1). The contraction of the 6*s* orbital in gold provides an explanation for its high electronegativity and electron affinity.[3]

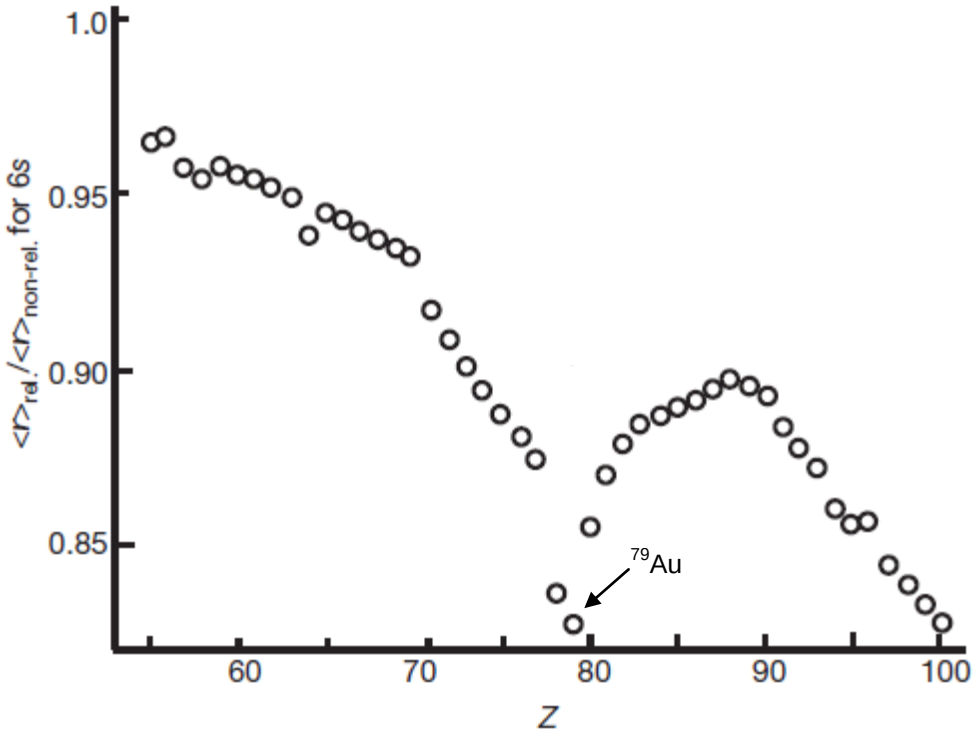

Figure 1. The calculated relativistic contraction of the 6*s* shell in the elements, compared to nonrelativistic calculations [Ca (*Z* = 55) to Fm (*Z*=100)].[16] The values are taken from the Dirac-Fock and Hartree-Fock calculations by Desclaux.[23]

The second effect is the reduction in spin-orbit coupling of the 5*d* and 6*p* orbitals (Figure 2). Spin-orbit coupling leads to an increase in energy between the 6*s* and 6*p* orbitals are observed. This leads to a loss of orbital mixing commonly between these two orbitals and promotes the formation of linear two-coordinate structures of gold(I), due to the compact 6*s* orbital hybridising with the lowest 6*p* orbital only ($6p_{1/2}$ orbital) to allow for 2-coordinate geometries. Copper and silver ions have a higher degree or *sp*-orbital mixing which results in an increase of coordination numbers.[12,13]

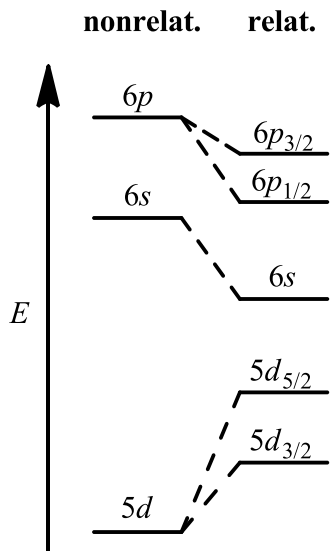

Figure 2. Schematic view of the molecular orbital energies for hypothetical gold compounds before and after relativistic considerations.[19]

The third effect is indirect. As the *s* and *p* shells are significantly contracted, the electrons in the outer 5*d* and 4*f* orbitals are better shielded, thus weaker nuclear attraction is felt, which results in expanded *d*-orbitals. The combined effect of the stabilisation of the 6*s* shell and the destabilisation of the 5*d* shell in gold leads to a substantially decreased 5*d*/6*s* band gap shown in Figure 3.[24]

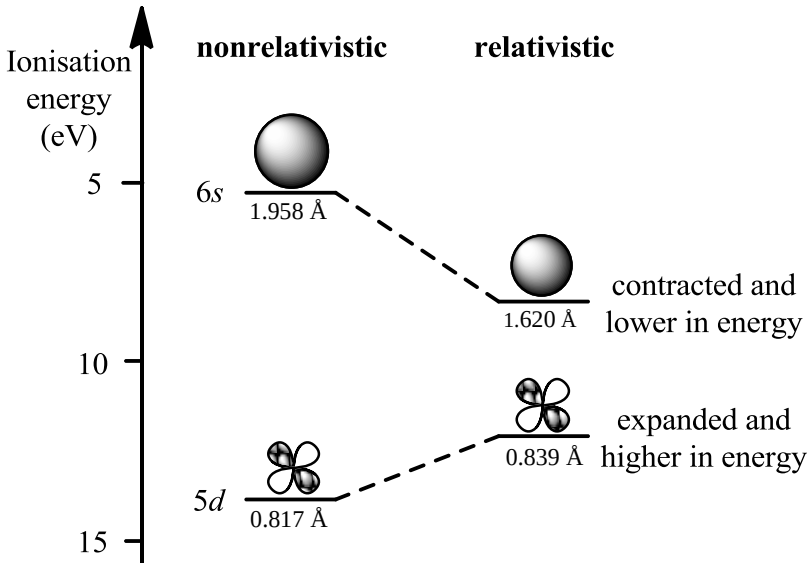

Figure 3. A comparison of the calculated sizes and energies of the 6*s* and 5*d* orbitals of gold with and without consideration of relativistic effects.[3]

The colour of gold metal is due to this intrinsic bandgap reduction; experimental reflectivities of a gold mirror show a sudden onset of absorption for the transition of an electron in the filled 5*d* band to the Fermi level (essentially the vacant 6*s* band), resulting in the absorption in the blue-green region of the visible spectrum (band gap at $h\nu$ = 2.38 eV, 521 nm; Figure 4). Silver, with its larger 4*d*/5*s* bandgap, absorbs in the UV region only (3.7 eV, 335 nm).[2]

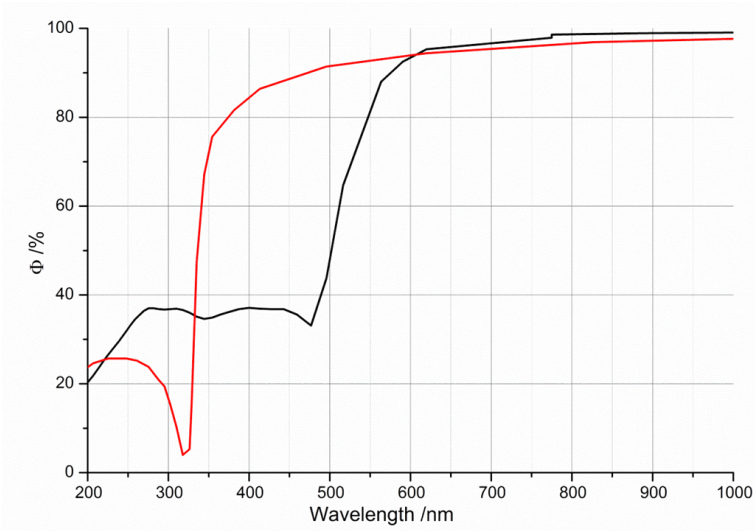

Figure 4. Spectral reflectance curves for silver (red) and gold (black) metal mirrors.[2]

1.2.1 Aurophilicity and Metallophilicity

Another inherent property of gold has been coined "metallophilicity" and "aurophilicity". "Metallophilicity" is commonly used to describe the bonding between select numbers of metallic elements (depicted in the abbreviated Periodic Table of elements in Figure 5), governed by relativistic effects. In relation to gold, experimental evidence of gold-heterometal bonding (Rh, Ir, Pd, Pt, Cu, Ag, Hg, Tl and Bi) is available,[25-29] but the theoretical calculations indicate none of these other interactions are as strong as Au···Au interactions.[30] Many of these metallophilic bonds are guided by electrostatic interactions and stabilised by weak metallophilic bonding.

						B	C	N
						Al	Si	P
	Fe	Co	Ni	Cu	Zn	Ga	Ge	As
	Ru	Rh	Pd	Ag	Cd	In	Sn	Sb
	Os	Ir	Pt	Au	Hg	Tl	Pb	Bi

Figure 5. Metallophilic elements in the Periodic Table.[31]

Aurophilicity is a term used to describe various kinds of bonding between gold centres in complexes and the properties observed as a consequence of these interactions. Aurophilic bond lengths are typically in the range of 2.7 to 3.6 Å (which are within the region of the sum of the van der Waal radii of two gold atoms at 3.32 Å)[2] with bond strengths in the region of 7-12 kcal mol^{-1}. Aurophilic bonds are comparable in strength to hydrogen bonding.[22]

Aurophilicity is believed to result from orbital mixing of molecular orbitals between two gold centres in their respective complexes. Figure 6 illustrates a simplified MO bonding diagram of $[(L)Au]_2^{2+}$ in d^{10} configurations.[31,32]

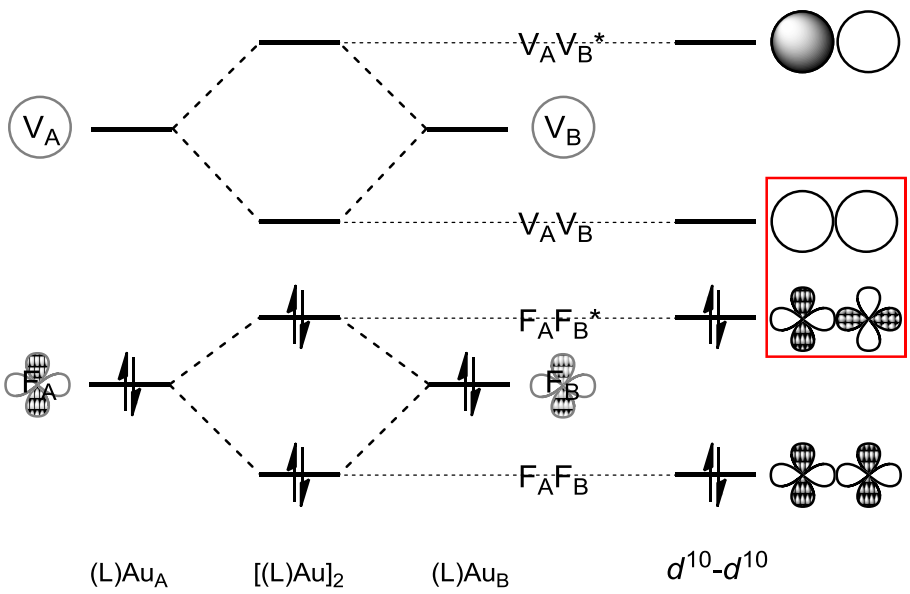

Figure 6. Generic MO scheme for metallophilic interactions, with orbital overlaps between pairs of d^{10} ((L)Au) ions in red.[33]

The frontier orbitals in gold centre **(L)Au$_A$** can mix with the orbitals in **(L)Au$_B$** on an adjacent molecule, creating a new set of molecular orbitals (Figure 6, left). The interactions of the filled (labelled **F$_A$** and **F$_B$**) and vacant (**V$_A$** and **V$_B$**) atomic orbitals create a new bonding and antibonding MO system (with **F$_A$F$_B$**, **F$_A$F$_B$***, **V$_A$V$_B$** and **V$_A$V$_B$*** orbitals). The band gap between the HOMO (**F$_A$F$_B$***) and LUMO (**V$_A$V$_B$**) bands in **(L)Au$_A$···Au$_B$(L)** is greatly reduced, compared to that observed in a single gold centre, with mixing of these newly created orbitals permitting aurophilicity. In the case of d^{10}-d^{10} systems (Figure 6, right) the empty 6*s* orbitals of **Au$_A$** are energetically low enough to mix with the filled $5d_{x^2-y^2}$ orbitals of like symmetry in **Au$_B$** (highlighted in red). This LUMO/HOMO mixing can also be envisaged in d^8-d^8 (HOMO: $5d_{x^2-y^2}$ and LUMO: $5d_{z^2}$) and d^{10}-d^8 systems, but with the relative instability of unfilled *d* shells and the increased steric repulsions between the ligands in the aggregates, attributed to the higher coordination number of gold(III), these interactions are significantly weaker and less commonly seen.[34] With the absence of such MO mixing, negligible interactions would be felt with these closed-shell centres at the distances observed, combined with the Coulombic repulsions of the gold cations expected at shorter distances.[18,32,35,36]

A recent review article by Schmidbaur and Schier provides a detailed survey of complexes containing aurophilic bonding and will not be discussed in detail here.[18] Aurophilic interactions are most commonly observed in Au(I) systems, with Au(I)···Au(I) bonds falling into two types: unsupported (intermolecular) or supported (intramolecular) bonding (Figure 7). These Au···Au distances can be observed in solid state by crystallographic techniques (at distances ranging from 2.8 to 3.1 Å), or by restricted structural flexibility in solution.[1,18,37,38]

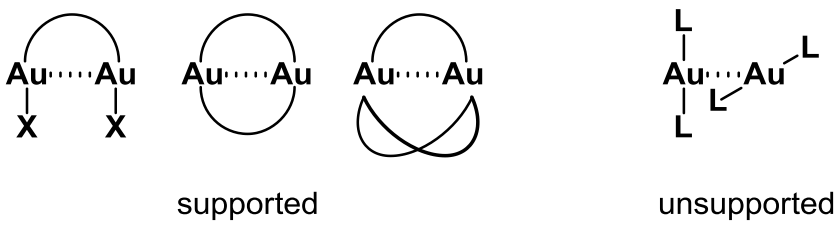

Figure 7. General forms of aurophilic interactions.[18,35]

Gold(III) complexes that exhibit aurophilic interactions (based on Au(I)···Au(III) or Au(III)···Au(III)) in molecular systems have only been crystallographically characterised in a small number of cases.[34] Examples of supported Au(I)···Au(III) bonding were found with distance between the two metal centres within the range of 2.8-3.0 Å. Au(III)···Au(III) systems, in unsupported aurophilic bonds are extremely rare, with relatively longer aurophilic bonds seen (3.4 to 3.6 Å).[35] No examples of supported Au(III)···Au(III) digold complexes have been structurally analysed, but possible candidates have been spectroscopically identified.[38]

Gold complexes which exhibit metallophilicity, aurophilicity, or a combination of both, have been used as tools for the assembly of supramolecular and polymeric gold compounds. Aurophilicity grants access to 1D and 2D lattices (Figure 8), with scope in their non-linear optical and electronic properties the focus of further research.[32,34,39]

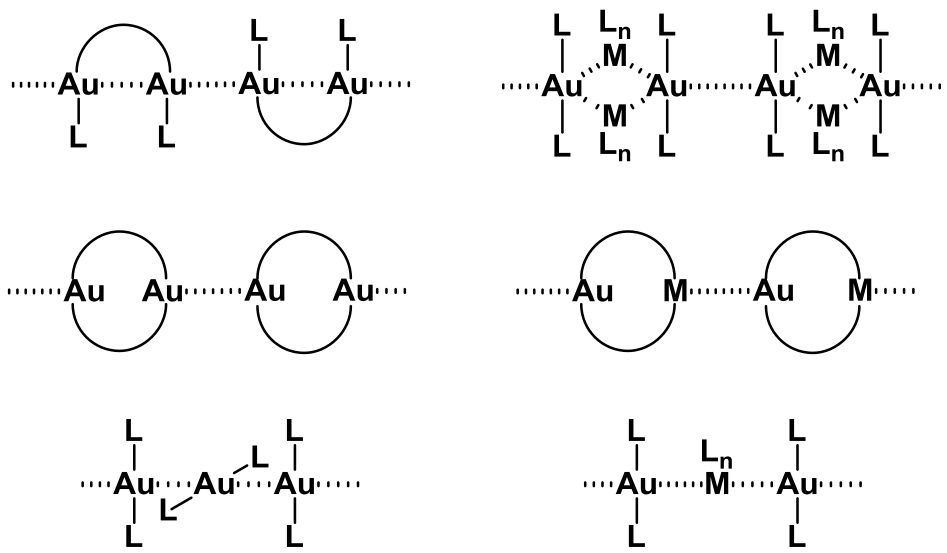

Figure 8. Skeletal representations of extended intra- and intermolecular metallophilic interactions with gold.[18,35]

Complexes of gold(I) and gold(III) (sometimes in combination with other metals) can often exhibit intense luminescence in the visible region of the electromagnetic spectrum.[40] Classifying the origins of photoluminescence has been found to be very difficult, but is thought to originate from a number of factors;

the nature of the ligands, the geometry around the gold centre and the presence of gold-metal interactions have been considered.[41]

For Au(I) complexes, it has been shown that luminescence can originate from the existence, type and distance of aurophilic bonds.[42] A prominent example of this is in the on-off switching of luminescence for complex **I**; interconversion of aurophilic bonding is achieved when acidic or basic vapours are passed over the compound (Figure 9).[42c] **I·(HOAc^F)$_2$** exhibits a single intramolecular Au-Au bond, whereas in the absence of trifluoroacetate **I** shows significant intermolecular Au-Au interactions. These two interactions are competitive, according to the external condition; the bulky trifluoroacetate groups hamper the formation of intermolecular bonds. Luminescence in Au(I)-M heteromultimetallic complexes which contain both aurophilic and metallophilic interactions are discussed in more detail in Section 4.2.

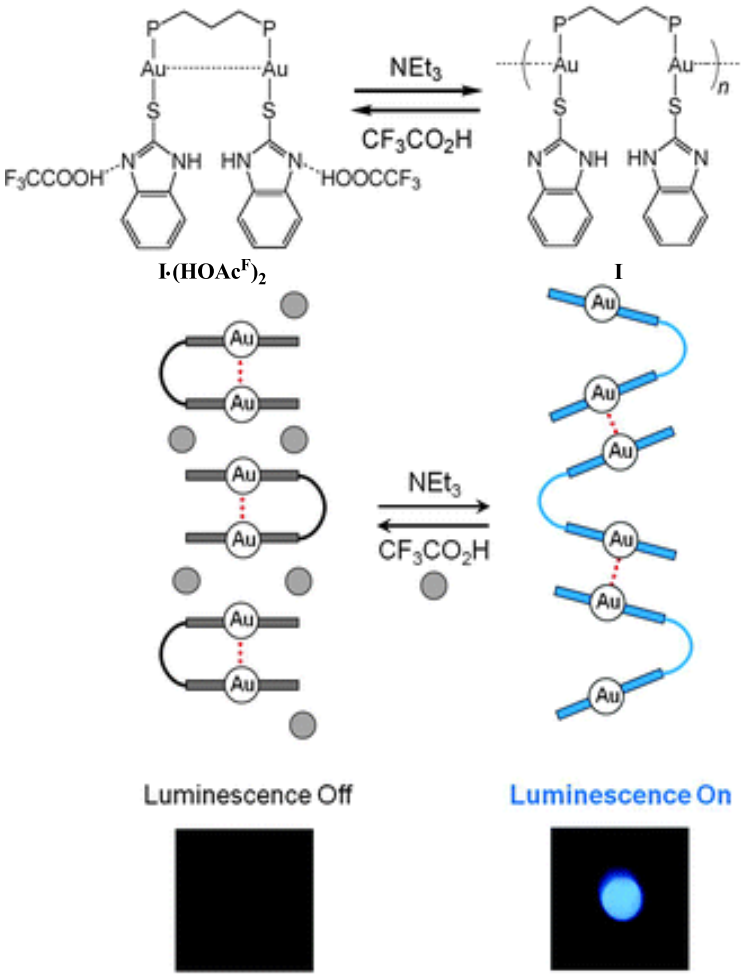

Figure 9. The on-off switching of luminescence in **I** as a consequence of the type of aurophilic bonding.[42c]

Gold(III) complexes that exhibit luminescence are believed to be based on π-π* transitions and LLCT mechanisms from the bound, often orthogonal, conjugated π-systems on gold. Although it is not responsible for the luminescence, aurophilicity plays an indirect, but significant role in the emissions of the Au(III) complexes, as the formation of supramolecular columns of planar Au units promotes π-π stacking of the conjugate ligands, causing a red shift in luminescence of up to 100 nm (an example is shown of the bis-cyclometallated gold(III) alkynyl complexes **II**; Figure 10). Aurophilic interactions of these complexes are only observed in the solid state, as dilute solutions of these complexes remain monomeric.[43]

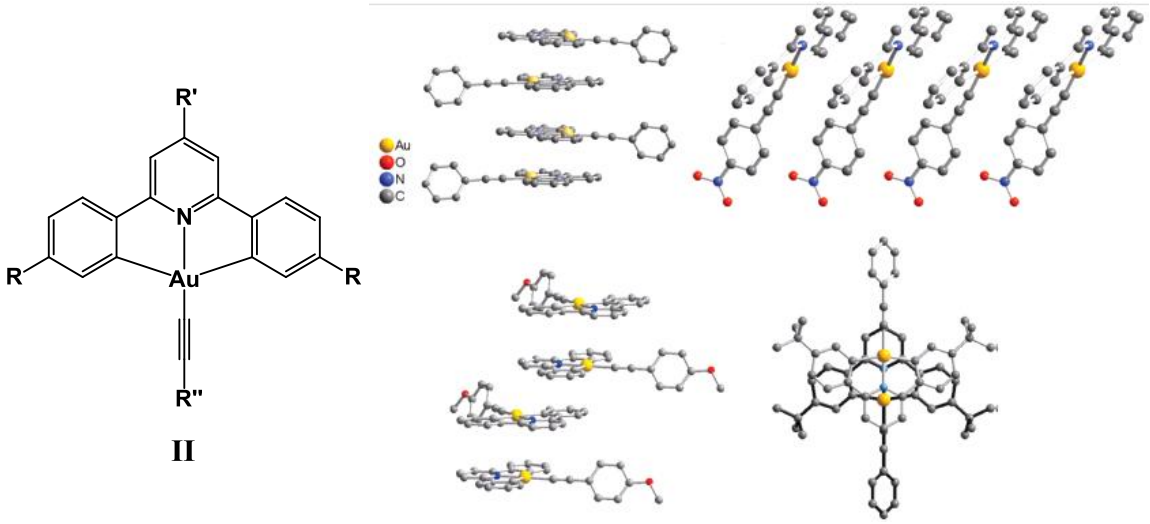

Figure 10. The family of bis-cyclometallated gold(III) alkynyl complexes (**II**, left) and crystal packing and 1D π-stacking of select examples, arising from aurophilicity.[43]

1.3 Lewis π-Acidity and π-Coordination

Due to the intrinsic effects upon the *s*, *d* and *p* orbitals of gold by relativity, the availability for bonding to organic substrates in differing manners has provided a flourish of organic transformations. The role of gold in organic synthesis has been extensively studied; within the last five years numerous reviews have been published, exploring both the activation and functionalisation of C-H and C-C bonds.[3,8,18,19,44]

The interactions of ligated gold cations $[(L)Au]^+$ with various electron rich bonds have been well investigated.[10,44f,45,46] The binding energies between $[(L)Au]^+$

and unsaturated organic substrates follows the trend; alkyne ≈ alkene >> arene.[45,47,48] The Dewar-Chatt-Duncanson (DCD) model of coinage metal-bonding to ethylene has been used to help describe the bonding nature of Au^+ to π-bonds (Figure 11).[49,50]

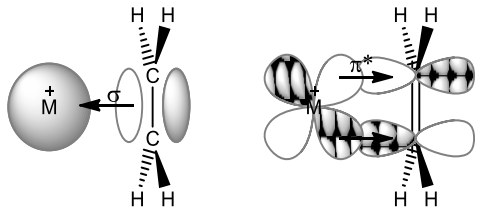

Metal	EA /eV	Promotion Energy /eV	BDE of $[M\text{-}(C_2H_4)]^+$ /kcal mol^{-1}
Cu	7.72	8.25	41.5
Ag	7.59	9.94	33.7
Au	9.22	7.83	69.0

Figure 11. The schematic representation of a group 11 metal-ethylene bonding model: donation to a vacant *s* orbital of the metal from the filled π-orbital of ethylene (left); back donation to the empty antibonding π*-orbital of ethylene from a filled *d*-orbital (right). The figure is accompanied by a table of atomic and molecular properties of the coinage metals.[2]

Both the electron affinities (which relates to the σ-accepting ability) and the promotion energies (correlates inversely with the π-donor property) indicates that gold is the best σ-acceptor and π-donor among coinage metals, due to the better overlap between the orbitals of the metal and the conjugate bond.[2,3,46] In addition, the theoretical bond dissociation energies of $M^+(C_2H_4)$ finds that Au^+ forms the strongest π-bonds with ethylene.[47,48] The bond dissociation enthalpies of $[Au\text{-}(C_2H_2)]^+$, $[Au\text{-}(C_2H_4)]^+$ and $[Au\text{-}(C_6H_6)]^+$ (calculated by DFT studies[47,48,51]) are -64.9, -72.9 and -3.9 kcal mol^{-1}, respectively. This suggests that comparable bond strengths to gold are calculated with both alkene and alkyne bonds, with the binding of Au^+ to arenes significantly weaker.

The relative π-coordination strengths of alkenes and alkynes to a ligand-stabilised gold cation was shown in the results of a $^1H\text{-}^1H$ NOESY experiment between the 1,7-enyne **III** and [{(*o*-biphenyl)(^{t}Bu)$_2$P}Au][SbF_6] (**IV**) at 223K. In solution the cationic gold centre has little thermodynamic preference in

coordination between the alkene and alkyne moieties in **III**, resulting in an approx. 1:1 mixture of the π-coordinated intermediates as shown in Scheme 1.[45c]

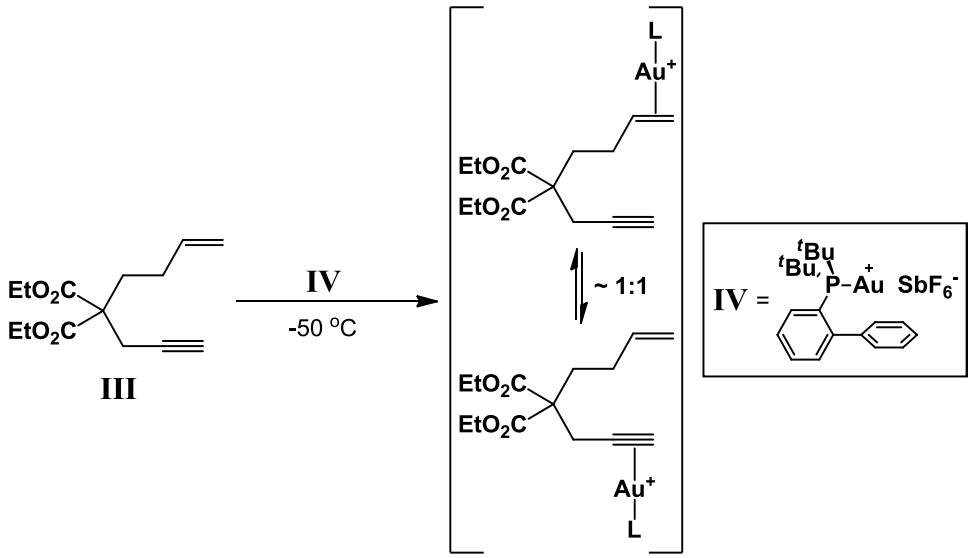

Scheme 1. The ratio between the aurated intermediates of **III** detected by ^{1}H-^{1}H NOESY NMR spectroscopy was close to 1:1.[52]

However the reactivity of such organics is not dictated by the preference on coordination sites of the gold cation, but by the difference in activity of the two different π-bonds upon gold-coordination.[45] This is shown by the addition of nucleophiles (such as water) to reaction mixtures of a) the alkyne **V** with the gold catalyst **IV** and b) the alkene **VI** with **IV** (Scheme 2), where C-C bond activation only occurs in the former reaction.[44j]

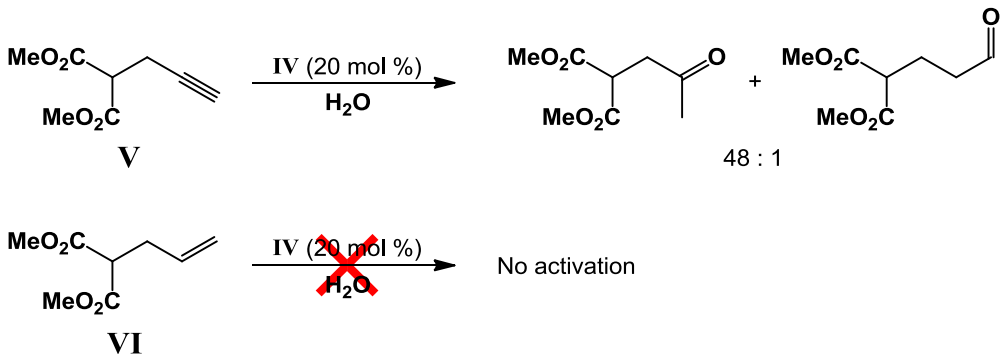

Scheme 2. Hydration of alkyne **V** by gold(I).[44j]

In light of such findings, understanding the nature of η^2-complexation of gold cations has been of particular interest, with the syntheses and isolation of gold complexes coordinated to π-bonds being targeted in research. Recent developments in the structurally and spectroscopically determined complexes of gold π-bonded to olefin, alkyne and arene ligands are documented below.

1.3.1 Gold(I)-(η^2)Alkene Complexes

Given the discovery of Zeise's salt ($K[Cl_3Pt\text{-}(\eta^2)C_2H_4]$) in 1827[53] (which was only crystallographically assessed in 1969;[54] see Figure 12) and the developing coordination chemistry of olefins and acetylenes to many late transition metals in the first half of the 20th century, it seemed unusual that no examples of gold π-coordination to olefins were available before 1964.

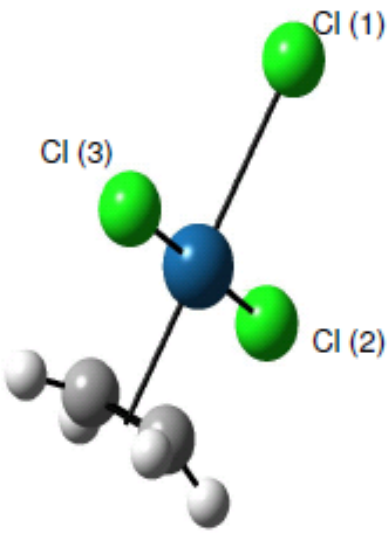

Figure 12. The crystal structure of the anionic component in $K[PtCl_3(C_2H_4)]$.[54]

Rudolf Hüttel *et al.* reported a series of olefin and alkyne complexes of Au(I) halides in the 1960's.[55] They showed that anhydrous AuCl, AuBr, $AuCl_3$ and $AuBr_3$ as the acceptors and simple linear and cyclic olefins as the donors gave gold-olefin complexes [(ene)AuX] (X = Cl, Br). However, most of the compounds showed very limited stability and decomposed at or below room temperature, with the exception of adducts of strained cyclic olefins. It also appeared that gold(I) halides formed the more stable complexes compared to the gold(III) counterparts with the same olefin,

which were invariably reduced to Au(I).[56] The relative weakness of the π-donation of olefins is backed by the lack of reactivity of olefins to (L)AuCl (L = RCN, R_3P, R_2S), where the strong σ-donor ligands act as poor leaving groups. Although the work is thorough, the identification of these complexes relied heavily on elemental analyses, vibrational spectroscopy and cryoscopic or osmometric molecular mass determinations,[55f] with no clear data of the gold-olefin bonding nature. It was only in 1987 that the first structurally characterised complex (*cis*-cyclooctene)AuCl (**VII**) was described, which gave valuable data on the π-acidity of gold, as well as information on the effect on the electron-rich bond, such as bond lengthening and loss of sp^2-hybrid character of the carbon atoms (Figure 13).[57]

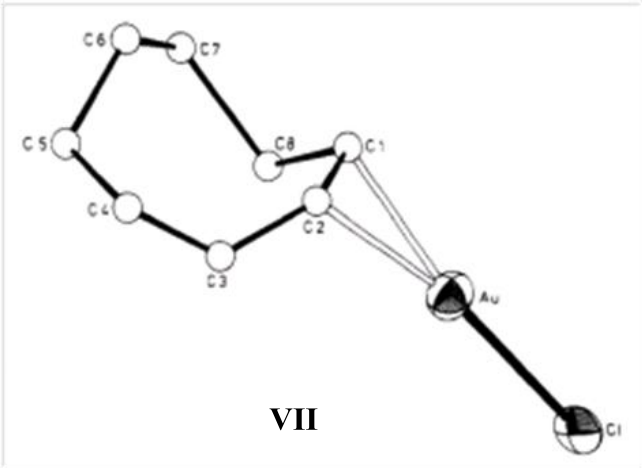

Figure 13. Ortep structure of (cis-cyclooctene)AuCl.[57]

While there is interest in gold(I) complexes bearing simple olefins for experimental and theoretical studies,[46a,56] isolation of these gold-alkene complexes are sparse, due in large part to the poor thermal stability, light sensitivity and high lability of the organic ligands, creating difficulties in the isolation of these complexes. This difficultly is most pronounced in the attempted syntheses of gold-(η^2)ethylene complexes.[46] Below describes the latest developments in the synthesis of gold-(η^2)olefin complexes.

1.3.1.1 Neutral Gold(I) Complexes

The work by Dias *et al.* provided neutral gold(I) ethylene complexes containing anionic tris(pyrazolyl)borate (**VIIIa-b** and **IX**)[58] and triazapentadienyl (**X**)[59] anions (Figure 14)

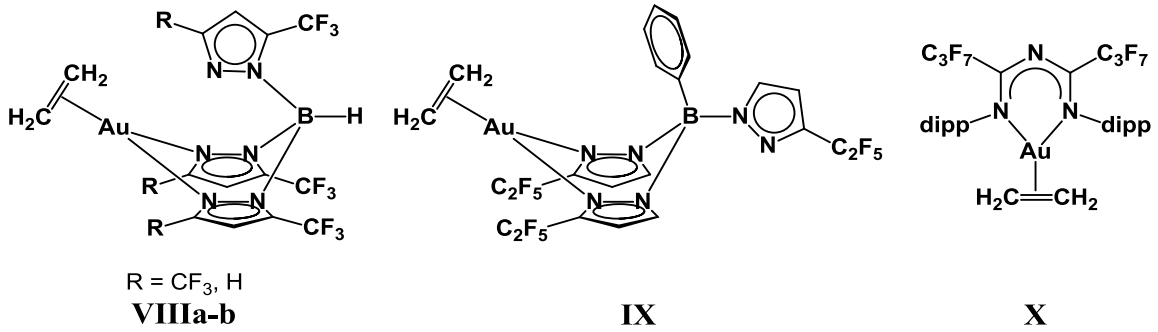

Figure 14. Neutral gold(I)-ethylene complexes.[58,59]

The gold centres in **VIII-X** are in distorted trigonal planar geometries, with the orientation of the C=C axis in the structures being virtually parallel to the (N^N) axes of the coordinated ligands. The relative strong π-bonding between the gold(I) cation and ethylene inhibits both lability in solution and the loss of the olefin when placed in a vacuum. The crystal structures indicate a significant lengthening of C=C bonds (from 1.313 Å of free ethylene to 1.38-1.41 Å when aurated), as well as symmetric Au-(C=C) bonding of the gold-ethylene unit.

1.3.1.2 Cationic Gold(I) Complexes

The formation of cationic gold complexes containing Au^{+}-(η^2)olefin bonds has been achieved by the treatment of [(L)AuCl] with silver salts (examples include $AgBF_4$, $AgPF_6$, $AgSbF_6$, AgOTf and $AgOC(O)CF_3$) in the presence of an olefin. These cationic complexes have been proposed as intermediates in many cationic gold(I)- and gold(III)-mediated transformations of olefins.[45c,60-62]

Complexes of the type $[(L)Au(ene)]^{+}$ have been described containing a variety of stabilising σ-donor ligands: Examples of structurally determined gold(I)-(η^2)alkene complexes are supported by 6,6'-substituted-2,2'-bipyridines $[(bipy^{R,R'})Au(ene)][PF_6]$ (**XI**$_{ene}$; ene = ethylene, styrene, 4-methoxystyrene,

α-methylstyrene, *cis*-stillbene, norbornene, and dicyclopentadiene),[63] *N*-heterocyclic carbenes [(NHC)Au(ene)][SbF_6] (**XII**$_{ene}$; ene = *cis*-2-butene, *iso*-butene, 2-methylbut-2-ene, 2,3-dimethyl-but-2-ene, 1-hexene, norbornene, styrene and 4-methylstyrene)[64] or (*tert*-butyl)phosphines [(R(^{t}Bu)$_2$P)Au(ene)][SbF_6] (**XIII**$_{ene}$; ene = isobutene, norbornene, *trans*-cyclooctene; R = ^{t}Bu, *o*-biphenyl).[64,65] All isolated complexes are colourless solids which are surprisingly stable to air and heat, with no olefin loss under vacuum or introduction of basic solvents. Crystallographic data of these complexes have shown that the gold atoms are in an almost perfectly planar (L)Au-(C=C) environment, with the exhibition of a slight extension in length and loss of double-bond character in the coordinated olefin bonds. In solution, these gold-olefin complexes exhibit rapid ligand exchange processes in the presence of excess olefin. Cationic gold(I) complexes containing *N*,*N*-chelates or strongly basic phosphine and NHC ligands are used as catalysts of choice for C-H and C-C functionalisation reactions.[44b,66,67]

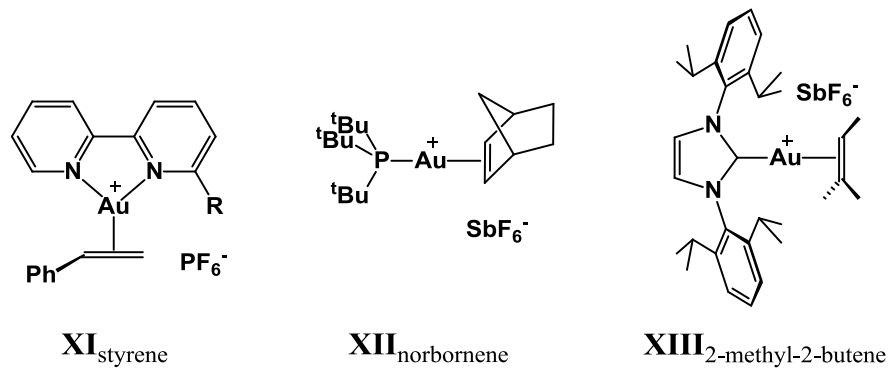

XI$_{styrene}$ **XII**$_{norbornene}$ **XIII**$_{2\text{-methyl-2-butene}}$

Figure 15. Select examples of supported gold(I)-(η^2)ene cations.[63-65]

Only gold-(η^2)olefin complexes which bear strongly basic ligands (such as tri-*tert*-butylphosphine and tricyclohexylphosphine) are stable at room temperature,[65] whereas treatment of olefins with (Ph_3P)Au^+ cations promote olefin C=C activation. The comparison of reactivity between (R_3P)AuCl/$AgSbF_6$ (R = Ph, Cy, ^{t}Bu; R_3 = (^{t}Bu)$_2$(*o*-biphenyl)) in the presence of cyclopentadiene (CpH) neatly shows the dependence of the substituents on the phosphine ligands. (Cy_3P)AuCl, (^{t}Bu$_3$P)AuCl and (^{t}Bu)$_2$(*o*-biphenyl)AuCl promotes the formation of stable η^2-bonding to CpH (**XIV**), whereas use of (Ph_3P)AuCl results in the activation of

the C=C bond in CpH, leading to a polymer blend comprising of 1,2- and 1,4-cyclopentene units (Scheme 3).[68]

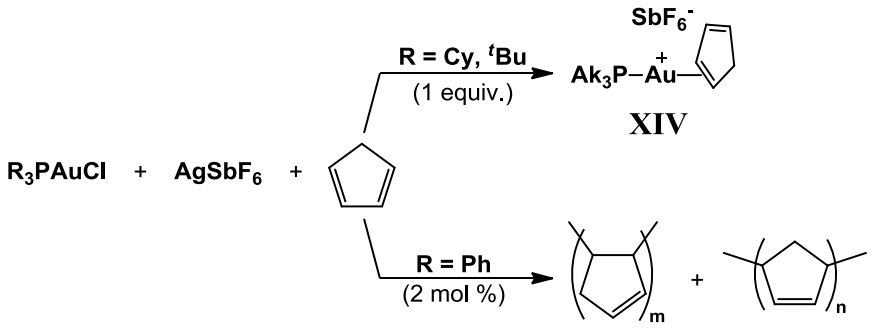

Scheme 3. The synthesis of a cyclopentadiene complex **XIV** and polycyclopentadienes by selection of $R_3PAuCl/AgSbF_6$.[68]

1D and 2D NMR spectroscopic evidence of $[(Ph_3P)Au(4\text{-methylstyrene})][BF_4]$ was only available at reduced temperatures, as cooling to -20 °C inhibits C=C bond activation.[69] The differences in reactivity between $[(Ph_3P)Au]^+$ and $[(Ak_3P)Au]^+$ have been ascribed to the umbrella-type shielding of the gold atom by the bulky ligand and the much more powerful donor effect of the alkyl groups on the phosphine, compared to that of phenyl groups.

Studies into the bonding of $[\{(o\text{-biphenyl})(^tBu)_2P\}Au][SbF_6]$ cation ($\mathbf{XV}_{diene}$) with dienes by experiment and theory established η^2-coordination is only observed. This is not surprising, as to the pronounced tendency of gold(I) to form two-, rather than three-coordinate complexes is apparent (Figure 16).[12,70]

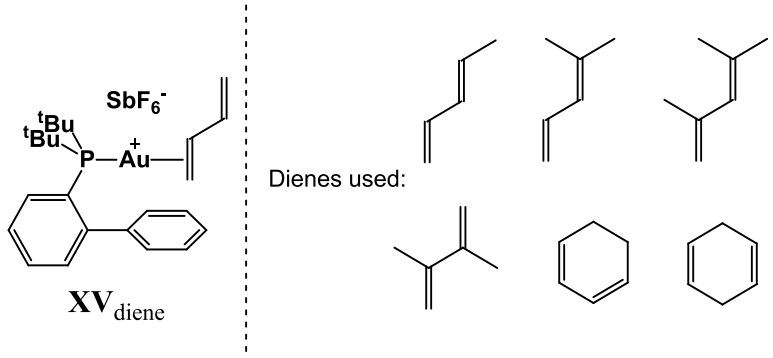

Figure 16. The isolated products of $\mathbf{XV}_{diene}$ and selected dienes that have been used.[70a]

Single crystal X-ray analyses of **XV**$_{diene}$ have shown that the $[(R_3P)Au]^+$ cation preferentially coordinates to the least-substituted double bond of the diene. In solution these compounds are fluxional with cold temperature ^{1}H NMR studies showing a migratory exchange step of the η^2-bond to the dienes, with kinetic findings concluding that the exchange probably occurs *via* an associative pathway through a cationic three-coordinate bis-(η^2)diene intermediate (Scheme 4).

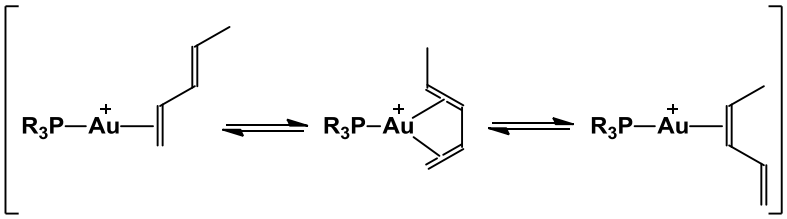

Scheme 4. The mechanism for π-bonding exchange of gold(I)-dienes.[70]

In the 1960s Hüttel *et al.* synthesised a family of gold-(η^2)olefin complexes in absence of a supporting ligand, which following the general formula $[Au(ene)_3][AuCl_4]$. In all cases, the yellow crystals isolated were thermally very unstable and highly sensitive to moisture.[55a,55g,55h] Only in 2008 was the structure of the $[Au(ene)_3]^+$ cation confirmed, from the product of AuCl and $AgSbF_6$ in dichloromethane under an ethylene atmosphere.[71] The choice of anion in $[Au(C_2H_4)_3][SbF_6]$ (**XVI**) results in a more stable derivative than the $[AuCl_4]^-$ containing complex in Hüttel's complexes. Crystallographic analysis, accompanied by theoretical calculations of $[Au(C_2H_4)_3][SbF_6]$ alludes to a strong Au-(η^2)C=C bond. The structure was found to be almost completely planar (regarding the non-hydrogen atoms), with in-plane orientation of the ethylene ligands, the same as in the isoelectronic Pt complex $[Pt(C_2H_4)_3]$[72] (Figure 17). The ethylene bonds exhibit the consequences of π-bonding, in terms of both C=C bond elongation and loss of sp^2 character. Subsequent discoveries by Russell[52] and Dias[73], describe numerous complexes of a ligand-free gold(I) cations bearing differing olefinic ligands (norbornene, cyclooctadiene, *trans*-cyclooctene; **XVIIa-c**). The structure of the norbornene and *trans*-cyclooctene complexes resembles that of the spoke-wheel arrangement seen in $[Au(C_2H_4)_3]^+$, whereas the (albeit poor) crystal data for the cyclooctadiene complex shows an increased coordination number to 4, to allow for

chelation of two diene units onto one cationic gold centre.[52] A comparison of the crystallographic properties of $[M(nbe)_3][SbF_6]$ within the coinage metals confirms that gold is the best candidate as a π-Lewis acid, with the bonding of gold to both ethylene and norbornene molecules deemed to the strongest.[73]

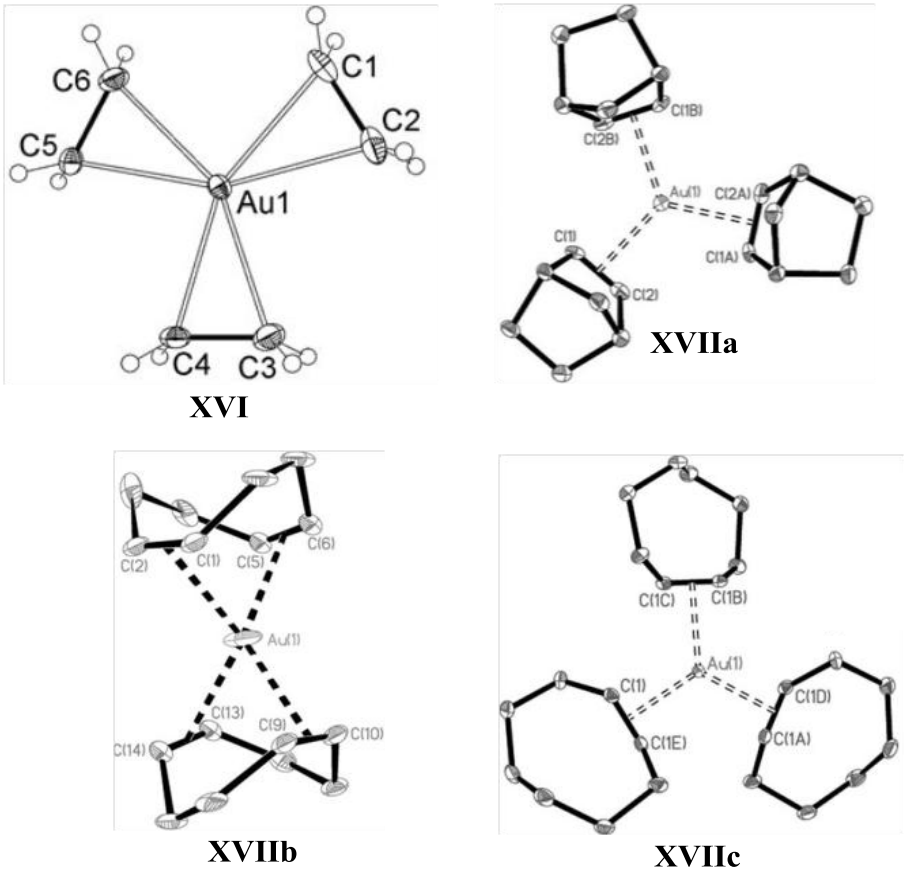

Figure 17. The crystal structures of the unsupported $[Au(ene)_n]^+$ cations **XVI** and **XVIIa-c**.[52,71,73]

1.3.2 Gold(I)-(η^2)Alkyne Complexes

As mentioned in section 1.3, the bond strength between a gold cation with alkynes and alkenes are comparable, but the increased reactivity of alkynes upon gold coordination means activation of the gold-(η^2)yne bond is preferred over isolation. This results in fewer structural examples containing a gold(yne) bond being documented.[45b,45c]

Structurally determined examples of neutral and cationic supported gold(I) complexes bearing simple internal alkynes ($[(L)Au(yne)_n]^{+/0}$) have been described with chloride (**XVIIIa-b**),[74,75] triazapentadienyl (**XIX**),[76] NHC (**XXa-b**)[77] and phosphine (**XXI** and **XXII**)[78,79] ligands (Figure 18). The effect of gold coordination

on the triple bond is similar to that of the olefinic equivalent, with (a) the lengthening of C≡C bond and (b) the loss of *sp* character on the alkynic centres.

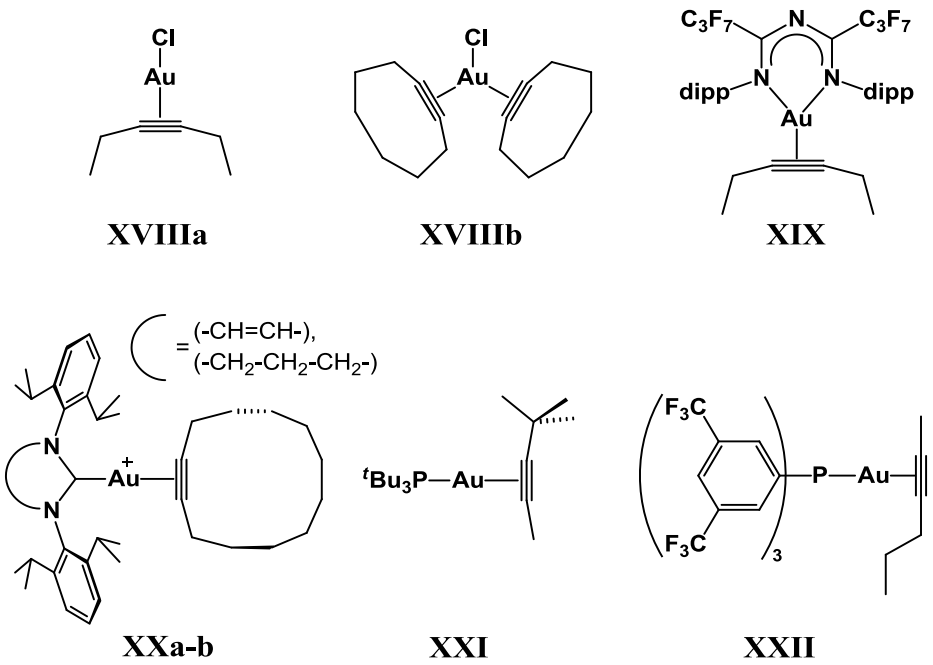

Figure 18. Neutral and cationic supported gold complexes containing an Au-(η^2)yne bond.[76-79]

The increase of acidity of the proton on terminal alkynes upon gold coordination was observed by Widenhoefer[80] and Finze[81]; treatment of terminal acetylenes with selected gold(I) complexes (at room temperature or 0 °C) yields the digold σ,π-acetylide complexes **XXIII**, **XXIVa-b** and **XXVa-b** as crystalline solids (Scheme 5). The two gold centres in these complexes support each other by aurophilic interactions (Au···Au_{intra} approx. 3.4 Å) with additional contacts observed with another digold σ,π-acetylide for **XXIVa-b**, resulting in a dimer complex (Au···Au_{inter} 3.0-3.1 Å). No dimerisation was observed for **XXIII** or **XXVa-b** due to the steric constraints of the supporting ligands. Suppression of C-H activation was achieved in the reaction of phenylacetylene with (IPr)AuCl/AgOTf when performed at -60 °C to furnish a gold-(η^2)alkyne complex (**XXVI**), identified by ^{1}H NMR spectroscopy. Once warmed to 0 °C, C-H activation of **XXVI** followed by coordination of a second gold cation gave the digold complex **XXIII**. Digold σ,π-acetylides have also been synthesised by the C-Si activation of ^{t}BuC≡CSiMe$_3$ with (^{t}Bu$_3$P)AuCl.[78]

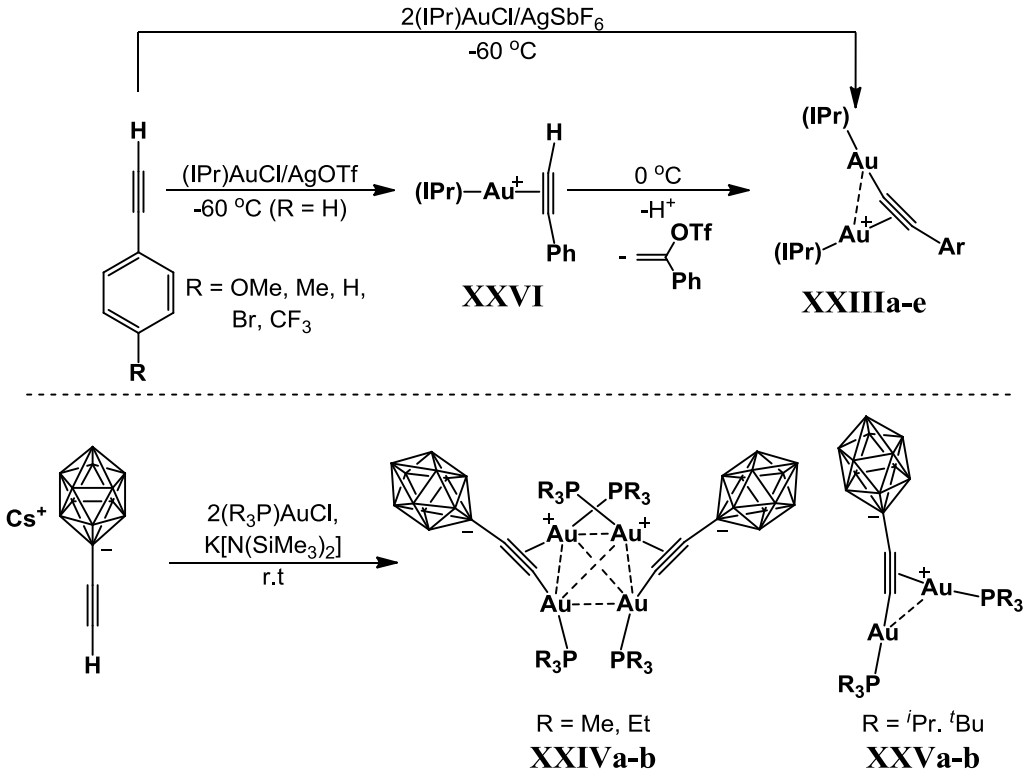

Scheme 5. Synthesis of a digold σ,π-acetylides **XXIII**, **XXIVa-b** and **XXVa-b**.[80,81]

The structural confirmation of gold(I)-alkyne complexes unsupported by strong donor ligands was only described in early 2012 by Dias *et al.*, with the synthesis of the moderately light- and air-sensitive complex [Au(cyclooctyne)$_3$][SbF$_6$] (**XXVII**, Figure 19).[74] Crystallographic analysis describes the structure of **XXVII** as a distorted spoke-wheel structure (the distortion was attributed to steric congestion). The cyclooctyne ligands experience lengthening of the C≡C bond, as well as an increase in torsion angle of the C-C≡C-C moiety, as a consequence of the loss of *sp*-character.

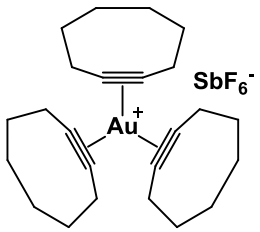

XXVII

Figure 19. The structurally characterised 'naked' gold(I)-alkyne complex **XXVII**.[74]

1.3.3 Gold(I)-(η^2)Arene Complexes

With the reduced interactions observed between gold centres and arenes,[45,47,48] it is not surprising that very few examples are available that exhibit gold-(η^2)arene bonding. The only such examples are accompanied by a strong σ-donating ligand, such as a (*o*-biphenyl)di(alkyl)phosphine (**XXVIIIa-b**)[60] or a NHC (**XXIX**)[82] group (Figure 20).

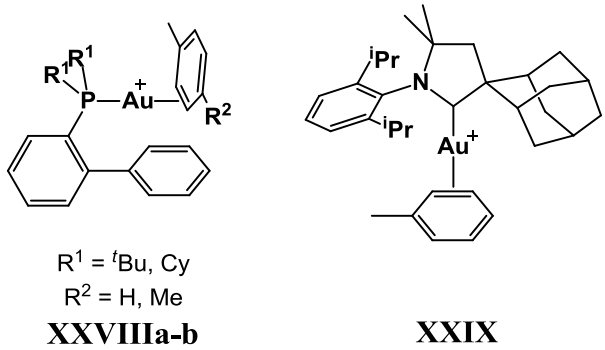

Figure 20. Isolated cationic gold(I)-arene complexes.[60,82]

The plane of the aromatic rings in **XXVIIIa-b** and **XXIX** are close to perpendicular to the $[(L)Au]^+$-arene bond. To date no information is available for attempts on the coordination of arenes by an unsupported, 'naked' gold cation.

1.3.4 Lack of Isolated Gold(III) π-Complexes

With the growing field of π-coordination of gold(I) to alkynes, alkenes and arenes appearing in literature, the lack of examples for such coordination to gold(III) is pronounced. Prior attempts by Hüttel *et al.* to treat various electron-rich bonds with $AuCl_3$, $AuBr_3$, $HAuCl_4$ or $NaAuCl_4$ in a number of conditions has resulted in either a C-H activation process, or reduction to form gold(I) π-complexes and metallic gold.[56] The only experimental evidence of gold(III) π-coordination available was observed in the reaction of $[(C_6F_5)_2AuCl]_2$ and phenylacetylene in methanol doped with trace water at 60 °C. NMR spectroscopic analysis suggests a $[(C_6F_5)_2AuCl(\eta^2\text{-PhC}\equiv\text{CH})]$ species could be identified as an intermediate to C-C activation (Scheme 6).[83]

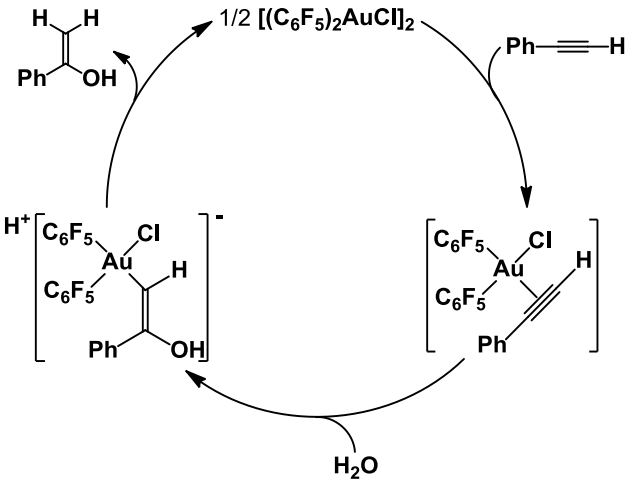

Scheme 6. The proposed catalytic cycle, with the possible gold(III) intermediates detected spectroscopically.[83]

1.4 Organic Transformations Mediated by Gold

With the explosive growth of homogeneous catalysis by gold(I) and gold(III) complexes in organic transformations of alkynes and alkenes,[44,84] many research groups have focused on the mechanistic understanding of the mechanisms of gold-mediated reactions.[44f,44j,44r] In catalysis, gold(I) $[(L)Au]^+$ and gold(III) $[(L)_3Au]^+$ cations act as soft, carbophilic Lewis acids to promote the activation of non-functionalised C-C and C-H π-bonds.[85] Many transformations of electron rich bonds (such as alkynes, alkenes and arenes) can also be promoted by Brønsted acid activation, but it has frequently been found that $[(L)_nAu]^+$ offers advantages, as activation occurs at far milder conditions, with greater control over the reaction products and stereoselectivity observed.[44s,86] This has opened up a huge synthetic potential for selective cyclisations and H-X additions to multiple bonds.

1.4.1 The Unknown Silver Effect in Activation

1.4.1.1 With (L)AuCl

In most homogeneously gold(I)-catalysed reactions, the active species is generated *in situ* by reacting the neutral two-coordinate complex (L)Au-Cl with silver salts containing weakly-coordinating anions (such as $AgSbF_6$, $AgBF_4$, $AgClO_4$, AgOTf and $AgOC(O)CF_3$), to generate a catalytically-active gold cation

and a silver chloride precipitate (Eq. 1). However, numerous studies have suggested this simple activation may not be the case.[87]

$$(L)Au\text{-}Cl + AgX \not\longrightarrow [(L)Au][X] + AgCl \qquad \textbf{(Eq. 1)}$$

Larrosa *et al.* have described a systematic assessment of the roles of gold and silver complexes in alkyne hydration (Table 3).[88]

Table 3. Silver effect in alkyne hydration.[88]

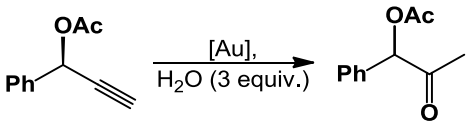

Entry	Catalyst[a]	Time /h	Yield
1	$[(Ph_3P)Au][A]^b$	12	0
2	AgA^b (10 mol %)	12	0
3	$(Ph_3P)AuCl/AgOTf$	12	90
4	$(Ph_3P)AuCl/AgSbF_6$	8	97
5	$[(Ph_3P)Au][SbF_6] + AgSbF_6$	12	91

a – 2 mol % loading unless otherwise stated, *b* – A = OTf, SbF_6 or BF_4.

None of the tested silver salts (AgA, A = OTf, SbF_6 and BF_4) catalyse the reaction, neither could the gold salts $[(Ph_3P)Au][A]$ (isolated by Celite filtration of the $(Ph_3P)AuCl/AgA$ mixtures). However, the mixtures of $(Ph_3P)AuCl$ and AgA employed without prior Celite filtration promoted the reaction to progress to completion. Interestingly, a mixture of $[(Ph_3P)Au][OTf]$ and $AgSbF_6$ also catalysed the reaction effectively, suggesting the combination of gold and silver cations makes alkyne activation possible. Closer inspection of $(Ph_3P)AuCl/AgOTf$ mixtures, both before and after Celite filtration, by XPS and ^{31}P NMR spectroscopy have confirmed that the combination of Ag^+ cation with $[(L)Au]^+$ results in the formation of an uncharacterised species in solution (Figure 21).

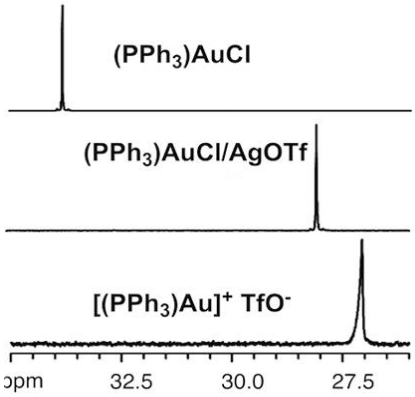

Figure 21. ^{31}P NMR spectra of $(Ph_3P)AuCl$ and a mixture of $(Ph_3P)AuCl/AgOTf$ both before and after filtration through Celite.[88]

1.4.1.2 With $[AuCl_3]_2$

$[AuCl_3]_2$ (which can be used as a catalyst on its own) is commonly used with silver salts, as it is believed to generate a more electrophilic Au(III) species $[AuCl_{3-n}][X]_n$ *in situ*. Reetz *et al.* described the findings of the reaction of $AuCl_3$ with three equivalents of AgOTf. No formation of the expected $Au(OTf)_3$ and AgCl compounds were observed, instead an orange precipitate formed which was found to be a mixture of Au(I), Au(III) and Ag(I) ions of approximate composition "$4AuCl_3 \cdot 5AuCl \cdot 11AgCl$", with the oxidation state of the gold species in solution unclear (Eq. 2). Similar products were seen when $AgSbF_6$ was employed.[89]

$$x[AuCl_3]_2 \;+\; 6x\ AgOTf \longrightarrow \text{“}Au_9Ag_{11}Cl_{28}\text{”} \;+\; \mathbf{?} \qquad \textbf{(Eq. 2)}$$

Other factors that are thought to influence catalysis include the metallophilic affinity of the two metals in their low oxidation states,[1,90] the known activity of Ag^+ with unsaturated organic substrates,[91] and the hygroscopic and light sensitive natures of silver salts, causing difficulties in keeping the reaction medium aprotic.[92]

1.4.2 Silver-Free Methods for Gold(I) Catalyst-Generation and Catalysis

Different tactics for gold(I) catalysis that omit the use of silver salts have been employed in recent times. One of these routes involves the development of stable, isolable complexes of $[(L)Au]^+$ stabilised by weakly coordinating ligands, to

give “single-component” catalysts. Examples in the literature include the synthesis of complexes incorporating solvate- (nitriles[60,93] and arenes[60,82]) and anionic- (triazolate,[94] triflimide,[92,95] triflates,[96,97] sulfonates[98] and trifluoroacetates[97-99]) ligands (Scheme 7). Additional work has shown that the well-known trinuclear gold oxonium complexes[100] (an example is shown in **XXXI**) can be employed as sources of $[(R_3P)Au]^+$ cations in organic transformations.[96,101]

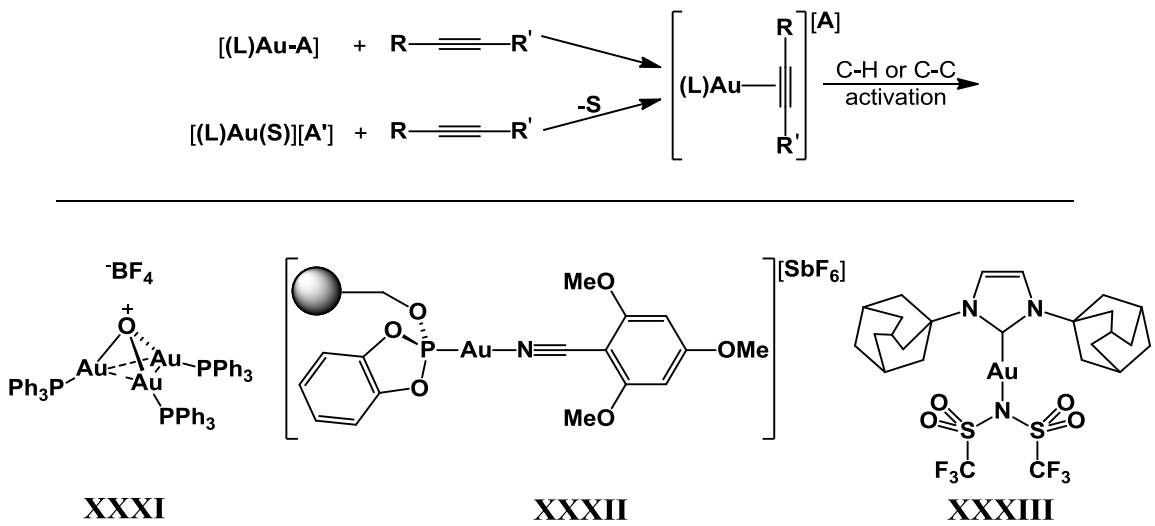

Scheme 7. General scheme for π-coordination of alkynes using chloride-free gold(I) salts (top) and a selection of gold(I) salts (**XXXI-XXXIII**) which have been used as catalysts for alkyne activation.[93a,95,96]

Other routes investigated involve the *in situ* generation of the gold(I) catalyst from (L)Au-Cl and weak bases[89,102] or of (L)Au-Me with Lewis acids.[103,104] Both methods have yielded catalysts that have activities comparable to (L)AuCl/AgX systems in similar conditions.

1.4.3 Activation of Unsaturated Organic Bonds by Gold

1.4.3.1 Activation of Alkynes by Gold(I) and Gold(III)

When considering the activation of alkynes, the modes of activation in homogeneous gold(I) and gold(III) catalysis are shown in Schemes 8-11.

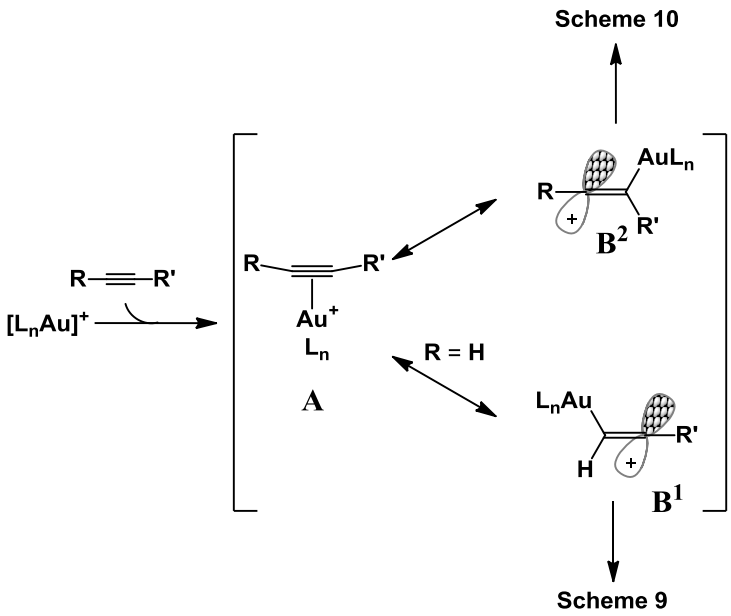

Scheme 8. The intermediates **A**, **B**^{1} and **B**^{2} from the reaction of $[L_nAu]^+$ and RC≡CR′.

The generally accepted mechanism shows that the treatment of alkynes with $[(L)_nAu]^+$ results, in the first instance, in a gold-(η^2)acetylene intermediate **A**. If R = H, the acidity of the alkynyl-proton increases, allowing for deprotonation (in the presence of a base) to form a gold-acetylide complex **XXXIV** *via* intermediate **B**^{1} (Scheme 9).[89,105,106]

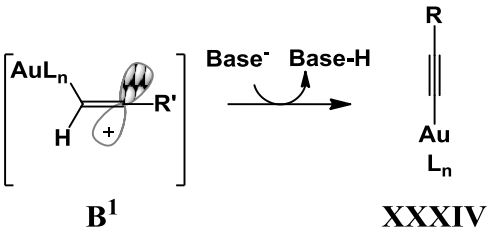

Scheme 9. The deprotonation step of intermediate **B**^{1}.

If no base is present, or R′ ≠ H, the aurated vinyl cation **B**^{2} (a resonance canonical of **A**) is susceptible to attack by a host of nucleophiles to give the intermediate **C** and its gold-carbenoid canonical **D** (Scheme 10). Intermediate **C** can undergo protodeauration to give the organic product **XXXV**, whereas **D** is involved in numerous organic transformations mediated by electrophilic attack.[44]

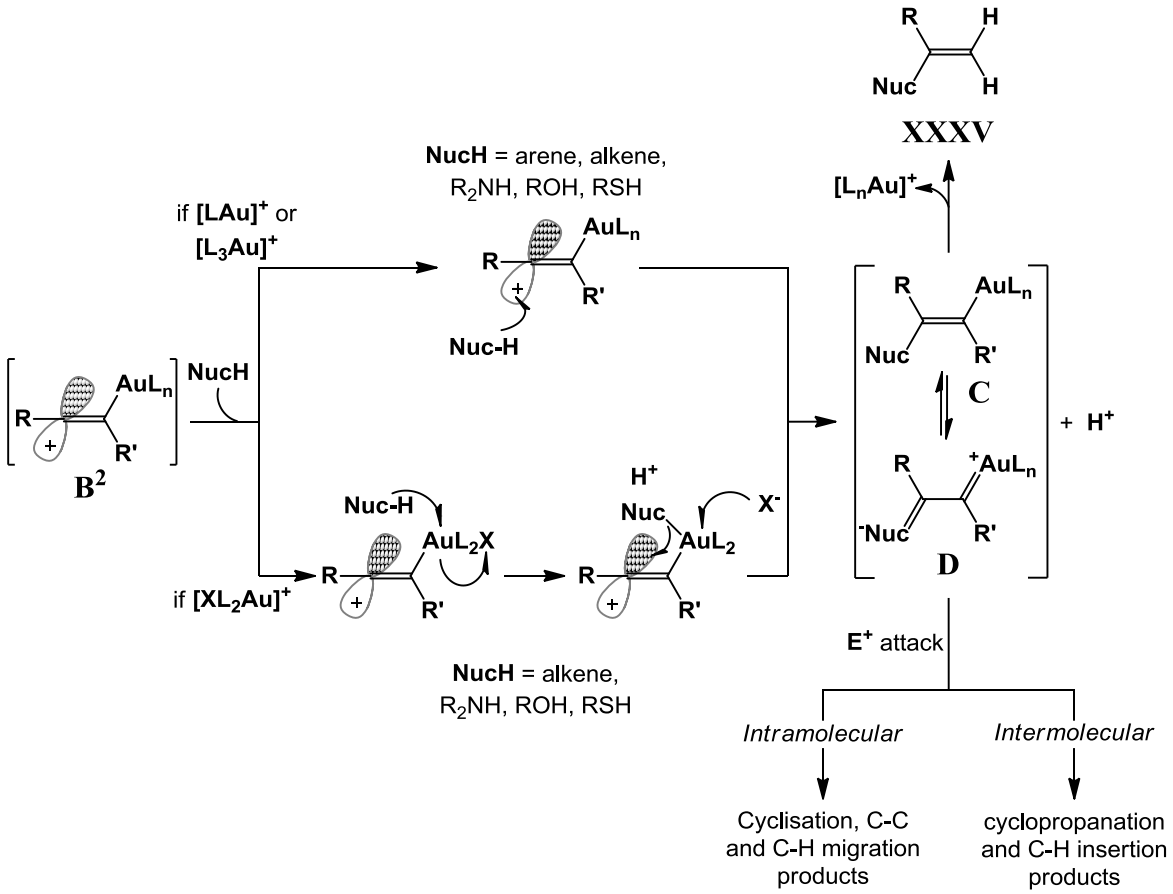

Scheme 10. The modes of nucleophilic attack observed by Au(I) and Au(III) cations.

The mode of attack is dependent on the composition of the gold cation employed; gold(I) or gold(III) cations containing non-labile ligands is thought to result in outer-sphere nucleophilic attack, whereas gold(III) cations containing a labile ligand can promote an inner-sphere coordination by auration of the nucleophile, followed by migratory attack.[107] In hydroarylation reactions, C-H activation of electron-rich arenes occurs *via* an electrophilic aromatic substitution mechanism, promoted by attachment of the vinyl carbocation **B²** to the π-cloud of the arene to give **XXXVI**; aryl C-H activation is not mediated by gold (Scheme 11).[106,108,109]

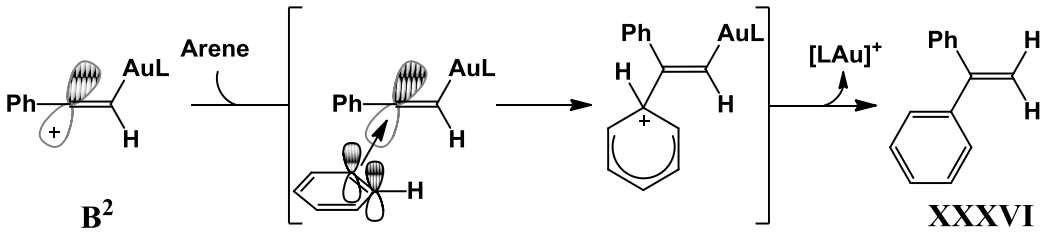

Scheme 11. The mechanism for hydroarylation to form **XXXVI** by gold(I).

Regioselectivity in these hydroarylation reactions is controlled by the electronic factors in the alkyne.[89,110] The electron-rich alkyne phenylacetylene, in the presence of $[AuCl_3]_2/AgSbF_6$, gives the 1,1-diarylethylene family in high yields under mild conditions. The inclusion of the electron-poor ethyl propiolate undergoes hydroarylation to give 1,2-disubstituted alkenes in a Z-configuration (Scheme 12). In the latter reaction, a number of gold catalysts can be employed, with both $[AuCl_3]_2/AgSbF_6$ and $(Et_3P)AuCl/BF_3{\cdot}OEt_2$ found to be efficient systems in this reaction.[89] Shi and He have developed this reaction further with evidence for hydroarylation of ethyl propiolate with methoxy-functionalised arenes by $[AuCl_3]_2/x AgSbF_6$ giving 1,2-disubstituted alkenes.[111]

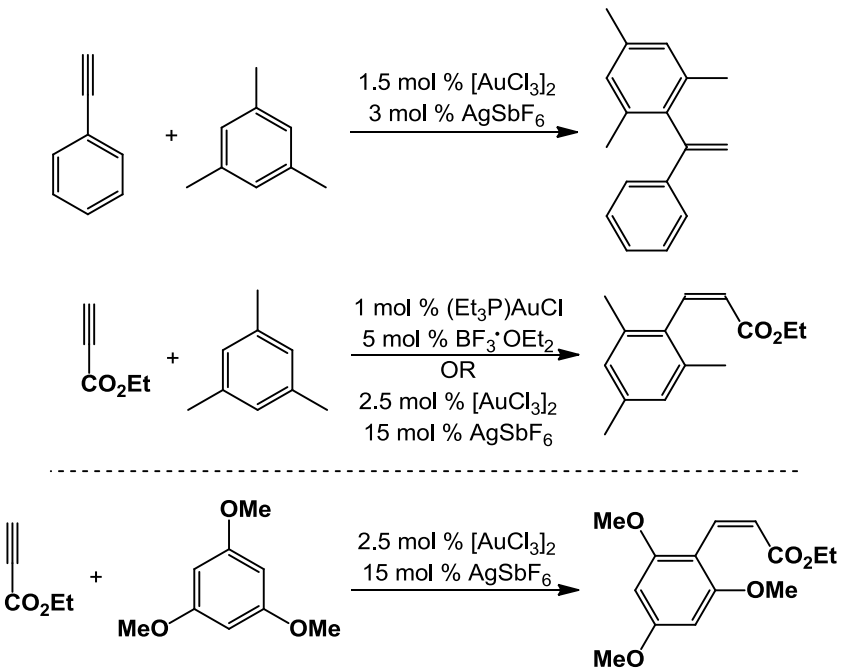

Scheme 12. Different hydroarylation products when mediated by Au(I) or Au(III) catalysts.[89,111]

1.4.3.2 Olefin Activation by Gold(I) and Gold(III)

The activation of olefinic bonds can be initiated by both gold(I) and gold(III) cations, with the mode of activation being similar to that of the activation of alkynes. Coordination of a gold cation with olefinic bonds yields a gold (η^2)-olefin intermediate **G** and its σ-bonded resonance canonical **H** (Scheme 13). The intermediate **H** is susceptible to nucleophilic attack to give the unsaturated organogold intermediate **J**, followed by protodeauration to complete the catalytic cycle and give **XXXVII** and the gold catalyst.[61]

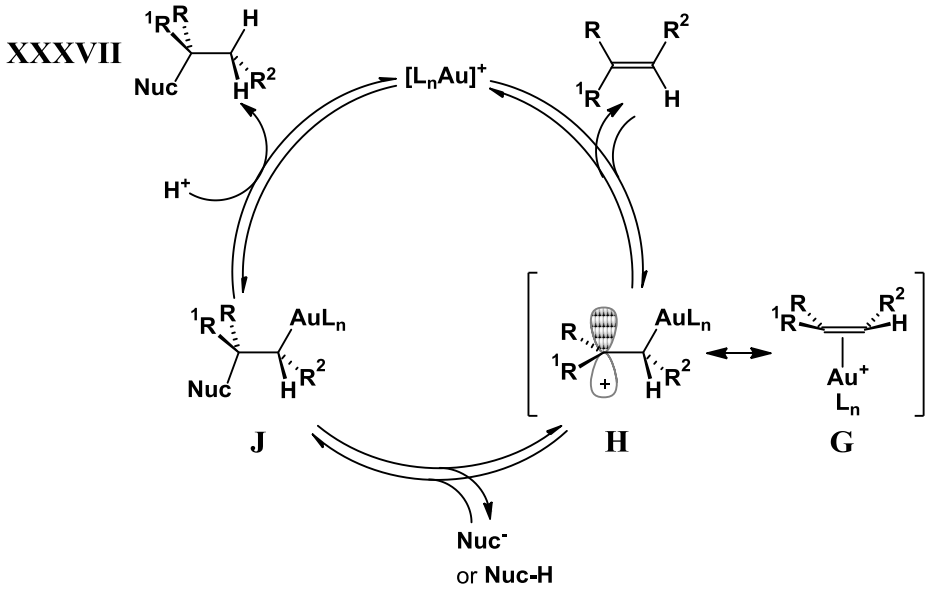

Scheme 13. The catalytic cycle of $[L_nAu]^+$ and alkenes.

1.4.3.3 Activation of Arenes

1.4.3.3.1 By Gold(I)

Despite the activity of other electron rich C-C bonds with gold(I), the first experimental evidence of direct C-H activation of arenes by gold(I) was only published in 2010.[112,113] The activation of electron-poor aromatic rings can be achieved by a concerted metalation-deprotonation step with a (L)Au-OPiv complex generated *in situ* (L = R_3P, IPr), where the coordinated pivalate ligand acts as a proton acceptor *via* a six-membered transition state (Scheme 14).[112,113a]

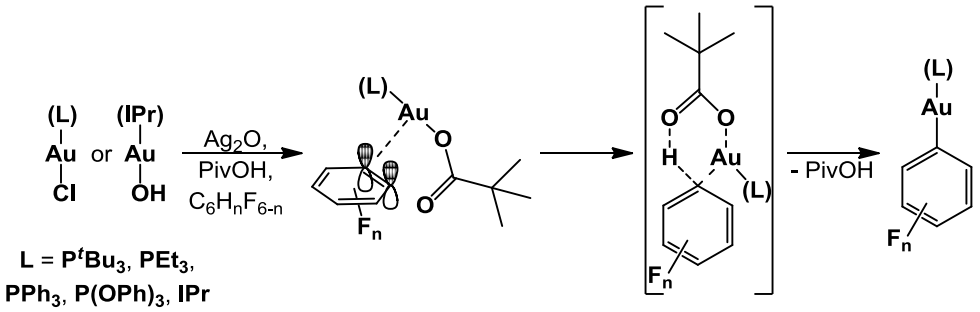

Scheme 14. Proposed Au(I) mediated C-H activation of electron deficient arenes.[112,113]

1.4.3.3.2 By Gold(III)

The activation of arenes by gold(III) is far more developed, with the chemistry established as early as 1931.[114] Two mechanisms are thought to operate in the activation of aromatic C-H bonds.

C-H activation of electron-rich arenes by $[AuCl_3]_2$ was first demonstrated by Kharasch and Isbell, with the synthesis of $[AuArCl_2]_2$ (**XXXIX**) and $[AuAr_2Cl]_2$ (**XL**) (Ar = C_6H_5, C_6H_4Me) *via* electrophilic aromatic substitution. These arylgold complexes were low yielding and unstable; readily reducing to ArCl and AuCl (Scheme 15).[114a] Stabilisation of the arylgold complex was achieved by the addition of a σ-donor ligand $[ArAuCl_2(L)]$ (L = PPh_3, C_5H_5N, S^iPr_2)[115] or by isolating the ligand-free dimer in carbon tetrachloride.[116] The synthetic yield of these products were always low (< 50 %). In 2001, Utsunomiya *et al.* had investigated these arylgold complexes and discovered the structural features of [Au(*p*-xylyl)Cl_2(2,6-lutidine)] (**XLI**), with similar arylgold(III) complexes containing benzene, toluene, *o*- and *m*- xylenes, mesitylene, cumene and anisole being spectroscopically characterised. Unless an alkali metal carbonate is employed, the maximum yield of these complexes was 50 % (in relation to $[AuCl_3]_2$), as HCl generated during auration consumes starting $[AuCl_3]_2$ to give $HAuCl_4$ (Scheme 15). A drastic reduction in yield was observed when electron withdrawing substituents (such as chlorobenzene) were incorporated into the arene substrate.[106]

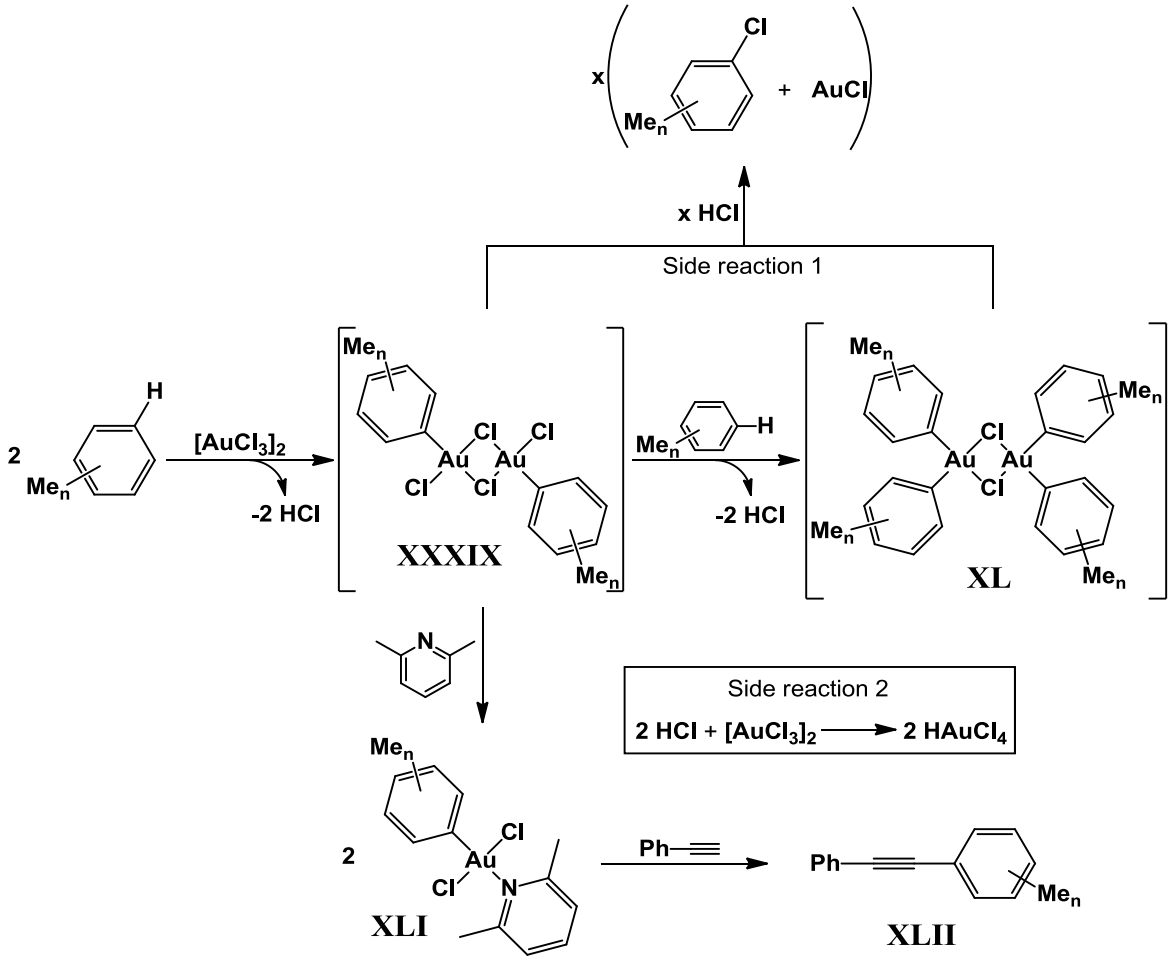

Scheme 15. The electrophilic aromatic substitution mechanism of arenes by $[AuCl_3]_2$.[106,114a,115,116]

In all cases the activation of only aromatic C-H bonds was seen; the aliphatic C-H bonds remain intact. Treatment of these arylgold(III) complexes with phenylacetylene results in the aryl-coupling of acetylene (**XLII**) (a Sonogashira-type reaction in the absence of a copper cocatalyst), with no evidence of a hydroarylation product.[106]

Electron deficient aromatics have also been found to be activated by organogold(III) intermediates (such as the intermediates **B**[2] and **C** in section 1.4.3.1, Scheme 10), where $[Au(III)]^+$ acts as a Lewis acid in a Friedel-Crafts acylation-type mechanism.

1.5 Concluding Remarks

This thesis will focus on understanding and developing the understanding of the reactivity of complexed gold centres with simple, π-donating organic compounds containing a C-C multiple bond. The work that makes up the following chapters was conducted in an effort to further contribute to and complement research in this field. As such, it focuses on the efficacy of a selection of σ- and π-donor ligands for gold coordination and the potential uses these new complexes as catalysts for many organic transformations. It is hoped that this work will lead to a better understanding on the mechanistic role of gold cations, as questions into the parts played by the numerous components of these reactions (the organic substrates, the role of silver salts as activators, *etc.*) are unanswered. Providing proof to answer these questions would surely be of tremendous academic interest.

2 - *N*-Coordinate Ligation to Gold(I) and Gold(III)

2.1 Topic 1: Synthesis of Gold(I)- and Gold(III)-Tetrafluorophthalimido Complexes

2.1.1 History of Gold Complexes Containing Monoimidate Ligands

Imidatogold complexes have a long history, with patents of gold(III) succinimidates, as well as other gold(III) complexes arriving as early as 1929.[117] In light of the well developed medicinal chemistry of platinum(II)[118,119] and the similarities between this metal and gold(III) imparted by their isoelectronic nature,[120] initial interest of gold(I) and gold(III) complexes containing biologically compatible ligands was in their uses as therapeutic compounds in the treatment of numerous harmful bodies both in *vivo* and in *vitro*. Closer to the present day, considerations of gold(III) and gold(I) imidates in terms of structural and catalytic properties have also yielded important developments.

2.1.1.1 Gold(I) Imidates

The first structurally identified gold(I)imidate complex was documented in 1978, with the synthesis of sodium bis(*N*-methylhydantoinato)gold·4H_2O (**XLIII**, Figure 22). Crystallographic studies show the gold anion exists in the usual [N-Au-N] linear geometry, with the sodium cation partially stabilised by coordination to one carbonyl group on each bound hydantoin ligand. **XLIII** was found to be moderately effective in animal anti-inflammatory trials. This work was the first to postulate that the therapeutic properties of gold(III) imidates that were tested prior to this work may actually originate from gold(I) imidates, as a consequence of reduction in biological media.[121]

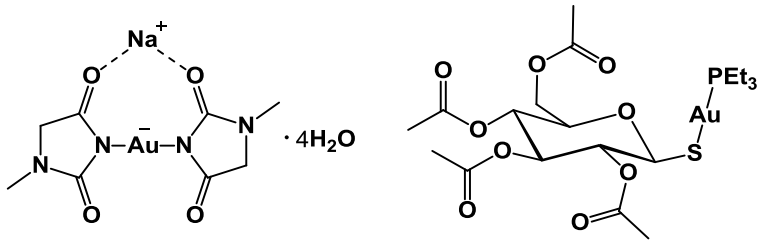

XLIII

Figure 22. Structures of sodium bis(*N*-methylhydantoinato)gold·$4H_2O$ (**XLIII**, left) and auranofin (right).[121,122]

With the developments of gold(I) phosphine complexes as anti-inflammatory agents (a prominent example being auranofin),[122] the incorporation of anionic imidates to phosphinegold(I) complexes for anti-inflammatory studies were targeted. The initial work concluded with the synthesis of a family of (triethylphosphine)gold(I) imidates (where the imidates are the anions of phthalimide (**XLIVa**), saccharin (**XLIVb**), 5,5-diphenylhydantoin (**XLIVc**), 3a,4,5,6-tetrahydosuccinimido[3,4b]acenaphthalen-10-one (**XLIVd**) and riboflavin (**XLIVe**); Figure 23). These complexes have anti-inflammatory properties with comparable activity to auranofin. The structural analysis of **XLIVa** confirms the expected linear geometry of the gold centre in $(Et_3P)Au(N\{CO\}_2C_6H_4)$. Oxidation to gold(III) by treatment of **XLIVa** with liquid bromine gave a complex mixture of $[(Et_3P)AuBr_n(phth)_{3-n}]$, with relatively little control on the products formed.[123]

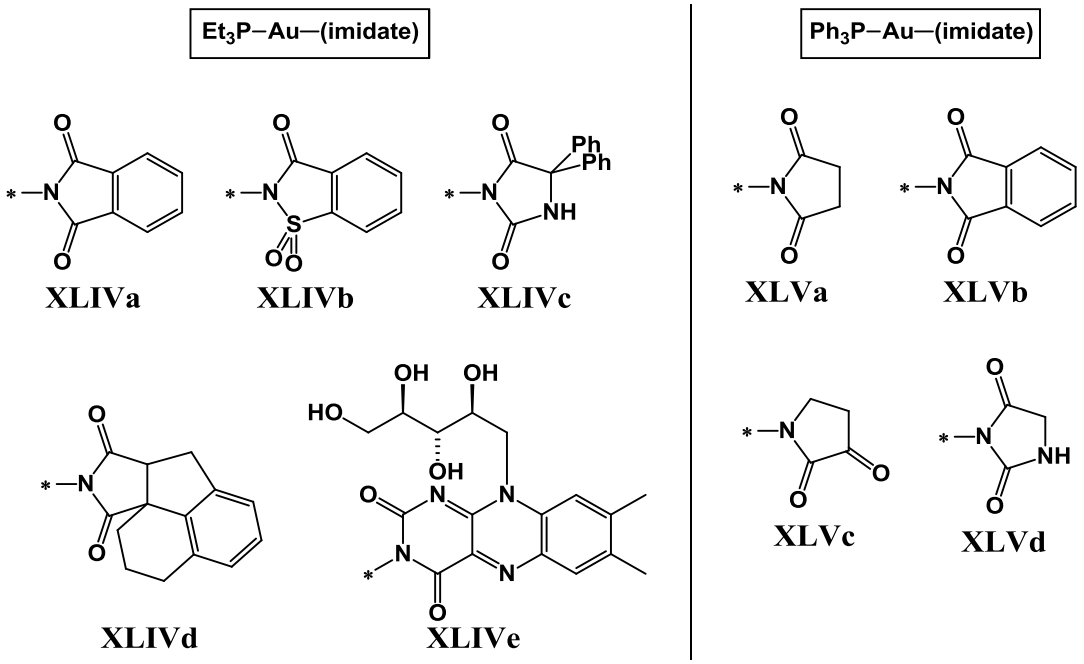

Figure 23. A selection of phosphinegold(I) imidate complexes.[123-127]

Further work resulted in the family of triphenylphosphinegold(I) complexes containing the anions of succinimide (**XLVa**),[125] phthalimide (**XLVb**),[124] 2,3-dioxoindoline (**XLVc**)[126] and hydrotoin (**XLVd**)[127] anions being just a few examples assayed for structural properties. All of these complexes show the coordination of the imidate anion in the expected linear fashion to the $[(Ph_3P)Au]^+$ cation (Figure 23).

The Au-N bond strength of these phosphinegold(I) imidates is considered to be weaker than traditional Au-N covalent bonds. In comparison with phosphinegold(I) bis(trimethylsilyl)amide, ($(Ph_3P)Au\text{-}N(SiMe_3)_2$; Table 4);[128] the gold-nitrogen bond lengths in the phosphinegold(I) imidates described above are up to 0.025 Å longer. This increase in bond length indicates that the Au-N bonds in gold(I)imidates are relatively weaker, allowing for the liberation of the $[(R_3P)Au]^+$. This property considered to be important for their observed therapeutic properties.[121]

Table 4. A summary of Au-N bond lengths in a selection of gold imidates.

Complex	Au-N (Å)	Reference
XLIII	1.94	121
XLIVa	2.05	123
XLVb	2.028, 2.040	124
$(Ph_3P)AuN(SiMe_3)_2$	2.027	128
$(Ph_3P)AuN(Tf)_2$ **XLVII**	2.102	92

The weakly coordinating nature of the imidate ions to gold has been observed with the reaction product of the silver salt of *o*-benzenedisulfonimide with (tht)AuCl. The gold cation is shown to preferentially coordinate to the neutral tetrahydrothiophene ligand over the anionic sulfonimide to form $[Au(tht)_2][C_6H_4NO_4S_2]$ (**XLVI**) in low yields. Crystallographic analysis portrays the weakly coordinating nature of the sulfonimide, with a long Au···N contact of 3.009(7) Å perpendicular to the linear [S-Au-S] bond(Figure 24).[129]

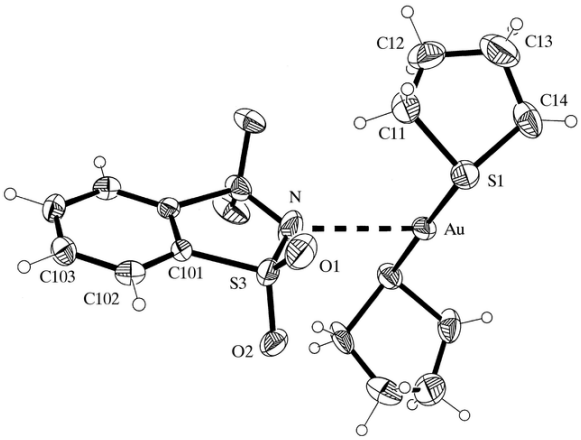

Figure 24. Molecular structure of $[Au(tht)_2][C_6H_4NO_4S_2]$ (**XLVI**).[129]

To date, there are no examples of gold(I)imidate complexes supported by thioether ligands, as the poor electronic donor capability of these dative ligands appears to be insufficient to stabilise a [(tht)Au(imidate)] configuration.

With phosphinegold(I)chloride complexes emerging as valuable precatalysts for organic transformations,[130] modifications to existing techniques of the activation of these gold complexes were desired to overcome the issues that come with the use of silver salts as activators (see section 1.4.1.1). An attractive alternative was first discovered by Gagosz *et al.*[92] with the isolation of $(Ph_3P)AuN(Tf)_2$ (**XLVII**). This class of phosphinegold(I) catalyst uses a bis(trifluoromethanesulfonyl)imidate moiety as a weakly coordinating counterion (comparison of Au-N bond lengths in Table 4 aids in this assignment, with a further elongation of the bond in comparison to gold(I)-imidates). These air-stable complexes have been found to be more convenient to prepare, store and handle and are exceedingly active catalysts for numerous activation processes for electron rich bonds.[131] Other sulfonimides have been used to synthesise $Ph_3PAuN(SO_2R)_2$ (R = 4-IC_6H_4, 4-ClC_6H_4, 4-FC_6H_4, 4-$(NO_2)C_6H_4$, CH_3).[132] The Au-N bond lengths from the crystallographic datasets were determined to be within 2.074-2.083 Å; considered a weaker bond than the imidatogold(I) complexes in Table 4, but stronger than the gold-nitrogen bond seen in **XLVII**.

2.1.1.2 Gold(III) Imidates

The early generations of gold(III) imidates consisted of four-coordinate gold anions in square planar geometries, paired with potassium cations (**XLVIII** and **XLIX**, Figure 25).[117a] These complexes are stable under atmospheric conditions but prone to reduction in biological media.

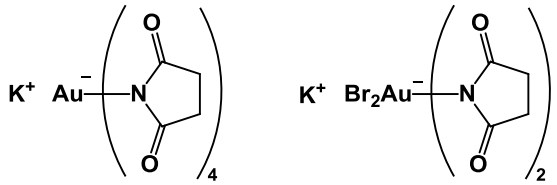

XLVIII **XLIX**

Figure 25. The first gold(III)imidates isolated by Kharasch and Isbell.[117a]

The use of bidentate chelates to produce cycloaurated complexes (typically with a bidentate C-N donor ligands) is currently the focus in the current generation of therapeutic gold(III) complexes.[133] The work by Henderson *et al.* in 2007 includes the synthesis of numerous cycloaurate(III) complexes containing imidate anions, with a selection showing excellent anti-tumour activity.[134] Structurally characterised examples of these cycloaurates (shown in Figure 26) found the geometry around the gold atom to be essentially square-planar. The two imidate ligands are in the *cis*-position with respect to each other, with the Au-N bond *trans* to the benzylpyridine-carbon being significantly longer than the benzylpyridine nitrogen ligand (due to the greater *trans*-influence of the phenyl group).

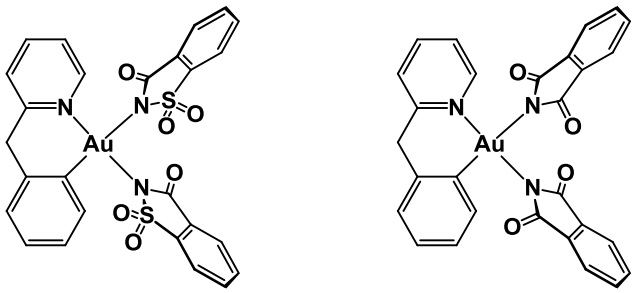

L **LI**

Compound	Au-$N_{Imidate}$	Au-N_{Py}	Au-C_{Benz}
L	2.118, 2.015	2.041	2.021
LI	2.117, 2.007	2.046	2.041

Figure 26. Cycloaurate(III) complexes structurally characterised by X-Ray crystallography; selected bond lengths in the accompanying table.[134]

Oxidation of the methylgold(I) complex **LII** by *N*-iodosuccinimide at reduced temperatures produced a poorly stable methylgold(III) succinimidate (**LIII**, Scheme 16). From the crystals grown, the Au-N was length determined to be 2.051(2) Å. This complex is temperature sensitive, as warming promoted reductive elimination to give the gold(I) succinimidate **LIV** and iodomethane.[135] It is believed that the species **LIII** may be an intermediate in the catalytic conversion of benzene to PhX (X = Cl, Br, I) by N-halosuccinimides in the presence of $[AuCl_3]_2$.[136]

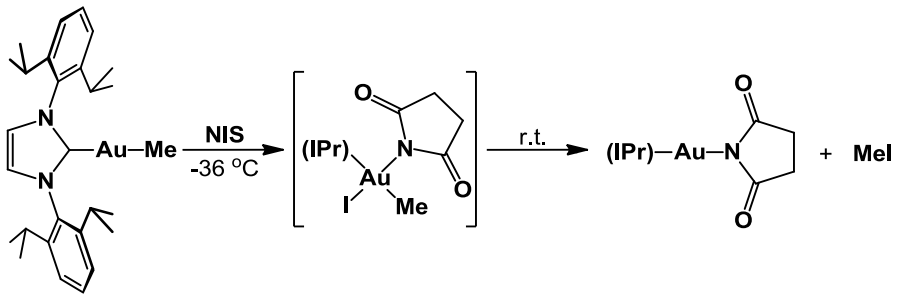

LII **LIII** **LIV**

Scheme 16. Oxidative addition of *N*-iodo succinimide to (IPr)AuMe (**LII**).[135]

Recent developments have shown that a gold(III) complex with 5,5-dimethylhydantoin ligands (dmh) can be used as an alternative source of gold metal to $[Au(CN)_2]^-$ in electrolyte solutions for electroplating.[137] The difficulties observed with using aurocyanide include: the use of hazardous cyanide solutions,

the poor stability in alkaline solutions and the electropotential ($E°$ = -0.61 V vs. Ag/AgCl) prohibiting the use of conventional water-soluble reducing agents; [Na][Au(dmh)$_4$] (**LV**) is found to be a useful alternative, as these issues are overcome with stability in aqueous alkaline solutions and efficient electrochemical reduction ($E°$ = -0.3 V vs. Ag/AgCl). The structure of the [Au(dmh)$_4$]$^-$ anion is square planar in geometry, with the imidate ligands arranged in a propeller-like shape. The Au-N bond distances in [Au(dmh)$_4$]$^-$ within the range of 1.96-2.01 Å (Figure 27).

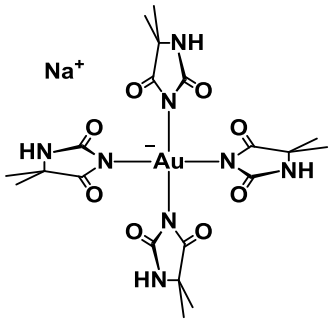

LV

Figure 27. A depiction of [Na][Au(dmh)$_4$].[137]

2.1.2 Targets and Objectives

The original target of this topic was to produce gold(I) and gold(III) complexes containing anionic phthalimidate ligands, which upon treatment with an electron rich bond (in the form of an alkene or an alkyne) would dissociate to allow for the formation gold complexes of the type [(R$_3$P)Au^I-(η^2)ene/yne][Phth] or [(R$_3$P)(C$_6$F$_5$)$_2$Au^{III}-{η^2}ene/yne)][Phth]. We have decided to explore the use of the anion of 1,2,3,4-tetrafluorophthalimide ([C$_6$F$_4$(CO)$_2$N]$^-$), since the electron deficient C$_6$F$_4$ backbone could extensively delocalise the electron density away from the imidate-nitrogen, coupled with the known ligand substitution mechanisms of succinimido and phthalimido units bound to gold with stronger donor ligands.[121] The presence of fluorine and C=O moieties can be used as reporter functions for charges in the electronic and bonding characteristics. To our knowledge, no gold complexes of the tetrafluorophthalimido ligand have been described before.

2.1.3 Results and Discussion

2.1.3.1 Synthesis of Tetrafluorophthalimido Precursors

Tetrafluorophthalimide (**2**) was first synthesised by Gething *et* al., who reacted tetrafluorophthalic acid with an aqueous solution of ammonia, followed by condensation and sublimation, although the yield was low.[138] A significant improvement is achieved using a two-step procedure *via* the anhydride **1**, followed by ammonolysis with urea.[139,140] The product was extracted into hot anisole to give the tetrafluorophthalimide **2** in 71% overall yield (Scheme 17).

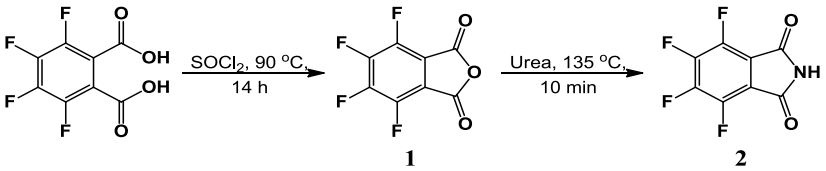

Scheme 17. Synthesis of tetrafluorophthalimide **2**.

Crystals of **2** were grown from slow cooling of an anisole solution and the compound was characterised by X-ray diffraction (Figure 28). The molecules are planar (C5-C6-N7-H7 torsion angle 179.8°), with extensive conjugation between the nitrogen atom and the C=O moieties. This is reflected in the low Lewis basicity of **2**, *i.e.* its failure to react with a number of strong Lewis acids (AlX_3, BX_3, where X = F, Cl, Br, C_6F_5). In the crystal the molecules form a hydrogen-bonded network in a corkscrew-like arrangement, where the N-H unit of one molecule interacts with one of the two oxygen atoms of a neighbouring molecule (N-H···O 2.07(3) Å).

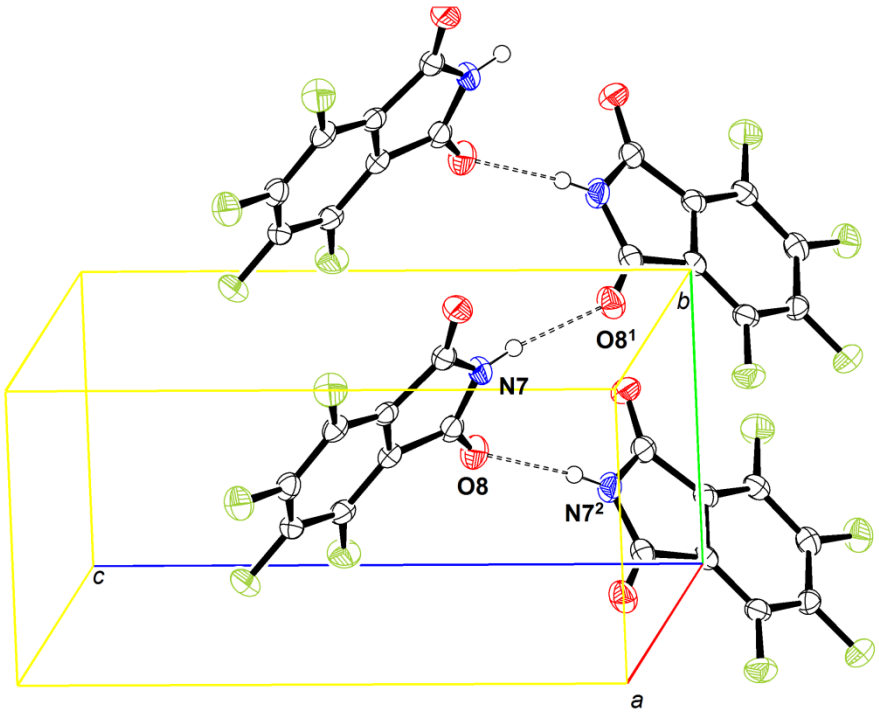

Figure 28. Crystal packing of **2**, with partial labelling scheme; unit cell depicted with the hydrogen bonding shown to illustrate the corkscrew orientation. Ellipsoids are drawn at the 50% probability level. Selected bond lengths (Å) and angles (°): C(6)-N(7) 1.389(3), N(7)-C(8) 1.380(3); C(6)-O(6) 1.205(3), C(8)-O(8) 1.212(3), N(7)-H(7) 0.80(3), H(7)···O(8') 2.07(3); N(7)-H(7)-O(8') 171(3).

The acidic N-H function of **2** can readily be metallated. Initial attempts to synthesise the lithium phthalimide **3** were unsuccessful; for example, the reaction **2** with of *n*-butyl lithium in THF solution at -78 ºC gave a deep red product, the ^{19}F NMR spectrum of which revealed a large number of broadened peaks, which we attribute to the possible susceptibility of the C_6F_4 backbone to nucleophilic lithation. Replacing *n*-butyl lithium with lithium bis(trimethylsilyl)amide under the same conditions generated the trimethylsilyl phthalimide **4** in moderate yield (~40 %; Scheme 18). The lithium phthalimide is however accessible in good yield from **2** and lithium diisopropylamide in diethyl ether as a red, amorphous solid. Attempts to obtain crystals were unsuccessful. The compound contained variable amounts of diethyl ether and a satisfactory elemental analysis could therefore not be obtained; however, the ^{19}F NMR and IR spectroscopic data confirmed the presence of the phthalimido anion. In particular, the ν(C=O) stretching frequency is reduced from 1740 cm^{-1} in **2** to 1640 cm^{-1} in **3**.

The trimethylsilyl derivative **4** was more conveniently prepared by treating **2** with triethylamine and excess trimethylsilyl chloride. An analogous procedure using Me_3SnCl affords the trimethylstannyl derivative **5**.

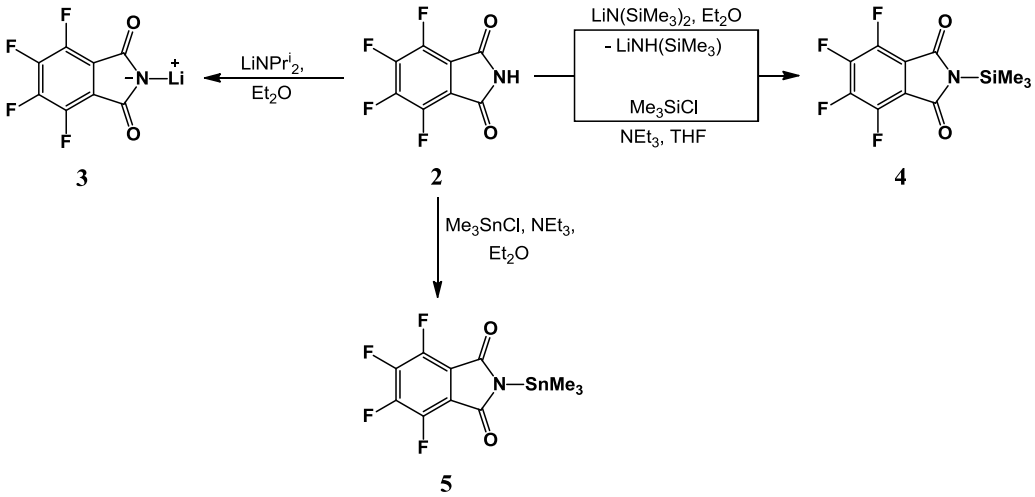

Scheme 18. Preparation of the *N*-substituted perfluorophthalimido compounds.

Crystals of **4** could be grown by cooling a light petroleum solution, while those of **5** were grown from diethyl ether. The molecular structures of **4** and **5** are shown in Figures 29 and 30, respectively. Both unit cells contain two independent but near-identical molecules but with very different packing arrangements: whereas the silyl compound shows approximately parallel but alternating stacking of the tetrafluorophthalimido groups, the tin analogue stacks in an end-to-face fashion.

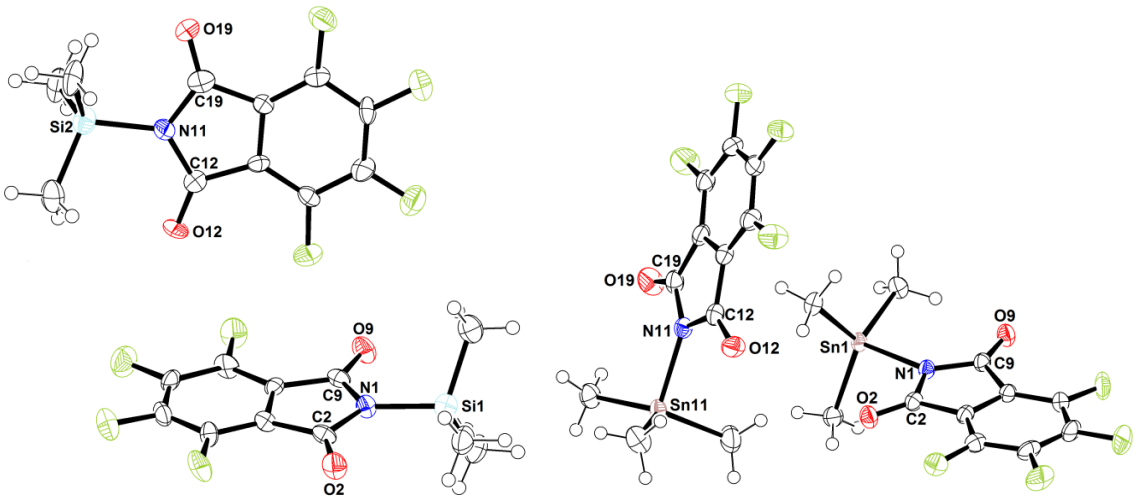

Figure 29. Molecular structures of two independent molecules of **4** (left) and **5** (right), showing a partial atomic labelling scheme (hydrogen atoms have been omitted for clarity). Ellipsoids are drawn at the 50% probability level. Selected bond lengths (Å): for **4** C(2)-N(1) 1.405(7), N(1)-C(9) 1.402(7), C(2)-O(2) 1.207(6), C(9)-O(9) 1.212(6), N(1)-Si(1) 1.821(5); for **5** C(2)-N(1) 1.390(3), N(1)-C(9) 1.383(3), C(2)-O(2) 1.208(3), C(9)-O(9) 1.217(3), N(1)-Sn(1) 2.183(2).

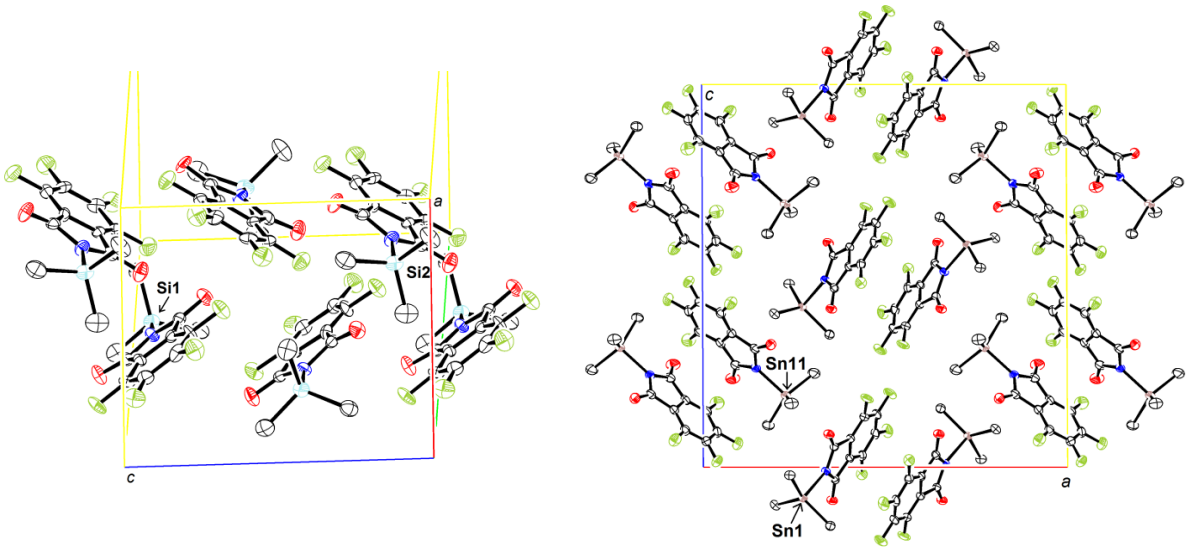

Figure 30. The packing in the crystals of **4** (left) and **5** (right), illustrating differences in packing within the unit cell (hydrogen atoms have been omitted for clarity). Ellipsoids are drawn at the 50% probability level.

The *N*-silyl derivative **4** is a useful phthalimide anion equivalent. Thus the reaction of **4** with AgF in acetonitrile at room temperature gives the argentate salt $Ag[Ag\{N(CO)_2C_6F_4\}_2]$ **6** in almost quantitative yield. While the solvent of crystallisation is readily lost under vacuum, recrystallisation of this complex from

acetonitrile layered with diethyl ether gives the adduct $[(MeCN)_2Ag][Ag\{N(CO)_2C_6F_4\}_2]$ as pale-brown crystals (Scheme 19). The same product can be obtained using the tin reagent **5** (91% yield); however, the relative efficiency for the removal of Me_3SnF by evaporation under reduced pressures compared to Me_3SiF, combined with its significantly higher toxicity makes the stannyl route less attractive.

The crystal structure of **6**·2MeCN (Figure 31) reveals that the compound contains two different silver environments: a linear bis(phthalimido)silver anion which coordinates in a chelate fashion to an $[Ag(MeCN)_2]^+$ cation *via* two of the carbonyl moieties. The discovery of only one ν(CO) band in the solid state IR spectrum, at 1587 cm^{-1}, instead of the expected two, brings uncertainty to whether this arrangement is seen in the solid state without coordinated MeCN. The geometry of the latter is a strongly flattened tetrahedron, with wide O-Ag-O and N-Ag-N angles in the range of 137-142° and consequently more acute N-Ag-O angles. The two planes of the phthalimido ligands are parallel to one another. The distance between the two silver atoms is 3.0172(3) Å, well above the sum of the covalent radius for Ag^- (1.33 Å) and the ionic radius of a tetra coordinate Ag^+ (1.15Å). The structure is reminiscent of the succinimidate $[Ag(H_2O)][Ag(suc)_2]$, which shows similar Ag-N distances of 2.079(5) and 2.067(5) Å but also coordination of the Ag^+ ion to an O-atom of a neighbouring succinimidate.[135]

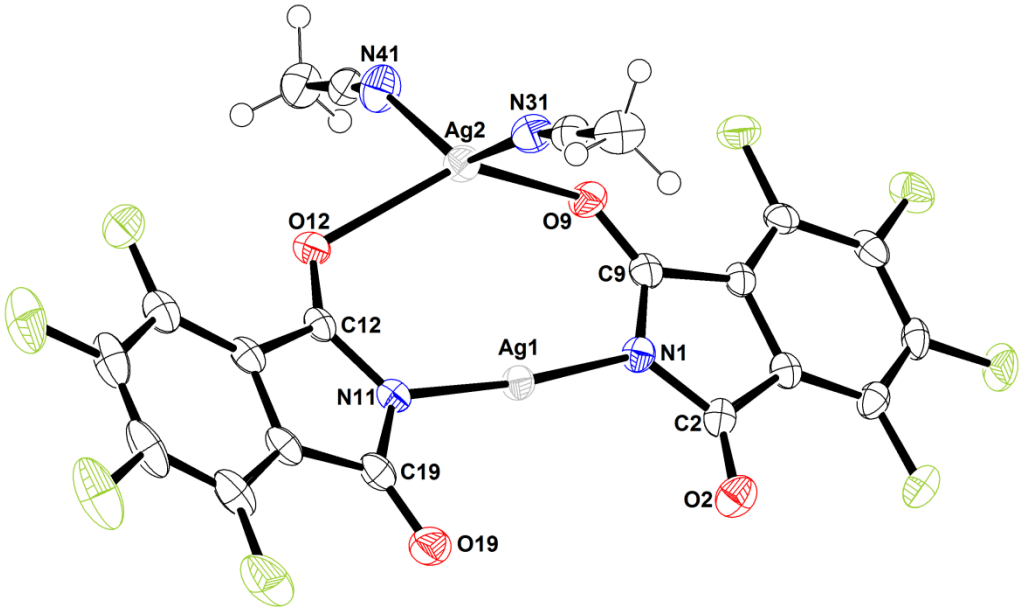

Figure 31. Molecular structure of $[(MeCN)_2Ag][Ag\{N(CO)_2C_6F_4\}_2]$ (**6**·2MeCN), with a partial labelling scheme (hydrogen atoms have been omitted for clarity). Ellipsoids are drawn at the 50% probability level. Selected bond lengths (Å) and angles (°): Ag(1)-N(1) 2.065(2), Ag(1)-N(11) 2.074(2), Ag(2)-O(9) 2.4616(17), Ag(2)-O(12) 2.4885(17), Ag(2)-N(41) 2.238(2), Ag(2)-N(31) 2.219(2), N(1)-C(9) 1.362(3), N(1)-C(2) 1.381(3); N(1)-Ag(1)-N(11) 174.16(8), O(9)-Ag(2)-O(12) 137.18(6), N(31)-Ag(2)-N(41) 142.45(9), O(9)-Ag(2)-N(41) 83.31(8), O(9)-Ag(2)-N(31) 112.53(7), O(12)-Ag(2)-N(41) 95.91(8), O(12)-Ag(2)-N(31) 93.95(7).

2.1.3.2 Synthesis of Gold(I)Tetrafluorophthalimides

The reaction of $(Ph_3P)AuCl$ with either the silver salt **6** or lithium phthalimide **3** in acetonitrile at room temperature gives (triphenylphosphine)gold tetrafluorophthalimide **7a** as colourless crystals in good yields (77 and 74 % respectively). This complex is stable to air and moisture. The carbonyl stretch is observed at 1678cm^{-1}, indicative of the accumulation of partial negative charge on the N-ligand. The tricyclohexylphosphine analogue **7b** was prepared similarly. A number of related succinimidato and heterocyclic gold(I) phosphine complexes are known.[6,125-127] Crystals of both products were grown from toluene.

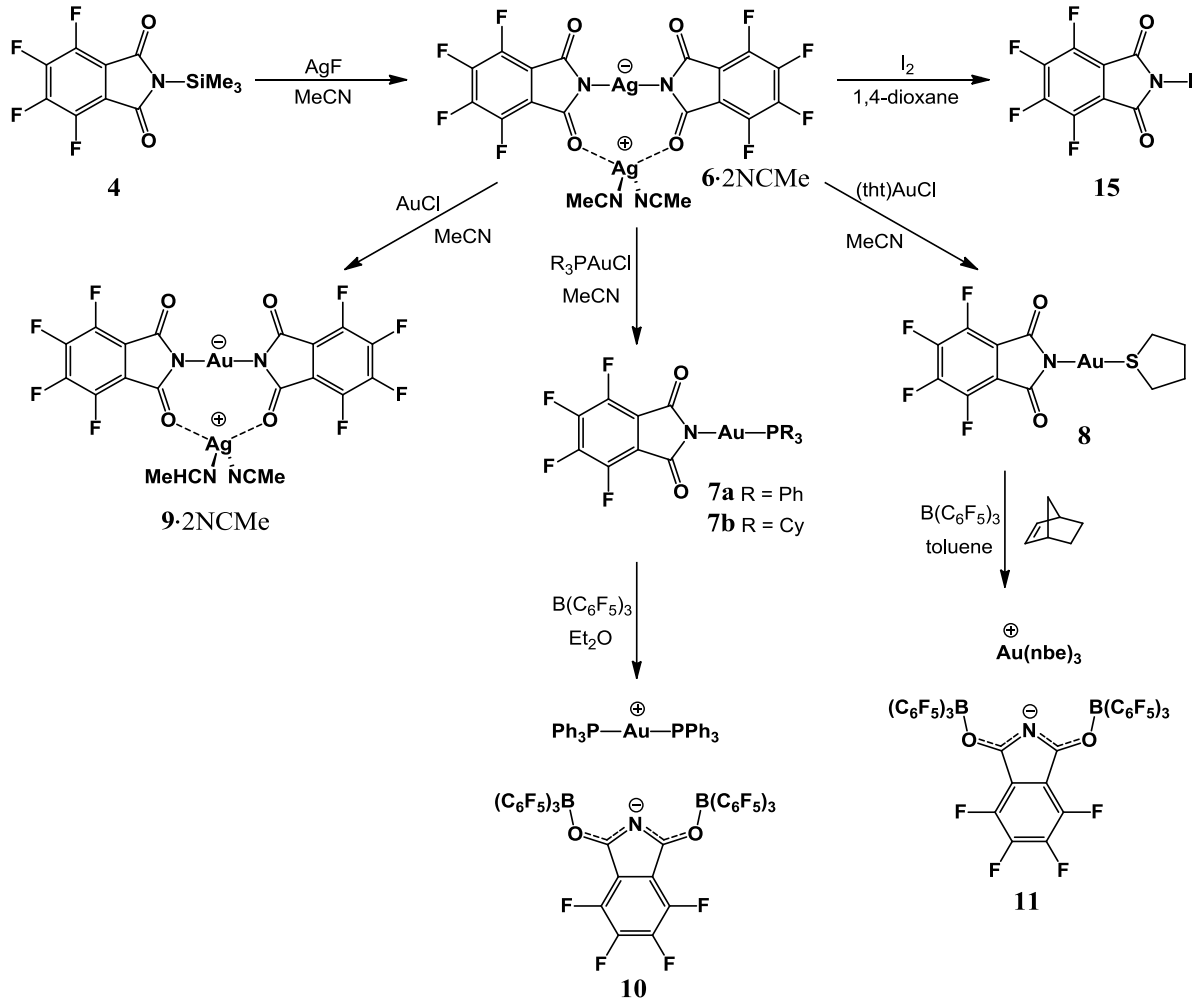

Scheme 19. Preparation and reactions of silver(I) and gold(I) tetrafluorophthalimido complexes.

The molecular structures of **7a** and **7b** are shown in Figure 32. Both have the expected linear gold coordination geometry. The unit cell of **7a** contains two independent molecules. The essentially coplanar phthalimido ligands are arranged at an angle of about 90°, such that a C=O moiety of one ligand is positioned on top of the six-ring of the second. Complex **7b** crystallises with a molecule of toluene. The molecules of **7b** are stacked in columns: pairs of phthalimide ligands are parallel about a centre of symmetry, with close contacts between overlapping edges, *e.g.* C(14)…F(14') 3.185, N(11)···C(14') 3.226, C(12)···C(14') 3.264, C(12)···C(13') 3.270 and C(13)···C(13') 3.272 Å. On the opposite faces, there are the disordered toluene molecules, tilted at 17.3(4)° to the phthalimide planes, with close contacts of F(14)···C(53) 3.183, C(14)···C(52) 3.304 and C(13)···C(52) 3.567 Å (Figure 33).

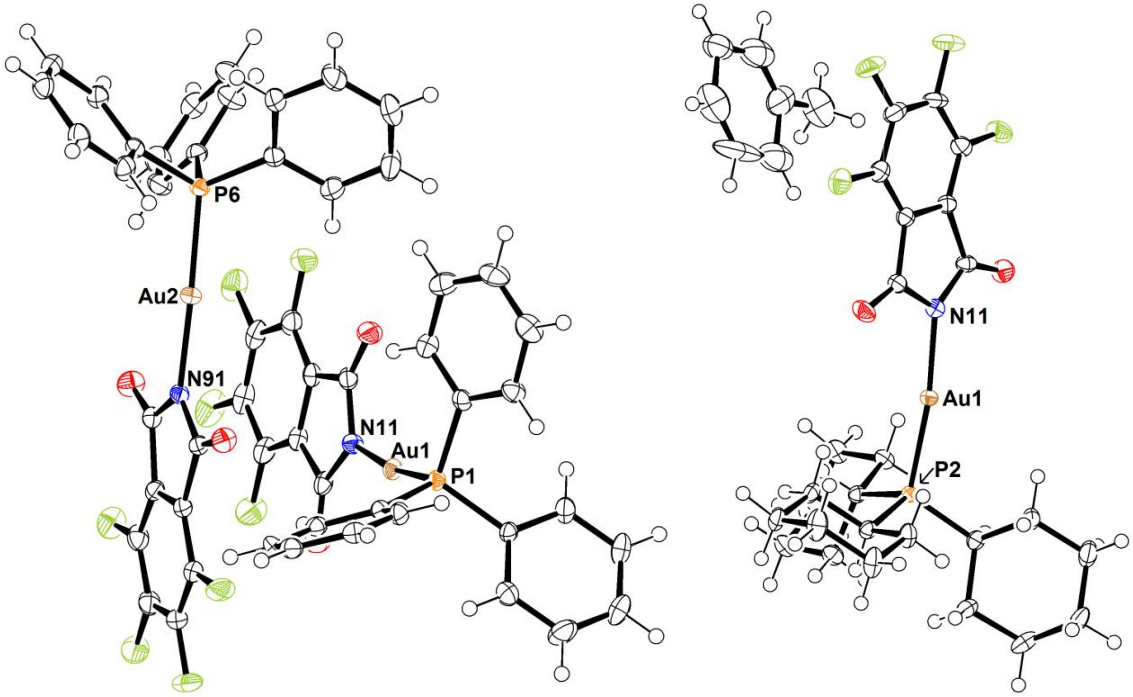

Figure 32. Molecular structures of two independent molecules of **7a** (left) and **7b** (right), showing a partial atomic numbering scheme. Ellipsoids are drawn at the 50% probability level. Selected bond lengths (Å) and angles (°) for **7a**: Au(1)-P(1) 2.2370(11), Au(1)-N(41) 2.058(4), Au(2)-P(6) 2.2336(12), Au(2)-N(91) 2.042(4); N(41)-Au(1)-P(1) 171.19(11), N(91)-Au(2)-P(6) 173.90(11). For **7b**: Au(1)-P(2) 2.2476(9), Au-N(11) 2.052(3); N(11)-Au(1)-P(2) 172.54(9).

The bond lengths show remarkably little variation with the nature of the R_3P ligands, with the tricyclohexylphosphine-derived **7b** showing a slightly longer Au-P and slightly shorter Au-N distance than its triphenylphosphine relative **7a** (Au-P **7a**, 2.2370(11) vs. **7b**, 2.2476(9); Au-N **7a**, 2.058(4) vs. **7b**, 2.052(3)). However, both compare well with related non-fluorinated complexes, notably $(Et_3P)Au\{N(CO)_2C_6H_4\}$ (**XLIVa**, Au-P 2.238(6), Au-N 2.05(2) Å)[123] and with $(Ph_3P)Au\{N(CO)_2C_6H_4\}$ (**XLVb**, Au-N 2.028(4) and 2.040(4) Å).[124] These Au-N bond lengths are longer than typical gold amide bonds, *e.g.* in $(Ph_3P)AuN(SiMe_3)_2$ (2.027 Å)[128]; they are however about 0.05 Å shorter than the Au-N distance in $(Ph_3P)Au(NTf_2)$ (Au-P 2.231, Au-N 2.102 Å),[92] a good indication that anionic charge delocalisation in phthalimides and perfluorophthalimides is much less effective than in the $N(SO_2CF_3)_2$ anion. In line with this observation, the complexes **7a** and **7b** do not form π-bonded systems (with diphenylacetylene, bis(trimethylsilyl)acetylene, cyclooctyne, norbornene, methyl acrylate), nor do they

displace the perfluorophthalimido moiety with strong σ-ligands (CO, trimethylsilyl isocyanide, *t*-butyl isocyanide or excess tricyclohexylphosphine).

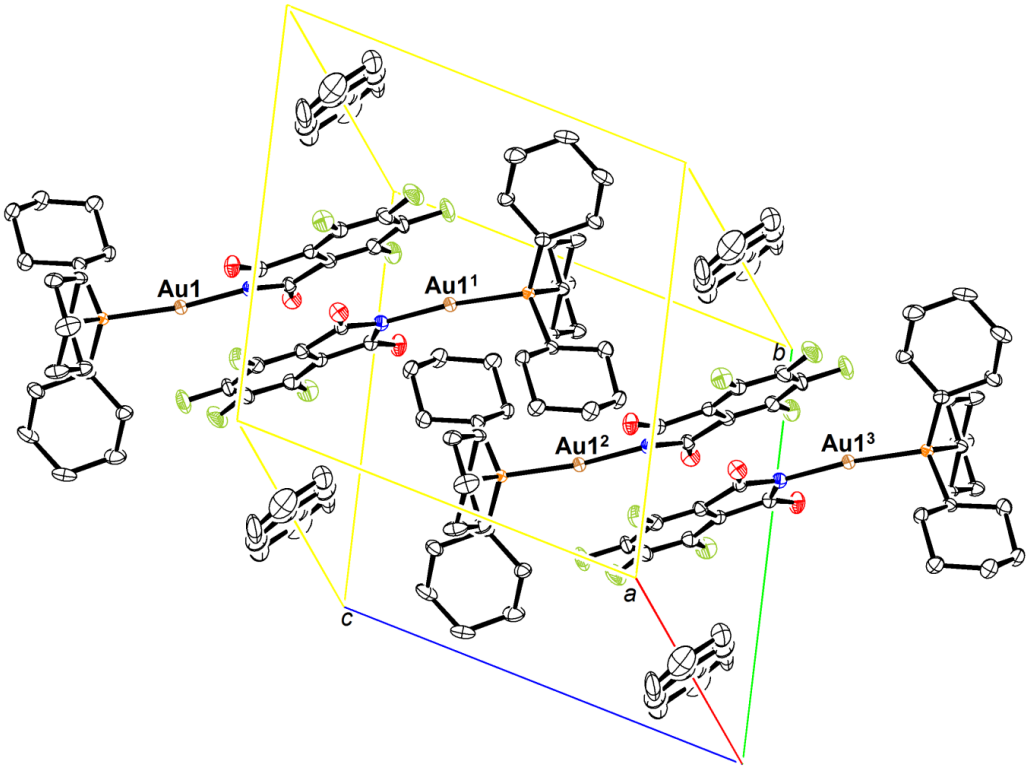

Figure 33. Stacking plot for the complex **7b**·toluene (hydrogen atoms have been omitted for clarity). Ellipsoids are drawn at the 50% probability level.

In an attempt to generate phthalimido complexes with more labile donor ligands, the tetrahydrothiophene complex (tht)Au{N(CO)$_2$C$_6$F$_4$} **8** was prepared by a similar route. The compound is stable to air and moisture but light sensitive, giving the colourless crystals a purple hue after exposure for a day. The molecular structure is shown in Figure 34.

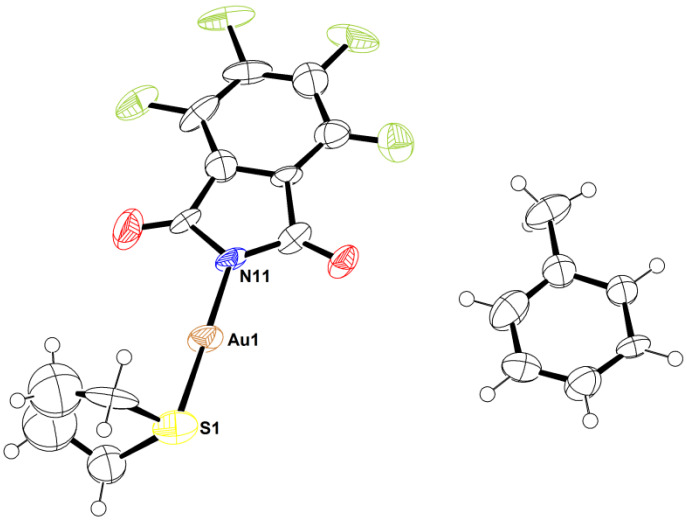

Figure 34. The molecular structure of **8**·toluene, with a partial labelling scheme. Ellipsoids are drawn at the 50% probability level. Selected bond lengths (Å) and angles (°): Au(1)-S(1) 2.264(4), Au(1)-N(11) 2.025(12), Au (1)-Au (1′) 3.3218(3); N(11)-Au(1)-S(1) 179.5(3); Au(1′)-Au(1)-Au(1″) 172.58(4).

The compound crystallises with one molecule of toluene. While the N-Au-S moiety has the expected linear geometry, the packing arrangement in the crystal is rather different from that in **7a** and **7b** and shows minimal overlap between the phthalimide ligands of two neighbouring molecules. Instead, the Au atoms are arranged to form an aurophilic interaction-mediated 1D polymer (Figure 35). These aurophilic interactions (Au(1)···Au(1`) 3.3218(3) Å) are within the sum of van der Waals radii. The toluene molecule sits stacked within the vicinity of two parallel tetrafluorophthalimido moieties in an offset face-to-face manner. The Au-N distance in **8**·toluene is notably shorter than in the phosphine analogues; evidently the weaker donor strength of the sulfur ligand is replaced by tighter anion binding and aurophilic interactions.

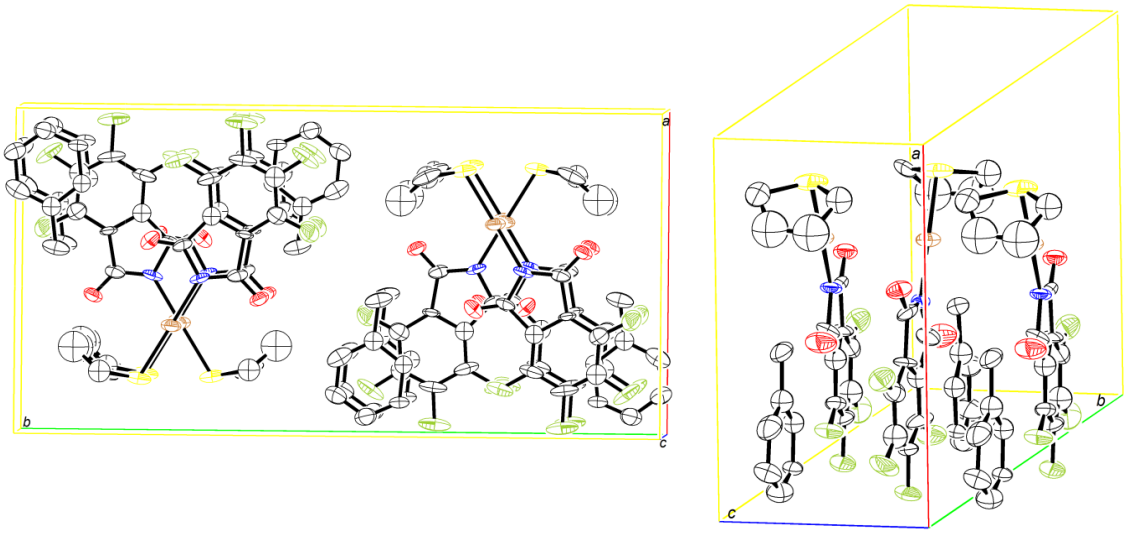

Figure 35. Two views of the packing arrangement of **8**·toluene (hydrogen atoms have been omitted for clarity). Ellipsoids are drawn at the 50% probability level.

Attempts to generate perfluorophthalimido complexes of the (L)AuX type with even weaker ligands L, such as acetonitrile, were only partially successful. Although the reaction of **6** with AuCl in a 1:1 stoichiometric ratio in acetonitrile gave a pale yellow solution which contained a single phthalimido complex (by ^{19}F NMR spectroscopy), the attempted isolation and crystallisation led to decomposition and formation of a gold film. On the other hand, the reaction of AuCl with two equivalents of Ag[Ag{N(CO)$_2$C$_6$F$_4$}$_2$] (**6**) in acetonitrile yielded the mixed-metal complex Ag[Au{N(CO)$_2$C$_6$F$_4$}$_2$] **9** as a brown powder. Crystals of this compound were grown by the slow cooling of a hot acetonitrile solution. This affords the adduct [(MeCN)$_2$Ag][Au{N(CO)$_2$C$_6$F$_4$}$_2$]·MeCN (**9**·3MeCN). The structure (Figure 36) resembles that of **6**·2MeCN, except that the phthalimido ligands have been transferred to gold.

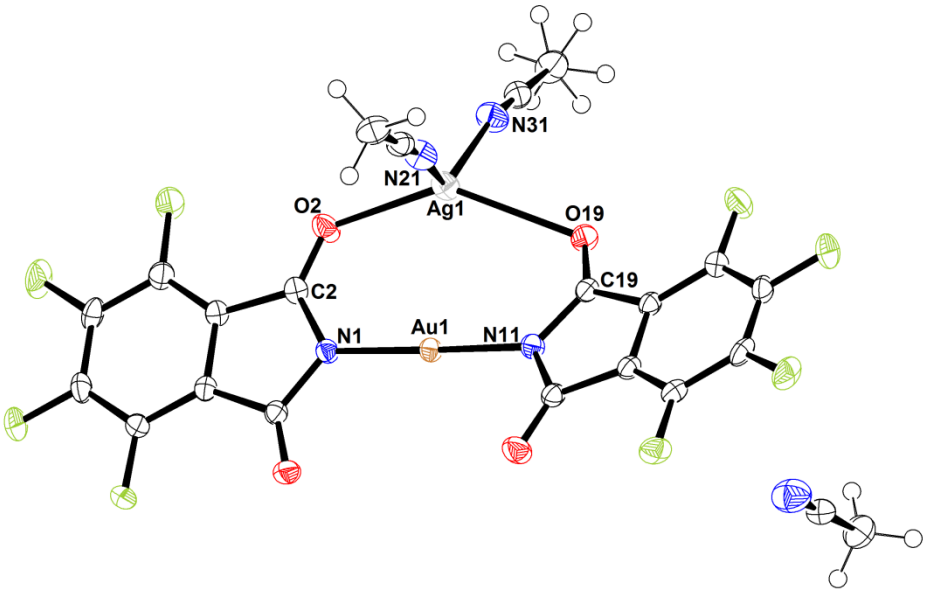

Figure 36. Molecular structure of $[(MeCN)_2Ag][Au\{N(CO)_2C_6F_4)\}_2]\cdot MeCN$ (**9**·3MeCN), showing a partial atomic numbering scheme. Ellipsoids are drawn at the 50% probability level. Selected bond lengths (Å) and angles (°):Au-N(1) 1.9972(17), Au-N(11) 2.0030(17), Ag-O(2) 2.4358(16), Ag-O(19) 2.6598(15), Ag-N(21) 2.207(2), Ag-N(31) 2.194(2). N(1)-Au-N(11) 177.73(7), N(21)-Ag-N(31) 130.95(8), O(2)-Ag-O(19) 140.68(5).

The bis(phthalimido)aurate anion is linear. The Au-N distances in **9** are *ca.* 0.03-0.05 Å shorter than in the neutral complexes **7a**, **7b** and **8**. We are aware of only one crystallographically characterised precedent for a structure of this type, in **XLIII**, for which a slightly shorter Au-N bond length of 1.94 Å has been reported.[121]

Unlike in **6**, the phthalimido ligands in **9** are twisted with respect to one another, with a dihedral angle of 14.8°. The aurate anion binds to a silver cation *via* two of the carbonyl oxygen atoms, but with two distinctly different Ag···O distances, unlike the near-symmetrical chelate found in **6**·2MeCN. The Ag···O coordination is reflected in the infrared spectrum which shows two C=O stretching bands at 1653 and 1620 cm^{-1} for the non-coordinated and the silver-bound C=O moieties, respectively. The non-bonding distance of the two metal centres is 2.9544(2) Å.

Attempts for incorporation of a CO ligand into a tetrafluorophthalimidogold species led to decomposition; to either the gold complex **8** or the reaction of **6** to AuCl in acetonitrile, gaseous CO was bubbled through the solution and observed

the precipitation of a purple solid within a minute. The data collected is inconclusive to whether CO uptake has occurred to form an unstable ($phth^F$)Au(CO) complex, which then degrades readily after synthesis.

2.1.3.3 Reactivity and π-coordination of Olefins to Gold(I) Tetrafluorophthalimides

While there was no evidence of lability of gold-bound phthalimide or its displacement by excess phosphine, the ligand is easily removed from the coordination sphere on addition of $B(C_6F_5)_3$. Thus, reacting **7a** with $B(C_6F_5)_3 \cdot Et_2O$ and PPh_3 in diethyl ether at room temperature for 15 min generates $[Au(PPh_3)_2][N\{COB(C_6F_5)_3\}_2C_6F_4]$ **10**, which contains a perfluorophthalimido-bridged diborate anion. The borane molecules are bonded to the O atoms; there is no evidence for formation of an *N*-bonded borate. The B-O bonding is reflected in the ν(CO) frequencies which change from 1678 cm^{-1} for **7a** to 1545 cm^{-1} in **10**. Crystals of **10** were grown from a minimum amount of toluene layered with light petroleum at -30 °C and obtained as pale yellow platelets. The structure of **10** (Figure 37) shows a linear $[Au(PPh_3)_2]^+$ cation supported by the bulky phthalimidodiborate anion; there are no close cation-anion interactions.

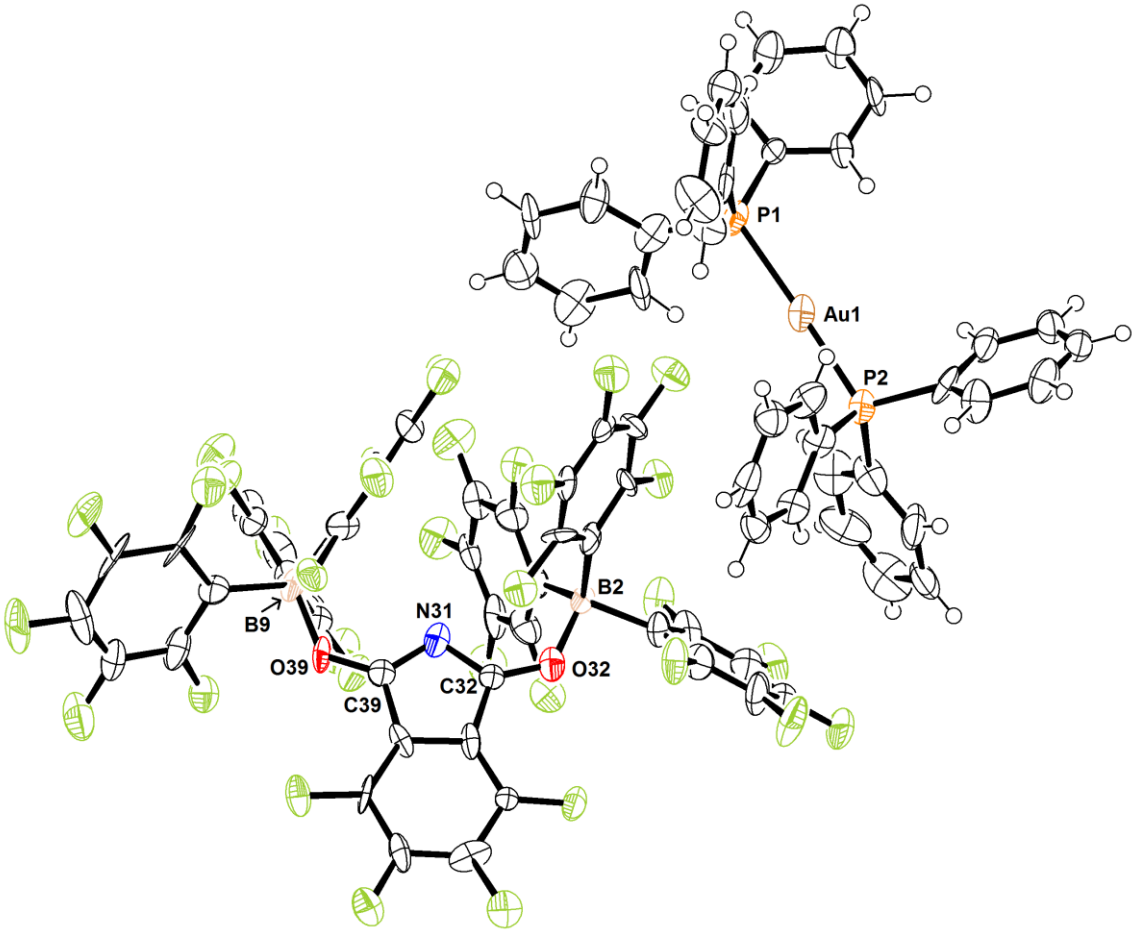

Figure 37. Crystal structure of $[Au(PPh_3)_2][\{N(COB(C_6F_5)_3\}_2C_6F_4]$ **10**, showing a partial atomic numbering scheme. Ellipsoids are drawn at the 50% probability level. Selected bond lengths (Å) and angles (°): Au(1)-P(1) 2.297(5), Au(1)-P(2) 2.301(5), B(2)-O(32) 1.57(2), B(9)-O(39) 1.55(3), N(31)-C(32) 1.31(2), N(31)-C(39) 1.31(2), C(32)-O(32) 1.23(2), C(32)-C(33) 1.48(2), C(33)-C(38) 1.37(2); P(1)-Au(1)-P(2) 169.53(19), B(2)-O(32)-C(32) 128.0(14), O(32)-C(32)-N(31) 131.8(17), N(31)-C(39)-O(39) 131.0(17), C(39)-O(39)-B(9) 127.1(14), C(32)-N(31)-C(39) 113.3(15).

Since the starting material for the synthesis of **10** has a P:Au ratio of 1:1, attempts were made to use this reaction for the preparation of mixed-ligand gold complexes of the type $[(R_3P)AuL']^+$ in the presence of L′ = norbornene or 1,5-cyclooctadiene (PR_3 = PPh_3 or PCy_3). There was no evidence for the formation of such compounds. However, the reaction of the more labile tetrahydrothiophene complex **8** with $B(C_6F_5)_3$ in toluene in the presence of excess norbornene at 0 °C resulted in the displacement of the sulfur ligand and formation of $[Au(nbe)_3][N\{COB(C_6F_5)_3\}_2C_6F_4]$ **11**. Crystals were grown from dichloromethane at -30 °C, which were found to be poorly stable when exposed to air. The $[Au(nbe)_3]^+$ cation has recently been reported as the SbF_6^- salt.[52,73]

2.1.3.4 Synthesis of Gold(III)Tetrafluorophthalimidate Complexes

The synthesis of gold(III) complexes containing a tetrafluorophthalimido ligand was the next target. The metal centre of $[(C_6F_5)_2AuCl]_2$, stabilised by Au-C bonds with the C_6F_5 groups, is a valuable synthon for many organogold(III) complexes and is synthesised in three steps: the bis(pentafluorophenyl)gold(I) anion $[^nBu_4N][Au(C_6F_5)_2]$ was previously synthesised by the reaction of excess $Li(C_6F_5)$ with (dimethylsulfide)gold chloride in the presence of tetra-*n*-butylammonium chloride.[141] Since the use of $Li(C_6F_5)$ is potentially dangerous,[142] we modified the synthesis of $[^nBu_4N][(C_6F_5)_2Au]$ by replacing the lithium salt with C_6F_5MgBr which gave comparable yields. Oxidation of $[^nBu_4N][Au(C_6F_5)_2]$ by treatment with condensed chlorine at -60 °C in dichloromethane yielded $[^nBu_4N][(C_6F_5)_2AuCl_2]$ in quantitative yields.[83] To obtain the gold(III) precursor, $[^nBu_4N][(C_6F_5)_2AuCl_2]$ was reacted with 1 equiv. of $AgSbF_6$ in dichloromethane to give, when isolated, $[(C_6F_5)_2AuCl]_2$ in quantitative yields.

The transmetallation reaction of $[(C_6F_5)_2AuCl_2]_2$ with 1.1 equiv. of the silver-tetrafluorophthalimido salt **6** and excess dimethylsulfide in acetonitrile produces $[(C_6F_5)_2Au(SMe_2)(N\{CO\}_2C_6F_4)]$ (**12**) in high yields (81 %, Scheme 20), with a small impurity, of $[^nBu_4N][(C_6F_5)_2Au(N\{CO\}_2C_6F_4)_2]$ (**14**, discussed later). Recrystallisation in a concentrated toluene solution at 2 °C gave pure crystals of **12**. The triphenylphosphine derivative $[(C_6F_5)_2Au(PPh_3)(N\{CO\}_2C_6F_4)]$ (**13**) was synthesised and purified in the same manner, but can also be synthesised by treatment of **12** with excess triphenylphosphine.

The complexes appear to be inert to moisture and oxygen exposure, but **12** can decompose if left at ambient temperatures overnight (presumably due to the lability of the thioether ligand). ^{19}F NMR spectroscopy at room temperature shows complexes **12** and **13** exist in different configurations: The thioether-containing complex **12** is not a single species, but a mixture of two configurations; a *cis*:*trans* ratio of 65:35 in chloroform-*d* was observed, whereas inclusion of triphenylphosphine into **13** favours the *trans*-configuration; none of the *cis*-isomer was observed. The preference of configuration appears to be dependent on the relative *trans*-stabilisation of the neutral ligand towards the $[C_6F_4(CO)_2N]^-$ anion *versus* the $(C_6F_5)^-$ moiety; the PPh_3 ligand in **13** is suited to this role, whereas the

poor donor capabilities of the dimethylsulfide ligand to gold results in a mixture of configurations seen in the ^{19}F NMR spectrum of **12**. X-ray diffractometry data, however, portrays the gold complexes **12** and **13** in their *cis*-forms only (shown in Figure 38), suggesting that a form of fluxionality is apparent in both complexes.

Crystallographic analysis confirms the gold atoms in **12** and **13** are four-coordinate and square planar, with the two perfluorophenyl groups in the *cis*-position (C(11)-Au-C(21) 86.8(2) and 87.09(9)° for **12** and **13**, respectively). The tetrafluorophthalimido-gold bonds (**12**, Au-N 2.057(4); **13**, 2.0538(19) Å) are similar to the bond lengths exhibited by the gold(I) complexes **7a** and **7b** (2.058(4) and 2.052(3) Å, respectfully) and compares well with the bond lengths observed for the gold(III) monoimidate complex **LIII** (2.051(2) Å), indicating a relatively strong bond.[135] The planes of the C_6F_5 groups and tetrafluorophthalimido ligands are angled away from the gold bonding plane as shown by the torsion angles.

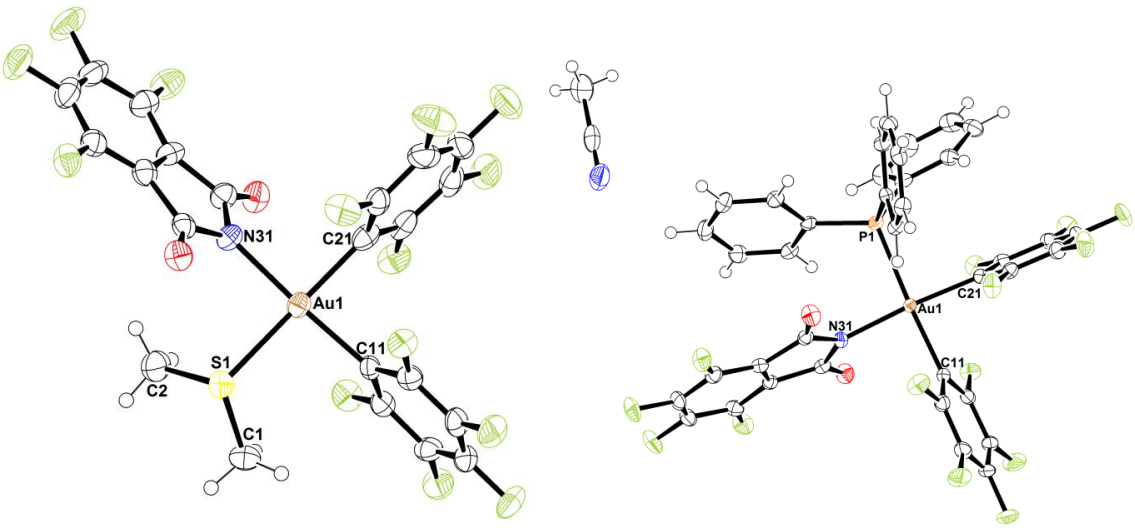

Figure 38. Molecular structures of **12** (left) and **13**·NCMe (right), with both showing a partial atomic numbering scheme. Ellipsoids are drawn at the 50% probability level. Selected bond lengths (Å), angles and torsion angles (°) for **12**: Au(1)-S(1) 2.3890(17), Au(1)-N(31) 2.057(4), Au(1)-C(11) 2.026(5), Au(1)-C(21) 2.016(5); N(31)-Au(1)-S(1) 90.12(5), N(31)-Au(1)-C(11) 175.84(19), N(31)-Au(1)-C(21) 90.3(2), C(11)-Au(1)-C(21) 86.8(2); S-Au···C(11)-C(12) 78.07, C(11)-Au···C(21)-C(22) 67.8, C(21)-Au-···N(31)-C(32) 62.0. For **13**: Au(1)-P(1) 2.3769(6), Au(1)-N(31) 2.0538(19), Au(1)-C(11) 2.060(2), Au(1)-C(21) 2.021(2); N(31)-Au(1)-P(1) 94.01(6), N(31)-Au(1)-C(11) 89.04(8), N(31)-Au(1)-C(21) 175.99(9), C(11)-Au(1)-C(21) 87.09(9); P(1)-Au···C(21)-C(22) 72.27, C(21)-Au···C(11)-C(12) 71.4, C(11)-Au···N(31)-C(32) 71.8.

Following the discovery of the bisphthalimido derivative as an impurity of the synthesis of **12**, we targeted the quantitative synthesis **14**. The reaction of $[^{n}Bu_4N][(C_6F_5)_2AuCl_2]$ with 2 equivalents of **6** yields $[^{n}Bu_4N][(C_6F_5)_2Au(N\{CO\}_2C_6F_4)_2]$ **14**. Unfortunately crystals grown from a concentrated toluene solution at 2 °C gave polycrystalline solids, therefore not suitable for structural analysis. We have tentatively assigned the geometry of the four-coordinate square planar gold(III) anion from ^{19}F NMR data; comparison of the *ortho*-C_6F_4 signal of **14** (δ -139.5 ppm) to *cis*-**12** (-137.2 ppm), *trans*-**12** (δ -138.8 ppm) and *trans*-**13** in $CDCl_3$ (and -139.8 ppm) indicates the *trans*-conformation is present in solution, although no definitive assignments can be made at this moment. IR spectroscopy gives a single signal for C=O stretches at 1695 cm^{-1} is in close agreement with the values obtained of the (tetrafluorophthalimidato)gold(I) complexes **7a**, **7b** and **8**, indicating no dative bonding of the carbonyl moiety is observed.

In an attempt to repeat the formation of gold(III)phthalimido complexes using a different gold(III) precursor, we attempted the reaction of **6** with $[(2,4,6\text{-}C_6H_2Me_3)_2AuCl]_2$ in the presence of tetrahydrothiophene or triphenylphosphine produces the gold(I) complexes $[C_6F_4(CO)_2NAu(SMe_2)]$ (**8**), $[C_6F_4(CO)_2NAu(PPh_3)]$ (**7a**) and $[\{C_6F_4(CO)_2N\}_2Au][Ag]$ (**9**) in moderate to good yields. On inspection of the toluene filtrate, the reduction of Au(III) is confirmed when the presence of dimesityl was detected by ^{1}H NMR spectroscopy.

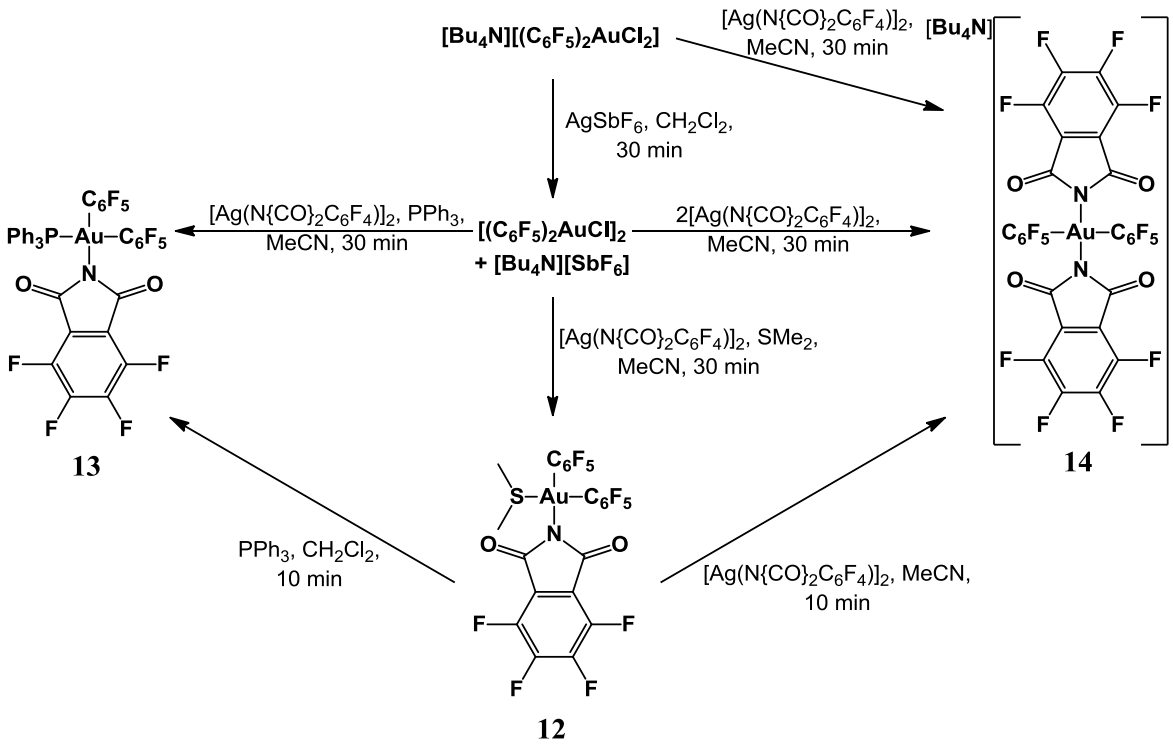

Scheme 20. The synthesis of Au(III) tetrafluorophthalimidates.

2.1.3.5 Other Tetrafluorophthalimido Compounds

The reactions of the Si and Sn compounds **4** and **5** with condensed Cl_2 and Br_2 under mild conditions gave only the parent phthalimide **2** as the only isolable product (small amounts of haloacid may be present in the condensed gases, protonating the phthalimide anion), while there was no reaction with iodine. However the reaction of the silver salt **6** with iodine in dry dioxane under the exclusion of light produced the *N*-iodo compound $C_6F_4(CO)_2NI$ **15** as a yellow powder in a high yield (82 %). The ν(CO) frequency was observed at 1702 cm^{-1}, slightly lower than that in **2** (1740 cm^{-1}). Crystals of **15**·MeCN were grown by recrystallisation from an acetonitrile solution at -28 °C. The crystal structure is shown in Figure 39. The whole of the phthalimide molecule lies on a mirror-plane of symmetry, with only the nitrogen atom of the MeCN solvent refined slightly away from the same plane. The molecular planes are separated by 3.152 Å (half the *b* cell length), but the phthalimide molecules overlap only peripherally with closest contact C(7)…C(7') at 3.173(2) Å. The phthalimide and the MeCN molecules are aligned with N(1)-I(1)···N(11)-C(12) almost linear, with a short I(1)···N(11) interaction.

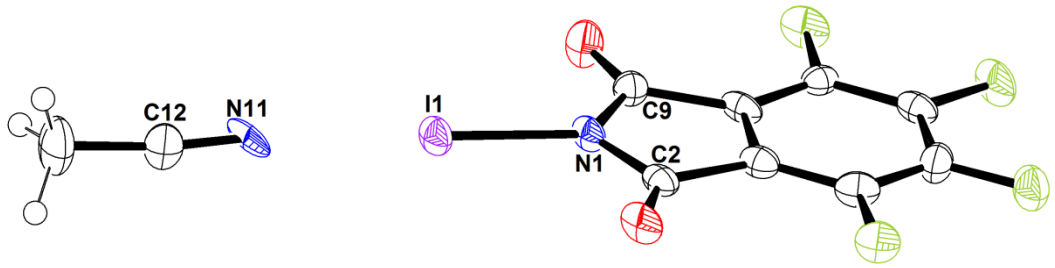

Figure 39. Molecular structure of $\{C_6F_4(CO)_2N\}I\cdot MeCN$ (**15**·MeCN), showing a partial atom numbering scheme. Ellipsoids are drawn at the 50% probability level. Selected bond lengths (Å) and angles (°): N(1)-C(2) 1.405(17), N(1)-C(9) 1.391(14), C(2)-O(2) 1.184(14), C(9)-O(9) 1.214(15), I(1)-N(1) 2.074(9), N(11)-C(12) 1.15(3), I(1)···N(11) 2.601(19); C(2)-N(1)-I(1) 121.2(7), C(9)-N(1)-I(1) 125.5(8), C(9)-N(1)-C(2) 113.4(9), O(2)-C(2)-N(1) 124.7(11), N(1)-I(1)···N(11) 174.6(3), C(12)-N(11)-I(1) 168.5(10).

In view of the electron withdrawing character of the $[C_6F_4(CO)_2N]^-$ moiety, compound **15** could be expected to readily undergo oxidative addition reactions, *e.g.* with gold(I) phosphine complexes. Unfortunately no evidence was found experimentally with only the starting materials being recovered.

2.1.3.6 Comparison of Spectroscopic Characteristics of the Complexes Containing a Tetrafluorophthalimidate Ligand

The tetrafluorophthalimido ligand allows the fluorine atoms and C=O functions to be used as probes for the electronic characteristics. A comparison of these data is given in Table 5. The C=O stretching frequencies show the expected reduction with increasing anionic character of the ligand but are little influenced by the donor strength of ligands coordinated to gold, *e.g.* the values for the PPh_3, PCy_3 and tht complexes are almost identical. The ionic O-chelate **9** shows two C=O bands, the higher of which is reduced by 87 cm^{-1} compared to that for the parent phthalimide **2**, while the second shows a further reduction by 33 cm^{-1} due as a result of coordination to Ag^+. There is however a more substantial reduction in C=O bond order on borane coordination; *e.g.* the corresponding absorption for compound **10** is almost over 190 cm^{-1} lower than that for ν(CO) in **2**.

Table 5. Comparison of IR and ^{19}F NMR data.

Compound	IR $\nu_{C=O}$ /cm^{-1}	Solvent	^{19}F NMR		
			Signal 1	Signal 2	Δδ
2	1740	$CDCl_3$	-134.7	-141.2	6.5
		CD_3CN	-139.9	-146.0	6.5
3	1640	THF-d_8	-143.7	-152.5	8.8
4	1706	$CDCl_3$	-137.0	-142.7	5.7
5	1706	$CDCl_3$	-137.9	-144.2	6.3
6	1587	CD_3CN	-143.6	-150.7	7.1
7a	1678	$CDCl_3$	-139.2	-145.9	6.7
7b	1679	$CDCl_3$	-139.7	-146.4	6.7
8	1678	$CDCl_3$	-138.8	-145.9	7.1
9	1653, 1620	CD_3CN	-143.0	-149.7	6.7
(phth^F)AuNCMe^a	1676	CD_3CN	-141.3	-145.9	4.6
10	1545	$CDCl_3$	-133.5	-141.0	7.5
11	n.d.	$CDCl_3$	-132.1	-141.3	9.2
12	1690	$CDCl_3$	-137.2	-143.9	6.7
13	1694	$CDCl_3$	-139.8	-146.9	7.1
14	1695	$CDCl_3$	-139.5	-146.1	6.6
15	1702	CD_3CN	-139.4	-146.5	7.1

a - not isolated.

By comparison, given the wide ^{19}F NMR spectroscopic chemical shift range, the variations of the ^{19}F signals for this set of complexes are quite small; in fact the chemical shift are more strongly influenced by the solvent than by any negative charge or donor ligands in the complex. In spite of the presence of F substituents, there is evidently very limited charge delocalisation over the C_6F_4 part of the phthalimido ligand.

It is difficult to differentiate between the families of phthalimido-gold(I) and gold(III) complexes by spectroscopic means, as little variation is observed in both the ^{19}F NMR (< 2 ppm) and IR (< 20 cm^{-1}) data.

2.1.4 Conclusions

Tetrafluorophthalimido ligands readily form complexes containing Li, Si, Sn, I, Ag and Au. The Si and Sn derivatives are useful phthalimide anion precursors for transmetallation. While gold complexes of the type [(L)Au(phthalimide)] have ample structural precedents, in the absence of donor ligands the less common linear anionic $[M(phthalimide)_2]^-$ are formed (M = Ag or Au) which generate

heterobimetallic structures with Ag^+ ions. The Au-N bonds in phosphine gold complexes [(L)Au{N(CO)$_2$C$_6$F$_4$}] are only very slightly longer than those in non-fluorinated analogues, which points to a surprisingly small influence of the C_6F_4 ring on the bonding character of this ligand. In line with this, there was no displacement of the [N(CO)$_2$C$_6$F$_4$]$^-$ ion by excess phosphines. On the other hand, the addition of the strongly Lewis acidic borane B(C$_6$F$_5$)$_3$ led to instantaneous phthalimide abstraction and the formation of a new non-coordinating tetrafluorophthalimidato-diborane anion. This synthetic methodology, combined with the use of the thioether-containing complex [C$_6$F$_4$(CO)$_2$NAu(tht)] allows for the generation of complex **11**; a [Au(nbe)$_3$]$^+$ cation accompanied by the bulky anion.

In addition, the first examples of gold(III) complexes containing tetrafluorophthalimidate ligands have also been described with neutral [(C$_6$F$_5$)$_2$Au(L)(N{CO}$_2$C$_6$F$_4$)] (L = PPh$_3$ (**12**) or Me$_2$S (**13**)) and anionic [^{n}Bu$_4$N][(C$_6$F$_5$)$_2$Au(N{CO}$_2$C$_6$F$_4$)$_2$] (**14**) examples presented within. Single crystal X-ray experiments of **12** and **13** depicts these complexes in *cis*-configurations, whereas ^{19}F NMR suggested some form of lability was observed, as mixtures the complexes in both *cis*- and *trans*-configurations were present in solution.

2.2 Topic 2: Attempted Oxidation of Gold *β*-Diketiminates

2.2.1 Introduction

2.2.1.1 Properties of (β-Diketiminato)Metal Complexes

Monoanionic *β*-diketiminates (also known as [nacnac]$^-$ ligands) can be used as ancillary ligands to stabilise a wide variety of metal complexes in various oxidation states across the periodic table (Scheme 21).[6,143] With its range of ligand variation in both the backbone and the substituents at the imidyl-nitrogen atom, the electronic and steric parameters of the $[R_1C\{C(R_2)NAr\}_2]$- anion can be adjusted with great flexibility.[144] With these controls, *β*-diketimidatometal complexes of generally high valent metals are active catalysts in many catalytic processes.[145]

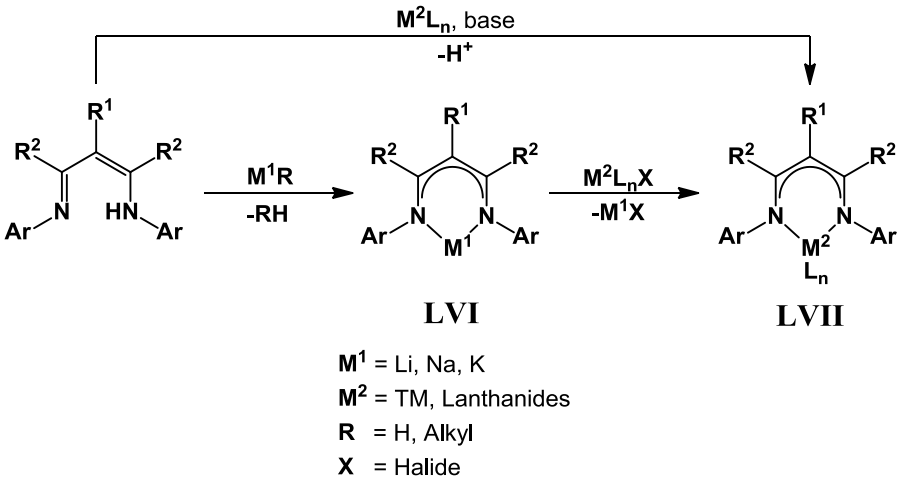

Scheme 21. A generalised scheme for the generation of metallated *β*-diketiminates **LVI** and **LVII**.[145]

In terms of structural chemistry, examples of low-coordinate M^+[nacnac]$^-$ complexes have pervaded the periodic table; investigations into the uses of these complexes include metal-metal bonding, small molecule activation and as catalysts for organic functionalisation. The formation of the well-known *N*,*N*-bonded chelate is observed in most cases, as seen in structures **LVI** and **LVII**.[145]

Among the coinage metals, copper has a rich history of complexes supported by *β*-diketimidate ligands. Numerous examples of

$L_nCu(I)[\kappa^2\text{-}(Ar)N\text{-}C(R^2)C(R^1)C(R^2)N(Ar)]$ have been synthesised for roles including: as model substrates to biological processes (such as dioxygen and O-, S- and *N*-organonitroso activation) and in small molecule activation.[145a] By contrast examples of silver- and gold(*β*)-diketiminates are sparse, with both metal atoms showing a pronounced tendency to exhibit linear coordination.[146,147]

2.2.1.1.1 The Scarcity of (β-Diketiminato)Silver(I), Gold(I) and Gold(III) Complexes

Prior to our research, the only examples of structurally characterised [Au(I)-nacnac] adducts were described by Dias *et al.*. He investigated the use of a non-substituted $[CH\{C(H)N(Ar)\}_2]^-$ diketiminate backbone; differing bulky, *N*-Aryl groups (Ar = 2,4,6-$C_6H_2Br_3$; 2,6-$C_6H_3{}^iPr_2$) were used to probe the electronic effects upon bonding. Treatment of $Tl[CH\{C(H)N(Ar)\}_2]$ with (tht)AuCl yielded the complexes $[Au\{\mu\text{-}(Ar)N\text{-}(CH)_3\text{-}N(Ar)\}]_2$ (Ar = 2,4,6-$C_6H_2Br_3$ **LVIIIa**; 2,6-$C_6H_3{}^iPr_2$ **LVIIIb**) in ~50 % yield (Scheme 22). Both **LVIIIa-b** are stable when exposed to air, light and heat. The crystal structures of these complexes revealed that the gold(I) *β*-diketiminate units dimerise to form a planar, 12-membered macrocyclic ring with a $[Au_2N_4C_6]$ core. The *β*-diketiminato ligands adopt a W-shaped conformation, with two gold centres coordinated in a linear N-Au-N manner. The gold-imide bonds in each molecule are in close agreement with each other, with Au-N bond lengths of **LVIIIa** (2.025(3), 2.027(3) Å) being marginally shorter than that in **LVIIIb** (2.029(5), 2.036(5) Å). This slight difference is due to the inductive effects of the substituted imido-phenyl rings.[146] The silver(I) analogue $[Ag]_2[\mu\text{-}(2,6\text{-}{}^iPr_2C_6H_3)N\text{-}(CH)_3\text{-}N(2,6\text{-}{}^iPr_2C_6H_3)]$ **LIX**, was also synthesised and is isostructural.[147]

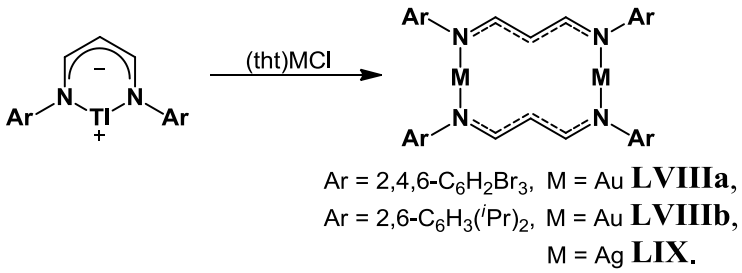

Scheme 22. Synthesis of the silver- and gold-dimer complexes **LVIIIa-b** and **LIX**, containing linear N-Au-N geometries.[146,147]

Two silver(I) *β*-diketiminate complexes have been structurally determined to form monomeric, 6-membered rings (Scheme 23). The first involved the CF_3-substituted ligand $H[CH\{C(CF_3)N(3,5\text{-}(CF_3)_2C_6H_3)\}_2]^-$ (**16a-H**). Treatment of **16a-H** with Ag_2O in the presence of triphenylphosphine or ethylene resulted in the isolation of **LXa** and **LXb**. When attempting to repeat the synthesis with the non-fluorinated *β*-diketiminate $H[HC\{C(Me)N(4\text{-}^tBuC_6H_4)\}_2]$, the precipitation of silver metal was observed. The only other example of such complexes was achieved in the screening of the potassium salt $K[HC\{C(Me)N(4\text{-}^tBuC_6H_4)\}_2]$ with numerous silver complexes ($(Ph_3P)AgNO_3$, $(Ph_3P)AgCl$, $(Me_2S)AgNO_3$, $(cod)AgNO_3$, $(Py)AgNO_3$ and (IMes)AgCl), with only the use of (IMes)AgCl forming a stable chelate of a non-fluorinated silver(I) *β*-diketiminate(**LXI**).[148]

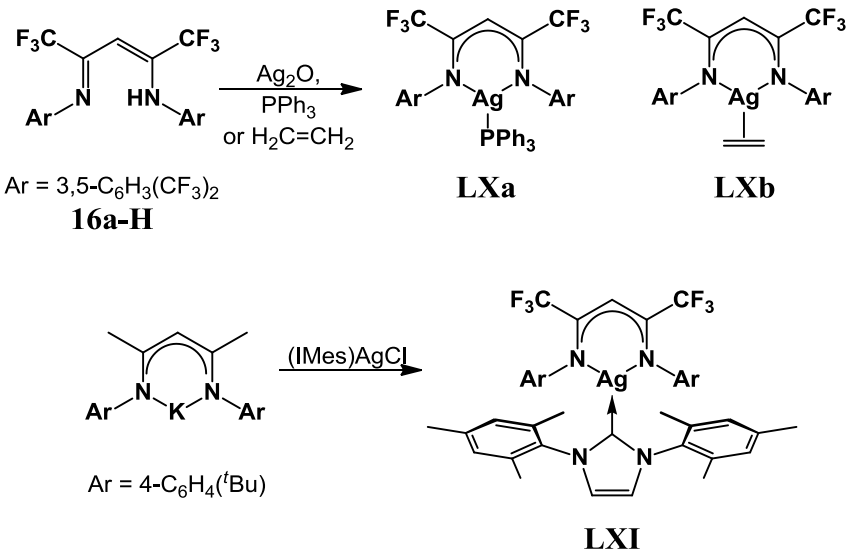

Scheme 23. Synthesis of the chelating silver *β*-diketiminates **LXa**, **LXb** and **LXI**.[148]

In 2005, Shi and co-workers employed Li[HC{C(Me)N(2,6-^{i}Pr$_2$C$_6$H$_3$)}$_2$] (6.3 mol %) with AuCl (5 mol %) to promote the aerobic oxidation of benzyl alcohols.[149] A subsequent review interpreted this as a gold(I)-chelate complex similar to **LVI** being formed *in situ* to stabilise the gold cation.[84]

By contrast to Au(I), dimethylgold(III) *β*-diketiminate complexes display a chelate structure to give an air stable but thermally sensitive (κ^2-HC{C(Me)N(2,6-Me$_2$C$_6$H$_3$)}$_2$)AuMe$_2$ (**LXII**; Scheme 24).[150] Further research of **LXII** has shown that the stable Au-C bond is resistant to electrophilic attack by triflic acid, resulting in protonation of the methine carbon in the diketiminato-chelate over demethylation (**LXIII**).

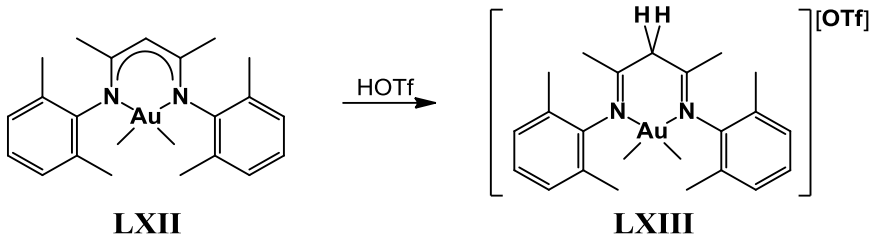

Scheme 24. Protonation of the diketiminate backbone in **LXII** by treatment with triflic acid.[150]

2.2.1.1.2 Gold coordination to 3-Heteroatom Substituted β-Diketiminates

Modifications to the 3-position *β*-diketiminate ligands have a profound influence on the structural chemistry of coinage metal complexes of these ligands. The 1,3,5-triazapentadienyl anions [N{C(C$_3$F$_7$)N(2,6-^{i}Pr$_2$C$_6$H$_3$)}$_2$]$^-$ (**LXIV**) are formally derived from [nacnac]$^-$ anions by replacing 3-CH with N. The resulting copper(I), silver(I) and gold(I) complexes form 6-membered metallocycles and give stable alkene and alkyne complexes of gold(I) (**LXVa-c** and **LXVIa-c**; Scheme 25).[59,76] Upon treatment of lithium 3-sila-*β*-diketiminates (**LXVII**) with phosphine salts of copper(I), silver(I) and gold(I), the delocalisation of the negative charge commonly seen with non-substituted diketiminate is absent, instead the 3-silicon atom carries the negative charge. The complexes **LXVIII**, **LXIX** and **LXX** show the preference of the more basic Si-M bonding.[151]

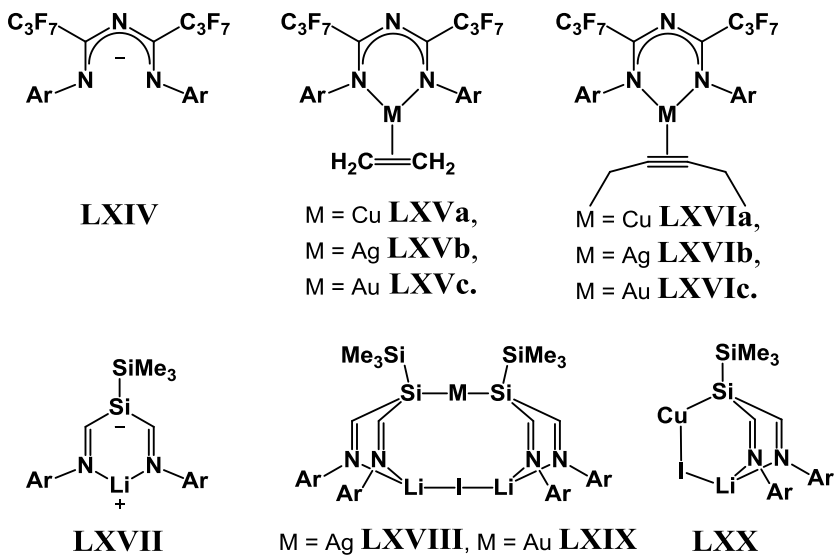

Scheme 25. π-coordination products of triazapentadienylgold(I) complexes and silyl-metallation of the 3-Si-substituted β-diketiminates.[73,76,151]

2.2.1.2 Gold-Oxo Complexes

An oxo-ligand is an oxygen atom bound to one or more metal centres. The ligand can exist as a terminal-bound or (more commonly) bridging atom (Figure 40). Terminal-oxo ligands are considered strong π-donor ligands.

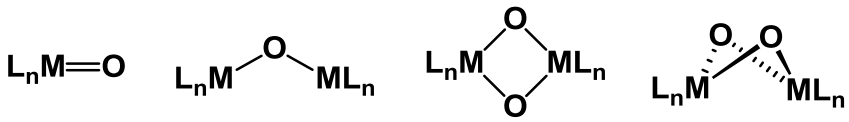

Figure 40. Model bonding modes of metal-oxo complexes of the type M=O, and M_2-(μ)O_n.

Metal-oxo compounds have significant uses as oxidising agents in organic synthesis. Moreover, metal-oxo complexes (both naturally-occurring and synthetic) have been found to be efficient catalysts for the oxidation of organics by C-H activation.[152]

The π-donor nature of a terminal-oxo ligand means that coordination to transition metals requires vacant *d*-orbitals of similar π-symmetry. Therefore terminal-oxo groups on group 3-8 transition metals are commonly seen, whereas for the metals in group 9-12 (with their occupied or partially occupied *d*-subshells) are rare.[153-155] It is this property (coined the "oxo-wall"), combined with the hard Lewis

basic nature of oxygen atoms that has resulted in a limited history of both terminal and bridging gold-oxo complexes.

Examples of gold(I) complexes containing an oxo-ligand are restricted to the bridging-oxonium family of complexes $[(R_3PAu)_3O]^+$ (an example is shown in Figure 41, **XXXI**), synthesised either by the reaction of $[R_3PAuCl]$ with Ag_2O and a suitable salt in acetone, or by reaction of $[AuPPh_3]^+$ (generated *in situ* from $[R_3PAuCl]$ and Ag^+) with water in basic media.[100] Applications of **XXXI** include as catalysis of electron-rich bonds[96,101] and as precursors for gold nanoparticle synthesis.[156]

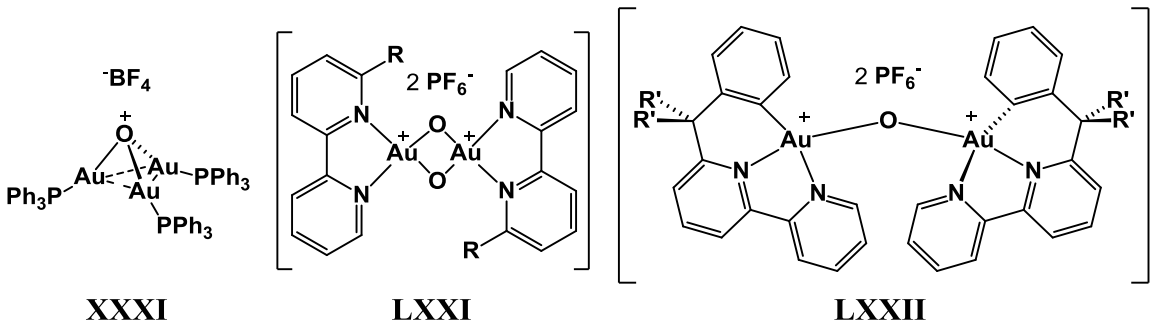

Figure 41. Bridged gold(I)- and gold(III)-oxo complexes.[63,100,157]

With the increase of coordination number, slight reduction of its Lewis softness and the availability of a vacant 5*d*-subshell, a small number of gold(III)-oxo complexes are known. Important discoveries of bridged gold-oxo complexes have been generated from the dehydration of hydroxyl-gold(III) intermediates supported by 6,6'-substituted-2,2'-bipyridine ligands (Figure 41).[157] The gold(III)-oxo complexes **LXXI** and **LXXII** are found to be prone to hydrolysis. Further work has found that when **LXXI** is treated with alkenes (styrene, norbornene, norbornadiene), numerous oxidation products are formed, including the auraoxetane complex (**C**), gold(I)-(η^2)olefin complex (**D**) and numerous hydroxy-functionalisations of norbornene.[63] The postulated mechanism describes the formation of a terminal (oxo)gold-(η^2-ene) as the first intermediate (intermediate **A**, Scheme 26).

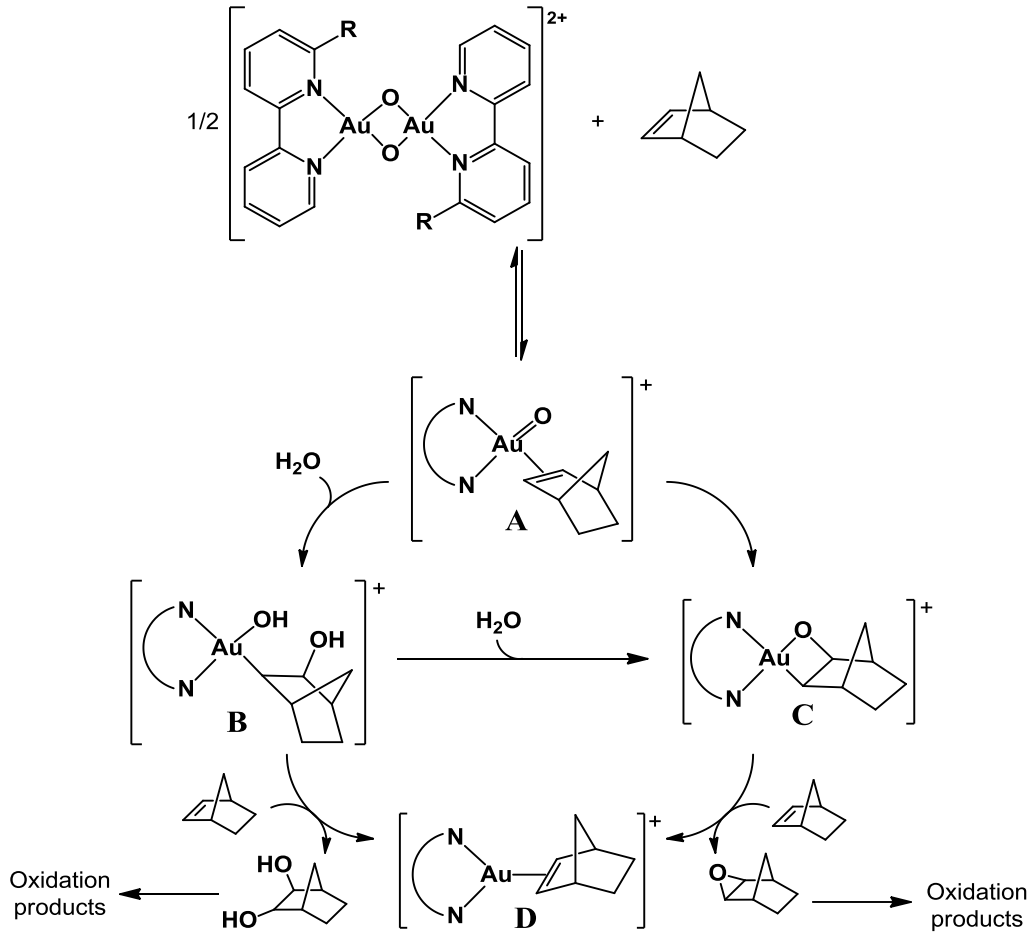

Scheme 26. Proposed reaction pathways for the reactivity of **LXXI** with norbornene (**A** and **B** are proposed intermediates).[63]

The only example of a terminal gold-oxo bond available is of the polytungstate-ligated complex **LXXIII** in which the terminal bonding nature was confirmed by ^{17}O NMR spectroscopy, X-ray and neutron diffraction studies (Figure 42).[158]

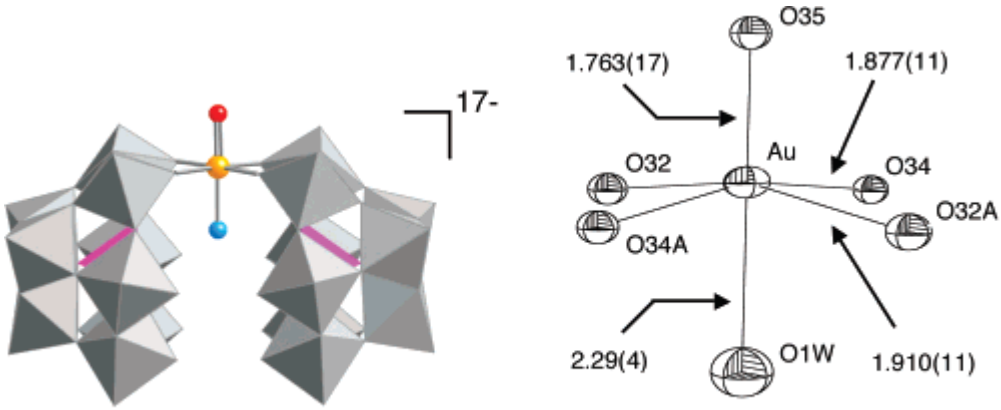

LXXIII

Figure 42. Combination polyhedral/ball-and-stick representation of **LXXIII** (the Au, O atoms, and aqua (H_2O) ligands are shown in yellow, red, and blue, left) and the X-ray structure around the Au atom (right).[158]

2.2.2 Objective of a Gold(III)-Oxo Complex Synthesis

The aim was to develop a gold(III) β-diketiminate complex bearing a terminal gold-oxo bond. As gold (in combination with an oxygen source) has been used as a homogeneous oxidation catalyst,[159,160] interest in the isolation of these rare species to develop the understanding of the catalytic oxidation process was targeted.

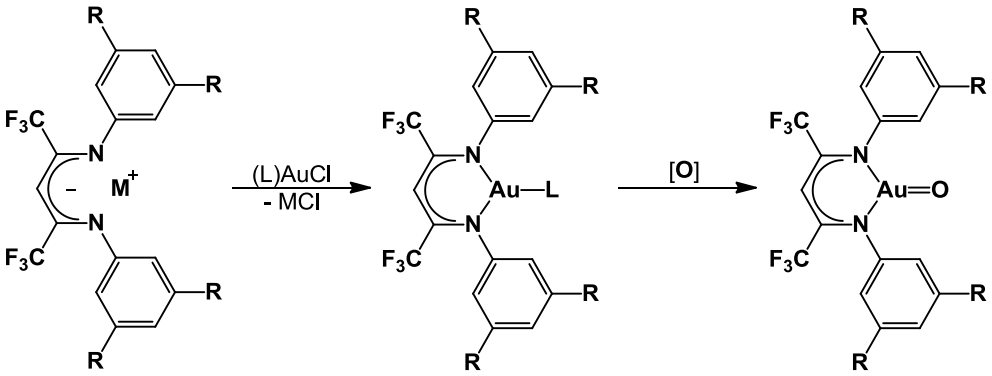

Scheme 27. Proposed reaction scheme for the synthesis of a gold(III)-oxo complex.

The structures of complexes **LVIIIa-b** show that an electron-rich ligand backbone promotes monodentate coordination. We were interested in modifying the backbone by inclusion of electron-withdrawing CF_3 groups, which have been shown to favour bidentate coordination in complexes of copper[161] and silver[148]. It was also of interest to tune the 3- and 5- positions of the *N*-aryl moieties, to see whether an

electron-withdrawing or electron-donating group aids in stabilising the gold centre upon coordination. It has been shown that the electronic influences in the 3- and 5-positions of the imido-aryl groups can significantly affect the bonding towards metals.[161]

2.2.3 Results and Discussion

2.2.3.1 Synthesis of Gold(I) Complexes Bearing Electron-Deficient β-Diketimide Ligands

Preliminary screening reactions of AuCl or (L)AuCl (where L = PPh_3, tht) with either Li[HC(2,6-$^{i}Pr_2C_6H_3$-NC(Me))$_2$] or Na[HC(4-$^{t}BuC_6H_4$NC(Me))$_2$] in THF/diethyl ether at 0 °C led in all cases to the rapid precipitation of metallic gold; evidently, these electron-rich ligands lead only to reduction. By contrast, the potassium salt of the less electron-donating trifluoromethyl substituted ligands **16a-K** and **16b-K** reacted cleanly with (Ph_3P)AuCl in diethyl ether at 0-20 °C gave the corresponding gold(I) diketiminato complexes **17a** and **17b** as orange powders in essentially quantitative yields (Scheme 28). In both the solid state and in solution these complexes are remarkably temperature-stable, with heating to 100 °C causing no decomposition.

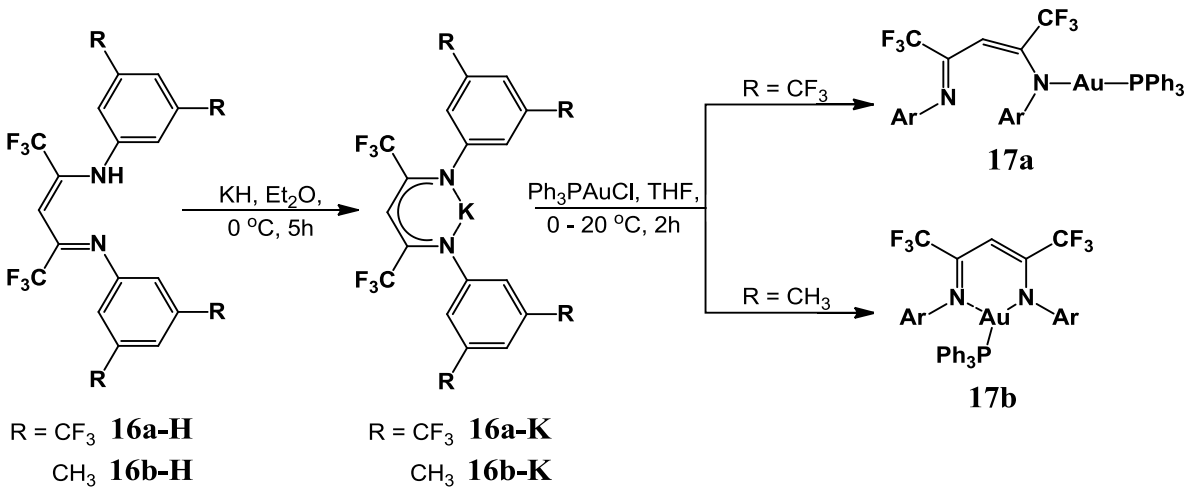

Scheme 28. Reaction scheme for the synthesis of **17a-b**.

Crystals of **17a** and **17b** were grown by cooling of concentrated diethyl ether solutions to -30 °C. Within the orange crystals of **17a** was a small quantity (<5 %)

of yellow platelets, which by X-ray diffraction were found to be the free ligand **16a-H**.[162]

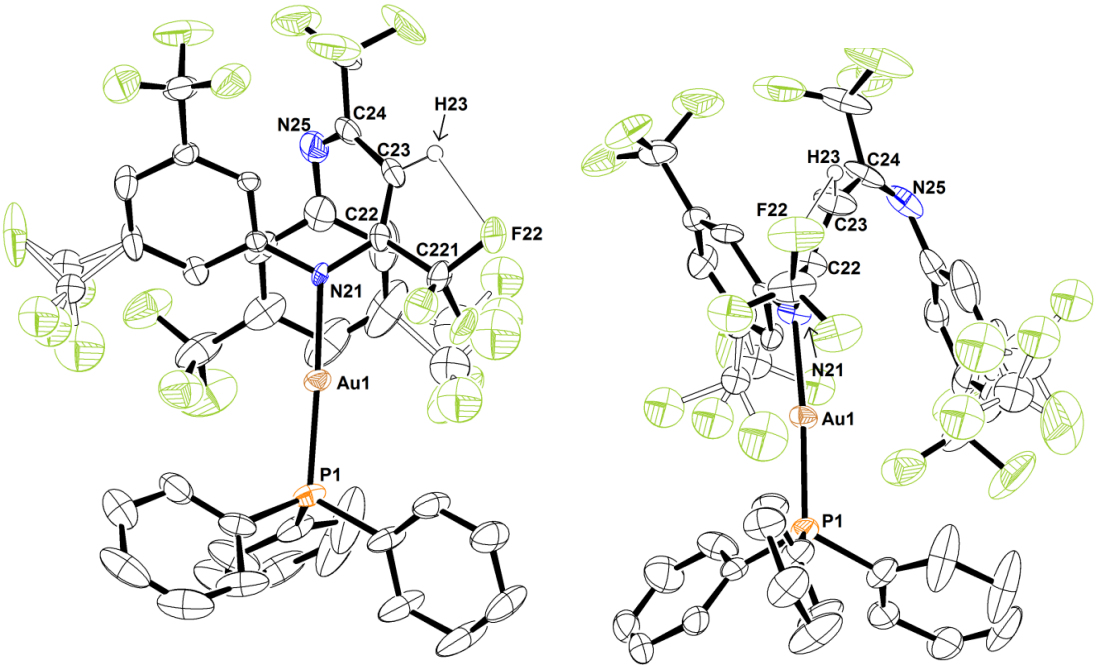

Figure 43. Two views of the molecular structure of **17a**, showing a partial atomic numbering scheme (hydrogens, except for the carbine-H, have been omitted). Ellipsoids are drawn at the 50% probability level. Selected bond lengths (Å) and angles (°): Au(1)-N(21) 2.075(4), Au(1)-P(1) 2.2360(12), N(21)-C(22) 1.368(6), C(24)-N(25) 1.263(7); C(22)-C(23) 1.342(7), C(23)-C(24) 1.467(7); N(21)-Au(1)-P(1) 175.59(11).

The crystal structure of **17a** (Figure 43) shows that the diketiminato ligand adopts a U-conformation, with a linear N-Au-P arrangement (see Table 6). There is no coordination to the second nitrogen atom. In the solid state both C-N bonds adopt *Z*-configurations; the $\{C_6H_3(CF_3)_2\}$ rings are approximately parallel to each other. By contrast, the structure of **17b** (Figure 44) shows that in this case both N-atoms of the diketiminato ligand are coordinated to the gold cation, albeit in an asymmetric manner. In line with this, the [NCCCN] backbone shows bond alternation, *i.e.* only partial charge delocalisation. The N(1)-Au(1)-P(1) moiety in **17b** is distorted significantly from linear towards a Y-shaped, three-coordinate geometry. The backbone of the diketiminato ligand and the gold-phosphine moiety exist within a symmetry plane, with only two phenyl groups from the phosphine and two from the N-aryl moieties protruding from this plane. The Au-N bond lengths

observed are longer than for those seen in the dimers of **LVIIIa-b** (which show Au-N bond lengths in the region of 2.030 Å).[146]

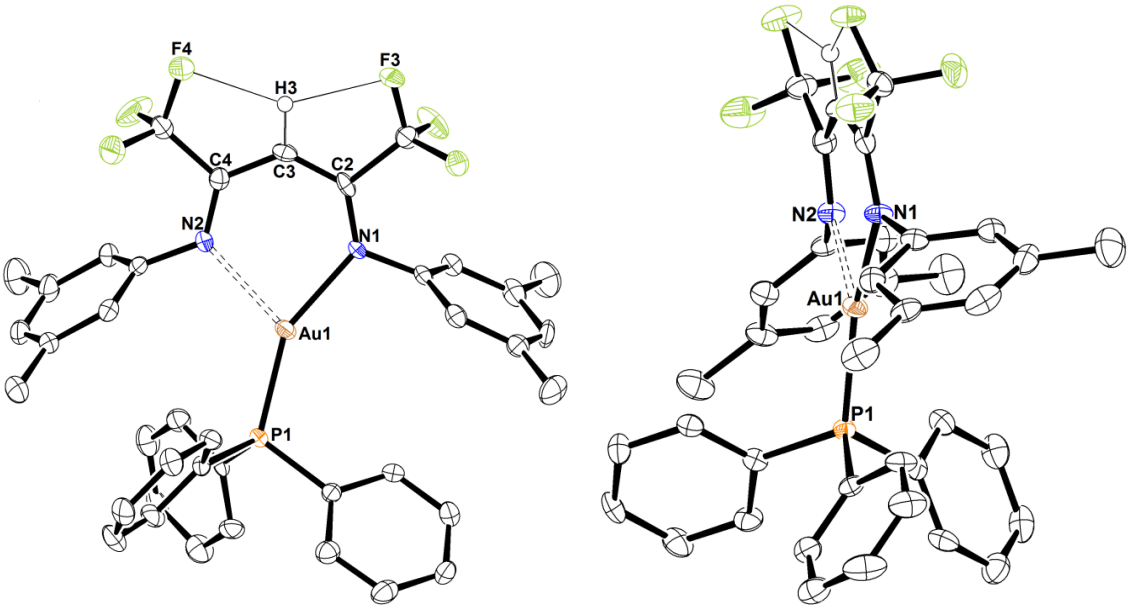

Figure 44. Two views of the molecular structure of **17b**, showing a partial atomic numbering scheme (hydrogens, except for the carbine-H, have been omitted). Ellipsoids are drawn at the 50% probability level. Selected bond lengths (Å) and angles (°): Au(1)-N(1) 2.137(4), Au(1)-N(2) 2.384(4); Au(1)-P(1) 2.2160(13), N(1)-C(1) 1.368(7), N(2)-C(3) 1.308(7); C(1)-C(2) 1.383(7), C(2)-C(3) 1.414(7); N(1)-Au(1)-P(1) 151.90(12); N(2)-Au(1)-P(1) 123.68(10).

Table 6. A comparison of the selected bond lengths and angles for **17a-b**.

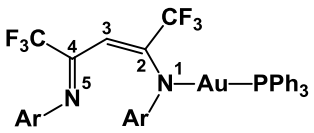

17a

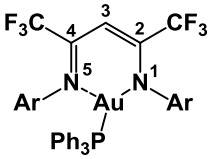

17b

Bond lengths/angles (Å or °)	**Complex 17a**	**Complex 17b**
N(1)-Au	2.0775(4)	2.137(4)
N(5)···Au	-	2.384(4)
Au-P	2.2360(12)	2.2160(13)
N(1)-Au-P	175.59(11)	151.91(12)
N(5)-Au-P	-	123.68(10)
N(1)-Au-N(5)	-	84.41(15)

Within the backbone of **17b**, there is evidence for strong intramolecular H···F interactions between one fluoride of both CF_3 groups and the methine C-H unit of the *β*-diketiminate ligand (F(3)-H(2) 2.20(5), F(4)-H(2) 2.20(6) Å).[163] In **17a**, only one of the CF_3 groups exhibited an intramolecular C-F···H-C interaction,

at a distance of 2.235 Å. An investigation of the X-ray data of related Cu and Ru complexes bearing CF_3-substituted diketiminato ligands suggest the existence of similar C-H···F-C bonding patterns, although these reports make no specific comments.[59,146,164,165] The fluorine-hydrogen bonding interactions of these compounds fall within the range of 1.9-2.2 Å, significantly shorter than the sum of the van der Waals radii (*ca.* 2.55 Å).

This difference in binding of gold to both ligands can be attributed to the subtle electronic nature of the bidentate ligand: The inductive effect of the 3,5-substituted moieties on the aryl-imide influences the basicity of the imidyl-nitrogen. The CF_3 groups on **17a** contribute to the withdrawal of electron density from the nitrogen lone pair, whereas its CH_3 equivalent in **17b** results in a sufficiently basic nitrogen centre to allow for dative bonding towards the gold cation.

The requirement of a strong donor ligand (such as triphenylphosphine) is paramount for the stabilisation of the gold cation in the presence of the *β*-diketiminate, as treating (tht)AuCl with either **16a-K** or **16b-K** in dichloromethane lead to colloidal gold suspensions when the solvent is removed.

2.2.3.2 Fluxional Processes

Both gold(I) *β*-diketiminate complexes are fluxional. In toluene-d^8 at 22 °C, two separate but broadened ^{19}F signals are observed for the two CF_3 substituents in 2- and 4-positions of the $[nacnac]^-$ ligand. For **17a**, the broadened signals are observed at δ -71.2 (Figure 45) and -65.5 ppm, with the corresponding signals at δ -70.2 and -64.3 ppm for **17b**. The coalescence temperatures (T_c) are 67 and 75 °C, respectively. For **17a** the signal has merged into a singlet at δ -66.5 ppm at 105 °C. This behaviour is consistent with the exchange of the metal centre between the two nitrogen donors of the diketiminato ligands, with a calculated rate constant (k_c = 3.6 × 10^3 s^{-1}) and Gibbs enthalpy ($\Delta G^{\ddagger}_c$ = 14.8 kcal mol^{-1}) at T_c. Unfortunately for **17b**, at 105 °C only a highly broadened signal can be seen at approx. -64.3 ppm, however, kinetic data could still be obtained at the coalescence temperature (k_c = 3.7 × 10^3 s^{-1}, $\Delta G^{\ddagger}_c$ = 14.8 kcal mol^{-1}). For both complexes, the chemical shift of the

coalescence singlet differs from the arithmetic mean of the two low-temperature resonances, suggesting the formation of a third component participates in the equilibrium. Conceivably a ligand rearrangement product of the type $[Au(PR_3)_2]^+[Au(nacnac)_2]^-$ is possible, which is not observed at lower temperatures but that contributes to the time-averaged chemical shift (Scheme 29).

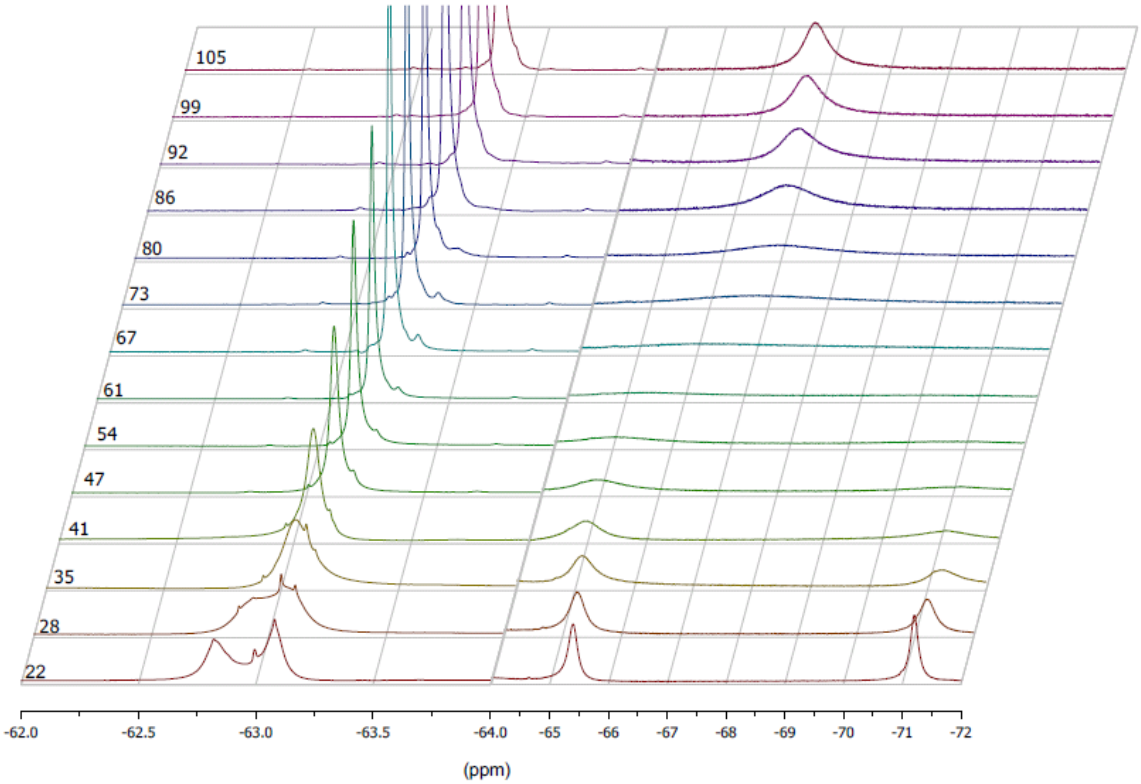

Figure 45. ^{19}F NMR spectra of **17a** run between 22 and 105 °C (toluene-d^8). At 22 °C the CF_3 substituents in 2- and 4-positions of the diazapentadienyl ligand are found at δ -71.2 and -65.5 ppm, respectively, while peaks around δ -63 ppm are due to aryl-CF_3.

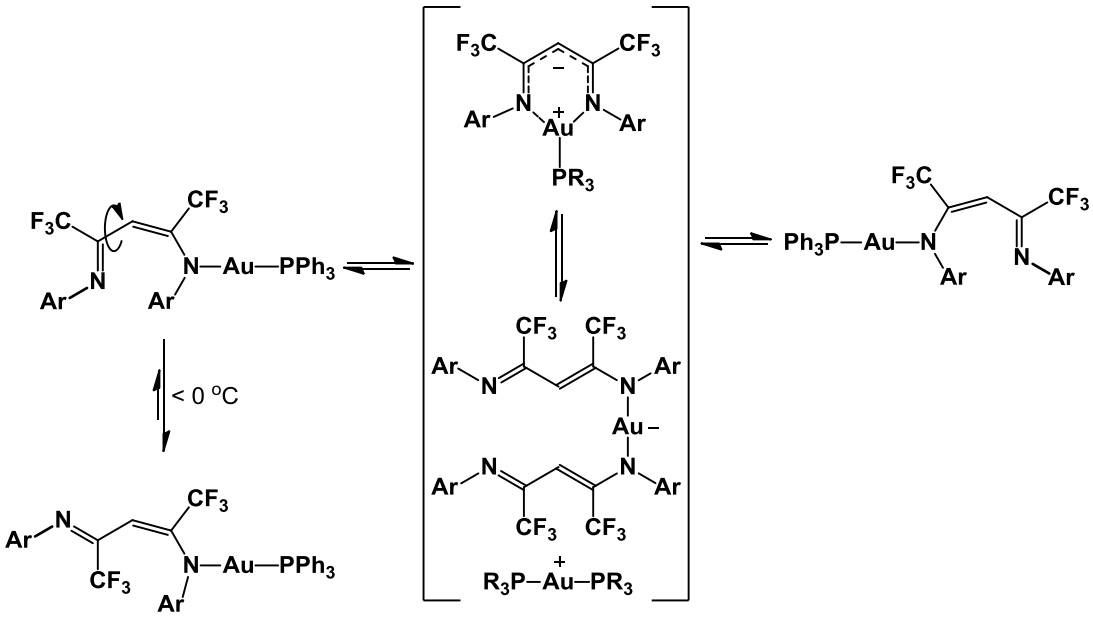

Scheme 29. Proposed fluxional processes observed with **17a** during variable temperature NMR studies.

Another form of fluxionality observed is from the rotation around the [C(CF_3)-C(H)] moiety in **17a**, indicated in Scheme 29. Low temperature NMR spectroscopy found that at room temperature the ^{19}F chemical shift at -65.5 ppm is apparently due to a mixture of *Z*- and *E*-isomers at this bond. Cooling to -94 °C shifts this equilibrium to yield a signal at -68.7 ppm, most probably towards the *Z*-isomer present in the crystal structure (Figure 46).

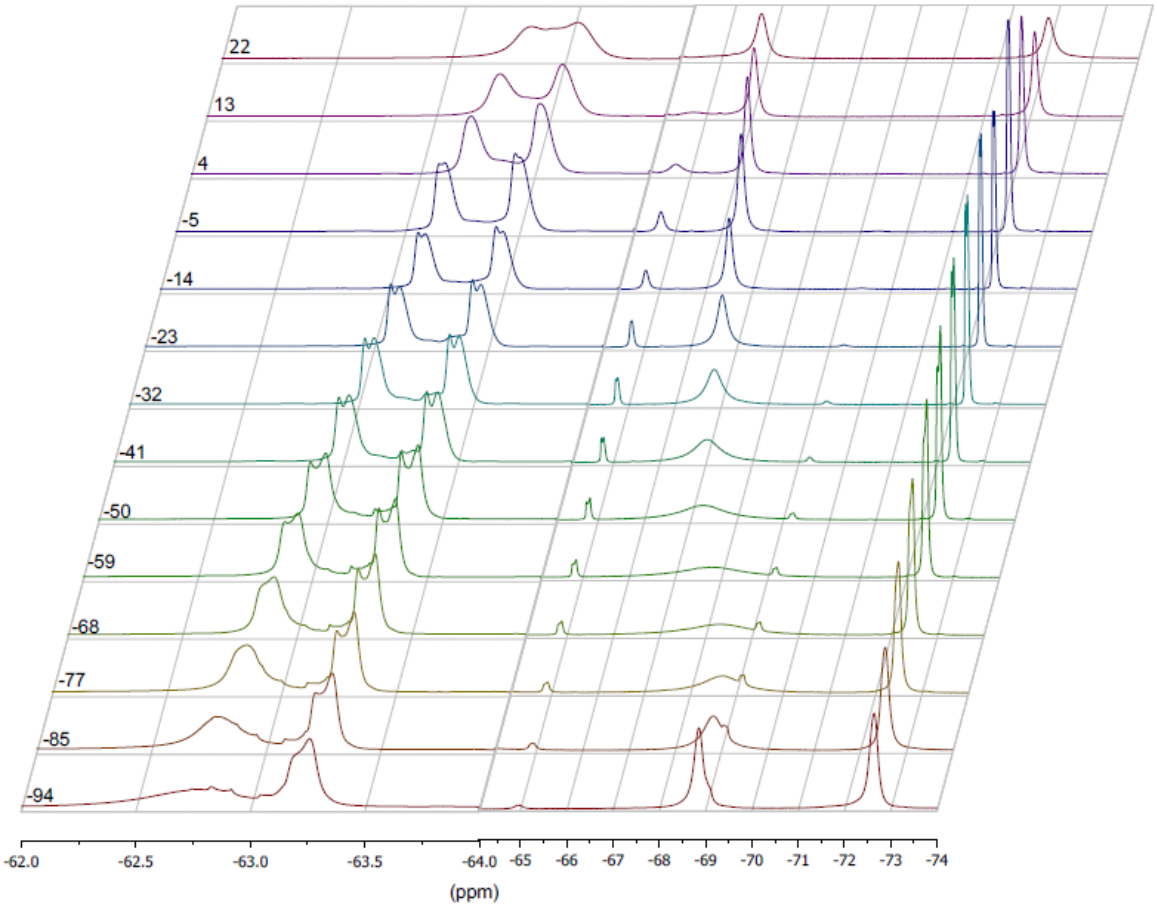

Figure 46. ^{19}F NMR spectra of **17a** run between -94 and 22 °C (CD_2Cl_2). At 22 °C the CF_3 substituents in 2- and 4- positions of the diazapentadiene are found at δ -71.2 and -65.5 ppm, respectively, while peaks around δ -63 ppm are due to aryl-CF_3.

2.2.3.3 Attempted Oxidation to Gold(III)β-Diketiminates

One of the aims of synthesising complexes **17a-b** had been the possibility of using these fluorinated nacnac ligands to stabilise an Au(III) oxo-species, [(nacnac)Au=O]. Numerous organic and inorganic oxidants were selected for this purpose.

The attempted oxidation of **17a-b** by Cl_2 or $PhICl_2$ gave a mixture of products when analysed by ^{19}F and ^{31}P NMR spectroscopy. Isolation of any species (by recrystallisation or column chromatography) was unsuccessful. Screening of peroxide oxidants (*tert*-butyl hydroperoxide, potassium monopersulfate, and magnesium bis(monoperoxyphthalate) hexahydrate) results in protonation, forming the free *β*-diketimide. Also observed in the reaction was a gold film, possibly

arising from the reduction of gold from the unstable [(Ph_3P)Au][OOR] byproduct believed to be produced from protonation of the ligand.

Use of $PhI(OAc)_2$, $PhI(OAc^F)_2$, $(PhI{=}O)_n$, or Dess-Martin periodinane (1,1,1-triacetoxy-1,1-dihydro-1,2-benziodoxol-3(1H)-one) appears to have a common influence on complexes **17a-b**. With each oxidant employed, ^{31}P NMR spectroscopic analysis of the crude reaction gives a signal at ca. 42 and 45 ppm, from the reactions with **17a** and **17b**, respectfully. In comparison to literature data, this suggests that the reactions do not produce the dissociation products [(Ph_3P)Au(O_2CCX_3)] (X = F, H)[97,166] or $Ph_3P{=}O$.[167] Unfortunately the diketimide backbone appears to have deteriorated with a large number of ^{19}F NMR spectroscopic signals within the window of the *β*-diketiminate region of the spectrum. Isolation of any products proved unsuccessful. Heating the dried products from the oxidation by iodine(III) to 300 °C produced a gold deposit, indicating that gold is present in a unknown form in the mixture.

In summary, numerous attempted oxidations of the gold cation have resulted in unclean products, shown by NMR spectroscopic techniques. Isolation by numerous means has so far been unsuccessful.

2.2.4 Conclusions

Treatment of triphenylphosphinegold chloride with the potassium salts of *β*-diketiminates with an electron-accepting backbone gave the first examples of mononuclear complexes of the type [CH{C(CH_3)N(3,5-$CX_3C_6H_3$)}$_2$]$AuPPh_3$ (X = F, H) which are stable in solution to > 100 °C. The electronic effect of the CX_3 groups on the *N*-aryl substituents has a profound effect on the solid state structures of these complexes: replacing CF_3 by CH_3 leads to a change from κ^1- to κ^2-coordination. Both complexes show an intricate fluxional behaviour, attributed to a metal migration, but yet undetermined complex mechanisms are apparent. All attempts of oxidation to gold(III)-oxo complexes were found to be unsuccessful and gave multiple reaction products.

3 - Benzylic C-H Activation of Electron-Rich Arenes by Gold(I)

3.1 Preliminary Observations and Objectives

Our initial vision into the chemistry of alkylbenzenes with gold cations was to compare the reactivity of a dichloromethane solution of $(Me_2S)AuCl/AgSbF_6$ in the presence of different electron-rich multimethylated arenes $[C_6Me_nH_{6-n}]$, since under analogous conditions the formation of a family of 'naked' gold cations stabilised by alkene coordination $[Au(ene)_n]^+$ is observed (Scheme 30).[71,52,73] Gold(I) cations containing an Au-(η^2)arene bond have only been described when the metal centre is supported by strong σ-donor ligands (such as alkyl phosphines, NHCs).[60,82] While there are numerous examples of arene complexes of silver,[168] thallium[169,170] and mercury[171-173] cations, the detection of such adducts in the "ligand-free" Au^+ system has so far not proved possible. Since hexamethylbenzene is electron-rich and gave the most stable complexes in the case of Tl^+,[169] it was chosen as the preferred substrate.

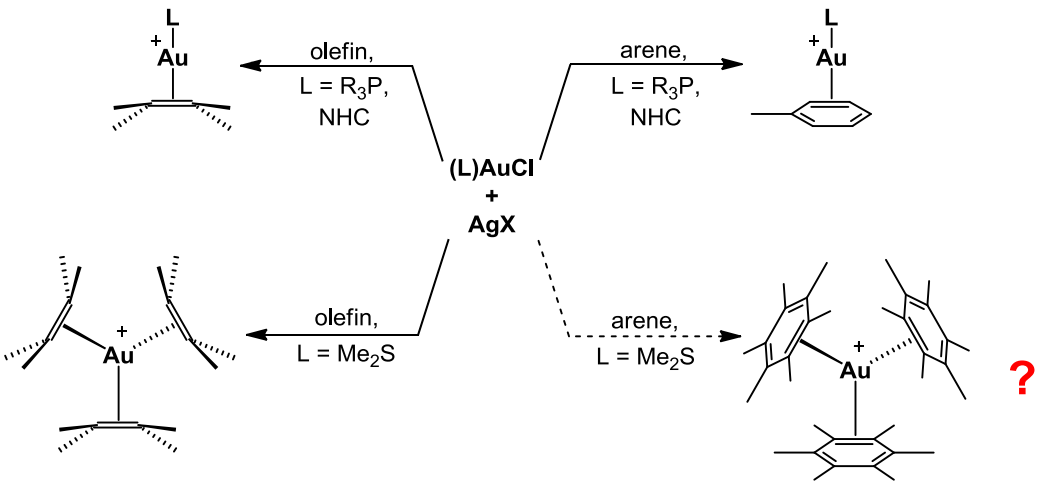

Scheme 30. Experimentally observed reactions of (L)AuCl and AgX in the presence of π-bonds, and the postulated reaction targeted in this chapter.

The reaction took a different course, however: There was no π-arene complexation, leading instead to benzylic (sp^3) C-H activation.

3.2 History of Benzylic C-H Activation

The functionalisation of sp^3 C-H bonds under mild conditions is a challenge to chemists, with motivation to develop important applications in natural gas conversion, as well as for green catalytic transformations from cheap materials.[8,174,175] Numerous obstacles inhibit such activations; the inertness of these aliphatic C-H bonds,[174] and the control of regio- and chemoselective activation of such bonds are particularly difficult without the incorporation of basic directing groups within the organic substrates.[176]

3.2.1 Benzylic C-H Activation by Late Transition Metals

The activation of benzylic sp^3 C-H bonds of methylarenes is a poorly studied area, as under standard conditions activation of aromatic C-H bonds is strongly favoured: ring-functionalisation >> benzylic-functionalistion.[177,178] The control of a number of reaction conditions, such as metal selection, ligand design or use of chemical additives can allow for the promotion of benzyl C-H activation. In particular, select late transition metal complexes (in groups 8-10) have been found to be effective in both catalytic functionalisations and metalation of benzylic C-H bonds in simple methylarenes.[177,178,181-183,185-192]

3.2.1.1 Group 8 Activators

Given the ability of the Cytochrome P-450 family of enzymes to convert alkanes to alcohols (often with high stereoselectivity),[179] synthetic iron(III)-porphyrin catalysts (amongst other late TM centres, in cooperation with oxygen donors) have been employed as oxidants.[180] Chemoselective hydroxylation of ethylbenzene is promoted photochemically by a chiral ferric-porphyrin catalyst (**LXXIV**, 1 mol %) in conjunction with iodosylbenzene (Scheme 31). The rate-determining step was found to be the abstraction of a hydrogen radical *exclusively at the α-carbon*; neither aryl-H nor *β*-C-H activation were observed. The secondary alcohols synthesised have moderate stereoselectivities.[181]

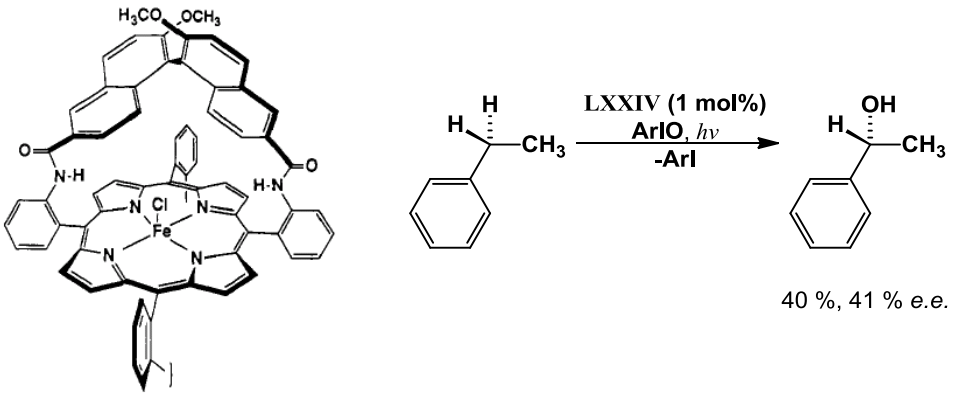

Scheme 31. The transformation of ethylbenzene to (α-methyl)benzyl alcohol by the chiral catalyst **LXXIV**.[181]

Indoles have been synthesised by the functionalisation of a benzylic C-H bond of 2-methylisocyanides mediated by [(dmpe)$_2$Ru(H)(napthyl)] (**LXXV**). The reaction of **LXXV** with 2,6-xylylisocyanide at 60 °C led to the formation of 7-methylindole (Scheme 32). Kinetic isotope studies have assigned an intramolecular oxidative addition step as the means of C-H activation.[182]

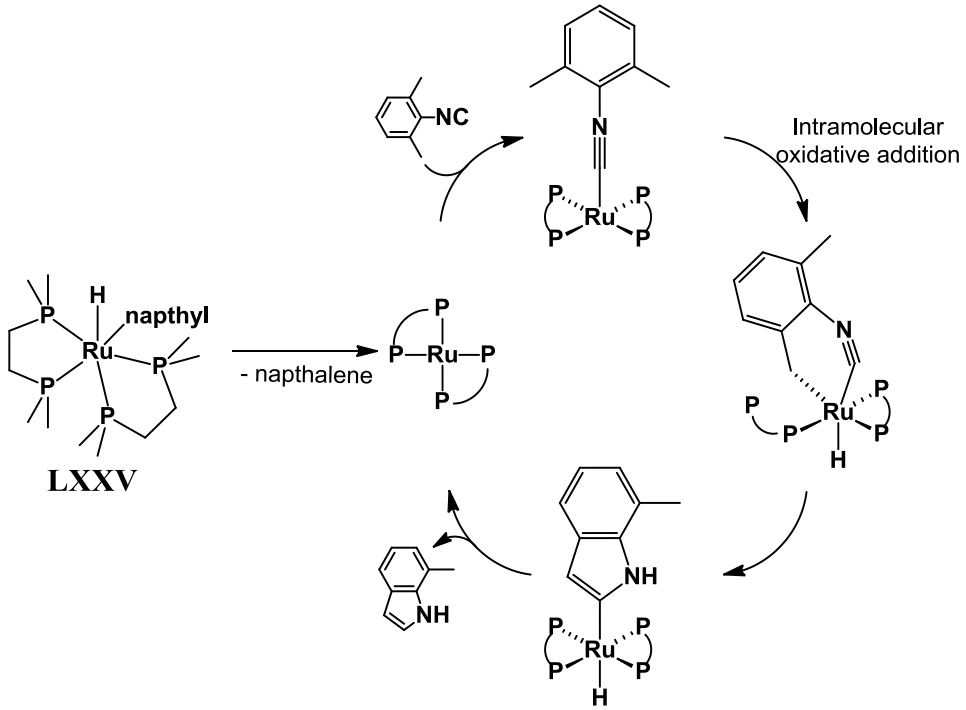

Scheme 32. The synthetic mechanism of 7-methylindole by complex **LXXV**.[182]

3.2.1.2 Group 9 Activators

A rhodium(II) porphyrinate complex (**LXXVI**) has been found to react with numerous alkylarenes (toluene, *o*-, *m*-, and *p*-xylenes, ethylbenzene, *n*- and *iso*-propylbenzene) in the presence of trace H_2O and O_2 to form the (porphyrin)rhodium(III) benzyl compounds (**LXXVII**) in near quantitative yields (Scheme 33).[183]

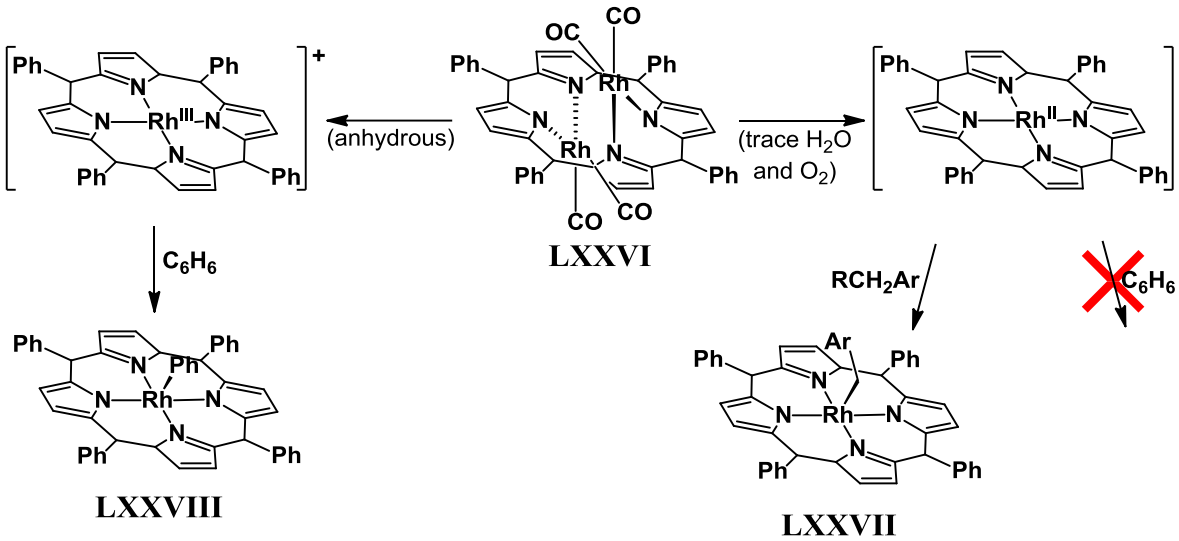

Scheme 33. Conversion of rhodium(II) porphyrinate **LXXVI** to benzyl- and aryl-rhodium(III) complexes **LXXVII** and **LXXVIII**.[183a]

C-H activation under atmospheric conditions is exclusively benzylic; water promotes the formation of the monometallic $[Rh^{II}(por)]$ intermediate, an active species for benzylic attack. The mode of activation is by homolytic cleavage of the sp^3 C-H bond by two $[Rh^{II}(por)]$ centres, *via* a trigonal bipyramidal transition state (Scheme 34). Under the same conditions the activation of aromatic C-H bonds are sterically prohibited (indicated by the destabilisation of geometry of the transition state), therefore a lack of reactivity with benzene is seen. In the absence of water, the activation of aromatic hydrogens is dictated by the active rhodium intermediate $[Rh^{III}(por)]^+$ promoting an electrophilic aromatic substitution step to yield a phenyl rhodium porphyrinate (**LXXVIII**).[183a]

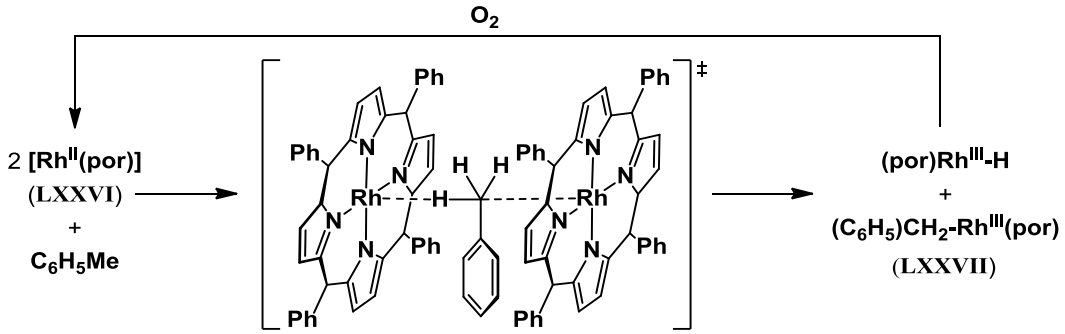

Scheme 34. The mechanistic transition state for the activation of toluene by [Rh^{II}(por)].[183a]

Photocatalytic conversion of toluene, *p*-xylene and mesitylene to benzylboronate esters produces an important class of synthetic intermediates for biological and organic chemistry.[184] [($^{i}Pr_3P)_2RhCl(N_2)$] (**LXXIX**) is an efficient and chemoselective catalyst for this transformation.[185] A mechanism for activation has been postulated, involving an oxidative addition of [$Me_nC_6H_{6-n}$] (n = 1-3) to form an η^3-benzylrhodium intermediate (Scheme 35).

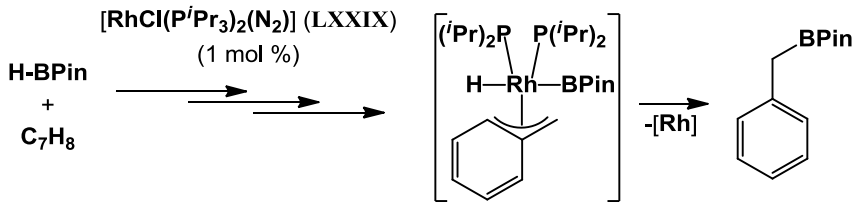

Scheme 35. The oxidative addition step for the activation of methylbenzenes by catalyst **LXXIX**.[185]

Intermolecular α-metalation of mesitylene by iridium has also been described. The formation of a benzyliridium complex [$Ir(acac)_2(Py)(CH_2\{3,5\text{-}C_6H_3Me_2\})$] (**LXXXb**) was achieved by the treatment of mesitylene with (**LXXXa**) under thermal conditions (Scheme 36). Activation of the benzylic C-H bond is by an oxidative addition step onto the metal centre, followed by reductive elimination of methane. Pyridine is displaced to allocate a vacant site for mesitylene addition; introduction of excess pyridine retards the rate of activation.[186]

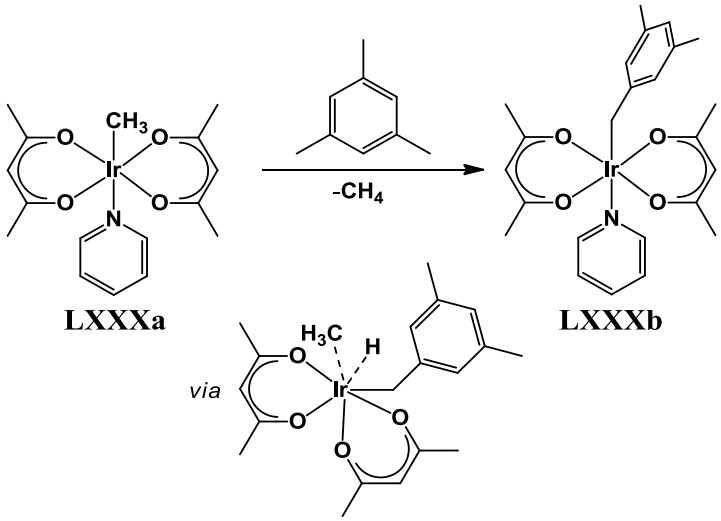

Scheme 36. α-metalation of mesitylene by iridium.[186]

The catalytic double C-H activation of mesitylene to afford benzyl aldehydes, esters and imines has been described by Crabtree and Voutchkova. The use of Ir/C in the presence of an oxidant (and a selected benzylic acid for ester formation) results in a mixture of oxidation products (poor yields and selectivity are observed due to uptake of adventitious water). The activation of the mesitylene is perceived to occur in two steps: homolytic cleavage, followed by liberation of H_2, to form a ArCH=Ir/C Schrock carbene (Scheme 37).[187]

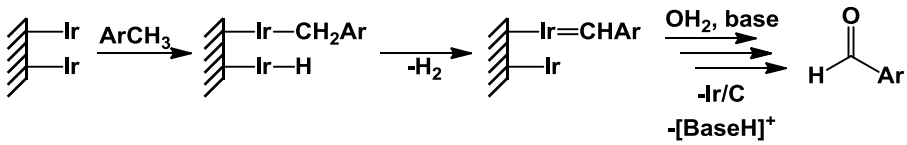

Scheme 37. The mechanistic overview of the double C-H activation of methylarenes on the surface of Ir/C.[187]

3.2.1.3 Group 10 Activators

Many palladium- and platinum-promoted C-H activation of methylbenzenes have a propensity for ring- over benzyl-metallation.[178] Whereas a selection of platinum(II) complexes containing neutral N^N bidentate ligands (**LXXXI** and **LXXXII**) can preferentially activate the benzylic position of methylarenes under mild conditions. Careful tuning of the ligands and reaction conditions allow for

such selectivity (Scheme 38). The C-H activation step has been determined to occur by associative substitution with the methyl groups on platinum.[177,188,189]

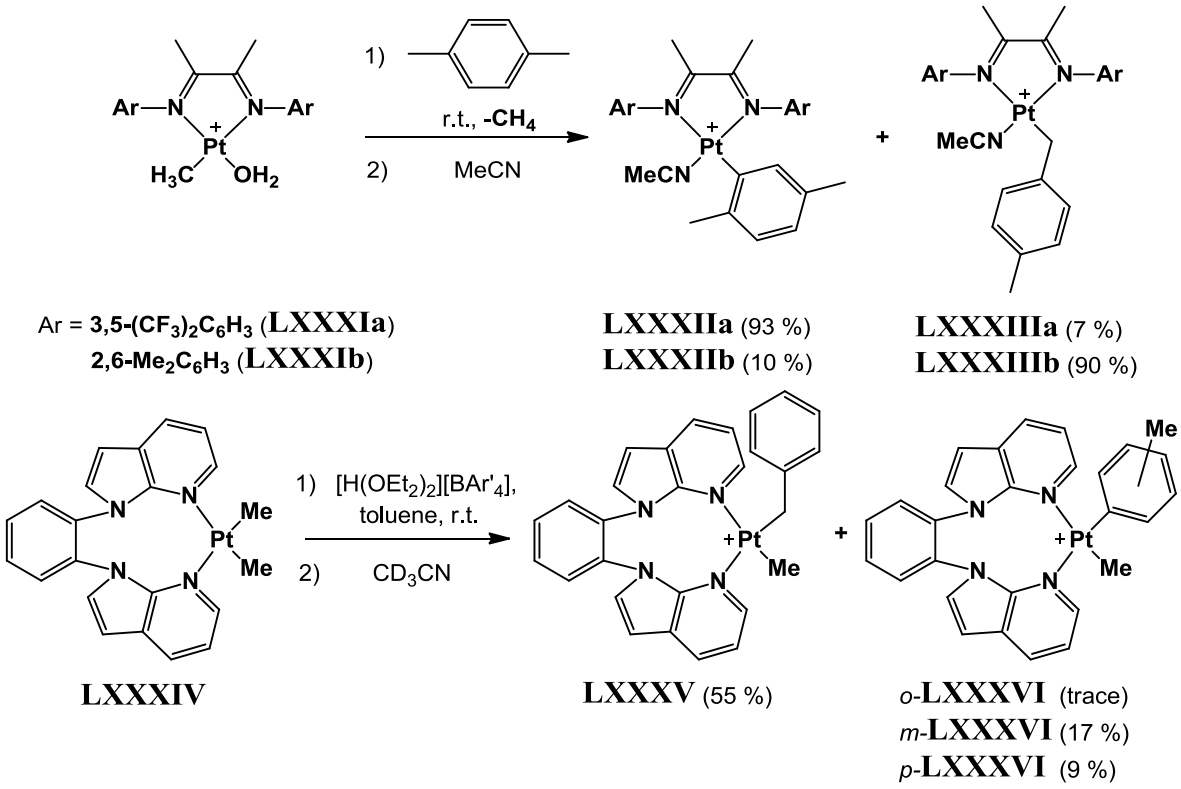

Scheme 38. Ligand selection allows for the control of benzylic- over aromatic-C-H metalation by Pt(II).[177,178,188,189]

Photoinduced activation of alkylbenzenes by Pt(II)-[190] and Pt(IV)-methyl complexes[191] leads to the formation of benzylic Pt-C bonds (Scheme 39). The activation of the alkylbenzenes was revealed to be by radical attack; photohomolytic cleavage of the Pt-alkyl bond gave a radical pair, $[R_3Pt]^{\cdot}Alkyl^{\cdot}$. A metathesis step with toluene or *p*-xylene yields $[R_3Pt]^{\cdot}[CH_2Ar]^{\cdot}$ and methane/2,2-dimethylbutane, followed by diradical association to yield the newly formed benzylplatinum complexes **LXXXVII** and **LXXXVIII**.

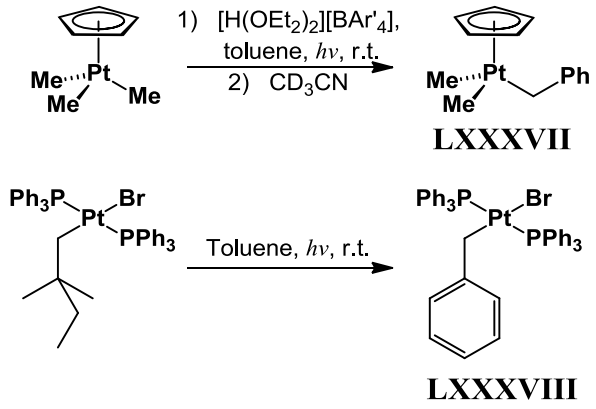

Scheme 39. Selective activation of toluene to give **LXXXVII** and **LXXXVIII**.[190,191]

Employment of the Shilov system for the catalytic oxidation of *p*-toluenesulfonic acid selectively activates the stronger methyl-C-H bond over the available aryl C-H bonds, albeit with moderate turnovers (Scheme 40).[192]

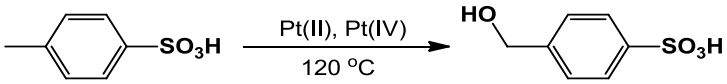

Scheme 40. The synthesis of (p-$HOCH_2$)$C_6H_4SO_3H$ by the Shilov system.[192]

Two mechanisms have been discussed for the two-electron oxidation by the Shilov system: the oxidative addition of R-H to give a platinum alkyl, and the oxidation of a side-on bonded alkane complex.[175a] This is discussed in more detail in Section 3.3.3.

3.3 Results and Discussion

3.3.1 Benzyl C-H Activation of Hexamethylbenzene

The reaction of equimolar amounts of $(Me_2S)AuCl$, $AgSbF_6$ and hexamethylbenzene in dichloromethane in the absence of light at room temperature was found to lead cleanly to the functionalisation of a benzylic C-H bond, giving $[C_6Me_5CH_2(SMe_2)][SbF_6]$ (**18**), alongside colloidal gold (Scheme 41).

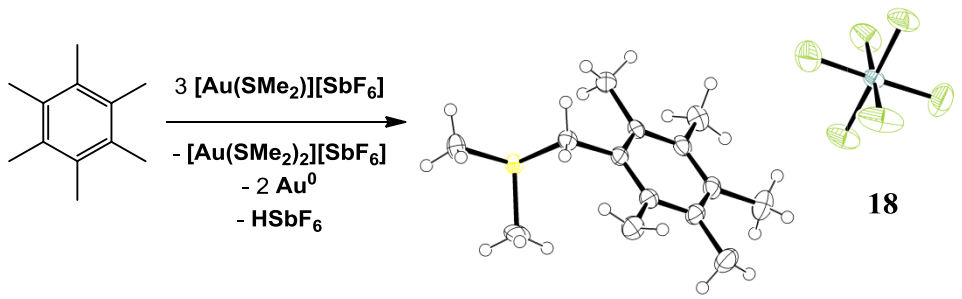

Scheme 41. The observed C-H activation of hexamethylbenzene by gold. Ellipsoids are drawn at the 50% probability level.

Monitoring the process by ^{1}H NMR spectroscopy showed that the reaction was accompanied by the formation of $[Au(SMe_2)_2][SbF_6]$ (**19**), which was characterised by X-ray crystallography (Figure 47). In the solid-state, the unit cell of **19** contains three independent gold cations. Any two cations are held together by a single unsupported aurophilic interaction (Au(1)-Au(2) 3.139(2), Au(3)-Au(3') 3.087(2) Å).

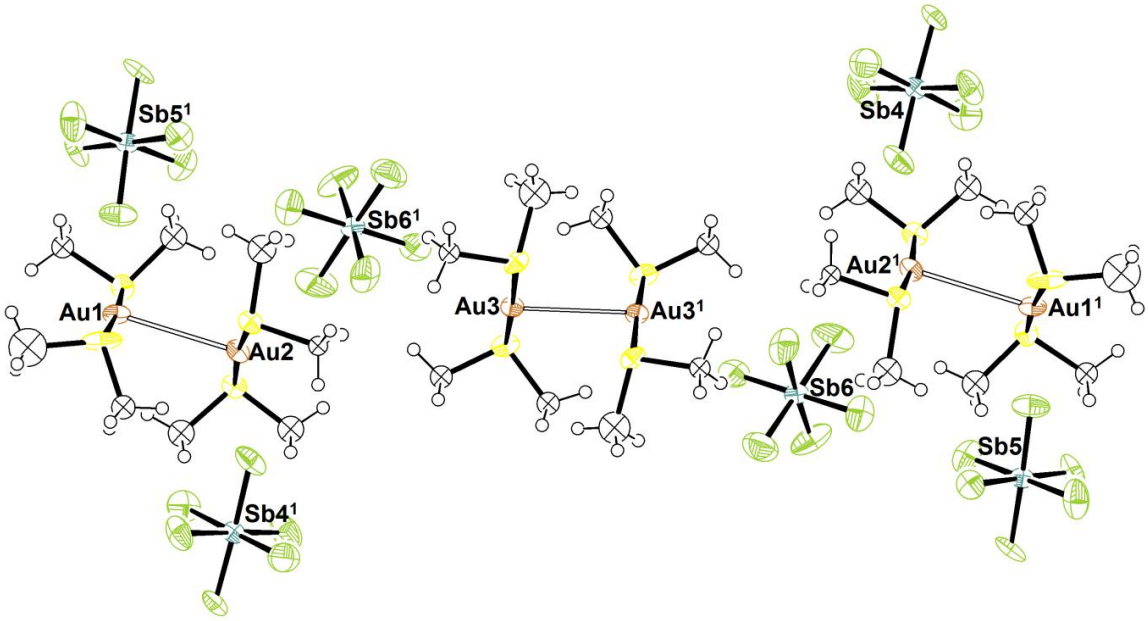

Figure 47. Two asymmetric units of $[(Me_2S)_2Au][SbF_6]$ (**19**). Ellipsoids are drawn at the 50% probability level. Au···Au distances are measured at approx. 3.1 Å.

There was no conversion of hexamethylbenzene with either $(Me_2S)AuCl$ or $AgSbF_6$ alone. The introduction of one or more equivalents of free dimethylsulfide

prior to addition of $(Me_2S)AuCl$ and $AgSbF_6$ gave only unreactive **19** in quantitative yield, without arene activation.

Formation of **18** was also observed using $AuBr_3(SMe_2)/3AgSbF_6$,[193] while (tht)AuCl gives the corresponding tht-sulfonium cation **20** (Table 7 and Figure 48). No reaction occurred with $(Ph_3P)AuCl$, (Py)AuCl and ligand-free AuCl (presumably due to the latter's insolubility). Thioether ligands are particularly suitable here since they not only help to solubilise the gold chloride precursors but also are sufficiently labile to undergo the ligand exchange reactions required to generate the active species. On the other hand, using $(^tBu_2S)AuCl/AgSbF_6$ led only to reduction to metallic gold, without C-H activation, as both $[(^tBu_2S)Au]^+$ and $[(^tBu_2S)_2Au]^+$ cations appear to readily break down at reduced temperatures. Other thioethers such as diphenylsulfide, thiophene and 2,5-dimethylthiophene when treated with $HAuCl_4$ failed to produce gold complexes.

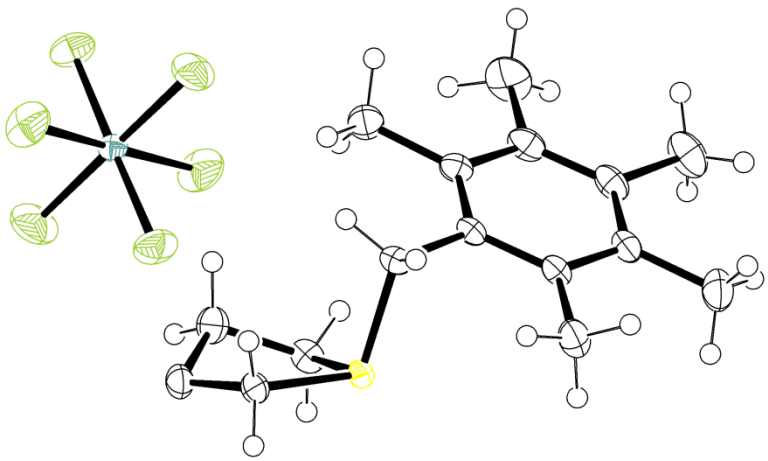

Figure 48. The crystal structure of **20**. Ellipsoids are drawn at the 50% probability level.

The nature of the silver activator ($AgSbF_6$, AgOTf, $AgBF_4$) is not critical, except in the case of $AgPF_6$. For the synthesis of $[C_6Me_5CH_2SMe_2][PF_6]$ (**23**), a yield of 14-17% was determined by ^{19}F NMR spectroscopy, along with the presence of PF_5 and AgF in solution in *ca.* 15% yield. The use of $NaBF_4$ and $^iPr_3SiOTf$ led to the formation of gold films only.

A dry, oxygen-free environment is not necessary for activation of hexamethylbenzene to occur, as a reaction performed under ambient conditions gave the sulfonium cation in the same yield. When the reaction was attempted in

methanol, no reactivity with the arene was apparent, but the production of $[(Me_2S)_2Au][SbF_6]$ and colloidal gold was observed.

The C-H activation reaction follows the stoichiometry given in Eq. 3:

$$C_6Me_5\text{-}CH_3 + 3\ [(R_2S)Au]^+ \rightarrow [C_6Me_5\text{-}CH_2(SR_2)]^+ + [(R_2S)_2Au]^+ + 2\ Au(0) + H^+ \qquad \textbf{(Eq. 3)}$$

For most arene substrates tested, an arene:gold molar ratio of 1:1 was employed and kept constant for comparison. The maximum achievable conversion of $Ar\text{-}CH_3$ was therefore 33% (Table 7). In agreement with Eq. 3, employing a C_6Me_6:Au ratio = 1:3 gave near-quantitative hydrocarbon conversion. The involvement of a carbocationic intermediate was demonstrated using the reaction of 2,4,6-trimethylbenzyl chloride with $AgSbF_6$ or $[Ph_3C][SbF_6]$, which in the presence of SMe_2 gives the expected sulfonium salt in quantitative yields.

Table 7. Benzylic C-H Activation of C_6Me_6 by gold.[a]

Entry	[Au]	Activator	Product	Conversion[b]
1	$(Me_2S)AuCl$	$AgSbF_6$	$[Me_5C_6CH_2SMe_2][SbF_6]$ **18**	33
2	$(Me_2S)AuCl$	-	-	0
3	-	$AgSbF_6$	-	0
4	$(Me_2S)AuBr_3$	3 $AgSbF_6$	$[Me_5C_6CH_2SMe_2][SbF_6]$ **18**	33
5	(tht)AuCl	$AgSbF_6$	$[Me_5C_6CH_2(tht)][SbF_6]$ **20**	30
6	$(Me_2S)AuCl$	$AgBF_4$	$[Me_5C_6CH_2SMe_2][BF_4]$ **21**	33
7	$(Me_2S)AuCl$	AgOTf	$[Me_5C_6CH_2SMe_2][OTf]$ **22**	32
8	$(Me_2S)AuCl$	$AgPF_6$	$[Me_5C_6CH_2SMe_2][PF_6]$ **23**	15
9	$(Me_2S)AuCl$	$NaBF_4$	-	0
10	$(Me_2S)AuCl$	$^iPr_3SiOTf$	-	0

a - Reaction conditions: C_6Me_6 (0.5 mmol), LAuCl (0.5 mmol), AgX (0.5 mmol), CH_2Cl_2 (15 mL), N_2 atmosphere, 20 °C, 1 h. *b* - Yields (%) determined by ^1H NMR spectroscopy, relative to initial C_6Me_6 concentration.

There was however no reaction between C_6Me_6 and $[Au(SMe_2)_2][SbF_6]$, nor was there any reaction in a mixture of 2,4,6-trimethylbenzyl chloride and $AgSbF_6$ in the presence of $[Au(SMe_2)_2][SbF_6]$ (**19**). This confirms that the $[Au(SMe_2)_2]^+$ ion is an unreactive side product. Attempts to reactivate the by-product by treating **19** with 1 equiv. of $B(C_6F_5)_3$ were made, but $B(Ar^F)_3$ was not found to act as a sulfide scavenger.

3.3.2 Kinetics of Activation.

The activation of hexamethylbenzene with $(Me_2S)AuCl$ and $AgSbF_6$ was monitored by ^1H NMR spectroscopy under anaerobic conditions. To a mixture of C_6Me_6 and $(Me_2S)AuCl$ in $CDCl_3$ at the required temperature was added a solution of $AgSbF_6$ in $CDCl_3$ and spectra were recorded at ~2 min intervals. Rate measurements were conducted in the presence of excess C_6Me_6, i.e. under *pseudo*-first-order conditions and show first-order dependence on the active gold species (labelled $[Au]^+$). Rates were determined from the growth of the signals for $[ArC\boldsymbol{H_2}SMe_2]^+$ (δ 4.75).

Measurements of conversion versus time, over a period of one hour were fitted to the below expression (Eq. 4) and used to calculate initial rates of reaction R_0.

$$\frac{d[Arene]}{dt} = R_0 = k[Arene]_0[Act] \qquad \textbf{(Eq. 4)}$$

The plot for determining R_0 shows that the trend does not intersect the origin, as the consumption of [Au] in a side reaction is evident at lower concentrations (< 0.04 M; Figure 49).

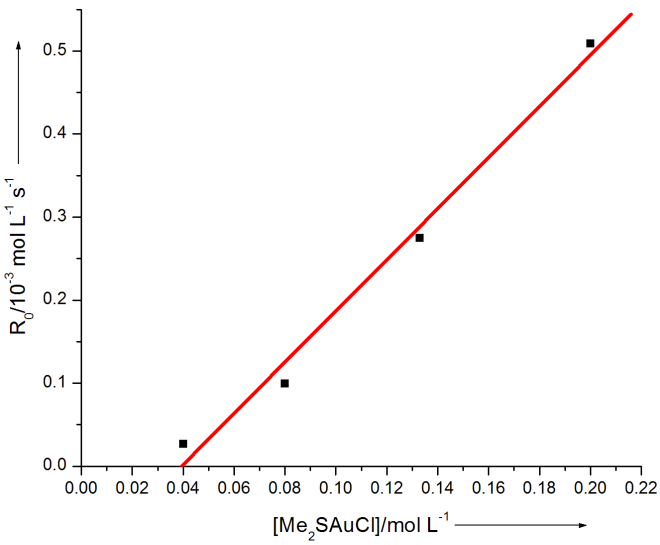

Figure 49. Plot of R_0 versus $[(Me_2S)AuCl]$ at 30 °C (from NMR reactions).

Where $[(Me_2S)AuCl]$ defines the initial concentration of the gold precursor for the reaction of $(Me_2S)AuCl$ and $AgSbF_6$. Over longer periods, the evolution of the yield

with time is non-linear. The negative curvature at longer times is attributed to the depletion of $[Au]^+$ within the reaction.

The observed rate constants (k_{expt}) is determined by plotting the concentration of hexamethylbenzene consumed within the reaction, according to Eq. 5 and shown in Figure 50.

$$ln\frac{[Arene]}{[Arene]_0} = -k_{expt}t \qquad \textbf{(Eq. 5)}$$

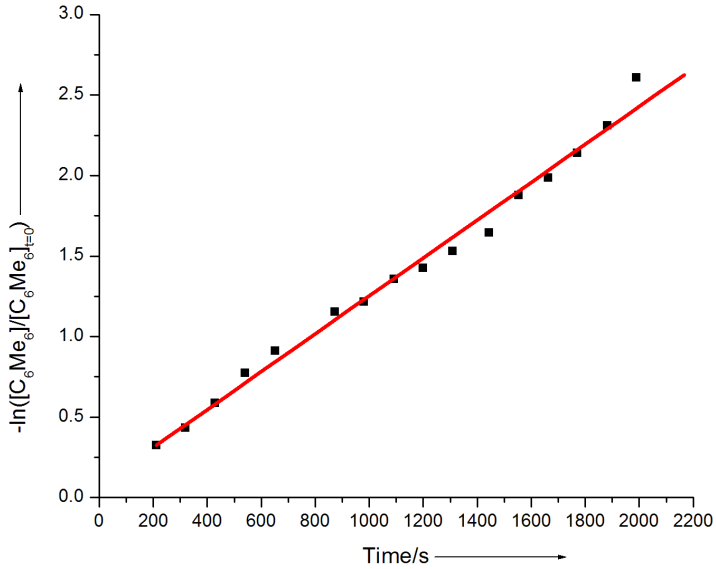

Figure 50. -ln([Arene]/[Arene]$_0$) vs. time (for NMR reaction)**;** C-H activation of hexamethylbenzene; 0.048 mmol $(Me_2S)AuCl$ and $AgSbF_6$, 0.082 mmol C_6Me_6, 30 °C, k_{expt} = 1.24 × 10^{-3} s^{-1}.

Table 8. Obtained values of k_{expt} by NMR spectroscopy from the C-H activation of hexamethylbenzene.

Entry	**Concentrations of reactants /mmol, in 0.6 mL $CDCl_3$)**			**Temperature /°C**	**k_{expt} /10^{-3} s^{-1}**
	[C_6Me_6]	**[$(Me_2S)AuCl$]**	**[$AgSbF_6$]**		
1	0.082	0.048	0.048	20	0.89
2	0.082	0.048	0.048	25	1.07
3	0.082	0.048	0.048	30	1.25
4	0.082	0.048	0.048	35	1.34
5	0.082	0.048	0.048	40	1.49
6	0.130	0.048	0.048	20	0.89
7	0.130	0.048	0.048	25	1.11
8	0.130	0.048	0.048	30	1.23
9	0.130	0.048	0.048	35	1.37
10	0.130	0.048	0.048	40	1.50
11	0.095	0.080	0.080	30	2.07
12	0.095	0.025	0.025	30	0.76

The 1st order dependence of the active gold species was confirmed when the increase or reduction in the concentrations of $(Me_2S)AuCl$ and $AgSbF_6$ results in an equivalent change in k_{expt}. (Table 8, Entries 11 and 12).

Arrhenius and Eyring plots were constructed as shown in Figure 51. The plots are linear and yields the thermodynamic values: E_a = 4.58 (± 0.44) kcal mol^{-1}, $\Delta H^{\ddagger}$ = 4.02 (± 0.42) kcal mol^{-1} and $\Delta S^{\ddagger}$ = -32 (± 24) cal K^{-1} mol^{-1}.

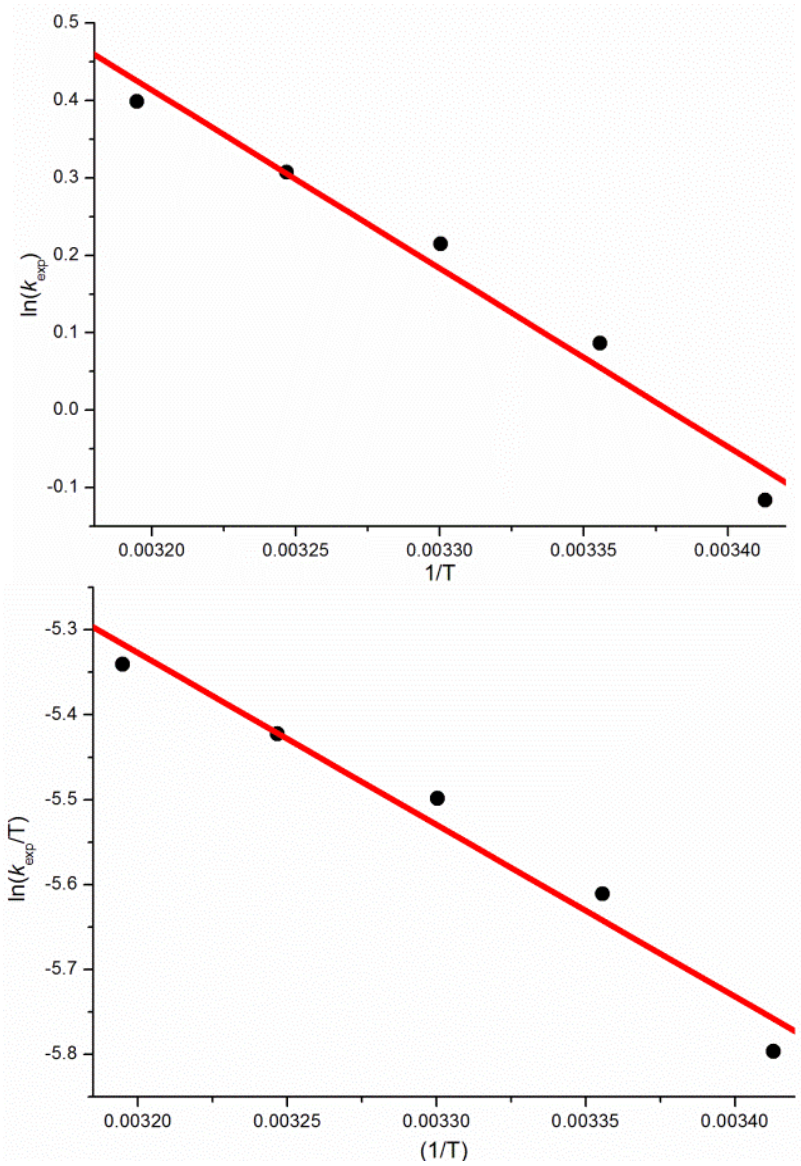

Figure 51. Arrhenius (top) and Eyring (bottom) plots of the activation of hexamethylbenzene determined from NMR reactions.

Monitoring the conversion of C_6Me_6-d^{18} to $[ArCD_2S(C\boldsymbol{H_3})_2]^+$ (δ 2.87) by ^1H NMR spectroscopy at varying temperatures provided a value for KIE at $k_H/k_D \approx 3.5$

(Table 9). This value is consistent with the breaking of a C-H bond in the rate limiting step.[194]

Table 9. Obtained values of k_{expt} by NMR spectroscopy from the C-H activation of hexamethylbenzene-*d*[18].

Entry	Concentrations of reactants /mmol, in 0.6 mL $CDCl_3$			Temperature /°C	k_{expt} /10^{-3} s^{-1}	k_H/k_D
	$[C_6Me_6\text{-}d_{18}]$	$[(Me_2S)AuCl]$	$[AgSbF_6]$			
13	0.090	0.048	0.048	20	0.25	3.57
14	0.090	0.048	0.048	30	0.34	3.67
15	0.090	0.048	0.048	40	0.44	3.40

Since each C-H bond activation is accompanied by formation of H^+ (in the form of $HSbF_6$), the reaction can also be independently monitored by pH measurements (Figure 52 and Table 10); the rate constants obtained by this and the NMR method are in close agreement.

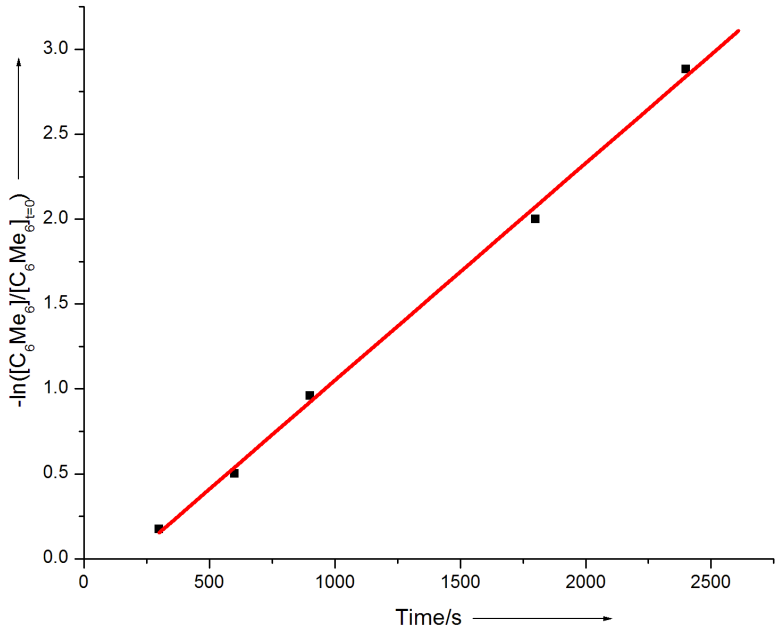

Figure 52. C-H activation of C_6Me_6 (CH_2Cl_2, 30 °C) determined from the pH change, $k = 1.28 \times 10^{-3}$ s^{-1}.

Table 10. Obtained values of k_{expt} by pH measurements from the C-H activation of hexamethylbenzene.

Entry	Concentrations of reactants /mmol, in 50 mL CH_2Cl_2			Temperature /°C	k_{expt} /10^{-3} s^{-1}
	$[C_6Me_6]$	$[(Me_2S)AuCl]$	$[AgSbF_6]$		
16	0.25	0.25	0.25	20	0.94
17	0.25	0.25	0.25	30	1.28
18	0.25	0.25	0.25	40	1.54
19	0.50	0.50	0.50	30	1.65

3.3.3 Possible Mechanisms of Benzyl C-H Activation

From observations, it is clear to see that a two-electron oxidation of the arene substrate occurs to form resonance-stabilized carbocations, followed by thioether coordination. It is unclear on the nature of the gold cation that activates the benzylic C-H bond ($[(Me_2S)Au]^+$ and solvated Au^+[generated by the ligand exchange equilibrium $2[(L)Au]^+ \rightleftharpoons Au^+ + [(L)_2Au]^+$] have been considered) is responsible for the activation process. In principle, there is the possibility that Au^+ disproportionates: $3Au^+ \rightarrow 2Au^0 + Au^{3+}$, to give Au^{3+} as the active species. Such an ion would, however, react preferentially with SMe_2 and, as is known for Au(III), lead to aryl ring metalation;[106,114a,115,116] none of these products are observed.

There was no evidence for the formation of gold π-complexes or benzylgold species. Monitoring the reaction by EPR spectroscopy failed to detect any involvement of radical species. It is clear from the yields obtained that a simple auration at the benzylic carbon is not the process that is observed. Two reaction pathways have been considered in the synthesis of the benzyl-sulfonium cations (Scheme 42):

The first is by the formation of a benzyl radical intermediate, initiated by an electron transfer from a gold(I) cation. The proposed activation by the solvated Au^+ cation gains some support from the reaction of Au^+ ions with benzene in the gas phase, which has been shown to proceed both by $Au(\eta\text{-}C_6H_6)^+$ and to Au^0 + $[C_6H_6]^{\bullet+}$.[41]

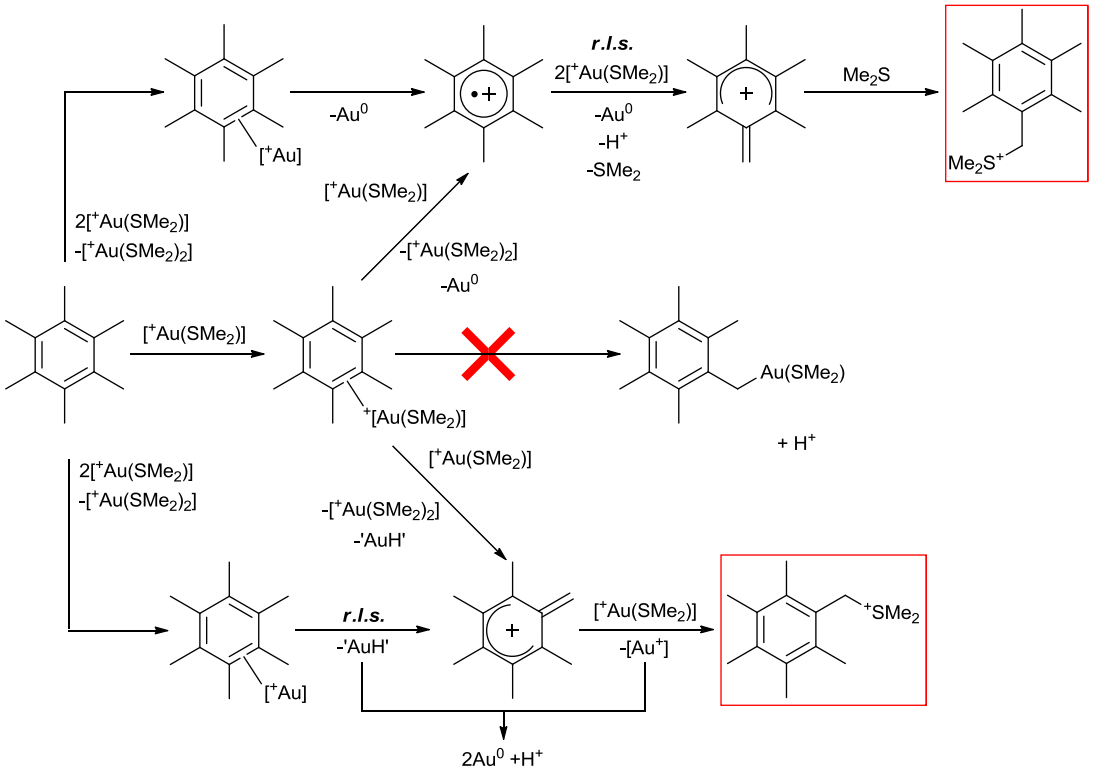

Scheme 42. Possible reaction mechanisms for the activation of hexamethylbenzene

The second refers to the oxidative C-H activation of hexamethylbenzene by Au^+, which has certain aspects in common with Shilov's oxidation of alkanes to alcohols. As stated in section 3.2.1.3, two possible mechanisms for such activation are the oxidative addition of Ar-H to give a platinum alkyl and the oxidation of a side-on bonded alkane complex (Scheme 43).[175a]

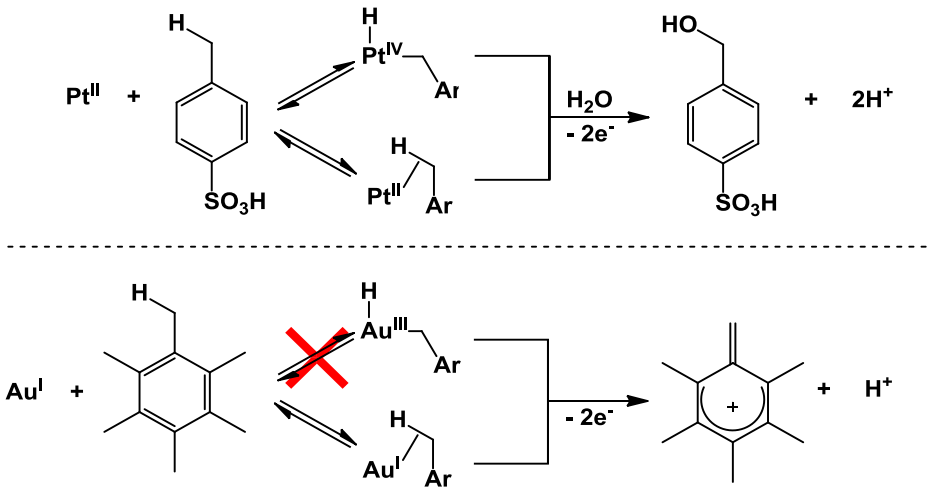

Scheme 43. A postulated activation of hexamethylbenzene by gold(I) from those seen by the Shilov system.

Gold is unable to undergo a oxidative addition-type activation under the mild conditions imposed, suggesting C-H activation could occur *via* the benzyl-auration step; the mechanistic similarities with the Shilov system are evident in Scheme 43, even though the Shilov system works under much more drastic conditions in acidic aqueous media at elevated temperatures (>100 °C).[175a,195,196]

3.3.4 Reactivity with Other Electron-Rich Substrates

Surveying a range of aromatic substrates revealed that the C-H activation is highly selective and *exclusively involves the benzyl CH_3 groups*, the C-H bonds of the arene ring remain unactivated (Table 11 and Figure 53).

Table 11. C-H Activation of methyl-substituted arenes.[a]

Entry	$^{Me}ArCH_3$	$[MeArCH_2SMe_2]^+$	Conversion (%)[b]
1[c]	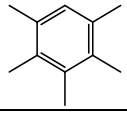	$[o\text{-}C_6Me_4CH_2SMe_2]^+$ **24a**	16.8
		$[m\text{-}C_6Me_4CH_2SMe_2]^+$ **24b**	9.6
		$[p\text{-}C_6Me_4CH_2SMe_2]^+$ **24c**	6.7
2	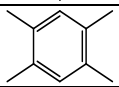	$[Me_3H_2C_6CH_2SMe_2]^+$ **25**	33

a - Reaction conditions: $ArCH_3$ (0.5 mmol), $(Me_2S)AuCl$ (0.5 mmol), $AgSbF_6$ (0.5 mmol) in CH_2Cl_2 (15 mL), 1 h. [b] Yields determined by ^1H NMR spectroscopy, relative to initial $ArCH_3$.[c] Conditions: 0 °C, 3 h.

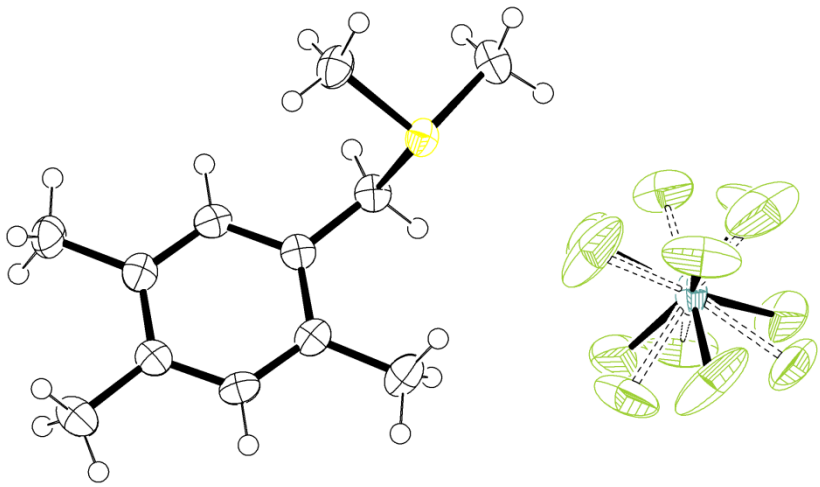

Figure 53. Crystal structure of **25**, with a disordered SbF_6 anion. Ellipsoids are drawn at the 50% probability level.

The oxidation potentials of arenes to their respective radical cations[197] suggest that pentamethylbenzene, 1,2,4,5-tetramethylbenzene (durene) and 1,2,3,5-tetramethylbenzene may be susceptible to oxidative activation by $[Au]^+$, while mesitylene, *o*-, *m*-, *p*-xylenes and toluene may not. These predictions have been borne out by our observations. Values for the Au^+/Au^0 couple in dichloromethane solvent are lacking. The standard potential for Au^+/Au^0 in aqueous acid of +1.83 V (vs. standard hydrogen electrode, SHE) compares with those of hexamethylbenzene (+1.34 V), pentamethylbenzene (+1.45 V), and tetramethylbenzenes (+1.51−1.58 V) in acetonitrile vs. SHE.

While hexamethylbenzene and durene react at 20 °C, pentamethylbenzene required cooling to 0 °C for quantitative C-H activation to take place, giving a mixture of *o*-, *m*- and *p*-regioisomers in a ratio 51:29:20. No reaction was observed with mesitylene, 1,2,4-trimethylbenzene, *o*- and *p*-xylene, or toluene. With the redox potentials for these aromatics previously established,[197] a relationship between reactivity of the methylated arenes with $[Au]^+$ and their redox potentials (under ambient acetonitrile conditions) can give an approximation of the redox potential for the gold cation in this solvent. From the data provided in Table 12, the redox potential of the gold cation in the above reaction is between the range of +1.51 and +1.67 V (vs. SHE).

Table 12. The redox potentials of methylated arenes in MeCN (vs. SHE).

Arene		E_{ox} **/V MeCN**
Benzene		+2.24[197a]
Toluene		+2.02[197a]
Xylene:	*o*-	+1.85[197a]
	m-	+1.86[197a]
	p-	+1.77[197a]
Trimethylbenzene:	1,3,5-	+1.81[197a]
	1,2,4-	+1.67[197a]
1,2,4,5-Tetramethylbenzene		+1.51[197a]
Pentamethylbenzene		+1.45[197b]
Hexamethylbenzene		+1.34[197b]

The relative reactivity of methyl-substituted arenes was probed by competition experiments, using equimolar mixtures of (i) hexamethyl- and pentamethylbenzene (0 °C, 2 h), and (ii) hexamethyl- and 1,2,4,5-

tetramethylbenzene in dichloromethane (RT, 1 h), in the presence of $(Me_2S)AuCl/AgSbF_6$. In each case the activation of C_6Me_6 was strongly favoured, (29.8 % and 1.5 % conversion for reaction (i); 28.8 % and 3.0 % for reaction (ii); in both cases the combined yield was close to the expected value of 33%.

Activation by a naked gold cation proved very sensitive to steric factors and heteroatoms.[198] Studies of the reactions of C_6Et_6 and 1,3,5-$^{i}Pr_3C_6H_3$ by NMR spectroscopy indicated that a reaction occurred, though no single product could be identified or isolated. There was no reaction with 1,3,5-tri-*tert*-butylbenzene, dodecahydrotriphenylene, cumene, pentamethylbenzyl alcohol, or electron-rich methyl-heterocycles such as 9-methylcarbazole or 2,5-dimethylthiophene.

The reaction of dimesitylmethane in our activation system takes a rather different and unexpected path: exposure to $[Au]^+$ in the presence of SMe_2 led predominantly to (sp^3)-(sp^2) C-C bond cleavage (Scheme 44). The major product is $[2,4,6\text{-}Me_3H_2C_6CH_2SMe_2][SbF_6]$ (**26**), accompanied by a small amount of a component derived from C-H activation of the methylene bridge (**27**). Signals consistent with the formation of $[Au(mesityl)]_5$[199] were also observed in the ^1H NMR spectrum of a reaction conducted at -10 °C over a 5 h period. Precedence of such (sp^3)-(sp^2) C-C activations by late transition metals is available, but have only been promoted in an intramolecular fashion to coordinated ligands containing such bonds.[200-203]

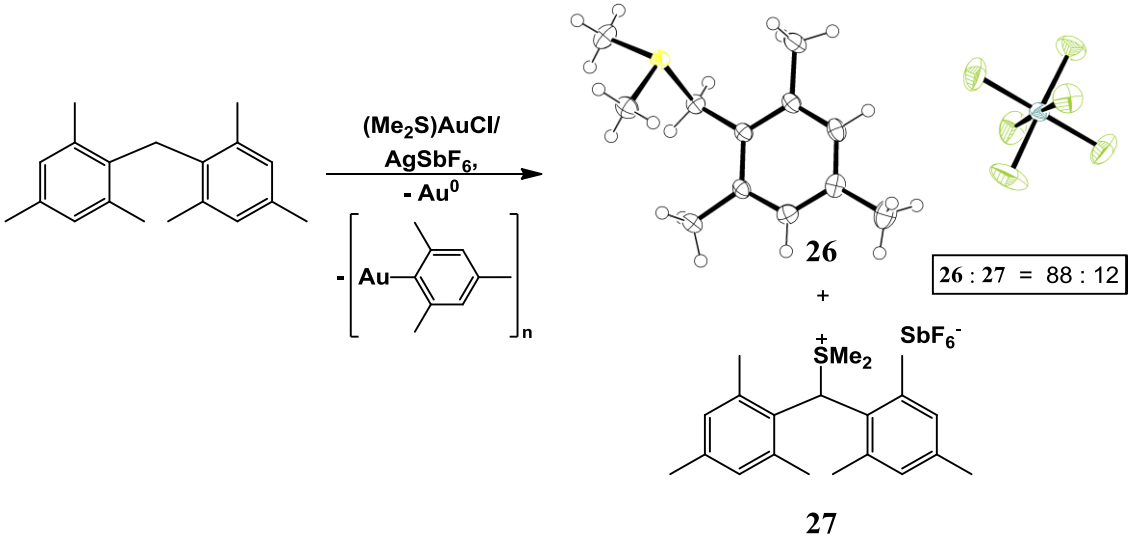

Scheme 44. C-C and C-H activation of dimesitylmethane by $(Me_2S)AuCl/AgSbF_6$. Ellipsoids are drawn at the 50% probability level.

Other electron-rich substrates, such as alkynes were also investigated. Employing $(Me_2S)AuCl$ and $AgSbF_6$ to a dichloromethane solution of phenylacetylene under analogous conditions quickly produced colloidal gold, analysis of the reaction shows free phenylacetylene in the presence of $[Au(SMe_2)_2][SbF_6]$ (**19**). This is believed to be from the instability of either the resulting π-bonded naked gold on acetylene, as cold temperature (-60 → 0 °C) NMR spectroscopy suggests that no C-H activation has occurred to form the gold coupling intermediate $[PhC{\equiv}CAu]^+$. The use of diphenylacetylene shows no reactivity to the gold cation during cold temperature NMR spectroscopic screening.

3.4 Conclusions

In situ generated gold(I) cations in weakly coordinating solvents react with benzylic C−H bonds of multimethylatedbenzenes ($C_6H_nMe_{6-n}$, n = 0, 1, 2) under remarkably mild (0−20 °C), non-acidic and non-aqueous conditions. The reactions proved highly selective for benzyl- over aromatic C-H activation. Unusually activation of dimesitylmethane preferentially proceeds *via* the C-C bond of the bridging carbon over sp^3-C-H activation bond. The reactivity of gold(I) cations differ in this respect from other electrophilic heavy-metal ions such as Ag^+, Tl^+, and Hg^{2+}, which readily form arene π-complexes; and from $AuCl_3$, which metallates arenes to give $[(aryl)AuCl_2]_2$. The observations are consistent with the formation of carbocationic intermediates, which are quenched by thioethers. Mechanistic and kinetic studies of these activation pathways are so far inconclusive, but evidence of important mechanism steps has been found.

4 - General Chemistry of Gold(I) and Gold(III)

4.1 Topic 1: Zwitterionic Complexes of Gold(I)

4.1.1 Introduction

With many organic transformations of electron-rich bonds mediated by cationic gold(I) catalysts or activated precatalysts, the accompaniment of an independent, weakly-coordinating anion to stabilise the cationic intermediates as an ion-pair have been found to play an important role within the catalytic cycle.[204,205] The polar nature of these cationic gold complexes means that their use does have disadvantages: their poor solubility in low-polarity solvents, inactivity in strongly basic ones and control of the counterion within mechanistic cycle is non-existent.[205]

Zwitterionic catalysts (neutral inorganic or organometallic catalysts comprising of a cationic metal centre supported by an outer-sphere counterion within the ligand manifold) have recently been explored for the identification of key reactive intermediates in catalysis. The benefits of zwitterionic complexes over their cationic equivalents have been explored in both metallocene[204] and platinum group[205] catalysts. The reviews found that the use of such zwitterionic complexes over their cationic alternatives benefitted from an increased solubility in non-polar solvents, control of a formal charge separation within the complex and the spectroscopic identification of important catalytic steps, whilst keeping activities high. In addition, a select number of cases have shown a divergence of the reaction to produce novel compounds from those observed in cationic catalyst-mediated processes (Scheme 45).[206]

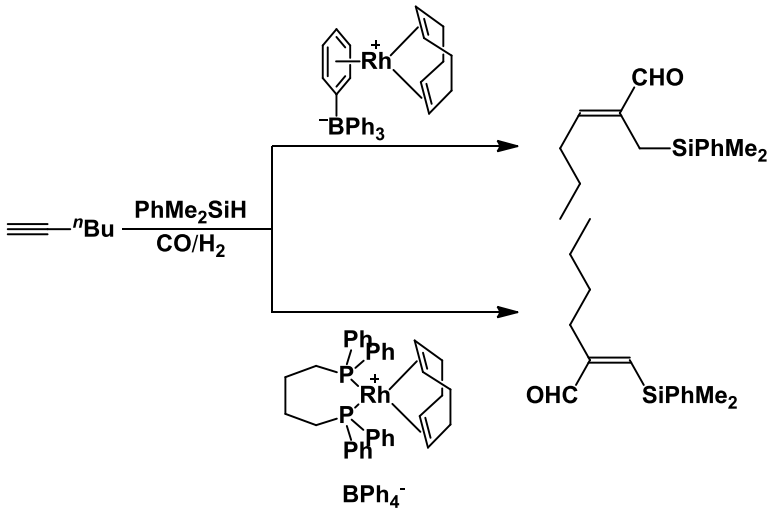

Scheme 45. An example of divergent product selectivity for the cationic and zwitterionic rhodium catalysts (1 mol %) in the silylation of terminal alkynes.[206]

4.1.1.1 Examples of Zwitterionic Gold Complexes

There are a number of examples of zwitterionic gold complexes available in literature, with their syntheses described below. The ligand [Et-NH(S)$Ph_2PN^+PPh_2C(S)N^-$Et] has been treated with coinage metal salts to give the complexes **LXXXIX-XCI** (Scheme 46), where a contrast in chelation is observed. The copper complex **LXXXIX** coordinates *via* κ^3-*S,N,S* chelation, with a Cu-N bond exhibiting ionic character. The silver derivative **XC** has been structurally characterised as a dimer; the ligand coordinates to the metal centres in both terminal and bridging modes with a four-membered planar Ag_2S_2 core. Only for the gold complex **XCI** was a zwitterionic species isolated; coordination to two sulfur atoms in a linear κ^2-*S,S* fashion gives rise to an eight-membered chelation ring.[207]

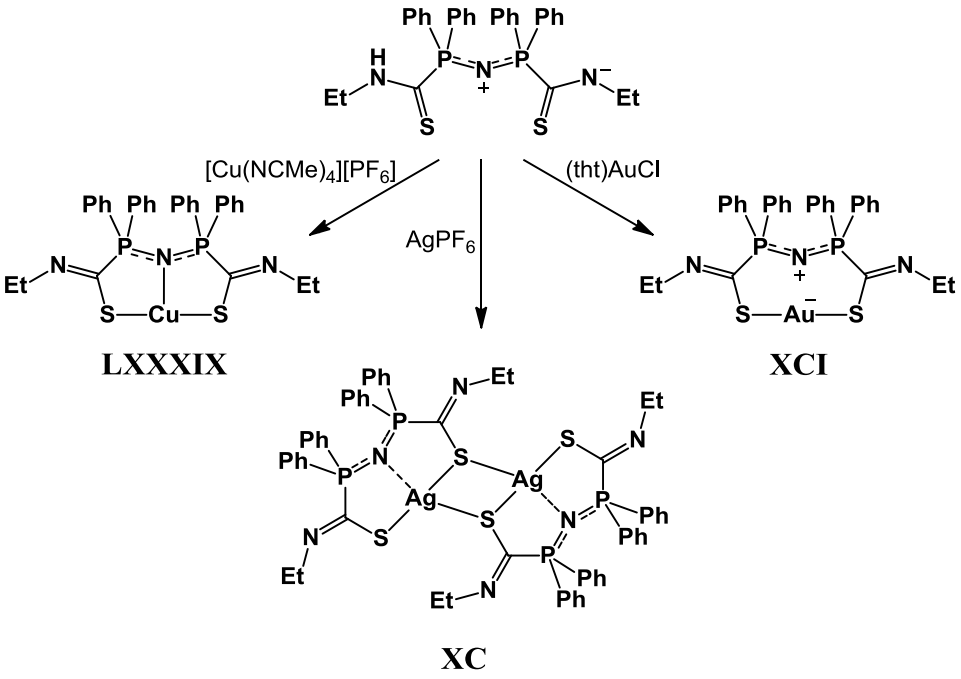

Scheme 46. The complexes of the type M[EtSNS], M = Cu, Ag and Au.[207]

The coordination chemistry of ambiphilic ligands (ligands containing one or more traditional donor groups in addition to a Lewis acidic element) has been explored by several groups.[208] Examples of Au(I) compounds include **XCIIa-d**[29a,209] and **XCIII**[210] (Figure 54). Both sets of complexes comprised of a gold atom coordinated to both phosphine sites in a linear fashion, but for **XCIII**, chloride transfer from gold to the Lewis acidic centre results in the formation of a gold zwitterion. Further exploration of **XCIV** in differing polarity solvents shows an interconversion between the neutral (**XCIV$_N$**) and zwitterionic (**XCIV$_{ZI}$**) was observed within NMR timescales.[211]

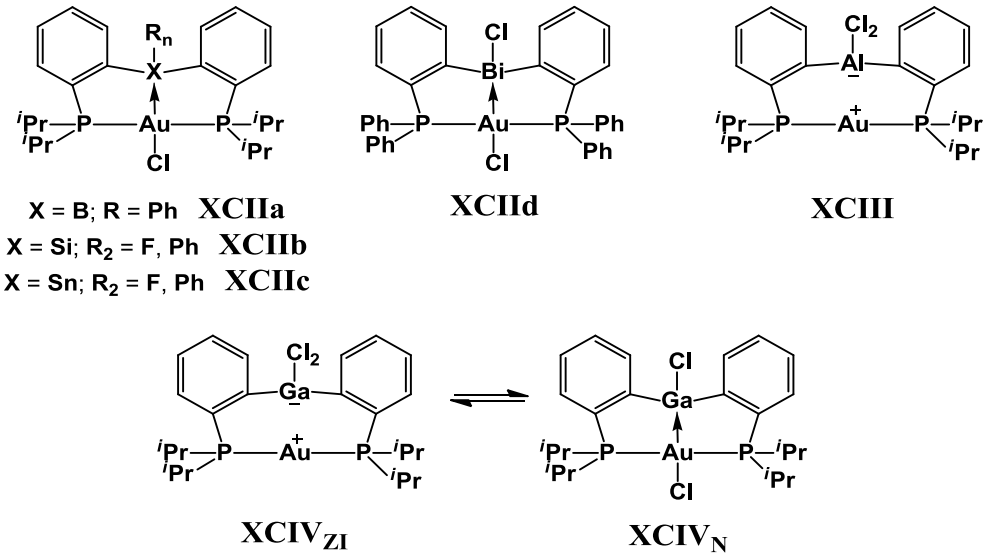

Figure 54. Neutral and zwitterionic complexes containing ambiphilic ligands.[29a,209-211]

A zwitterionic gold(III) complex has been described by Stradiotto *et al.* (Figure 55); the reaction of $[Me_2AuCl]_2$ with a lithium salt of **XCV-H** gives the square planar complex **XCVa**. The carbocyclic framework in **XCVa** exhibits a more delocalised structure consistent with a 10 π-electron indenide anion, unlike the platinum derivative **XCVb** which has localised C-C and C=C bonds.[212]

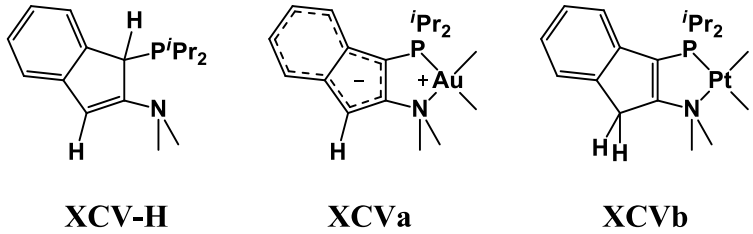

Figure 55. Neutral Pt(II) and zwitterionic Au(III) supported by a *P*,*N*-functionalised indene ligand.[212]

The zwitterionic compound **XCVa** is resistant to hydrolysis, as the anionic bidentate ligand coordinates strongly to the $AuMe_2^+$ fragment.[212] Unfortunately due to the requirement for strongly donating neutral ligands to stabilise the gold cation, the zwitterionic gold complexes **XCII**, **XCIII**, **XCIV** and **XCVa** are inactive in catalysis.

4.1.2 The Aim for Zwitterionic Gold(I) Catalysis

Our objective was to try to develop a zwitterionic gold species which incorporates an anionic *o*-(diphenylphosphine)benzylsulfonate chelate ligand (**28**$^-$), previously used with other late transition metals for applications, which include as water-soluble and biphasic catalysts for olefin polymerisation (Ni, Pd), regioselective functionalisation (Ru) and coupling reactions (Pd).[213-215] Since most Au(I) catalysts are generated *in situ* from gold chloride complexes and silver salts, it was hoped to generate a family of relatively stable chloride- and silver-free "single component" catalysts for transformations of electron-rich organic bonds.

The reaction of the sulfonated phenylphosphine ligand **28-H** or its metal salt **28-M** with $(R_2S)AuCl$ was to be tested as a route to synthesising gold(I) zwitterionic complexes (Scheme 47). With the known linear conformation of gold(I) centres, combined with its poor affinity with anionic oxygen centres, a stable dimer or macrocyclic aurate ring would be expected to be isolated. If the zwitterionic complex is stable, an initial screening of its catalytic properties would also be attempted.

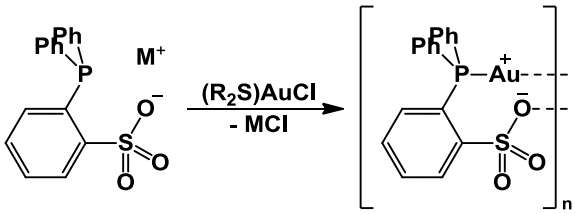

Scheme 47. Proposed zwitterionic gold(I) complex stabilised by an *o*-(diphenylphosphine)benzylsulfonate chelate.

4.1.3 Results and Discussion

4.1.3.1 Transmetallation Precursors

The synthesis of the sulfonated arylphosphine was based on the procedure by Claverie *et al.*[215e] The dilithated salt of toluenesulfonic acid was treated with diphenyl(chloro)phosphine to give 2-$(Ph_2P)C_6H_4SO_3H$ (**28-H**). The potassium and silver salts **28-K** and **28-Ag** were synthesised in quantitative yields by the addition

of potassium hydride or silver oxide into dichloromethane solutions of **28-H** (Scheme 48).

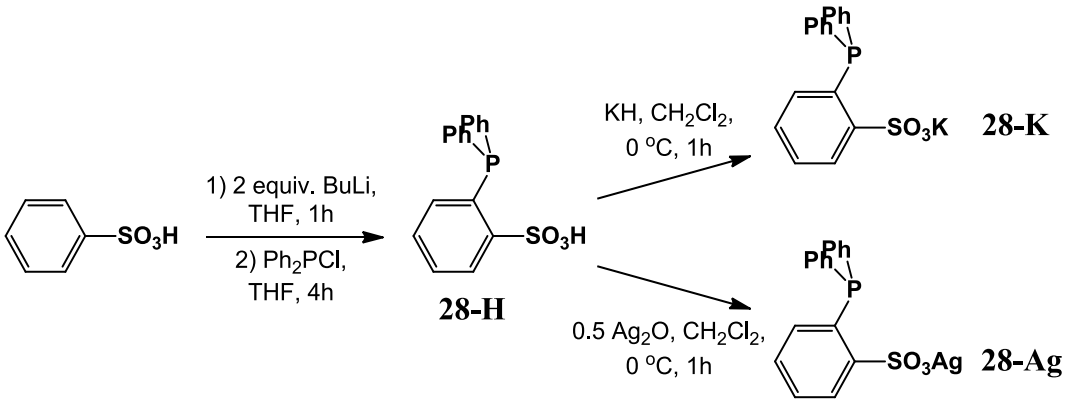

Scheme 48. Reaction scheme for the synthesis of **28-K** and **28-Ag**.

4.1.3.2 Auration of 2-(Ph_2P)$C_6H_4SO_3M$ (M = K, Ag)

The addition of (tht)AuCl to a dichloromethane solution of **28-H** resulted in two reaction products, indicated by two signals in the ^{31}P NMR spectrum at 41.9 and 33.8 ppm (in approx. ~2:1 ratio). It has proved not possible to purify the mixture by recrystallisation. On the other hand it was found that the treatment of the potassium (**28-K**) and silver (**28-Ag**) salts with (tht)AuCl gave a single, but differing product each.

The addition of (tht)AuCl with **28-K** in THF did not precipitate KCl as expected. After isolation, ^{1}H NMR spectroscopic analysis indicated loss of tetrahydrothiophene. These factors gave a tentative assignment to a non-zwitterionic, bimetallic gold-potassium complex **29** (Scheme 49).

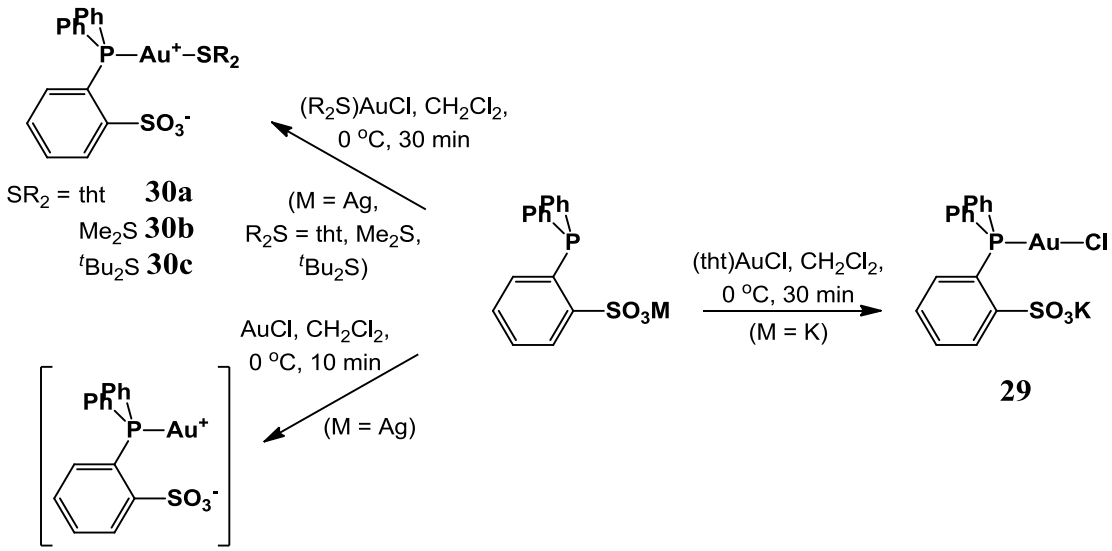

Scheme 49. Synthesis of gold(I)-sulfonated diphenyl(aryl)phosphines, **29** and **30a-c**.

Colourless crystals were grown by slow evaporation of a chloroform-*d* solution containing **29**, with X-ray diffraction studies confirming the heterobimetallic nature; the potassium cation was incapable of abstracting the chloride from gold (Figure 56). The unit cell contains two molecules of **29** in alternating directions, accompanied by a chloroform-*d* molecule. The gold centre coordinates in an essentially linear fashion.

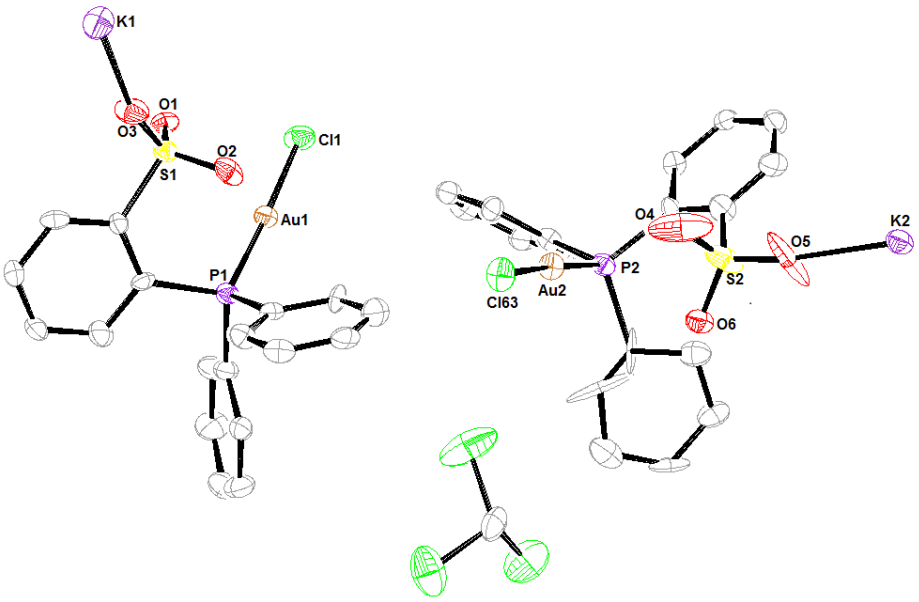

Figure 56. The molecular structures of two independent molecules of **29**, showing a partial atomic labeling scheme (hydrogens have been omitted). Ellipsoids are drawn at the 50% probability level. Selected bond lengths (Å) and angles (°):(Au(1)-P(1) 2.225(3), Au(1)-Cl(1) 2.259(4), Au(2)-P(2) 2.227(3), Au(2)-Cl(63) 2.298(4) Å; P(1)-Au(1)-Cl(1) 175.77(12), P(2)-Au(2)-Cl(63) 176.37(12)°.

In combination with adventitious water uptake in partial occupancies (O(7) 82% and O(8) 54% occupancy), Ar–SO_3^-, OH_2 and K^+ moieties contribute to an intricate network of intra- and intermolecular linkages between molecules of **29**. This results in a supramolecular column, with a core consisting of K-O bonds within the range of 3.10-3.35 Å. The Ar_3P-Au-Cl moieties are in a twofold screw-axis symmetry operation, with the P-Au-Cl bonds running parallel to the outer surface of the column (Figure 57). The two molecules of **29** in each asymmetric unit contribute to two different column structures running in parallel with each other, with the cross-section showing the two different environments of Au(1) and Au(2) within the column (Figure 58).

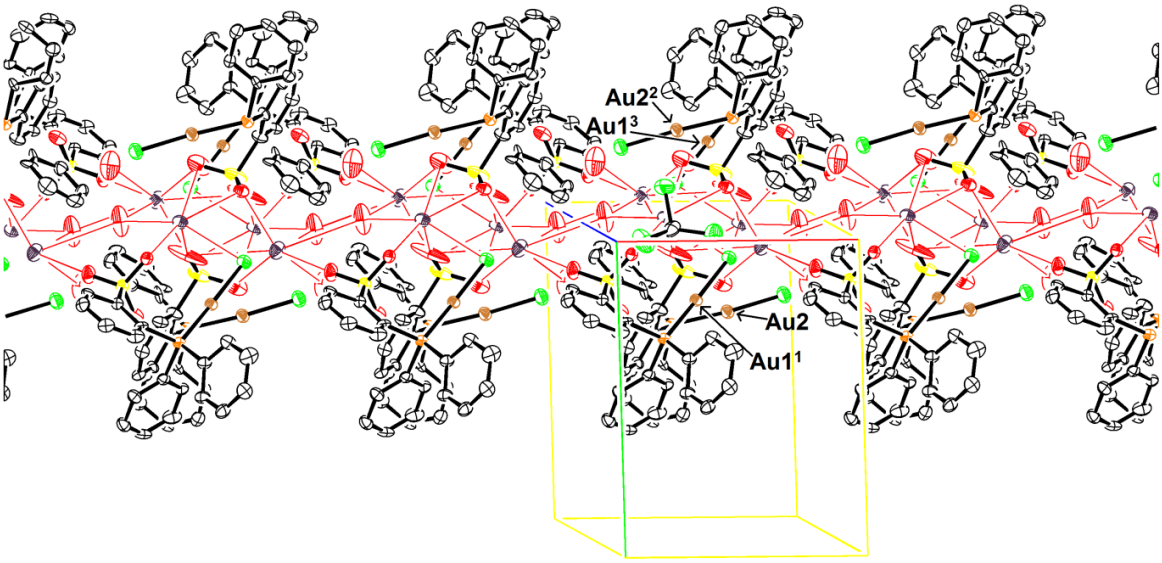

Figure 57. The supramolecular column of **29**, with hydrogen bonding highlighted red. (hydrogens have been omitted). Ellipsoids are drawn at the 50% probability level.

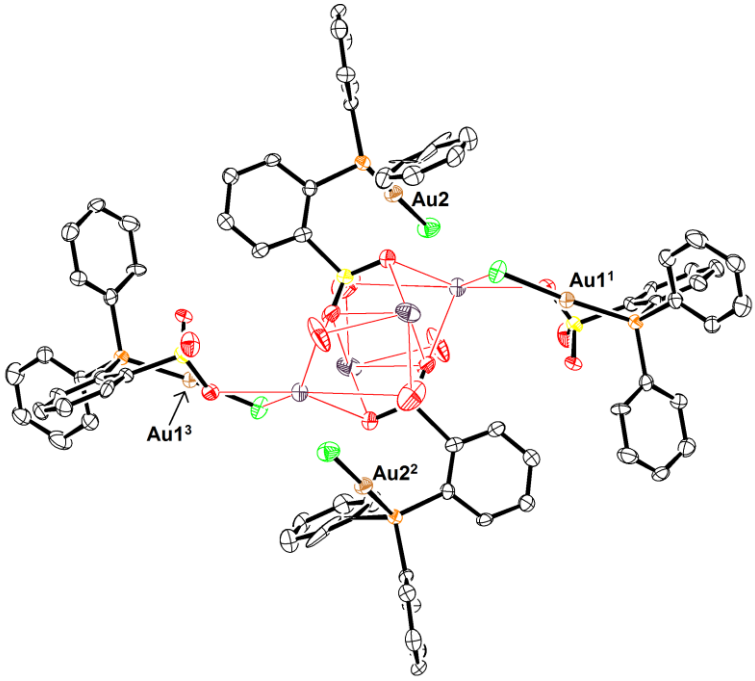

Figure 58. A view through the cross-section of the column in Figure 57. (hydrogens have been omitted). Ellipsoids are drawn at the 50% probability level.

With this configuration, intramolecular connections of K···Au and K···Cl are apparent, as their distances are significantly shorter than the sum of the van der Waals radii of these atoms (Figure 59; selected distances in Å; Cl(1^2)···K(1) 3.116(5), Cl(1^2)···K(2) 3.176(5), Cl(63^1)···K(2) 3.312(5), Au(2^1)···K(2) 3.495(3); sum of van der Waals radii = 4.5 and 4.41 Å, for K···Cl and K···Au, respectively).

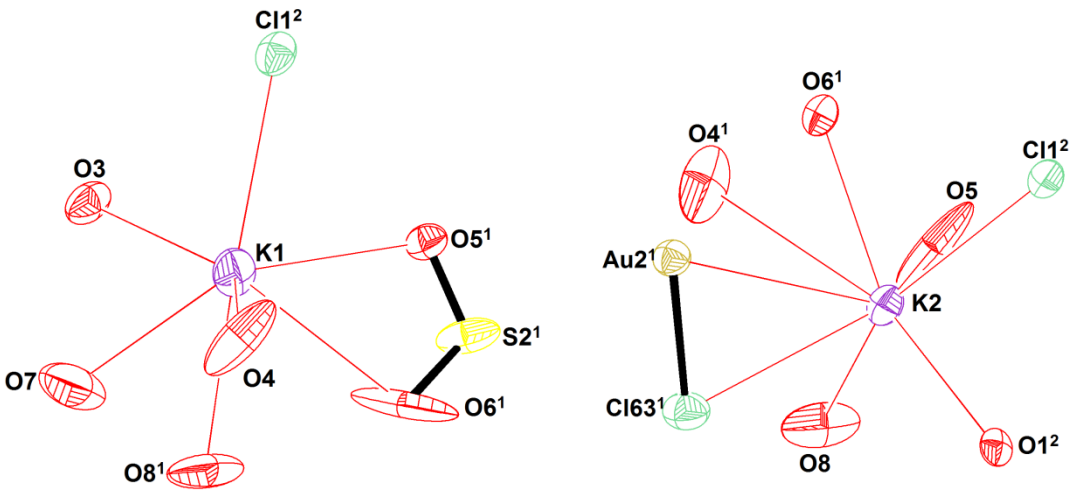

Figure 59. Spheres of enclosures set at 3.5 Å for the potassium cations K(1) and K(2); they exhibit a mix of intra- and intermolecular interactions within the lattice.

Treating **28-Ag** with $(R_2S)AuCl$ (R_2S = tht, Me_2S, $^tBu_2S$) in THF yielded colourless solutions as well as a white precipitate, which after a short exposure to light turned a purple hue; indication of the decomposition of a AgCl byproduct. Filtration and isolation of the colourless solutions produced white powders. NMR spectroscopic analysis of each product revealed the presence of a coordinated thioether within the complex in an equimolar ratio to the phosphine ligand. Elemental analysis confirmed the synthesis of the zwitterionic-type gold(I) complexes of **30a-c** in quantitative yields (Scheme 49). Attempted removal of the sulfides by vacuum evaporation, or ligand exchange with electron-rich organics (phenylacetylene, ethyl propiolate, norbornene, 1,5-cyclooctadiene) were unsuccessful, suggesting that coordination of thioether ligands render **30a-c** catalytically-inert. Crystals of **30b** (R_2S = Me_2S) were grown from a dichloromethane solution layered with light petroleum, but were found to be unsuitable for crystallographic analysis. To date, no information on the supramolecular structure of the family of **30a-c** could be attained.

In an attempt to produce a thioether-free gold zwitterion, **28-Ag** was reacted with AuCl in dichloromethane. This gave initially an off-white powder with ^1H and ^{19}F NMR spectra indicating the possible formation of the zwitterionic complex, [*o*-$(Ph_2PAu)C_6H_4SO_3$]; see Scheme 49. Unfortunately the stability of the new compound was poor and over a three hour period at -30 °C, reduction to gold colloids was seen, indicated by the appearance of a purple hue.

4.1.4 Conclusions

Metallated complexes of the (*o*-diphenylphosphine)benzylsulfonate ligand [*o*-$(PPh_2)C_6H_4SO_3M$ (M = Ag, K)] readily react with $(R_2S)AuCl$ (R_2S = tht, Me_2S, $^tBu_2S$) to form gold(I) phosphine complexes bearing a SO_3^- moiety. It appeared the nature of M produces different products: The potassium salt did not promote halide abstraction, instead forms a bimetallic salt, with its crystal structure describing a supramolecular column with metallophilic Au···K contacts present. The silver salt produces a family of zwitterionic gold complexes stabilised by thioether ligands. These R_2S supports are not labile, resulting in no generation of a vacant site on gold

to promote olefin coordination. Attempts to generate the thioether-free complexes have provided evidence of a poorly stable gold-zwitterion species.

4.2 Topic 2: Luminescence Studies and Anion Coordination of Unsupported Gold-Silver Tetrametallic Clusters

4.2.1 History of Luminescent Heteromultimetallic Clusters

Gold-heterometal complexes incorporating both aurophilic and metallophilic bonding (allowing for aggregation into cluster systems) have given rise to a distinct field of photoluminescent materials with possible uses as sensors and molecular switches.[42b]

These materials are synthesised by an acid-base reaction between basic diaryl- or dialkynyl-aurate centres and other coinage metal cations. The use of copper(I) and silver(I) salts has led to broad families of compounds displaying different structural arrangements, ranging from small clusters, to complex polymeric and supramolecular lattices (Figure 60).[216-220]

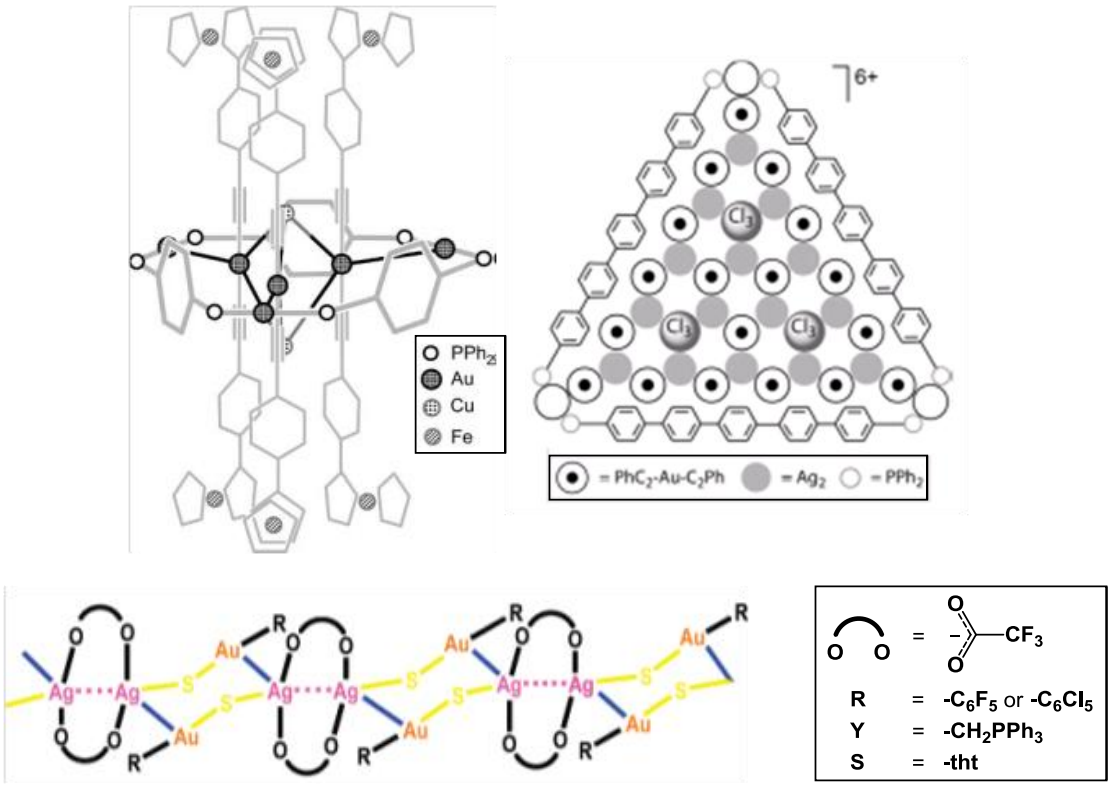

Figure 60. Metallophilic bonding between gold and heterometals (Ag, Cu) governs the shape of clusters isolated.[216e,216k,218e]

Luminescence in heteromultimetallic clusters are influenced by the interactions between the frontier orbitals of the two closed-shell metals (see section 1.3.2). Lowering of the electronic bandgap can lead to emission in the visible region of the spectrum. The origins of emission are by either direct excitation of the M-M frontier orbitals, or metal-metal to ligand charge transfer (MMLCT) as a result of the metals bonding with ligands.[41]

In this chapter introduction, we will focus on describing recent developments in heteromultimetallic clusters of $[R_2Au]^-$ with copper and silver.

4.2.1.1 Structural and Optical Studies on Unsupported $[(C_6X_5)_2Au(I)]\cdots[M]$ Complexes

Heterometallic complexes containing Au···Cu or Au···Ag interactions can be made selectively as linear 1D polymers, or as multimetallic clusters, with the core stabilised by metallophilic bonding.[216-218] These complexes show great diversity in structure, electronic and optical properties (Scheme 50).[217a,219,220] In recent years, $[Au(C_6X_5)_2]^-$ anions have been the target substrate for cluster formation, as the gold(I) centres are sufficiently stabilised by electron-withdrawing perhalophenyl groups to resist reduction. Below describes the research in both cluster and 1D polymer formations of $(C_6F_5)_2Au$-group 11 metal complexes.

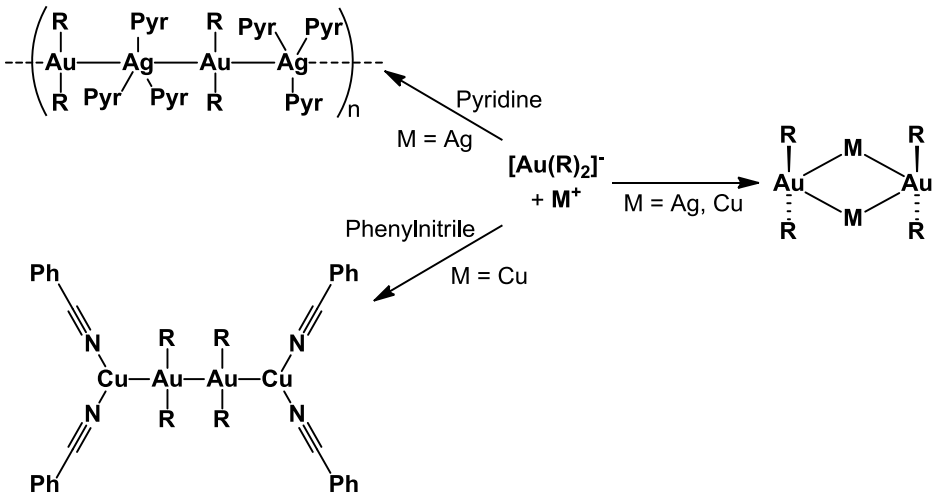

Scheme 50. The formation of differing structures from the reaction of $[R_2Au]^-$ and Cu^+/Ag^+ cations.

For the tetrametal [Au_2Ag_2] clusters which do not incorporate pentafluorophenyl ligands (**XCVI-XCIX**, Figure 61 and Scheme 51), no intermolecular aurophilic bonding were observed.

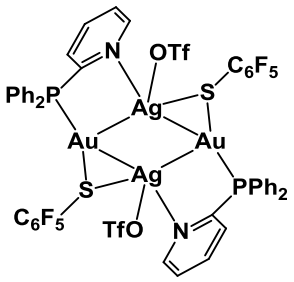

XCVI

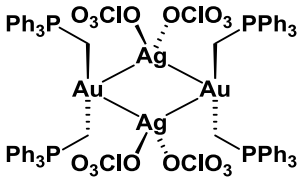

XCVII

Figure 61. Tetrametallic [Au_2Ag_2] clusters which do not incorporate perhaloaryl ligands.[217a,220]

For complexes **XCVI** and **XCVII**, the crystallographic data shows the clusters are monomeric, whereas careful selection of the halogenated silver acetate reacted with **C** can promote the formation of polymeric (**XCVIII**) or monomeric (**XCIX**) clusters.[219]

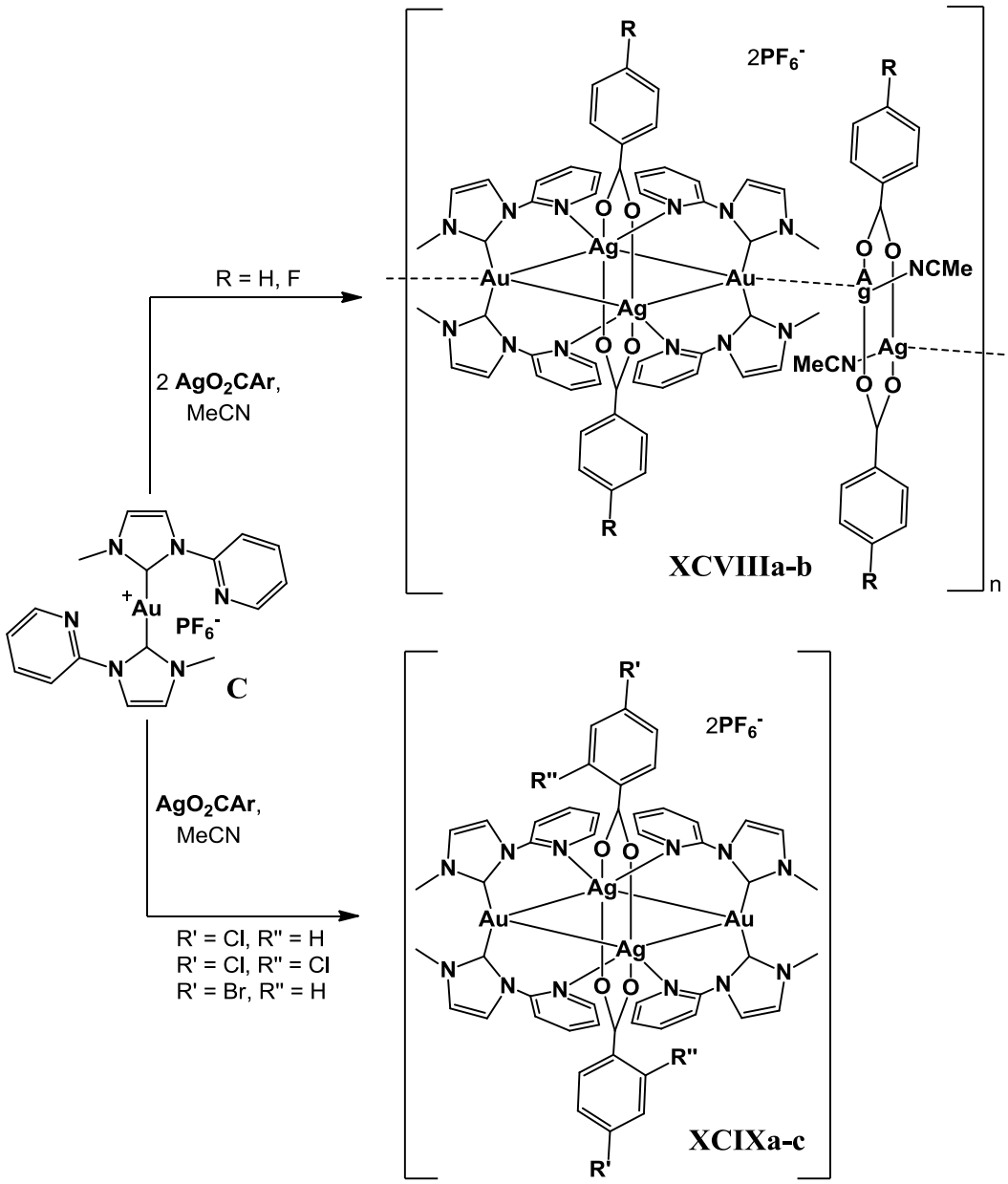

Scheme 51. The synthesis of the $[R_4Au_2Ag_2]$ clusters (**XCVIII** and **XCIX**) with the choice of monomer or polymer formation.[219]

4.2.1.1.1 Tetrametallic $[(C_6X_5)_4Au_2M_2]$ Clusters

In 1981, Usón and co-workers reported the first tetrametallic cluster containing $[Au(C_6F_5)_2]^-$ anionic units.[221] The treatment of $[^nBu_4N][Au(C_6F_5)_2]$ with $AgClO_4$ gave the polymeric product **CI** (Scheme 52), which was the nucleus for a series of communications from the research labs at Universidad de Zaragoza over the last 30 years.

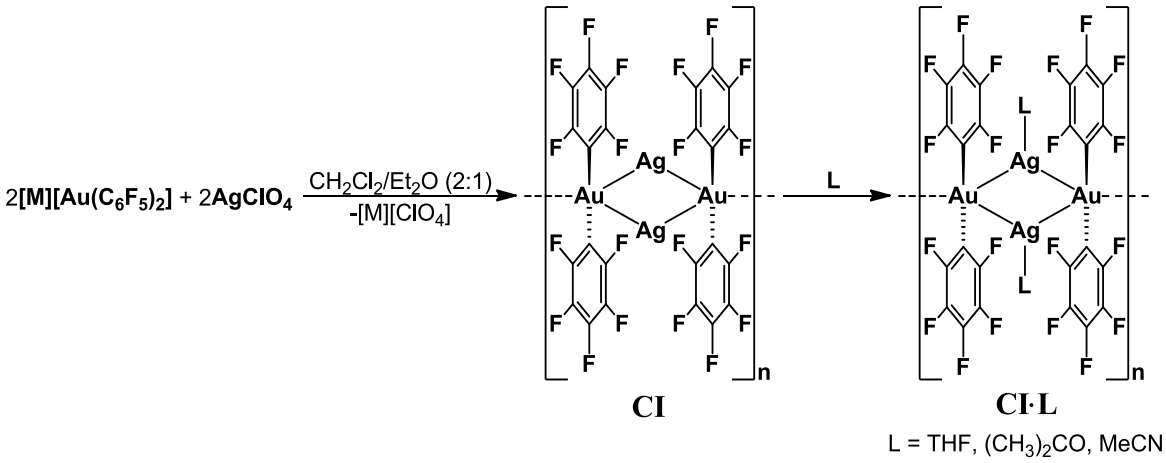

Scheme 52. General reaction scheme for the synthesis of the polymer **CI** and its solvated adducts.[221]

One of the properties of **CI** is vapochromism.[218d,218g] Exposure to vapours of volatile organic compounds (VOCs) such as THF, acetone or acetonitrile (amongst other basic solvents) results in changes in its solid state luminescence when exposed to UV light (Figure 62). These vapochromic complexes have been envisaged for uses as threshold monitors in chemical laboratories, and as environmental sensors of VOCs in the field.[222] Examples of π-coordination of alkynes, alkenes and arenes with the vacant site at the silver cations within the cluster have also been described, but their luminescent properties were not investigated.[221,223]

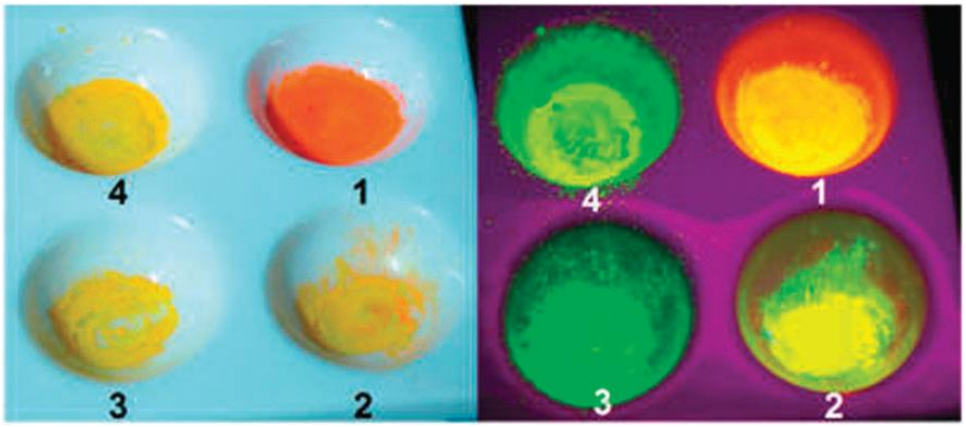

Figure 62. Vapochromism of $[(C_6F_5)_4Au_2Ag_2]$ (**CI**, 1) when exposed to (2) acetone, (3) THF, (4) MeCN.[218d]

Subsequent modification of the perhalophenyl rings has led to the isolation of the $[(C_6X_5)_4Au_2Ag_2]$ clusters **CII-CIV**, which show varying structures and

luminescent behaviours (Scheme 53).[224-226] Transmetallation of **CI** and **CIV** with CuCl yields the analogous $[(C_6X_5)_4Au_2Cu_2]$ clusters **CV** and **CVI**, which exhibit similar structural, vapochromic and luminescent properties to their gold-silver relatives.[218g]

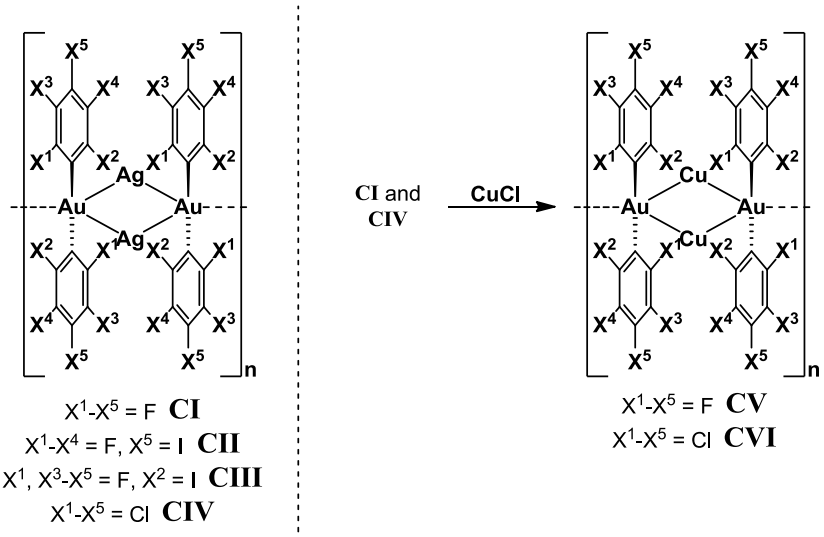

Scheme 53. Synthesis of the $[(C_6X_5)_4Au_2M_2]$ family of clusters.[218g,221,224-226]

All the adducts of **CI·L** described in the literature are found to be polymeric in the solid state; infinite chains based on Au···Au bonding between the gold atoms of neighbouring cluster units.[218d,218g,221-223] In the case of **CII·L**, the crystals of the acetone and acetonitrile adducts gave the polymeric structures akin to **CI·L**, whereas the crystals grown of **CII·THF** from a THF solution gave rise to two different crystal morphologies (red needles and orange blocks). The red needles represented the expected polymer 1D lattice (Figure 63, left), while the orange blocks were of a unit cell containing a molecular $[Au_2Ag_2]$ cluster unit with no intermolecular aurophilic interactions (Figure 63, right). Instead the units are connected to each other by Au···I interactions in a 2-dimensional lattice.[222]

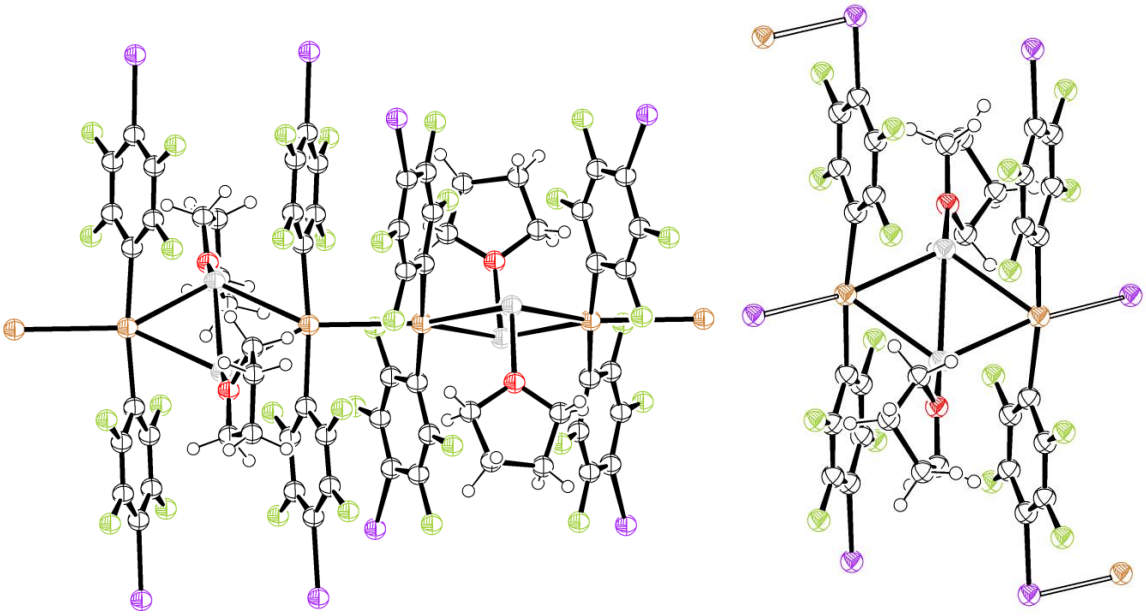

Figure 63. Two different crystal morphologies of $[(4\text{-}C_6F_4I)_4Au_2Ag_2(THF)_2]$ (**CII·THF**) isolated.[225]

In consideration to the cluster **CIII**, a relationship between the extent of intermolecular aurophilic bonding between cluster units and its luminescent colour was established. The incorporation of anionic ligands within the clusters was achieved by the reaction of $[^nBu_4N][Au(2\text{-}C_6F_4I)_2]$ with silver trifluoroacetate to give **CIII·tfa** as a green-luminescing powder. The conversion of **CIII·tfa** to the neutral, yellow-emitting solids **CIII** was promoted by the addition of $[^nBu_4N][ClO_4]$, with acetonitrile addition (by liquid or vapour exposure) producing the red glowing solids of **CIII·NCMe** (Scheme 54).[224] Crystals of **CIII·tfa**, **CIII** and **CIII·NCMe** have been crystallography tested and were found to have a difference in the number of intermolecular aurophilic bonds. The monomeric cluster **CIII·tfa** contains no intermolecular Au···Au contacts, whereas the dimer **CIII** contains a single aurophilic bond and **CIII·NCMe** exist as a 1D polymer chain, promoted by aurophilic bonding.

In comparison to the luminescence signals, the conversion of **CIII·tfa** to **CIII** shifts the emission signature by ~40 nm, with MeCN addition to **CIII** further red-shifts by about 80 nm (Scheme 54) this shift is (at least in part) attributed to the extent of aurophilic bonding observed.[224]

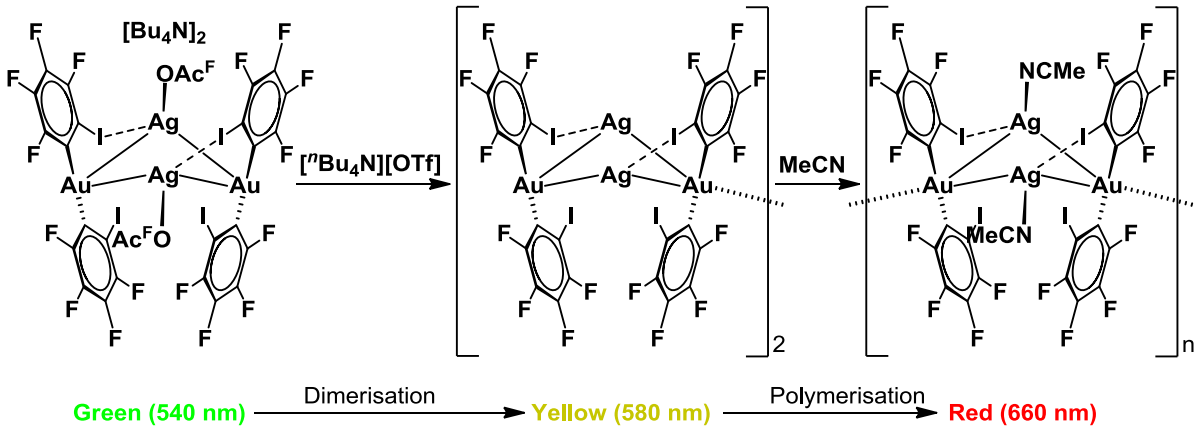

Scheme 54. The emission colours can be used as an indicator of the extent of polymerisation observed in the family of **CIII** clusters.[224]

The butterfly-shaped conformations of the $[Au_2Ag_2]$ cluster core in **CIII·tfa**, **CIII** and **CIII·NCMe** are attributed to the additional internal bonding observed of the Ag^+ cation with the iodine centres present within the cluster.[224]

With the difficulty in assigning the origins of luminescence of heavy metal complexes and clusters, a definitive conclusion for the root cause of the emission in the $[(C_6X_5)_4Au_2M_2]$ cluster systems cannot be given, although spin-allowed fluorescence is tentatively suggested, based on the short lifetimes and small Stokes' shifts observed.[41]

4.2.1.1.2 Linear $[(C_6F_5)_2Au\text{-}M]$ Polymers, Dimers and Monomers

To obtain linear, 1-dimensional polymer chains containing metallophilic interactions, an inclusion of a base is required to inhibit aggregation to clusters. The reaction of $[Au(C_6F_5)_2]^-$ and $[AgClO_4]$ in the presence of excess pyridine gives the formation of $\{[(C_6F_5)_2Au][Ag(Py)_3]\cdot Py\}_n$ (**CVII**; Figure 64).[218h] Single crystal analysis shows an extended, one-dimensional chain of alternating gold and silver ions of $[Au(C_6F_5)_2]$ and $[Ag(Py)_3]$. The combination of Au-Ag ion pairs and π-stacking between pyridine and C_6F_5 ligands gives the linear formation its structural support. No information on its luminescent properties is available.

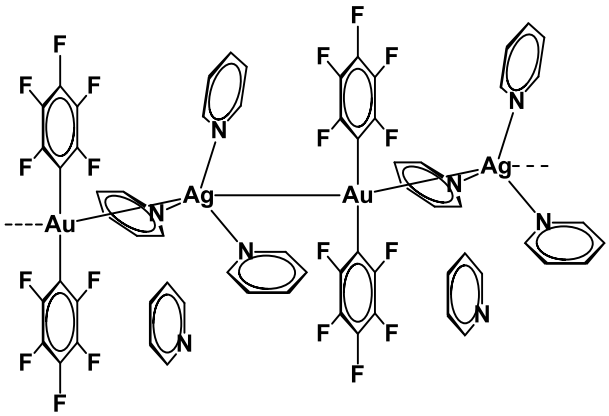

CVII

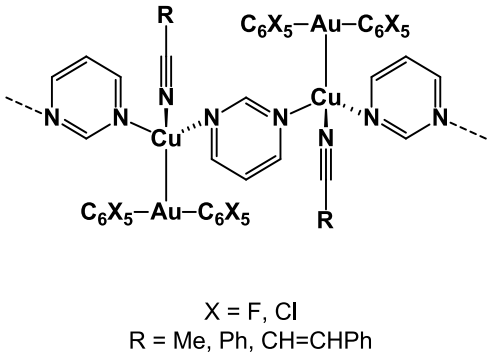

CVIIIa-d

Figure 64. Examples of Au···Ag and Au···Cu bond-containing 1D polymers.[218b,218h,227]

Gold and copper containing polymers are synthesised from the metathesis reaction of **CI·NCMe** or **CIV·NCMe**, CuCl and excess pyrimidine in acetonitrile to give $\{[(C_6X_5)_2Au][Cu(NCMe)(\mu^2\text{-}C_4H_4N_2)]\}_n$ (**CVIIIa-d**; Figure 64). The bridging pyrimidine ligands gave a one-dimensional corkscrew-type polymer. In this case, the Cu···Au interactions do not contribute to the polymer backbone; the $[Au(C_6F_5)_2]$ units are pendants, branched out from the chain (Figure 64).[227] Further studies revealed that the electronic features of the *N*-donor ligand have a profound effect on its photoluminescence properties: Acetonitrile and benzonitrile promote phosphorescence in these clusters whereas the alkene bond-containing cinnamonitrile quenches luminescence, resulting in non-radiative decay.[218b]

Selective control to form discrete bi- and tetrametallic Au···Cu complexes was achieved by treatment of **CI·NCMe** with CuCl in nitrile solvents. This generates monomeric and dimeric complexes containing Coulombic (Au···Cu) and aurophilic (Au···Au) contacts (**CIX** and **CX**; Scheme 55).[218c] The crystals isolated luminesce under UV excitation, with the emission considered to be from spin-allowed fluorescence.

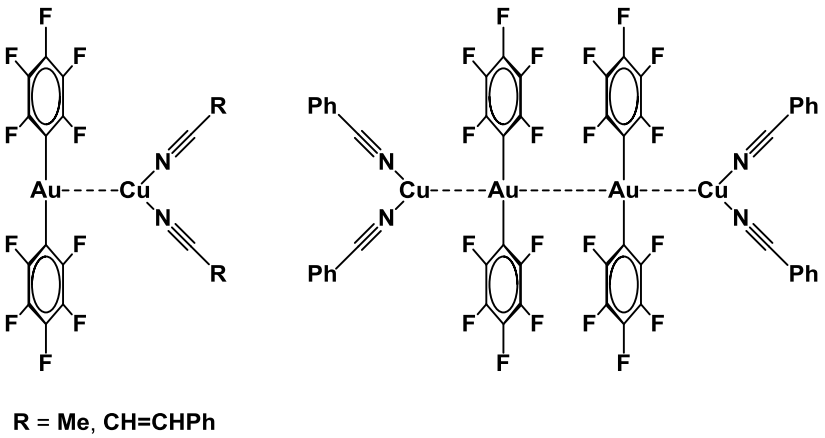

Scheme 55. Structures of **CIX** and **CX**.[218c]

4.2.2 Aims for Developing $[(C_6F_5)_4Au_2Ag_2]$ Luminescence Properties by Anion Addition

Prior to this work, the reactivity of $[(C_6F_5)_4Au_2Ag_2]_n$ (**CI**) with protected amino acid esters (*e.g.* *L*-methylglycinate) were observed, to determine whether coordination of the functional groups of the amino acid esters towards the silver centre was possible, causing a shift in the luminescence signature of the cluster. The work was viewed as the initial steps towards the development of the cluster as possible luminescence sensors for proteins. Unfortunately it was found that the amino acid esters were too labile in the presence of strong donors, but the report disclosed the affinity of nitrate and trifluoroacetate anions towards the cluster, causing a distinct change in its fluorescence signature.[228]

At the time of experimentation, work by Laguna *et al.* on the clusters based on the **CIII** skeleton had not been reported,[224] with investigations into the uses of anions on the $[\{(C_6X_5)_2AuAg\}_2]_n$ clusters unexplored beforehand. The target was to screen the use of numerous silver salts containing weakly basic anions (nitrate, acetate, sulfonate) with $[M][(C_6F_5)_2Au]$ (M = $^nBu_4N$ and Ph_4P) to observe the structural and photoluminescent variations that occur from the resulting complexes. One hope was to be able to correlate anion donor strength of the anion-containing clusters, as measured by Hammett parameters, with the luminescence emission wavelength.

4.2.3 Results and Discussion

4.2.3.1 Synthesis and Characterisation of $[(C_6F_5)_4Au_2Ag_2]$ Clusters Bearing Anions

The nitrate-containing clusters stabilised by bulky, inert cations (M = $^nBu_4N$ **31a**, Ph_4P **31b**) were initially obtained by the reaction of $[M][Au(C_6F_5)_2]$ with $AgNO_3$ in 1:1 molar ratio in $CH_2Cl_2/Et_2O/MeOH$ (2:2:1 ratio). The trifluoroacetate complexes (M = $^nBu_4N$ **32a**, Ph_4P **32b**) were synthesised from AgO_2CCF_3 and $[M][Au(C_6F_5)_2]$ in CH_2Cl_2/Et_2O (1:1). The triflate-coordinated compounds (M = $^nBu_4N$ **33a**, Ph_4P **33b**) were the products of the addition of AgOTf to $[M][Au(C_6F_5)_2]$. Evaporation of the solvents gave brightly coloured powders which luminesced under a UV lamp. The colouration and luminescence suggested the formation of a polymer (based on aurophilicity between $[(C_6F_5)_4Au_2Ag_2]$ units) with coordination of the anions perturbing colours seen for the neutral $[(C_6F_5)_4Au_2Ag_2]$ complex.[218d]

We found that all of these compounds could be obtained in two distinct forms, each with its own characteristic colour and emission signature, depending on the method used for isolating these solids from a dichloromethane solution. For example, different coloured powders were obtained by either (a) vacuum evaporation of the dichloromethane solution or (b) careful precipitation by drop wise addition of light petroleum before isolating the powders by filtration. The observed luminescent colours are shown in Table 13. It appears that the nature of the counter-cation plays a role in the colour change, as the (tetra-*n*-butyl)ammonium cation-containing complexes have a wider shift in colours in their two forms than their tetraphenylphosphonium equivalents.

Table 13. Fluorescence colours of clusters **31a-33b** with extraction methods.

Cluster	Colour of fluorescence after extraction by:	
	Evaporation	**Precipitation**
$[^nBu_4N][\{(C_6F_5)_2Au\}_2(AgNO_3)_2]$ **31a**	Orange	Green
$[Ph_4P][\{(C_6F_5)_2Au\}_2(AgNO_3)_2]$ **31b**	Red	Orange
$[^nBu_4N][\{(C_6F_5)_2Au\}_2Ag_2OAc^F]$ **32a**	Red	Orange/Yellow
$[Ph_4P][\{(C_6F_5)_2Au\}_2Ag_2OAc^F]$ **32b**	Red/Orange	Orange/Yellow
$[^nBu_4N][\{(C_6F_5)_2Au\}_2Ag_2OTf]$ **33a**	Orange	Green
$[Ph_4P][\{(C_6F_5)_2Au\}_2Ag_2OTf]$ **33b**	Red/Orange	Orange

These complexes are stable to air and moisture, both in solution and as solids, for at least one hour in the dark. The ^{19}F NMR spectra showed the expected (albeit broadened) signals for the pentafluorophenyl groups bound to gold(I) centres. The IR spectra of these complexes displayed $[(C_6F_5)_2Au]^-$ absorptions at 1499-1505 and 953-964 cm^{-1} corresponding to ν(C-F) and 781-788 cm^{-1} for the ν(Au-C) stretching mode. Furthermore, **31a-b** displayed bands at 1296-1298 and 826-831 cm^{-1} for the nitrate anions, **32a-b** gave bands at 1661, 1193-1195, 1136-1140, 835-837 and 780-781 cm^{-1}, attributed to the trifluoroacetate anions and **33a-b** had bands at 1155-1140 cm^{-1} from the triflate anions.

4.2.3.2 Crystallographic Analysis

Slow diffusion of light petroleum to dichloromethane solutions containing the complexes at -30 °C produced single crystals of **31a**, **31b** and **32a** which were stable for days without degradation. The details of the crystallographic structure of the asymmetric $[(C_6F_5)_4Au_2Ag_2]$ units are documented in Table 14 (page 132).

*4.2.3.2.1 Structures of the Clusters **31a^1**, **31a^2**, **31b** and **32a***

Crystals of $\{[Ph_4P][\{(C_6F_5)_2Au\}_2(AgNO_3)_2]\}_n$ (**31b**) exist solely as red needles. X-ray diffraction studies revealed that the compound consists of clusters based on a planar $[Au_2Ag_2]$ core, with two C_6F_5 groups linearly bound to each gold centre in an essentially perpendicular manner with respect to the $[Au_2Ag_2]$ plane (Figure 65). There is one NO_3^- anion coordinated to each silver cation, in an asymmetric κ^2-fashion (Ag-O bonds are seen at 2.35 and 2.44Å), in a close-to perpendicular orientation to the $[Au_2Ag_2]$ cluster base. Each $[(C_6F_5)_4Au_2Ag_2]$ cluster unit is therefore dianionic and stabilised by two closely associated $[Ph_4P]^+$ counterions.

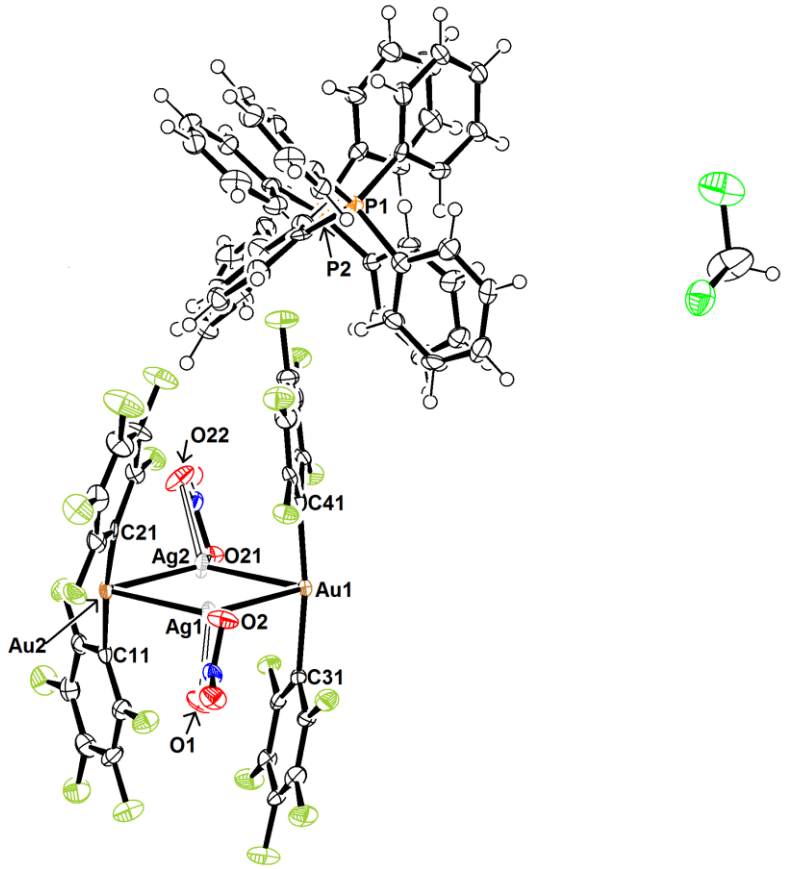

Figure 65. Molecular structure of a monomeric unit of **31b**·CH_2Cl_2 with a partial atomic numbering scheme. Ellipsoids are drawn at the 50% probability level. Bond lengths and angles of the $[(C_6F_5)_4Au_2Ag_2]$ base are in Table 14. Selected bond lengths (Å) and angles (°) in relation to the NO_3^- ligands: Ag(1)-O(1) 2.448(5), Ag(1)-O(2) 2.342(5), Ag(2)-O(21) 2.351(5), Ag(2)-O(22) 2.433(5); O(1)-Ag(1)-O(2) 53.46(16), O(21)-Ag(2)-O(22) 53.37(17).

These building units form a linear polyanionic 1D chain along the *x*-axis, held together by aurophilic bonding (Figure 66). The planes of neighbouring $[Au_2Ag_2]$ bases run parallel to one another.

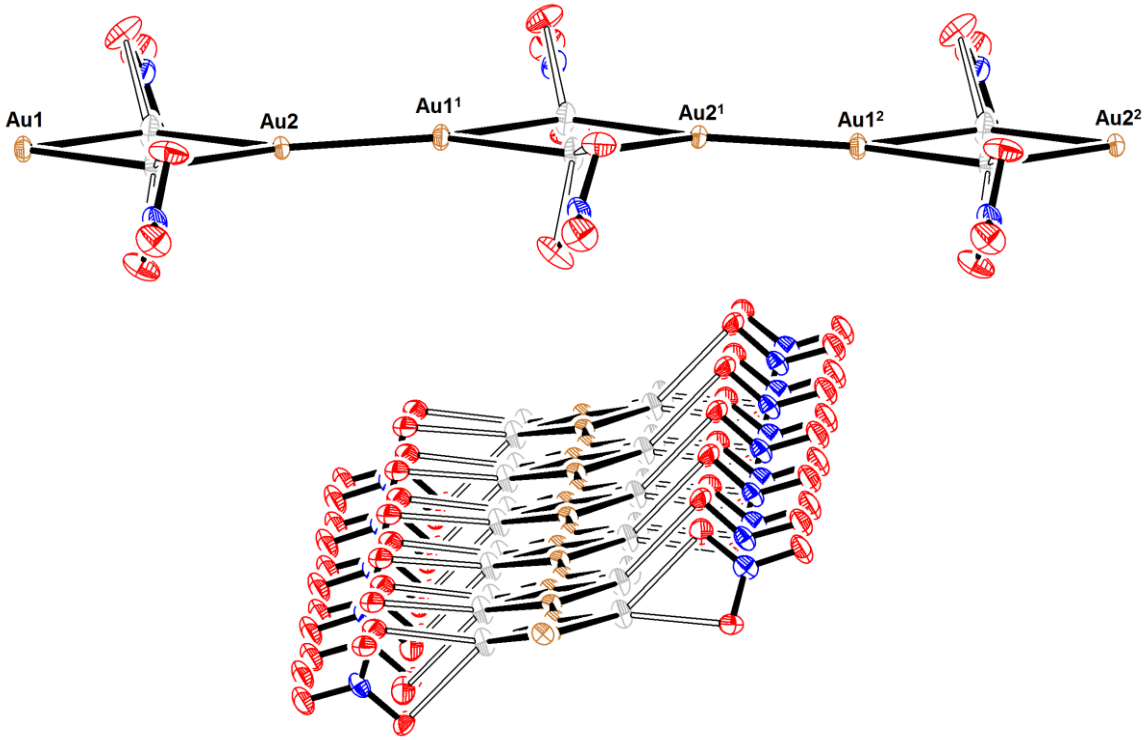

Figure 66. Two views of the polymeric arrangement of the $[Au_2Ag_2(NO_3)_2]^{2-}$ skeleton in **31b**·CH_2Cl_2. Ellipsoids are drawn at the 50% probability level.

Crystallisation of $\{[^nBu_4N]_2[\{(C_6F_5)_2Au\}_2(AgNO_3)_2]\}_n$ (**31a**) afforded two distinct crystal forms: yellow plates which upon UV exposure emitted green light, and needle-shaped crystals which luminesce orange (Figure 67). Both the yellow plates (**31a**^{1}) and the orange needles (**31a**^{2}) were analysed by X-ray diffraction techniques. Due to the severe disorder in the $[^nBu_4N]^+$ cations, the data of **31a**$^{1\text{-}2}$ were poorly defined.

Figure 67. Photos of the crystals obtained of **31a**^{1} (left), **31a**^{2} (centre) and **31b** (right), with the images shot in the dark under UV light exposure (bottom).

Crystals of **31a**^{1} were twinned, giving two different unit cells of poor quality. Nonetheless it was possible to establish that the structure of the anionic component is similar to that of **31b**, that is to say it is based on planar tetrametallic clusters $[\{(C_6F_5)_2Au\}_2\{Ag(NO_3)\}_2]$. However in contrast to **31b**; the clusters in **31a**^{1} do not form a polymer chain, but the tetra-anionic complex $[\{(C_6F_5)_2Au\}_2\{Ag(\kappa^1\text{-}NO_3)\}_2]_2^{4-}$ is held together by a single Au···Au bond which is significantly longer than the aurophilic bonds in **31b** (3.039(3) and 2.8171(6) Å, for **31a**^{1} and **31b**, respectively; Figure 68). The poorly resolved C_6 ring atoms have been constrained in the refinement process to lie in a regular hexagon with C-C bond lengths at 1.39 A. The linear $[Au(C_6F_5)_2]$ moieties are perpendicular to the plane of the $[Au_2Ag_2]$ core, but the (C_6F_5)-Au-(C_6F_5) bonds do not align with a plane which intersects the core across the gold atoms, instead are tilted away from this plane (*ca*. 57° from Au(1) and 42° from Au(2)). The nitrate anions in this case appear to be bonded to only one O-atom, supported by a second, weaker attraction of silver with the second oxygen of the nitrate. The two $[Au_2Ag_2]$ planes in **31a**^{1} are rotated about the Au-Au bond so that their normals form an angle of ca. 76°. These dimer units arrange themselves within the crystal lattice so that the axes of the Au(2)···Au(1)···Au(1^{1})···Au(2^{1}) units run parallel with other dimer units (Figure 69).

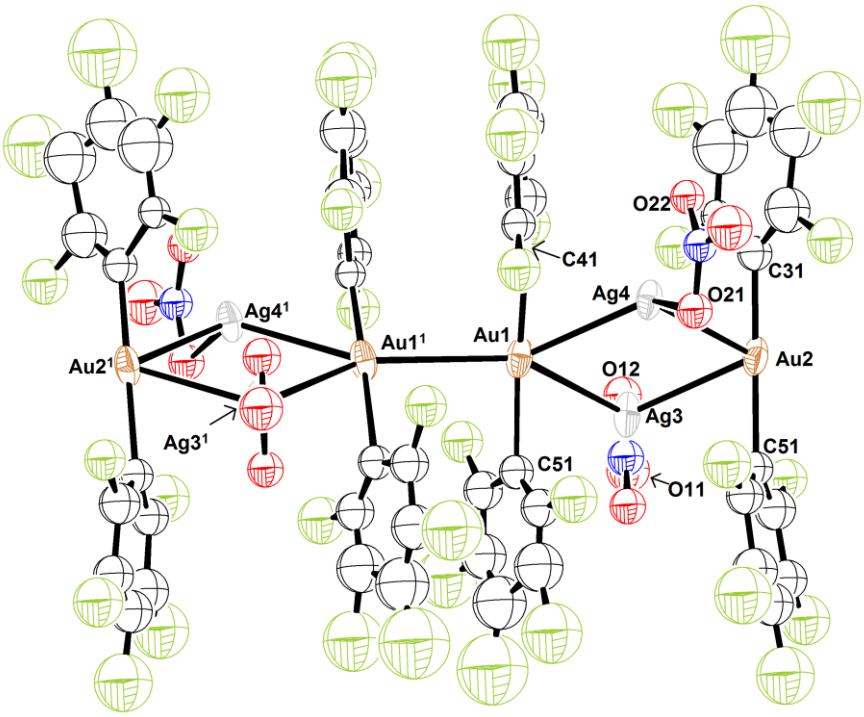

Figure 68. An Ortep view of the anionic components of the dimer cluster **31a**[1] at 30% ellipsoid probability. A partial atomic labelling scheme is shown. Bond lengths and angles of the $[(C_6F_5)_4Au_2Ag_2]$ base are in Table 14. Selected bond lengths (Å) and angles (°) in relation to the NO_3^- ligands: Ag(3)-O(51) 2.65(2), Ag(3)-O(52) 2.32(2), Ag(4)-O(61) 2.30(2), Ag(4)-O(62) 2.57(3); O(51)-Ag(3)-O(52) 52.1(9), O(61)-Ag(4)-O(62) 51.4(10).

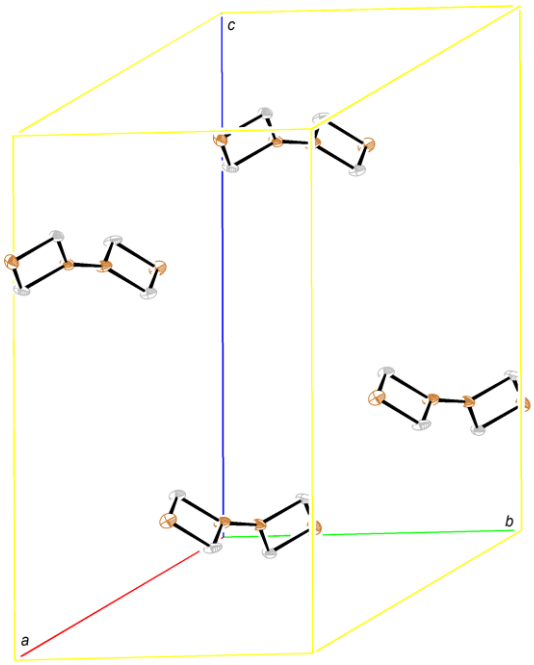

Figure 69. An Ortep of the unit cell packing of **31a**[1] at 30% ellipsoid probability.

The two $[^{n}Bu_4N]^+$ cations are not so clear; the principle arrangements for most of the two cations can be seen in Figure 70, but only when partial occupancy was applied as these cations are extensively disordered.

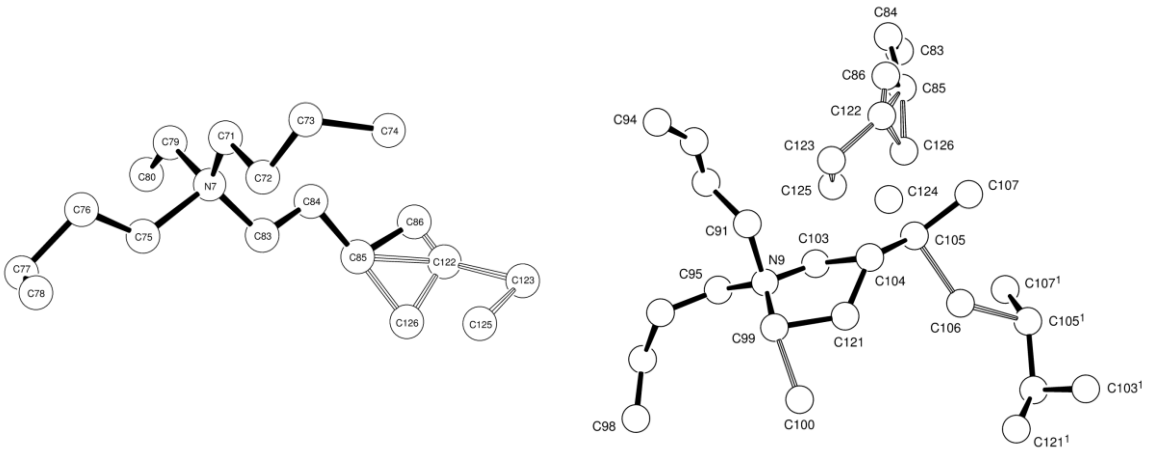

Figure 70. Atoms of the principal components of the two, independent, disordered $^{n}Bu_4N$ cations in **31a**[1], together with neighbouring, partially occupied atoms (designated as carbon atoms), which are presumed parts of minor cation components.

The poor data obtained from a crystal of **31a**[2] reveal a generally well defined anionic $[(C_6F_5)_4Au_2Ag_2]$ ribbon polymer (except for disorder in one C_6F_5 ligand and in one of the Ag ligands, assumed to be nitrate, but was not resolved). A unique unit consists of half of a $[Au_2Ag_2]_3$ polymer fragment ($[^{n}Bu_4N]_{ca.2.5}[Au_3Ag_3(C_6F_5)_6(NO_3)_2X]$, where X is probably a nitrate ion ligand; Figures 71 and 72). The cluster forms polymeric corkscrew chains in which the butterfly-shaped $[Au_2Ag_2]$ are linked through Au···Au bonds. Currently there is no explanation why the clusters adopt this arrangement, as no additional coordination to silver is observed to perturb the expected planar structure. In the asymmetric $[(C_6F_5)_4Au_2Ag_2]$ unit, the silver atoms Ag(4) and Ag(5) are coordinated by nitrate ions by a single O-atom, supported by a weak interaction to a second nitrate-oxygen. The two Au atoms Au(2) and Au(3) have pairs of C_6F_5 ligands arranged linearly about them. A twofold symmetry axis passes through the midpoint of the Ag···Ag vector in the second $[Au_2Ag_2]$ moiety of the asymmetric unit, with each Ag(6) atom coordinated to an unresolved array of 'O' atoms at a distance of approx. 2.55 Å, which might be parts of disordered and unresolved nitrate ions. The Au(1)

atom has the normal linear coordination of C_6F_5 ligands. Again, the $[^nBu_4N]^+$ cations are highly disordered, with only partial occupancy of the cations observed.

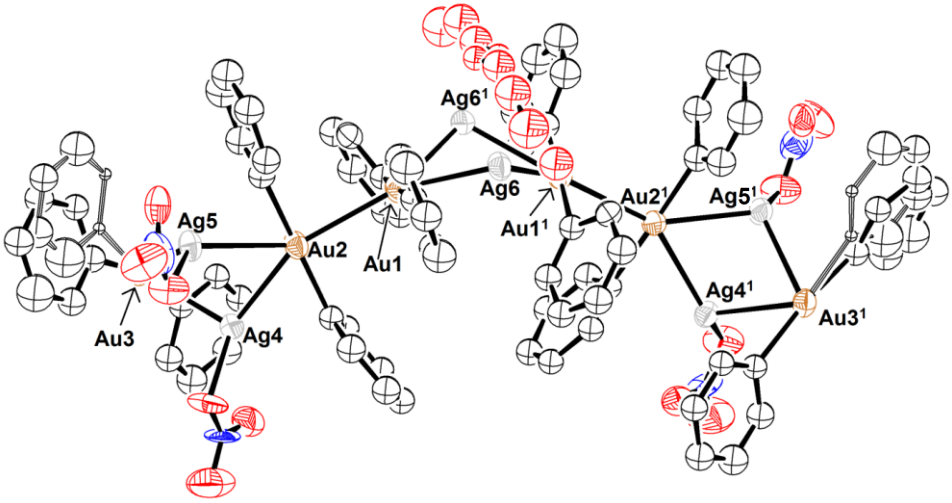

Figure 71. Two asymmetric units of the anionic component **31a²** with a twofold rotational symmetry element observed across the Ag(6)-Ag(6¹) plane (hydrogens and fluorines have been omitted). Ellipsoids are drawn at the 25% probability level. A partial atomic numbering scheme is shown. Bond lengths and angles of the $[(C_6F_5)_4Au_2Ag_2]$ base are in Table 14. Selected bond lengths (Å) and angles (°) in relation to the resolved NO_3^- ligands: Ag(4)-O(91) 2.29(2), Ag(4)-O(92) 2.54(3), Ag(5)- Ag(5)-O(81) 2.29(2), Ag(5)-O(82) 2.55(3) Å; O(91)-Ag(4)-O(92) 52.8(9), O(81)-Ag(4)-O(82) 54.1(9).

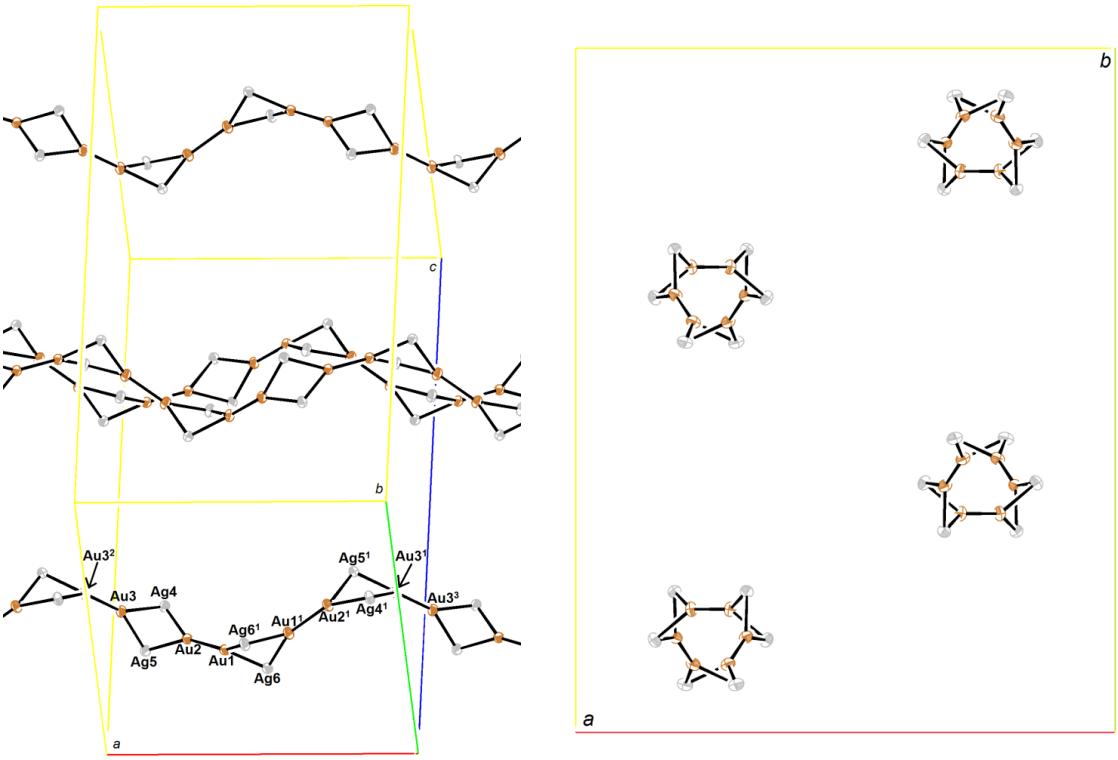

Figure 72. Two views of the $[Au_2Ag_2]$ polymer ribbon of **31a²**.

From the two crystal forms of **31a**, it is clear that the degree of association of the $[(C_6F_5)_4Au_2Ag_2]$ clusters dictates the emission wavelengths observed, *i.e.* polymeric **31a**^{2} emits in the orange/red region of the visible spectrum and the dimeric **31a**^{1} glows a green colour.

The crystalline blocks of the trifluoroacetate containing cluster $\{[^nBu_4N][(C_6F_5)_2Au\}_2Ag_2(O_2CCF_3)]\}_n$ **32a** fluoresce red under UV excitation. X-ray crystallography shows that this compound contains a single trifluoroacetate ligand that bridges both silver cations in the cluster. This forces the $[Au_2Ag_2]$ framework to adopt the butterfly configuration (Figure 73).[229]

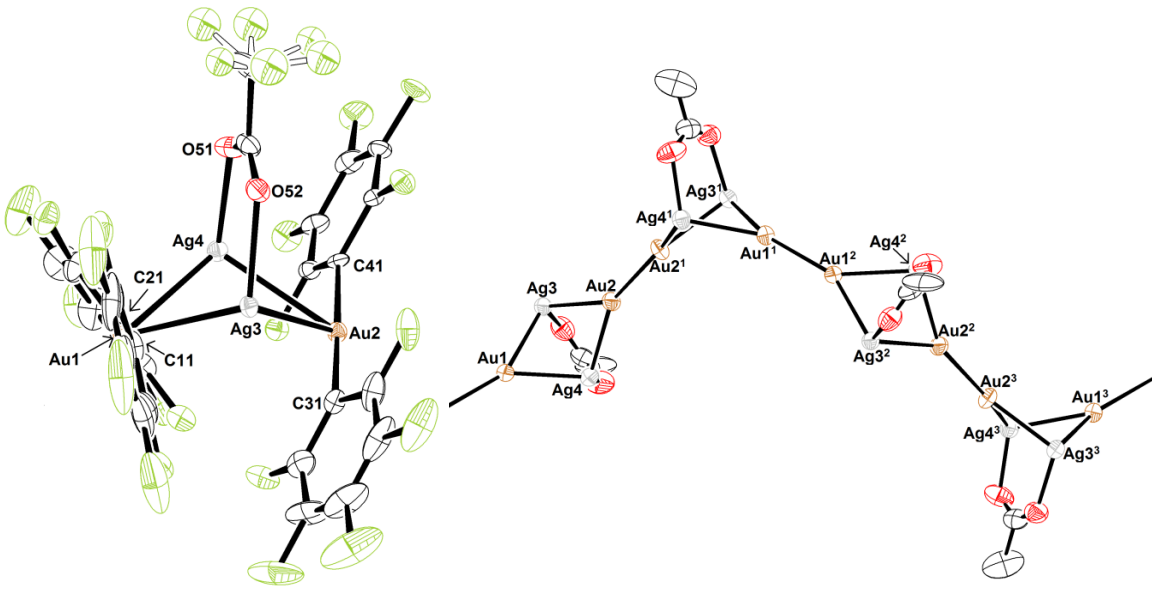

Figure 73. A view of the anionic $[(C_6F_5)_4Au_2Ag_2(\mu\text{-}OAc^F)]$ monomer (left) and the polymer skeleton of **32a** with a partial atomic numbering scheme. Ellipsoids are drawn at the 50% probability level. Bond lengths and angles of the $[(C_6F_5)_4Au_2Ag_2]$ base are in Table 14. Selected bond lengths (Å) and angles (°) in relation to the OAc^F ligand: Ag(3)-O(52) 2.267(12), Ag(4)-O(51) 2.301(12).

Aurophilic linkage promotes a 1D polymeric corkscrew-type lattice along the *x*-axis, with the best planes through the $[AuAg_2]$ moieties of neighbouring units being orientated perpendicular to one another (Figure 74).

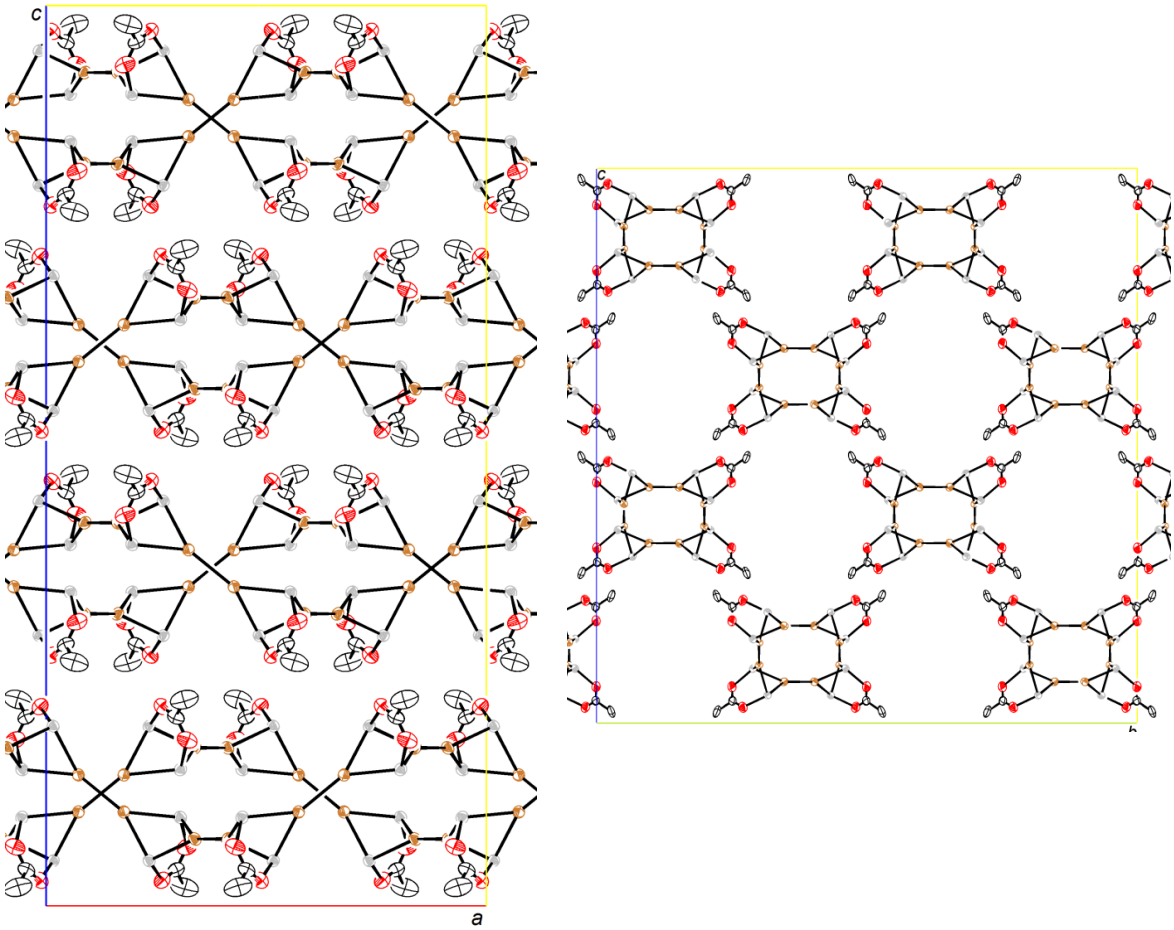

Figure 74. Views of crystal packing along the *x*- and *y*-axes of the $[Au_2Ag_2]$ backbone for the polymer **32a**.

Unfortunately crystals of the $[Ph_4P]^+$ analogue **32b** were polymorphic. Crystals of the (trifluoromethyl)sulfonate-containing compounds **33a** and **33b** were poorly stable at room temperature after an hour period, resulting in a precipitation of a metallic deposit when redissolved in solution. With the poor stability of **33a-b**, attempted structure determinations were unsuccessful, but ^{19}F NMR spectroscopy indicates the ratio of the (perfluorohalo)phenyl groups to triflate anion is approximately 4.5:1. This leads us to conclude that the triflates have a similar structure to the trifluoroacetates, with one $[O_3SCF_3]^-$ anion bridging two silver cations per each $[(C_6F_5)_4Au_2Ag_2]$ unit.

4.2.3.2.2 Comparison of Structures

Table 14 shows the bond lengths (Å) and angles (°) for selected atoms in the $[(C_6F_5)_4Au_2Ag_2]_n$ backbone of the clusters **31a**[1-2], **31b** and **32a**. The main feature of interest arises from the differing aurophilic bond lengths observed in the clusters: The planar polymer **31b** has far shorter Au···Au distances than the dimer **31a**[1]. The consequence of a shorter Au···Au bond is the lengthening of the bonds to the C_6F_5 rings, as **31a**[1] has Au-C bonds ~0.05 Å shorter than **31b**. The butterfly clusters **31a**[2] and **32a** have aurophilic bond lengths inbetween these two extremes, possibly as a consequence of the small changes in both the Au-Ag bonds and the Ag-Au-Ag angles observed in these complexes altering the frontier orbital shape of gold.

4.2.3.3 Trends in Emission Colours

With the dependence of the colour of luminescence on the chain lengths established for the different crystals of **31a**, we will now focus on the trends observed with the isolated powders shown in Table 15.

When isolated by vacuum evaporation, all of the complexes emit in the orange to red region of the spectrum (566-620 nm), indicative of the powders being of polymeric chains. Slow precipitation from dichloromethane solutions of **31a** and **33a** with light petroleum gave green luminescent powders, in agreement with the formation of a dimer cluster system seen in **31a**[1]. Unusually when the complexes **31b**, **32a**, **32b** and **33b** were isolated by slow precipitation, their colours do not shift away from their polymeric equivalents as much, with emissions colours in the yellow/orange region of the spectrum (553-582 nm). On closer inspection, when the products were first precipitated with light petroleum, yellowish-green luminescence were always observed, but after five minutes, a shift of emission towards the red region of the spectrum is seen, but never reach the hues seen by the evaporation products (example of **31b** shown in Figure 75). This time-dependent shift is believed to arise from aggregation of the dimeric clusters to form oligomeric or polymeric isomers.

Table 14. Selected bond lengths and angles for the clusters **31a**[1], **31a**[2], **31b** and **32a**.

Asymmetric Unit:	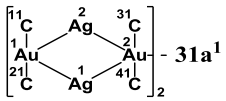 **31a**[1]	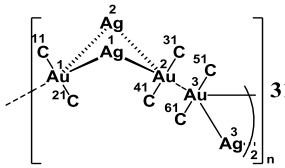 **31a**[2]	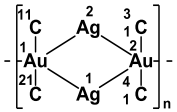 **31b**	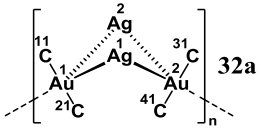 **32a**
Au(1)-Ag(1)	2.773(4)	2.797(3)	2.7097(7)	2.8409(13)
Au(1)-Ag(2)	2.770(3)	2.833(3)	2.7045(7)	2.8023(13)
Au(2)-Ag(1)	2.750(3)	2.773(3)	2.7161(7)	2.7921(13)
Au(2)-Ag(2)	2.746(4)	2.799(3)	2.7262(7)	2.8282(12)
Au(3)-Ag(3)	-	2.804(3)	-	-
Au(1)-C(11)	1.96(3)	2.101(14)	2.074(6)	2.066(13)
Au(1)-C(21)	2.06(2)	2.099(2), 2.100(2)[a]	2.048(7)	2.074(15)
Au(2)-C(31)	2.07(2)	2.083(3)	2.062(6)	2.083(15)
Au(2)-C(41)	1.95(2)	2.112(3)	2.046(6)	2.070(17)
Au(3)-C(51)	-	2.107(16)	-	-
Au(3)-C(61)	-	2.101(17)	-	-
Ag(1)-Au(1)-Ag(2)	67.10(10)	62.47(8)	66.36(2)	61.46(3)
Ag(1)-Au(2)-Ag(2)	67.74(10)	63.21(8)	65.98(2)	61.73(3)
Au(1)-Ag(1)-Au(2)	112.49(11)	101.10(9)	113.91(3)	98.12(4)
Au(1)-Ag(2)-Au(2)	112.67(11)	99.57(9)	113.75(3)	98.18(4)
Ag(3)-Au(3)-Ag(3^1)	-	62.24(10)	-	-
C(11)-Au(1)-C(21)	176.4(12)	163.6(13), 174.2(14)[a]	175.5(3)	178.3(6)
C(31)-Au(2)-C(41)	178.8(12)	176.2(10)	172.0(2)	176.5(7)
C(51)-Au(3)-C(61)	-	178.0(8)	-	-
Dihedral Angles[b]:				
Au(1)Ag_2 *vs.* Au(2)Ag_2 planes	0.5(2)	51.72(8)	0.72(2)	56.81(4)
Au(3)Ag_2 *vs.* Au(3^1)Ag_2 planes	-	51.61(7)	-	-
Aurophilic Bonds:	3.039(3)	2.910(2), 2.901(3)	2.8171(6)	2.8997(12), 2.9319(12)

a - dimensions in each of two disordered conformations, b - angles between the normals of the two $AuAg_2$ planes in each Au_2Ag_2 core.

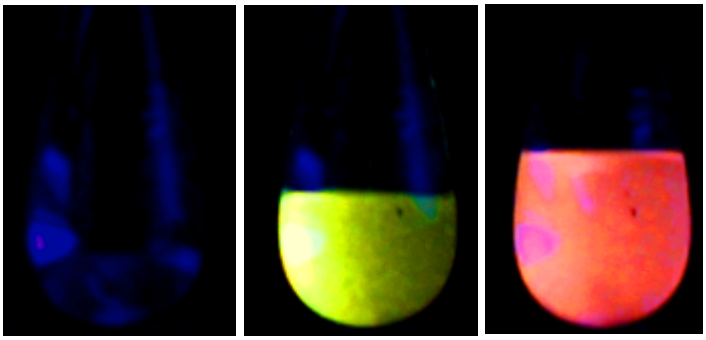

Figure 75. Pictures of (left) **31b** in a dichloromethane solution under UV illumination, (centre) initial luminescence upon precipitation by addition of light petroleum and (right) luminescence 5 minutes after precipitation.

The tetra-*n*-butylammonium counterion seems to promote the formation of smaller oligomers than (tetraphenyl)phosphonium, as the slow precipitation products of the $[^{n}Bu_4N]^+$ containing clusters are further blue-shifted away from the emissions seen for the polymer products; a fine balance between aurophilic attraction and Coulombic repulsion is apparent with the position of this equilibrium is apparently influenced by the cations, as well as the method of crystallisation.

4.2.3.4 Anion Studies

The formation of the anion-containing clusters is always favoured over their neutral counterpart $[Ag_2(Au\{C_6F_5\}_2)_2]_n$ (**CI**), shown by treatment of **CI** with 1 equiv. $[^{n}Bu_4N][A]$ (A = NO_3, $OC(O)CF_3$, $OS(O)_2CF_3$) to give clusters in quantitative yields. The weakly coordinating nature of the anions was evident by the behaviour of dichloromethane solutions of **31a-33b**, which show colour changes when acetone or THF were added, to yellow and green, respectively. The solvent displaces the anions to form **CI·CO(CH$_3$)$_2$** and **CI·THF** by both solution and vapour exposure to the solvents. The reactions of **31a**, **32a** and **33a** with methanol also led to anion displacement, as the orange solids isolated fluoresce green under UV excitation. This reaction was found to be reversible; vacuum evaporation, redissolution in dichloromethane and precipitation by light petroleum gave the parent clusters in quantitative yields.

Table 15. Uv-vis, fluorescence and lifetime measurements of the clusters **31a-33b**.

Compound	Absorbance / nm ($\epsilon = \times 10^3$ L mol^{-1} cm^{-1})	Fluorescence (in CH_2Cl_2 solutions, ~2×10^{-4} mol)			Fluorescence (solid state)			
					Evaporates		Precipitates	
		λ_{max}^{Ex} / nm	λ_{max}^{Em} / nm	Lifetime / ns (χ^2)	λ_{max}^{Ex} / nm	λ_{max}^{Em} / nm	λ_{max}^{Ex} / nm	λ_{max}^{Em} / nm
31a	231 (6.7), 258 (3.6)	405	538	τ_1 = 56, τ_2 = 183 (1.33)	433	579	407	532
31b	233 (7.1) 263 (2.3) 268 (2.2) 277 (1.9)	410	528	τ_1 = 66, τ_2 = 112 (1.18)	429	609	418	588
32a	239 (6.4) 261 (4.1)	402 410	500 621 (vw)	τ_1 = 41, τ_2 = 93 (1.18) n/a	425	582	401	555
32b	233 (6.5) 261 (2.3) 269 (2.5) 276 (2.1)	402 n/a	499 ~615 (vvw)	τ_1 = 52, τ_2 = 137 (1.39) n/a	432	599	404	553
33a	233 (6.9) 259 (4.8) 292 (6.8)	411	529	τ_1 = 98, τ_2 = 167 (1.17)	430	620	398	525
33b	232 (6.9) 263 (2.3) 269 (2.5) 277 (2.8) 293 (2.9)	408	531	τ_1 = 125, τ_2 = 179 (1.11)	434	566	431	584

In an attempt to observe a correlation between differing anions of the same type with its luminescence signatures, numerous acetate- and sulfonate-anions were targeted to replicate the synthesis of the trifluoroacetate- and triflate-containing clusters. A series of silver acetates ($Ag(O_2CR)$, R = Me, Ph, *p*-C_6H_4Br, C_6F_5 or CBr_3) were treated with $[^nBu_4N][Au(C_6F_5)_2]$; however, there was no reaction. Only with silver trichloroacetate was a positive result seen; a bright orange solid was isolated *via vacuo*, but its stability was limited to less than 30 minutes in dichloromethane, resulting in a precipitate and a change in its fluorescence colour in the solid state suggestive of the neutral cluster $[(\{C_6F_5\}_2Au)_2Ag_2]_n$. The reactions of silver (methane)- and (*p*-tolyl)sulfonate with $[^nBu_4N][Au(C_6F_5)_2]$, produced colourless powders which exhibited a feint green and blue fluorescence upon UV exposure. Unfortunately these compounds break down readily in dichloromethane and give non-fluorescing samples after 5 minutes exposure to the solvent. In addition silver sulfate or silver methanephosphonate were found to be unreactive towards $[^nBu_4N][Au(C_6F_5)_2]$.

4.2.3.5 Fluorescence Spectroscopy of 31a-33b

The complexes **31a-33b** luminesce in the solid state at room temperature, with only a very faint luminescence observed in dichloromethane solution, when exposed to UV light. The results of the luminescence studies are summarised in Table 15.

The emission spectra of dichloromethane solutions (*ca.* 2 x 10^{-4} M) give rise to intense signals at 499-538 nm when excited within the region of 400-410 nm. The excitation spectra of the complexes show very complicated profiles with poorly resolved absorbencies within the region of excitation (Example of **31a** in Figure 76).[230] Secondary excitations for **32a-b** give rise to very weak emissions in the orange region of the visible spectrum. The intense emissions within the green region are from dimers in solution, with the weak signals in the orange-red region occurring from aggregation in solution. The lifetime measurements in dichloromethane solutions (~2 × 10^{-4} mol) at room temperature are within the

nanosecond time scale, together with the short Stokes' shifts suggests the emissions are associated with spin-allowed fluorescent transitions.[231]

Fluorescence data in the solid state is also available; data for powders isolated in both the precipitated or evaporated forms are collated in Table 15. For complexes **31a** and **33a**, the slow precipitation method produced a bright green glowing powder, with emission properties somewhat matching that of the solution fluorescence (see Figure 76). The other clusters give emissions within the yellow/orange region of the spectrum (553-588 nm). The poorly resolved excitation signals in the solid state spectra closely correspond to the fluorescence spectra in solution. When isolated by vacuum evaporation, the luminescent complexes gave a broad emission signal with some fine structure in the red-region of the spectrum, attributed to the formation of a mixture of aggregates. The emissions from the solution precipitates are narrower, within the green to yellow region of the spectrum, suggestive of a more homogeneous mixture. The red-shift is attributed to the change from dimerisation to polymerisation of the clusters *via* Au···Au contacts to form 1D polymers.

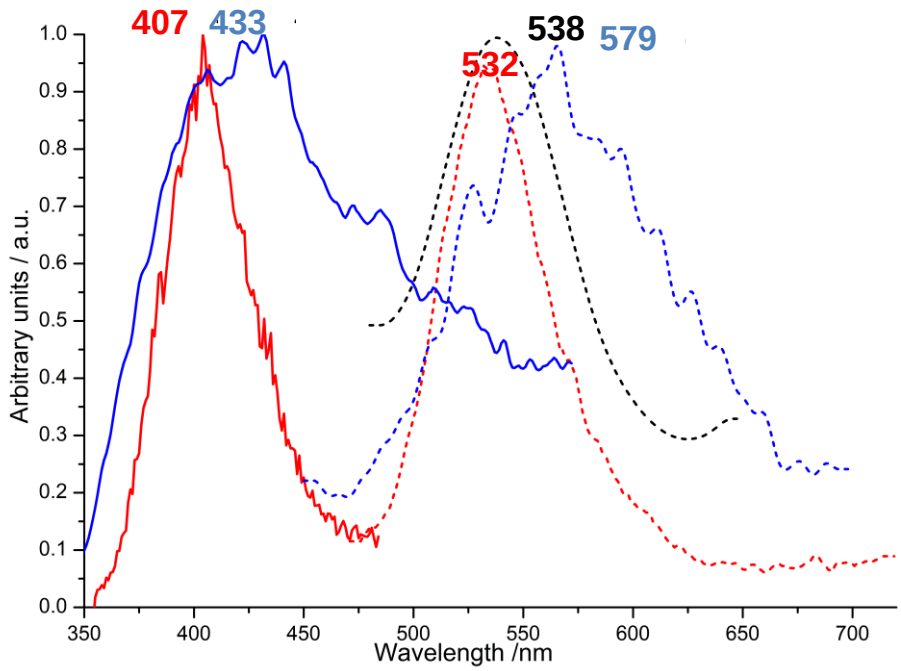

Figure 76. Nominalised photoluminescence of **31a**: (a) Emission spectrum in CH_2Cl_2 (~2 × 10^{-4} mol, black dashed), (b) excitation (red solid) and emission (red dashed) spectra of the precipitate and (c) excitation (blue solid) and emission (blue dashed) spectra of the evaporate.

The observed emissions are believed to be from the transitions influenced by gold(I)-silver(I) closed-shell (M···M) interactions with aurophilic interactions evidently lowering the emission energy to a varying degree; the polyaurophilic interactions of **31a**^{2} lower the bandgap more than the dimeric compound **31a**^{1}.[232] This conclusion is backed-up by similar results seen with other $[(C_6X_5)_4Au_2Ag_2]$ clusters.[233]

The UV-vis spectra for the clusters, measured at room temperature in CH_2Cl_2 (~2 $\times 10^{-4}$ M), are shown in Figure 77; the units of the calculated extinction coefficients (ε) are in L mol^{-1} cm^{-1}. The tetra-*n*-butylammonium salts **31a, 32a** and **33a** show highly similar profiles; high energy bands are observed at 231 (ϵ = 6.7 $\times 10^3$) and 258 nm (ϵ = 3.6 $\times 10^3$) for **31a**, 239 (ϵ = 6.4 $\times$ 10^3) and 261 nm (ϵ = 4.1 $\times$ 10^3) for **32a** and 233 (ϵ = 6.9 $\times$ 10^3) and 259 nm (ϵ = 4.8 $\times$ 10^3) for **33a.** The signals observed have been assigned to the allowed π-π* transitions in the pentafluorophenyl rings.[218d] For the tetraphenylphosphonium complexes **31b, 32b** and **33b**, bands at 233 (ϵ = 7.1 $\times$ 10^3), 233 (ϵ = 6.5 $\times$ 10^3) and 232 nm (ϵ = 6.9 $\times$ 10^3), respectively, compliment observations, but the signals at *ca.* 260 nm have been replaced with a three-band structure between 262-277 nm, attributed to the absorption by the C_6H_5 rings on $[Ph_4P]^+$.[234] A broadened signal is seen for each of the triflate anion-containing clusters **33a-b**, observed at 292 (ϵ = 6.8 $\times$ 10^3) and 293 (ϵ = 2.9 $\times$ 10^3) nm, respectfully.[235] Use of any other solvent (acetone, THF, MeCN, MeOH, EtOH) results in anion loss to form the solvated clusters.

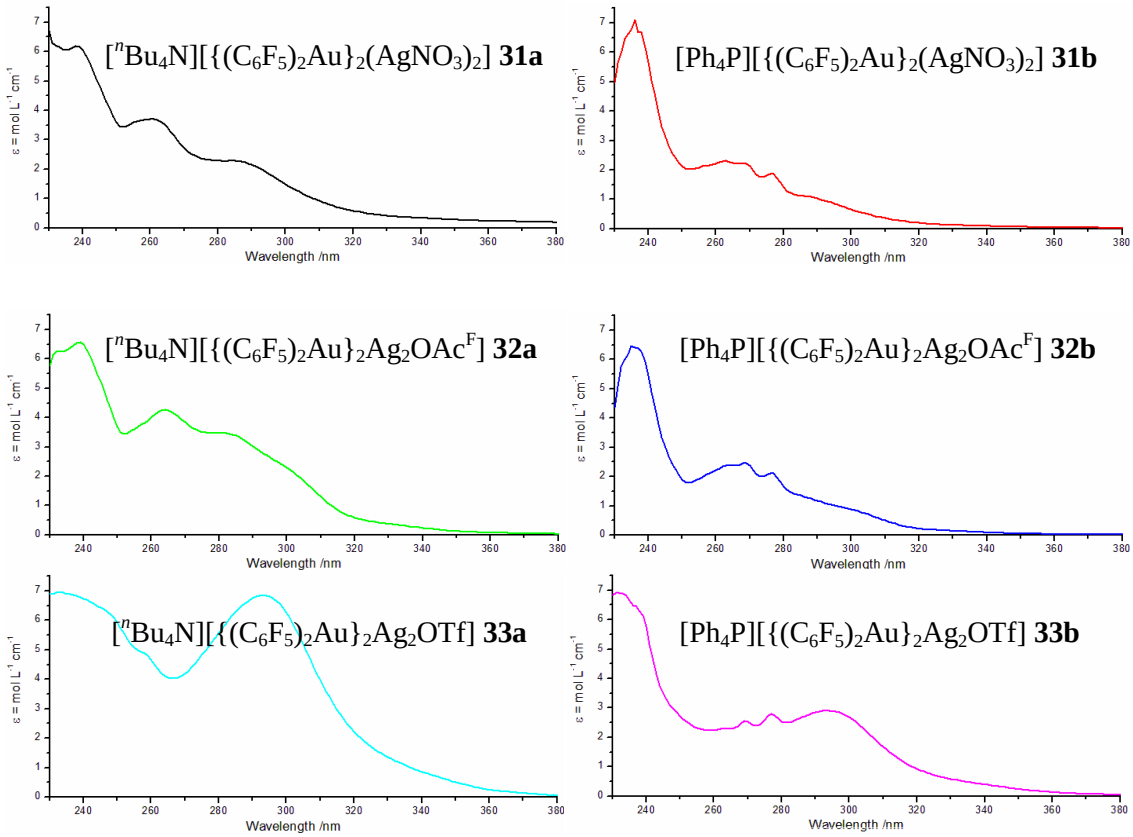

Figure 77. UV-vis plots of the clusters (2 × 10^{-4} mol).

4.2.4 Conclusions

The use of nitrate, trifluoroacetate and triflate salts of silver with $[(C_6F_5)_2Au]^-$ readily gave $[(C_6F_5)_4Au_2Ag_2]$ clusters which incorporate these anions by bonding to the silver cations. The clusters photoluminesce in both the solid state and in dichloromethane solutions, with its origins thought to arise from fluorescence mechanisms. By modifying the methods for cluster isolation, we can obtain powders which contain varying degrees of aurophilic bonding; polymeric powders of these clusters have ample structural precedents, whereas the cluster dimers that contain a single Au···Au bond have only been identified in a few cases.

X-ray crystallography has shown (a) the shape of the $[Au_2Ag_2]$ core can differ, depending on the anion coordinated to silver, (b) the shape of the $[Au_2Ag_2]$ core can affect the Au···Au bond lengths in the polymer lattices by up to 0.1 Å and (c) the comparison of clusters containing planar $[Au_2Ag_2]$ cores found that a polymer structure exhibits aurophilic bonds ~ 0.2 Å shorter than those for the dimer equivalent.

A relation between the degree of polymerisation and its luminescence in the solid state was established by fluorimetry measurements. The powders being of polymeric cluster chains emit in the orange-red region of the spectrum, as well as the powders which luminesce green being dimers. All clusters, when in dilute dichloromethane solutions, luminesce green which indicates the clusters exists as dimers in solution.

4.3 Topic 3: Gold(III) Reactivity and Catalysis with Simple Arenes

4.3.1 Objectives of Reaction Screenings

The catalytic and structural chemistry of $[^{n}Bu_4N][(C_6F_5)_2AuCl_2]$, as well as its neutral dimer counterpart $[(C_6F_5)_2AuCl]_2$ are of interest, as these complexes have shown a greater resistance to reduction than $HAuCl_4$ and $AuCl_3$.[236] We envisage these complexes as precursors for the synthesis of alkene, alkyne and arene complexes of the type $[(C_6F_5)_2Au(\eta^2\text{-}L)_2]^+$; in an attempt to hopefully generate the first examples of well-characterised gold(III) C=C π-bonded complexes.[237] Usón *et al.* has described the transformation of $[^{n}Bu_4N][(C_6F_5)_2AuCl_2]$ to $[(C_6F_5)_2Au(OEt_2)_2][SbF_6]$ (**CXI**) by dehalogenation with two equivalents of $AgSbF_6$ in diethyl ether.[83,236] The Au-O bonds in $[(C_6F_5)_2Au(OEt_2)_2][SbF_6]$ are considered weak; the diethyl ether is easily exchanged by acetone, acetonitrile, dimethyl sulfide. We hoped that it might also be possible to displace the ether ligands with alkenes to provide gold(III) complexes containing, for example, cycloalkenes or chelating 1,5-cyclooctadiene (Scheme 56). If successful, the synthesis of alkyne and arene π-complexes by the ether displacement method was also to be explored.

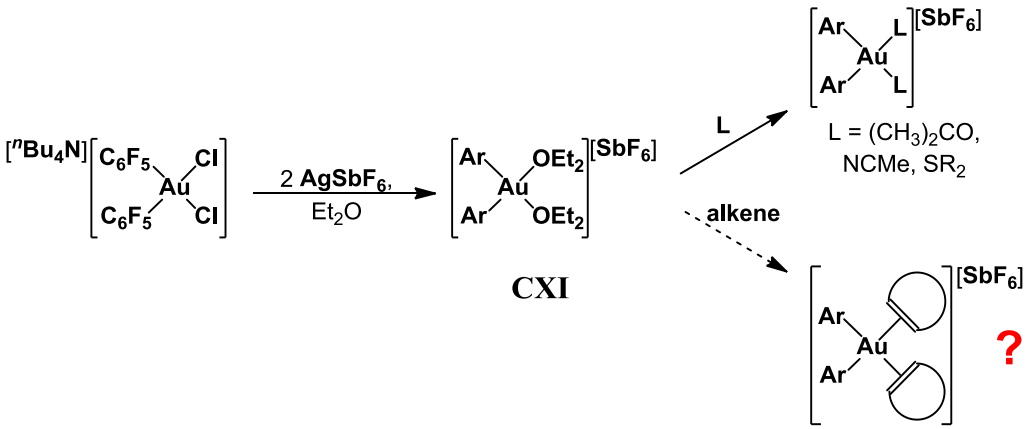

Scheme 56. Synthesis and proposed chemistry of **CXI** with alkenes.

In addition, the poor understanding of the active gold(III) species in organic transformations was highlighted by Reetz and Sommer in hydroarylation reactions of simple alkynes.[89] In their attempt to replace $[AuCl_3]_2$ by the more electrophilic

Au(III) triflate, they reacted $[AuCl_3]_2$ with three equivalents of AgOTf (discussed in more detail in Section 1.4.1.2), but found that the mixed-valence, mixed metal gold-silver chloride amalgam formed instead.[89] There is of course, always the possibility that electrophilic reactions, ostensibly catalysed by Au(III), are in fact simply promoted by protons, for example the use of hygroscopic $AgSbF_6$ may introduce trace amounts of water, which could result in reactions such as hydroarylations proceeding *via* Brønsted acidic or Au(I) catalysed processes.[44s,111,238] There is also the question of the role of silver in the activation of arenes.[88]

We planned to answer these questions by monitoring the reaction of pentamethylbenzene and ethyl propiolate mediated by $[(C_6F_5)_2AuCl]_2/2[(Et_3Si)_2H][B(C_6F_5)_4)]$. We anticipated that the pentafluorophenyl ligands would provide sufficient stability towards reduction and the silyl salt would produce the gold(III) cation in the absence of both silver and trace water. In these investigations, the perfluoroaryl ligands could also be used as valuable NMR reporter functions for determining the oxidation state of the gold centre within these reactions.

4.3.2 Background of the Interactivity of Gold(III) Cations with Arenes

Although gold(III) complexes are extensively used in catalytic transformations of organic substrates, very little of the mechanistic processes have been identified experimentally. This is shown by (a) the lack of evidence for π-bonding to gold(III) (see section 1.4.2)[83] and (b) the poor mechanistic understanding of C-H and C-C activation processes mediated by gold.

Theoretical considerations into π-bonding to gold(III) (*e.g.* $(C_2H_4)AuCl_3$ and $(C_2H_2)AuCl_3$) have shown low, if not repulsive, bonding interactions between the gold and the π-bond (-7.9 and +1.5 kcal mol^{-1}, respectively) when compared to Au(I) analogues ($(C_2H_4)AuCl$ -38.5 and $(C_2H_2)AuCl$ -34.2 kcal mol^{-1}).[45c,47d] Computational studies have predicted a square planar (bipy)Au(III)-benzene complex ($[(bipy)Au(C_6H_5)(\eta^1\text{-}C_6H_6)]^{2+}$, Scheme 57) to be stable. No experimental

evidence is available for the existence of such an arene complex, as all attempts of synthesis have resulted in reduction to metallic gold.[239]

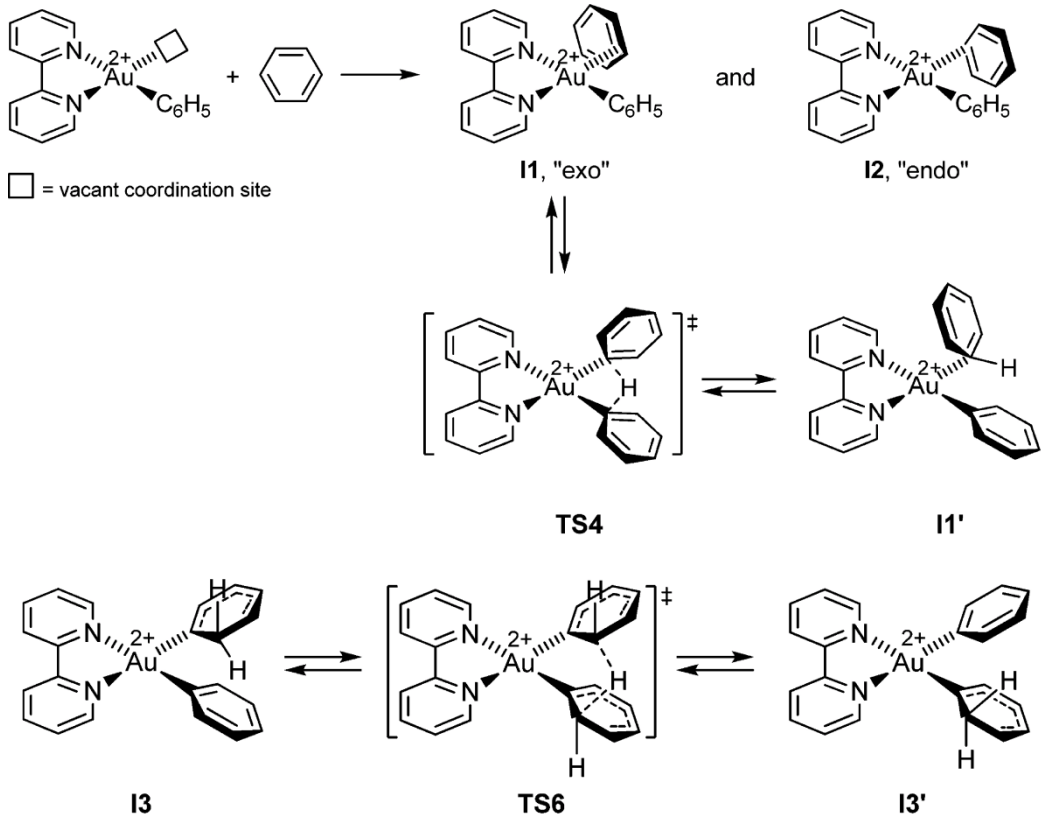

Scheme 57. Theoretical intermediates and transition states in benzene C-H exchange reactions of $[(bipy)Au(C_6H_5)(\eta^1\text{-}C_6H_6)]^{2+}$.[239]

4.3.3 Results and Discussion

4.3.3.1 Attempted synthesis of $(C_6F_5)_2Au(III)$-Alkene and -Arene Complexes.

The gold(III) etherate complex $[(C_6F_5)_2Au(OEt_2)_2][SbF_6]$ **CXI**, generated *in situ* by the reaction of $[^nBu_4N][(C_6F_5)_2AuCl_2]$ and 2 equiv. $AgSbF_6$, was treated with either an excess of norbornene (nbe) or 1,5-cyclooctadiene (cod) in diethyl ether, but afforded no change in the gold species. This indicates the π-acidity of gold(III) in $[(C_6F_5)_2Au(OEt_2)_2]$ does not bind preferentially to alkenes. When $[^nBu_4N][(C_6F_5)_2AuCl_2]$ was treated with 2 equiv. $AgSbF_6$ and an olefin (nbe or cod) in dichloromethane, ^1H NMR spectroscopy indicated a gold-(η^2)olefin species had been produced, but further investigations showed this to be the known complexes

$[Au(nbe)_3][SbF_6]$ and $[Au(cod)_2][SbF_6]$, respectively, in high yields (Scheme 58). The by-product, perfluorobiphenyl $(C_6F_5)_2$, was identified in the diethyl ether washings by ^{19}F NMR spectroscopy as the product of a reductive elimination from the $[(C_6F_5)_2Au]^+$ cationic intermediate. Although the C_6F_5 ligand is strongly electron withdrawing and can generally be equated to a halide ligand in its electronic characteristics, reductive elimination is still the preferred reaction pathway for Au(III).

Attempts to inhibit reduction by adding dimethyl sulfide to the dichloromethane reaction of $[^nBu_4N][(C_6F_5)_2AuCl_2]$, $AgSbF_6$ and norbornene in CH_2Cl_2 unfortunately results in the isolation of white solids containing $[Au(nbe)_3][SbF_6]$ in a moderate yield, among other unidentified products.

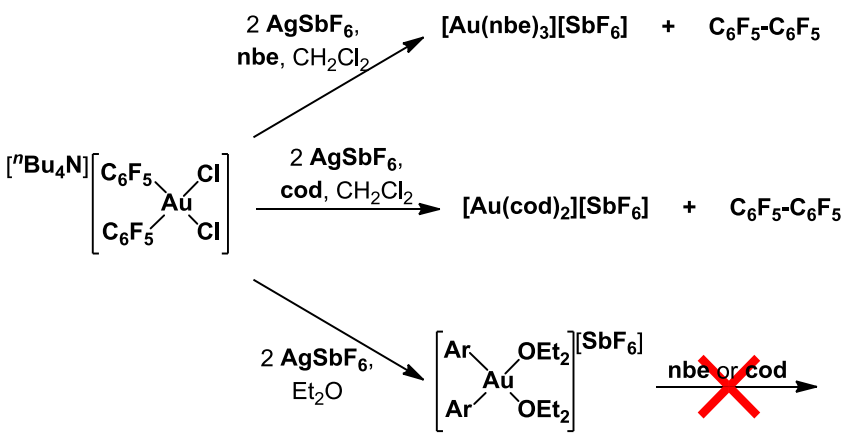

Scheme 58. The observed reaction products of $[^nBu_4N][(C_6F_5)_2AuCl_2]$ and $AgSbF_6$ in the presence of an olefin.

A family of 'naked' gold(I)-(η^2)olefin complexes has been reported[52,71,240] by the treatment of (tht)AuCl and $AgSbF_6$ in a dichloromethane solution infused with selected olefins. The new, thioether-free method established above allows us to test for the formation of gold(I)-(η^2)arene complexes, as there will be no competition between thioether coordination and the weak gold(I) π-interactions We hoped this might boost the chances of isolating a 'naked' gold(I)-(η^2)arene complex.[56] Indeed, a number of reactions were undertaken to screen the reactivity of $[^nBu_4N][(C_6F_5)_2AuCl_2]$ with 2 equivalents of $AgSbF_6$ in a dichloromethane solution containing a range of methylated arenes. For the reactions with mesitylene, 1,2,4-trimethylbenzene, durene, pentamethylbenzene and hexamethylbenzene, a

fine gold film was formed, with no evidence of a gold-arene complex existing in solution. For benzene, toluene and the xylenes (*o*- and *p*-), white powders were isolated by precipitation from the dichloromethane solutions with diethyl ether at room temperature, but unfortunately developed a purple hue within a few minutes of precipitation in all cases. ^{19}F NMR spectroscopy of the filtrate identified signals assignable to $(C_6F_5)_2$, confirming a reductive elimination step is present. Keeping the powders at low temperatures (-30 °C) did not seem to stabilise the products.

4.3.3.2 Hydroarylation of Terminal Alkynes Catalysed by Gold(III)

The hydroarylation of C_6HMe_5 and $HC{\equiv}CCO_2Et$ mediated by gold was first observed by Shi *et al.* using 1.25 mol-% $[AuCl_3]_2/6AgSbF_6$ as the catatalyst.[111] We used the same catalyst loadings for direct comparison but employing $[(C_6F_5)_2AuCl]_2/2AgSbF_6$. The reactions were monitored by ^{1}H NMR spectroscopy in chloroform-*d* (Entries 3-4, Table 16).

Table 16. Comparison of synthesis of **34** by gold/silver and gold/triethylsilyl systems.

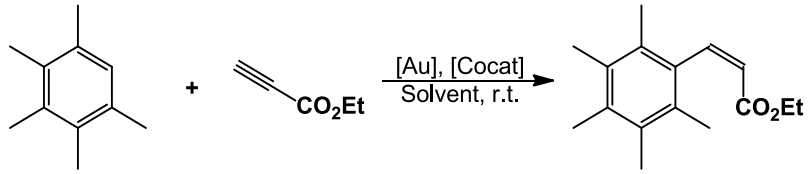

34

Entry	[Au][a]	[Cocatalyst][b]	Solvent	Time (h)	Yield (%)
1	$[AuCl_3]_2$	$6AgSbF_6$	$CDCl_3$	24	74
2				48	98
3	$[(C_6F_5)_2AuCl]_2$	$2AgSbF_6$	$CDCl_3$	24	71
4				48	98
5	$[(C_6F_5)_2AuCl]_2$	$2AgSbF_6$	C_7D_8	48	87
6[c]	$[(C_6F_5)_2AuCl]_2$	$2AgSbF_6$	C_7D_8	120	83
7	$[(C_6F_5)_2AuCl]_2$	$2Ag[B(C_6F_5)_4]$	C_7D_8	24	26
8				48	34
9	$[(C_6F_5)_2AuCl]_2$	$2[(Et_3Si)_2H][B(C_6F_5)_4]$	C_7D_8	0.5	18

a – 1.25 mol % catalyst; *b* – 2.5 mol % cocatalyst; *c* – 0.5 mol % $[(C_6F_5)_2AuCl]_2$, 1.0 mol % $[AgSbF_6]$

It is clear to see that in chloroform-*d*, the catalytic properties of $[(C_6F_5)_2AuCl]_2$ mirror that of $[AuCl_3]_2$, in terms of conversion rate at both 24 and 48 hour intervals. Due to the formation and aggregation of AgCl in the reaction vessel, monitoring the progress of hydroarylation by ^{19}F NMR spectroscopy proved difficult, as broadening of signals was seen. This issue was overcome by employing a silyl salt $[(Et_3Si)_2H][B(C_6F_5)_4]$,[241] as a) the by-products of chloride abstraction (Et_3SiCl and Et_3SiH) will remain in solution and b) with the silyl cation inertness to gold cations and arenes, there is no ambiguity in the nature of the gold catalyst. Given the reactivity of $[(Et_3Si)_2H][B(C_6F_5)_4]$ with chlorinated solvents, toluene-d^8 was selected. Prior testing showed that the catalytic reaction of toluene and ethyl propiolate using $[C_6F_5AuCl]_2/2AgSbF_6$ (1.25 mol %) has a greatly reduced activity (6 % conversion over 120 h). Reducing the catalyst loading to 0.5 mol % (with respect to $[(C_6F_5)_2AuCl]_2$) slowed the rate of conversion but achieved similar yields (Entry 6). The replacement of the silver activator with $Ag[B(C_6F_5)_4]$ greatly reduces reaction conversion, but the catalyst remains active for at least 24 hours (26 % over 24 h, 34 % over 48 h Entry 10).

The hydroarylation of ethyl propiolate by a $[(C_6F_5)_2AuCl]_2/2[(Et_3Si)_2H][B(C_6F_5)_4]$ catalyst system was monitored by ^1H and ^{19}F

NMR spectroscopy. No signals within the ^{1}H NMR window could be assigned to any aryl- or alkynyl-gold intermediates, but was used to identify the production of Et_3SiCl within the reaction. Upon initiation, the ^{19}F NMR spectrum of the reaction mixture points to a change in conditions of the gold complex; initiation with the silyl salt, signals corresponding to the $[(C_6F_5)_2Au]^+$ cation were observed (Figure 78, □), confirming that the gold was in oxidation state +III at this point. As the reaction time increased, the signals for the gold(III) cation are lost, with numerous signals (◊ and △) arising as the products of a reductive elimination process,[242] in addition to a slight change (< 0.2 ppm) in environment for the borate anion (○); the gold(III) cation does not remain stable in the reaction medium and reduction is apparent. Unfortunately, up to this point there was no evidence to determine whether catalysis proceeds *via* gold(III) or gold(I), therefore no conclusions can be made in relation to the question of the oxidation state of the active species (see Section 4.3.1.2). The silyl salt employed ensured that the reaction mixture remained aprotic, with hydroarylation still observed, confirming that the reaction occurs by activation of gold. However, it is also clear that silver is a non-innocent species in the reaction, as the $[(C_6F_5)_2AuCl]_2/2Ag[B(C_6F_5)_4]$ system employed was active at least 50 times longer than its $[(C_6F_5)_2AuCl]_2/2[(Et_3Si)_2H][B(C_6F_5)_4]$ catalyst equivalent.[87,89,112]

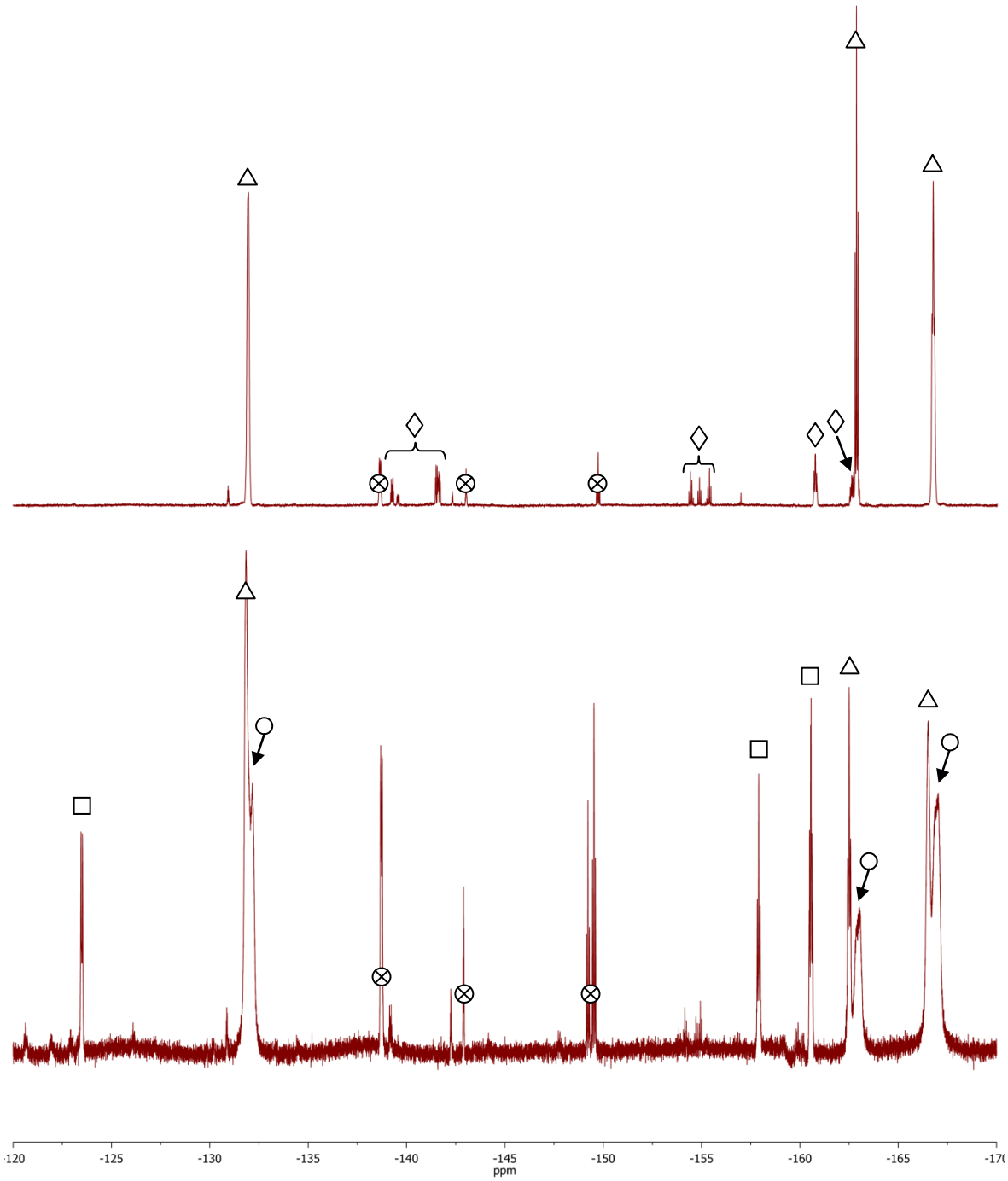

Figure 78. ^{19}F NMR spectra of the reaction of C_6Me_5H + $HC{\equiv}CCO_2Et$ promoted by 1.25 mol % $[(C_6F_5)_2AuCl]_2$/2$[(Et_3Si)_2H][B(C_6F_5)_4]$ after 5 minutes (bottom) and 30 minutes (top); The symbols corresponds to the signals of C_6F_5 ligands from the $[(C_6F_5)_2Au][B(C_6F_5)_4]$ (□ for the cation, ○ for the anion), the diaryl by-products (◊) and a by-product containing a second $[B(C_6F_5)_4]^-$ anion (△). ⊗ represents signals of unknown origin.

4.3.4 Conclusions

Although bis(pentafluorophenyl)gold(III) cations of the type $[(C_6F_5)_2Au(OEt_2)_2]^+$ are well known to contain labile ether ligands, there was no

observable exchange of the ether ligands with olefins or arenes. On the other hand, the reaction of $[^{n}Bu_4N][(C_6F_5)_2AuCl_2]/2AgSbF_6$ in dichloromethane dosed with an olefin resulted in the synthesis of the well-characterised $[Au(ene)_n]SbF_6$ complexes; the first synthetic methodology to quantitatively produce such π-coordinated gold cations in the absence of thioethers. The application of this reaction to introduce arenes to a gold cation allowed for the formation of powders, which appeared to be the first examples of a family of $[Au(arene)_n][SbF_6]$ complexes, akin to its well defined alkene- and alkyne-coordinated analogues, but these proved to be too unstable for any characterisation to be carried out.

In gold-catalysed hydroarylation reactions, the oxidation state of the active gold species responsible for alkyne hydroarylation is still unknown, as no conclusive proof could be obtained from ^{1}H and ^{19}F NMR spectroscopic observations of the reaction. However, we have determined that hydroarylation was only promoted by a gold cation generated *in situ*. The silver additives employed appear to have no activity to such catalysis, but were found to exhibit non-innocent behaviours, as its inclusion as the activators greatly increased the catalyst lifetime to that of catalysis initiated by a related silyl-containing activator.

5 - Miscellaneous Results

5.1 Attempted Synthesis of an Oxidative Fluorinating Agent for Gold

5.1.1 Introduction

5.1.1.1 Alternative Methods of Oxidative Halogenation of Gold: Possible Route for Oxidative Fluorination?

The common routine for oxidation of metallic gold is by treatment with aqua regia to give $HAuCl_4 \cdot xH_2O$. An alternative route was briefly explored using chloro- and bromosulfonium halides ($[Me_2S\text{-}Cl][Cl]$ and $[Me_2S\text{-}Br][Br]$), as these reagents can oxidise gold metal to numerous Au(I) and Au(III) species depicted in Scheme 59.[243,244]

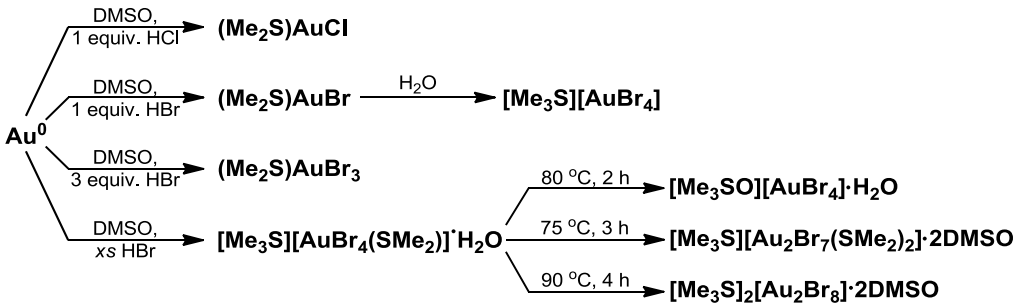

Scheme 59. Gold complexes produced from the reaction of DMSO + HX (X = Cl, Br) in the presence of powdered gold.[243,244]

The fluorosulfonium cation equivalent has been produced with inert counterions; $[Me_2SF][BF_4]$ and $[Me_2SF][AsF_6]$ (**CXIIa-b**, Scheme 60).[245] Two reaction routes were established in synthesis: the reaction of Lewis pair compounds $Me_2S \cdot BF_3$ or $Me_2S \cdot AsF_5$ with xenon(II) fluoride at -23 °C yielded $Me_2SF_2 \cdot BF_3$/$Me_2SF_2 \cdot AsF_5$, followed by warming to 35 °C. Alternatively, fluorination of dimethyl sulfide with XeF_2 gave Me_2SF_2, followed by addition of BF_3 or AsF_5 at -23 °C gave the salts $[Me_2SF][BF_4]$ and $[Me_2SF][AsF_6]$, respectively.

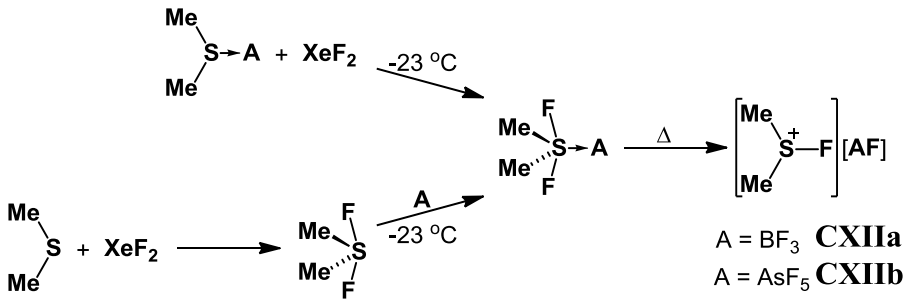

Scheme 60. Synthesis of **CXIIa-b**.[245]

CXIIa-b are stable at room temperature, but their high-polarity meant they were only soluble in HF solutions. Further development resulted in the family of the methyl(trifluoromethyl)sulfonium cations $[Me(CF_3)SF]^+[AF]^-$ (where A = AsF_5, SbF_5, $SbCl_5$, **CXIIIa-c**).[246] To date, no evidence is available for the use of **CXIIa-b** or **CXIIIa-b** as electrophilic fluorinating agents.

5.1.1.2 Known Gold Complexes Containing Au-F Bonds

Many gold fluoride complexes are highly reactive, moisture-sensitive materials which require specialized equipment for their synthesis, manipulation and characterization. Unlike the heavier halides, the hard Lewis base of F^- is poorly accommodated by a large, soft gold centre, resulting in a weak Au-F bond.[21,247]

Gold(I) fluoride is highly unstable and disproportionates easily ($3\ AuF \rightarrow AuF_3 + 2\ Au^0$). AuF has been generated in the gas phase[248] and isolated under immense pressures.[249] Strong σ-donating NHC ligands give the thermally stable complex (IPr)-Au-F (**CXIV**).[250,251] Noble metal atoms have also been found to coordinate to AuF by laser ablation methods to give (Ng)-Au-F (Ng = Ar, Kr, Xe; **CXIVa-c**), with the bonding of (Ng)-Au^+ based on Lewis acid/base bonding; Au^+ is the only cation which bonds to noble gases in this manner, as other metals experience electrostatic interactions to the noble metal only.[252]

A small number of complexes containing gold(I) or gold(II) centres exist which show coordination to complex fluoride anions and HF(**CXVI** – **CXIX**; Figure 79).[253] Only recently the synthesis of a dimeric gold(II) complex **CXX** with terminal Au-F bonds has been described.[254]

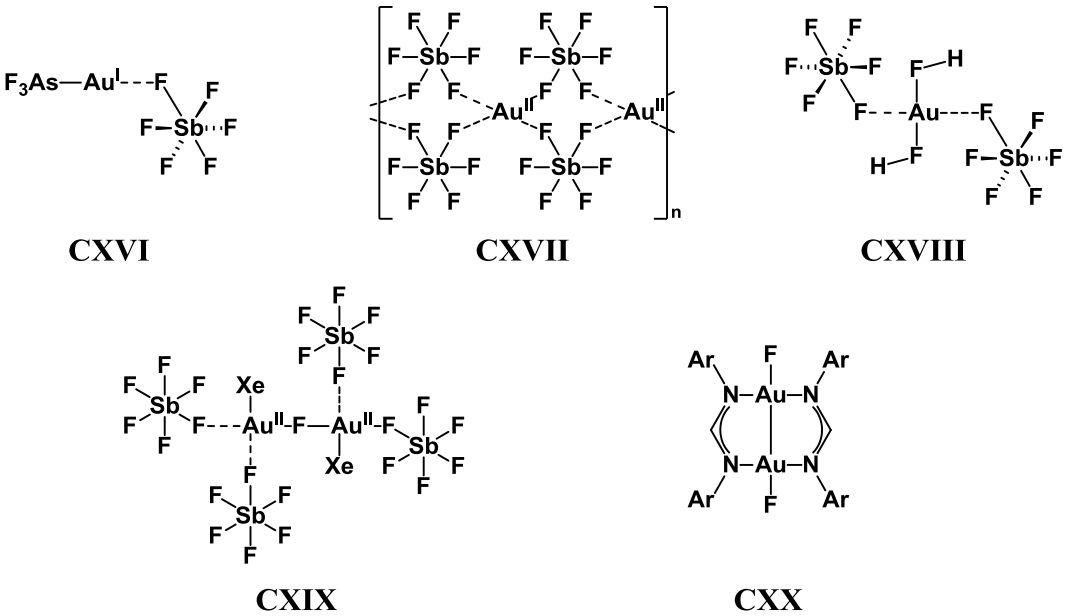

Figure 79. Examples of Au(I) and Au(II) fluoride complexes.[253,254]

Gold(III) fluoride (**CXXI**) has been known for over 60 years and is commonly used as a precursor for most of the known gold fluoride compounds.[255] Gold(III) fluoride is prepared in the reaction of $AuCl_3$ with F_2 or BrF_3, with the products being highly reactive towards water and organic compounds.[247,256] The structure of **CXXI** consists of a fluoride bridged helical polymer (Figure 80), very different to the chloride- and bromide-bridged dimers $[AuCl_3]_2$ and $[AuBr_3]_2$.[257]

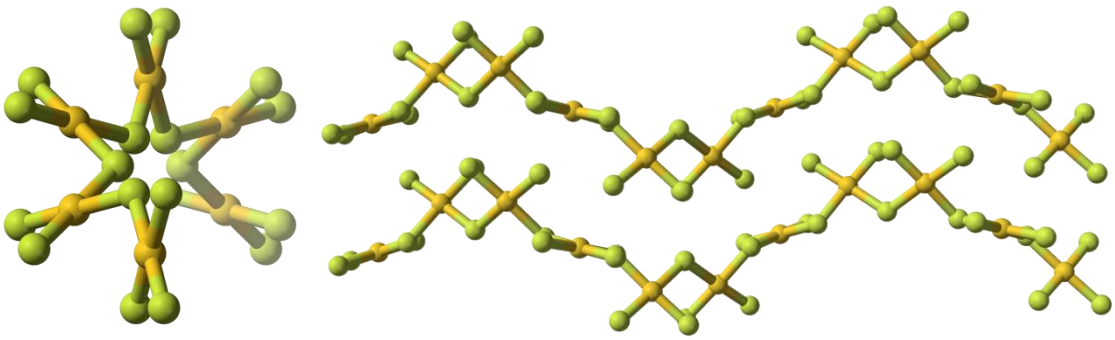

Figure 80. Two view of polymeric chain of $(AuF_3)_n$, **CXXI**.[255]

AuF_3 reacts with a wide range of metal fluorides to give complexes containing the square planar $[AuF_4]^-$ anion.[258] Alkylgold(III) fluorides containing NHC σ-donors (**CXXII** and **CXXIII**) have recently been synthesised by Toste and

Mankad (Scheme 61), with uses in C-C coupling reactions[259] and reductive elimination processes to yield alkyl fluorides.[251]

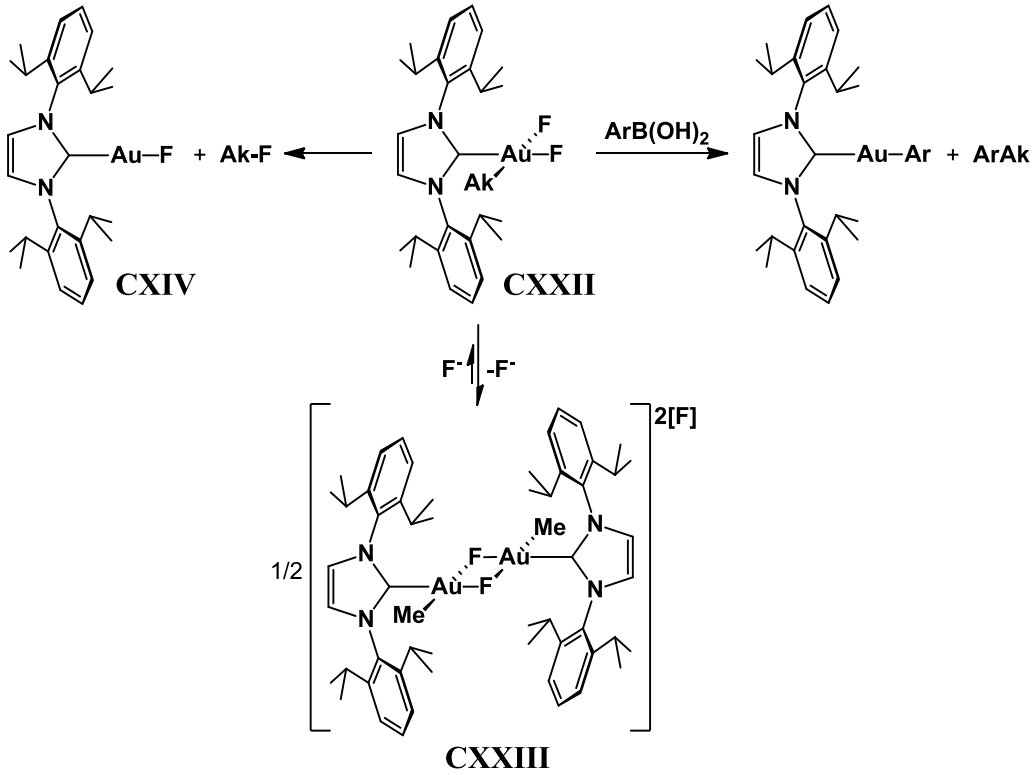

Scheme 61. Chemistry of [(IPr)Au(F)$_2$Me], **CXXII**.[251,259]

Gold in the oxidation state +V exists in both the neutral $[AuF_5]_2$ (**CXXIV**)[260] and numerous salts M[AuF_6] (**M[CXXV]**),[261] including the krypton fluoride compound **[KrF][CXXV]** shown in Figure 81.

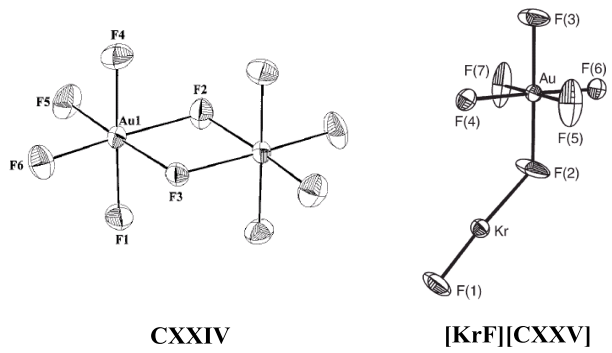

Figure 81. X-ray structures of **CXXIV** and [**KrF**][**CXXV**].[260,261e]

5.1.2 Aims and Objectives

Fluorinating agents for gold are limited to elemental fluorine or xenon difluoride. With the efficiency of chloro- and bromosulfonium systems for oxidation of metallic gold, we were interested to see whether a fluorosulfonium cation could be employed as a new reagent for the generation of gold(I) and gold(III) complexes that contain an Au-F bond (Scheme 62).

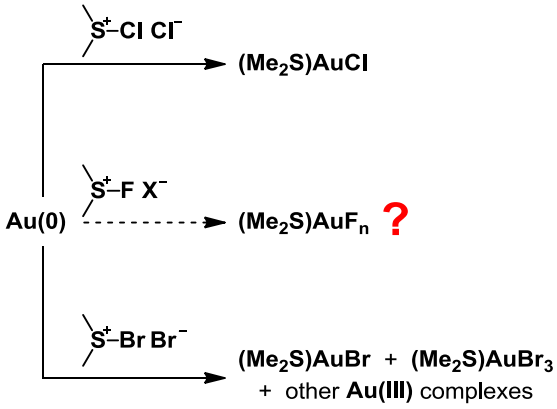

Scheme 62. The reactions of metallic gold powder with $[(Me_2S)Cl][Cl]$, $[(Me_2S)Br][Br]$ and the proposed reaction with $[(Me_2S)F][X]$.

With the inherent danger of using HF as a solvent, combined with the solubility issues experienced in $[Me_2SF][BF_4]$ and $[Me_2SF][AsF_6]$,[245] the composition of the fluorosulfonium cation will be modified in an attempt to promote solubility of the salt in organic solvents. If an electrophilic fluorinating agent can be synthesised, treatment of this compound with metallic gold powder will be attempted.

5.1.3 Results and Discussion

5.1.3.1 Synthesis of Organic Solvent-Soluble Fluorosulfonium Salts

Attempts to oxidise dimethyl sulfide by XeF_2 in dichloromethane resulted in the generation of the CFC gases $CHCl_2F$ and CCl_2F_2. The use of acetonitrile as the solvent in the same reaction produced Me_2SF_2 in near quantitative yields, with a relatively small amount of CH_2FCN as a byproduct (Scheme 63). Observing this

reaction by cold temperature NMR techniques in CD_3CN revealed the mechanism; fluoride extraction by dimethylsulfide produces the salt $[Me_2SF][XeF]$. The $[XeF]^-$ anion was unstable at temperatures above -20 °C, and dissociates to produce Me_2SF_2 and xenon gas.

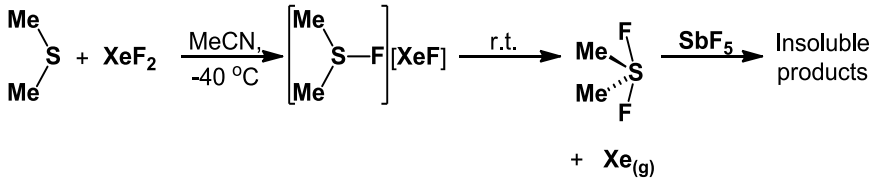

Scheme 63. The determined intermediates of the reaction of dimethyl sulfide and xenon(II) fluoride.

The use of SbF_5 as the Lewis acid, akin to those seen in the reported procedures[245,246] looked to be beneficial, but difficulties were experienced in handling at NMR scale quantities and the poor solubility of the reaction products in organic solvents (MeCN, THF, CH_2Cl_2 and $CDCl_3$) were seen. IR spectroscopy was the only method that could be used for analysis, which showed the presence of an SbF_6 anion at 658 cm^{-1}.

Replacing SbF_5 with $B(C_6F_5)_3$ resulted in the reaction products remaining soluble in acetonitrile, allowing for an NMR spectroscopic handle. The NMR scale reaction of $Me_2S{\cdot}B(C_6F_5)_3$ in acetonitrile-d^3 with XeF_2 at -40 °C initially yielded no reaction. When warmed to -20 ˚C a reaction was initiated. After about 30 minutes there was approx. ~30% conversion to $[Me_2SF][FB(C_6F_5)_3]$ (**35**). After one hour at -20 °C the intensities of the ^{19}F signals corresponding to the S-F signal at δ -189 ppm had degraded. Warming to room temperature drove the subsequent reaction to completion, with ^1H and ^{19}F NMR spectra suggesting the formation of a C-H functionalised disulfide cation $[Me_2SCH_2SMe]^+$ (**36**; Scheme 64).[262] This indicated the sulfuryl fluoride produced was sufficently electrophilic to promote cleavage of the methyl C-H bond of a second $[Me_2SF]$ cation to form a $[MeSCH_2F]$ intermediate, which was then attacked by the Me_2S byproduct. Similar results were observed when a solution of Me_2SF_2 in CD_3CN was treated with $B(C_6F_5)_3$ under identical thermal conditions.

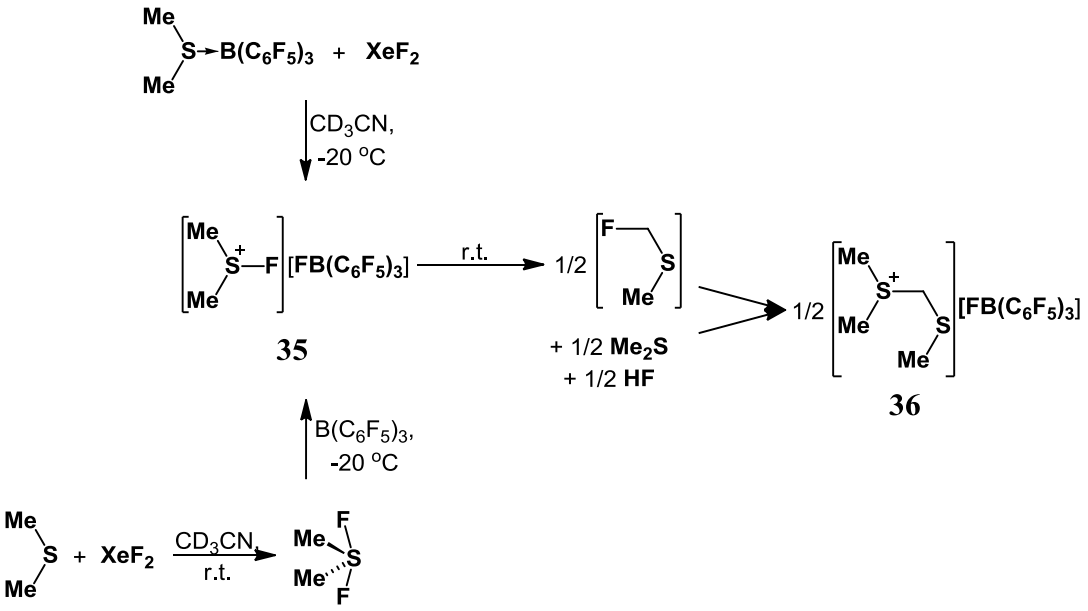

Scheme 64. Products and intermediates from the reaction of SMe_2, XeF_2 and $B(C_6F_5)_3$.

Replacing Me_2S with diphenyl sulfide to hinder electrophilic C-H activation was attempted: The reaction of $Ph_2S{\cdot}B(C_6F_5)_3$ with xenon difluoride at -20 °C results in full conversion to $[Ph_2SF][FB(C_6F_5)_3]$ (**37**) over an hour period. The fluorosulfonium compound **37** appeared to be stable for at least a short period at -30 °C (< 7 days). Warming to 0 ˚C initiated a subsequent reaction and yielded complicated ^1H and ^{19}F NMR spectra in less than 30 minutes. Only fluorobenzene could be unambiguously identified, a possible byproduct from an electrophilic substitution mechanism. Other by-products may have arisen from aryl C-H activation of the diphenylsulfide ligand.

Introducing electron withdrawing substituents, such as $-NO_2$, on the phenyl ring to inhibit electrophilic attack on the phenyl rings resulted in a reduced basicity of the thioether relative to acetonitrile, as the formation of $(\{4\text{-}NO_2\}Ph)_2S{\cdot}B(C_6F_5)_3$ was not seen. Instead the borane·acetonitrile adduct was formed in the presence of $S(p\text{-}C_6H_4NO_2)_2$. The NMR reaction of $(\{4\text{-}NO_2\}Ph)_2S$, xenon(II) fluoride and $B(C_6F_5)_3$ in acetonitrile-d^3 was initiated at -10 ˚C, but produced scattered ^1H and ^{19}F NMR spectra after 30 minutes. No observation of the $[(\{4\text{-}NO_2\}Ph)_2SF]^+$ cation was seen, with only one species from the number of byproducts identified as (4-nitro)fluorobenzene.

5.1.3.2 Alternative Elements For $[R_nX\text{-}F]^+$ Formation

A brief study was conducted to see whether an S(IV) species can undergo oxidation to S(VI) under similar conditions to $R_2S(II) \rightarrow R_2S(IV)F_2$. Dimethyl sulfoxide was dissolved in acetonitrile before the addition of XeF_2 at room temperature. No oxidation was seen, confirmed by NMR spectroscopy. The use of the smaller, calcogen centre as the F^+ carrier was found to be unsuccessful. The reaction of diphenyl ether with $B(C_6F_5)_3$ and XeF_2 at 0 °C produced $[Xe(C_6F_5)][F_2B(C_6F_5)_2]$ only,[263] with the ether not taking part in the reaction.

The diffusion and stabilisation of the charge of the $[R_nX\text{-}F]^+$ cation with higher period elements was probed; The use of Ph_3BiF_2 was targeted as a synthetic alternative to R_2SF_2. The added attraction here was that the formation of bismuth fluorides does not require expensive XeF_2. Synthesis of triphenylbismuth difluoride was a two-step process: Chlorination of Ph_3Bi with sulfuryl chloride in dichloromethane at -78 °C gave Ph_3BiCl_2,[264] followed by halide exchange with two equivalents of KF in acetone at room temperature.[265]

The reaction of Ph_3BiF_2 with a acetonitrile-d^3 solution of $B(C_6F_5)_3$ was monitored by ^{19}F colt temperature NMR spectroscopy (Figure 82). Fluoride abstraction from the bismuth(V) compound occurs below -40 ˚C, with the observation of three sets of signals (approx. 1:1:1 ratio, with reasons for this splitting currently unclear, but possiblities of intermolecular interations have been considered), as well as the M-F peaks corresponding to the $[Ph_3BiF]^+$ cation (broad singlet at -175 ppm) and an $[F\text{-}B(C_6F_5)_3]^-$ anion (broad doublet at -177 ppm). As seen before, an increase in temperature led to further reactions and at 0 ˚C results in the loss of the signals corresponding to $[Ph_3Bi\text{-}F]^+$ and $[F\text{-}B(C_6F_5)_3]^-$.

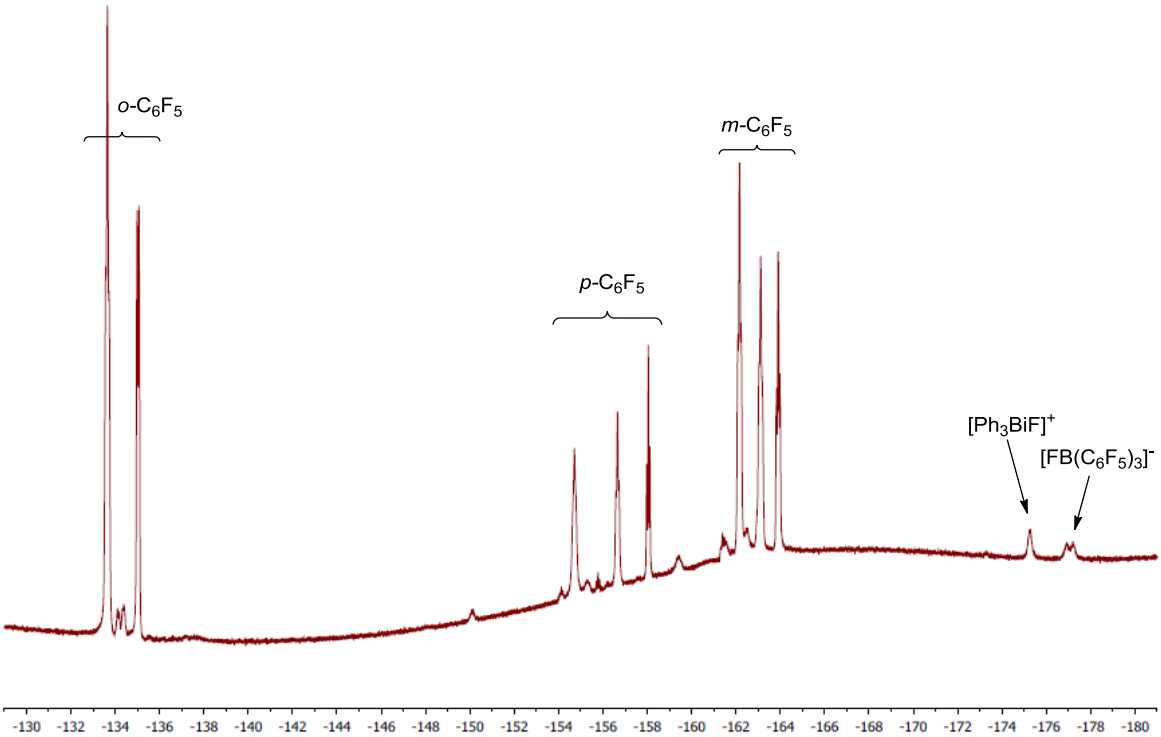

Figure 82. ^{19}F NMR spectrum of the reaction product(s) from Ph_3BiF_2 and $B(C_6F_5)_3$ at -40 °C.

Single crystals of what was believed to be $[Ph_3BiF][FB(C_6F_5)_3]$ were obtained when the reaction mixture was cooled from -40 to -80 ˚C. Any anaylses of these crystals was unsuccessful, as the temperature-sensitive material could only be manipulated under ambient conditions, resulting in a powdery residue with no single crystals viable for diffractometry studies.

5.1.4 Conclusions

Treatment of $R_2S{\cdot}B(C_6F_5)_3$ with xenon difluoride at reduced temperatures gave temperature sensitive fluorosulfonium compounds. These compounds are highly electrophilic and promote decomposition by cleaving C-H and C-C bonds of the thioether moieties at room temperature. An alternative viewpoint saw the use of a softer, larger bismuth centre that appeared to furnish a fluorobismuth cationic species at -40 °C, but characterisation and isolation of this species was inhibited by the poor stability at ambient temperatures.

6 – Experimental Section

6.1 Methods and Materials

All manipulations of air-sensitive materials were performed under dry nitrogen gas, employing exclusion of oxygen and moisture. Flame-dried Schlenk-type glassware was used on a dual-manifold Schlenk line or in a N_2-filled Saffron Scientific Alpha glove box. Unless indicated otherwise, solvents were purified by distillation under nitrogen from: sodium (low-sulfur toluene and 1,4-dioxane); sodium-benzophenone (tetrahydrofuran and diethyl ether); sodium-benzophenone with diglyme indicator (light petroleum, b.p. 40 – 60 °C); or calcium hydride (dichloromethane and acetonitrile). NMR solvents were degassed by several freeze-pump-thaw cycles and dried over activated 4 Å molecular sieves.

The compounds used which have previously been synthesised in literature are documented here. *Ligand precursors:* $[CH\{C(CF_3)N(3,5\text{-}(CF_3)_2C_6H_3)\}_2]H$,[161] $[CH\{C(CF_3)N(3,5\text{-}Me_2C_6H_3)\}_2]H$,[161] $Ph_2P(o\text{-}SO_3HC_6H_4)$,[215e] $Ph_2P(o\text{-}SO_3KC_6H_4)$,[215e] $(C_6F_5)MgBr$,[266] $[Hg(2,4,6\text{-}C_6H_2Me_3)_2]$,[267] $(Ph_4C_4)Sn$.[268] *Gold(I) complexes:* (tht)AuCl,[269] $^tBu_2SAuCl$,[270] $(Ph_3P)AuCl$,[271] $(Cy_3P)AuCl$,[272] $[(C_6F_5)_4Au_2Ag_2]_n$.[218d] *Gold(III) complexes:* $[^nBu_4N][Au(C_6F_5)_2Cl_2]$,[83] $[Au(C_6F_5)_2Cl]_2$,[83] $[(C_6F_5)_2Au(OEt_2)_2][SbF_6]$,[83] $[^nBu_4N][AuCl_4]$,[273] $[^nBu_4N][Au(2,4,6\text{-}C_6H_2Me_3)_2Cl_2]$,[274] $[^nBu_4N][Au(2,4,6\text{-}C_6H_2Me_3)_2Cl]_2$[243] Me_2SAuBr_3.[243] *Counterion and Lewis acidic precursors:* $Et_2O{\cdot}B(C_6F_5)_3$,[142] $B(C_6F_5)_3$,[142] $[Li(OEt_2)_3][B(C_6F_5)_4]$,[275] $[CPh_3][B(C_6F_5)_4]$,[276] and $[Et_3Si][B(C_6F_5)_4]$,[276] $AgO_2C(p\text{-}C_6H_4Br)$,[277] and $AgO_2C(C_6F_5)$,[277] $AgOSO_2CH_3$,[278] $AgOSO_2(p\text{-tol})$,[278] AgO_2CCCl_3,[279] and AgO_2CCBr_3,[279] NaO_2CCF_3,[280] NaO_2CCCl_3,[280] NaO_2CCH_3,[280] $NaOSO_2CF_3$,[281] $[^nBu_4N][O_2CCF_3]$,[282] $[^nBu_4N][O_2CCCl_3]$,[282] $[^nBu_4N][OSO_2CF_3]$.[283] *Miscellaneous reagents:* $LiN(Pr^i)_2$,[284] $LiN(SiMe_3)_2$,[285] PhIO,[286] $PhI(OAc^F)_2$,[287] Ph_3BiCl_2,[288] Ph_3BiF_2.[265]

The following compounds were prepared by other members of the faculty: $[CH\{C(CF_3)N(3,5\text{-}CH_3C_6H_3)\}_2]AuPPh_3$ (**17a**) was first prepared by Dr. Nora Carrera Aguado; The cluster complexes $[^nBu_4N]_4[(C_6F_5)_4Au_2Ag_2(NO_3)_2]_2$ (**31a**) and $[^nBu_4N]_2[(C_6F_5)_4Au_2Ag_2(\mu^3\text{-}OAc^F)]_2$ (**32a**) were first synthesised by Mr. Luke Wilkinson. Data collection and refinements of the X-ray crystallographic analysis

were performed by Dr David Hughes, Dr Mark Schormann, Dr Anna-Marie Fuller and the researchers at the EPSRC National Crystallography Service.

All NMR spectra were recorded on a Brüker Advance DPX-300 spectrometer. ^{1}H NMR spectra (300.1 MHz) were referenced to the residual protons of the deuterated solvent used. ^{13}C{^{1}H} NMR spectra (75.5 MHz) were referenced internally to the D-coupled ^{13}C resonances of the NMR solvent. ^{11}B (96.3 MHz), ^{19}F (282.4 MHz) and ^{31}P (121.5 MHz) NMR spectra were referenced externally to $BF_3{\cdot}Et_2O$, $CFCl_3$ or 85 % H_3PO_4, respectively. IR spectra were recorded on a Perkin Elmer Spectrum BX spectrometer equipped with a diamond ATR attachment. UV-visible absorption spectra were recorded using a Perkin Elmer Lambda 35 UV/VIS spectrometer. Excitation and emission spectra of solutions as well as lifetime experiments were recorded in a (TCSPC) FluoroLog Horiba Jobin Yvon spectrofluorometer using quartz cuvettes, with solid samples run on a Perkin Elmer LS55 Fluorescence Spectrometer with a solids mount attachment. Crystals were examined at 140(1) K on an Oxford Diffraction Xcalibur-3/Sapphire3-CCD diffractometer equipped with Mo-Kα radiation and graphite monochromator, or at 120(2) K on either a Brüker-Nonius KappaCCD diffractometer or a Rigaku AFC12 Kappa-3-circle, Saturn724+ CCD diffractometer (at the EPSRC National Crystallography Service). Elemental analysis was carried out by London Metropolitan University.

6.2 Experimental

6.2.1 *N*-Coordinate Ligation to Gold(I)

6.2.1.1 Synthesis of Gold(I)- and Gold(III)Tetrafluorophthalimidate Complexes

*o-$C_6F_4(CO)_2NH$ (**2**)*

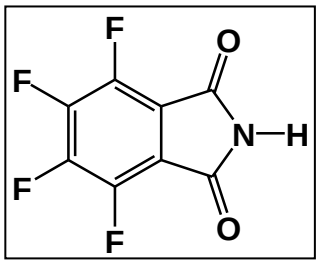

The synthesis was adapted from literature procedures.[139,140] Thionyl chloride (40 mL) was added drop-wise over 15 minutes to 1,2,3,4-tetrafluorophthalic acid (25.1 g, 105.4 mmol) at 60 °C. The subsequent white suspension was heated to 90 °C overnight to afford a light brown solution. The excess thionyl chloride was removed *in vacuo* and the resulting ivory solid dried under vacuum overnight. The crude tetrafluorophthalic anhydride **1** (21.1 g, 95.9 mmol, 91 %) was used without further purification. The analytical data for this compound was in agreement with the literature data.[139]

For the conversion into the phthalimide, a mixture of **1** (5.70 g, 25.9 mmol) and urea (1.63 g, 27.2 mmol) was heated at 135 °C for 10 min under a nitrogen atmosphere, upon which the contents melted and then re-solidified. The crude phthalimide was dissolved in the minimum amount of hot anisole (40 mL), filtered and recrystallised at 2 °C to produce yellow crystals of **2** (4.42 g, 20.2 mmol, 78 %).

^{19}F NMR ($CDCl_3$): δ -134.7 (2F, m, *o*-C_6F_4), -141.2 (2F, m, *m*-C_6F_4). ^{19}F NMR (CD_3CN): δ -139.9 (2F, m, *o*-C_6F_4), -146.0 (2F, m, *m*-C_6F_4). IR (powder): 1740 cm^{-1} *ν*(C=O).

*Li[$C_6F_4(CO)_2N$] (**3**)*

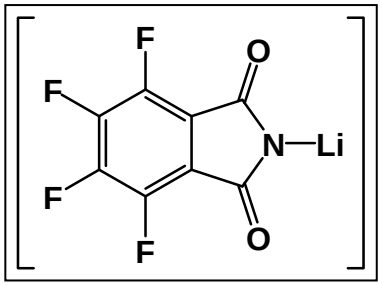

To a solution of **2** (1.05 g, 4.8 mmol) in diethyl ether (20 mL) cooled to -78 °C was added a solution of LiN^iPr_2 (0.512 g, 4.8 mmol) in diethyl ether. The mixture was stirred for 1 h to give an orange solution which was allowed to warm to room temperature. Removal of the solvent produced **3** as an orange solid. The attempted

recrystallisation by dissolving this solid in diethyl ether (20 mL) and layering with toluene at 2 °C resulted in the precipitation of an orange powder (740 mg, 3.3 mmol, 69 %).

^{19}F NMR (THF-d_8): δ -143.7 (2F, br. s, *o*-C_6F_4), -152.5 (2F, br. s, *m*-C_6F_4). IR (nujol mull): 1640 cm^{-1} ν(C=O).

*$Me_3Si[C_6F_4(CO)_2N]$ (**4**)*

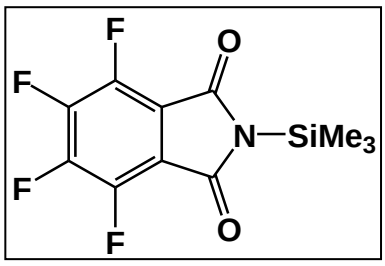

A solution of **2** (13.6 g, 62 mmol) in dry THF (300 mL) was cooled to -80 °C before addition of trimethylchlorosilane (15.7 mL, 124 mmol), followed by dry triethylamine (8.7 mL, 62 mmol). A white precipitate formed. The reaction was warmed to 20 °C and stirred for 1h before the solvent was removed *in vacuo*. The residue was dissolved in light petroleum and recrystallised at 2 °C to yield yellow needles which were filtered and washed with cold light petroleum to produce **4** as pale yellow needles (8.1 g, 28 mmol, 45%).

^{1}H NMR ($CDCl_3$): δ 0.48 (9H, s, Me). ^{19}F NMR ($CDCl_3$): δ -137.0 (2F, m, *o*-C_6F_4), -142.7 (2F, m, *m*-C_6F_4). ^{13}C{^{1}H} NMR ($CDCl_3$): δ 166.5 (s, C=O), 144.3 (dm, J_{CF} = 278 Hz, *o*-C_6F_4), 142.4 (dm, J_{CF} = 271 Hz, *m*-C_6F_4), 115.81 (s, *ipso*-C_6F_4), -0.51 (s, Me). IR (powder): 1706 cm^{-1} ν(C=O). Anal. found: C, 45.41 H, 3.00; N, 4.91 %. Calcd for $C_{11}H_9F_4NO_2Si$: C, 45.36; H, 3.11; N, 4.81.

*$Me_3Sn[C_6F_4(CO)_2N]$ (**5**)*

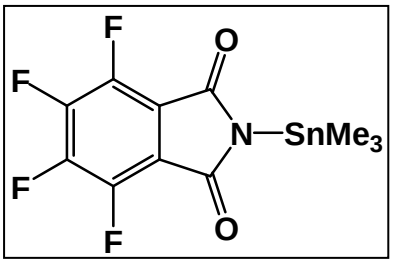

The compound was made following the procedure described for **4**, with the exception that the product was recrystallised from diethyl ether at 2 °C to give yellow crystals of **5** (5.65 g, 14.9 mmol, 67 %).

^{1}H NMR ($CDCl_3$): δ 0.72 (9H, s, Me). ^{19}F NMR ($CDCl_3$) δ -137.9 (2F, m, *o*-C_6F_4), -144.2 (2F, m, *m*-C_6F_4). ^{13}C{^{1}H} NMR ($CDCl_3$): δ 169.0 (s, C=O), 144.6 (dm, J_{CF} = 274 Hz, *o*-C_6F_4), 142.6 (dm, $J_{C\text{-}F}$ = 263 Hz, *m*-C_6F_4), 116.4 (s,

ipso-C_6F_4), -3.7 (s, Me). IR (powder): 1706 cm^{-1} ν(C=O). Anal. Found: C, 34.71; H, 2.45; N, 3.70. Calcd for $C_{11}H_9F_4NO_2Sn$: C, 34.58; H, 2.38; N, 3.67 %.

*$Ag_2[C_6F_4(CO)_2N]_2$ (**6**).*

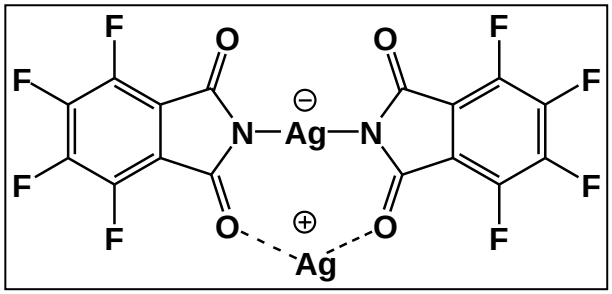

The silyl compound **4** (4.40 g, 15.1 mol) was dissolved in 70 mL dry acetonitrile before silver fluoride addition (1.92 g, 15.1 mmol). The mixture was stirred at room temperature for 30 min to yield a hazy solution. The solvent was removed *in vacuo*. The pale yellow solid residue was redissolved in dry acetonitrile (20 mL). Precipitation by addition of diethyl ether (50 mL) yielded a fluffy straw-coloured solid which was filtered off, washed with diethyl ether and dried to give **6** (4.51 g 6.9 mmol, 92%). The compound can be obtained free of coordinating solvent by prolonged evacuation. For single crystal X-ray analysis, the product was recrystallised from acetonitrile layered with diethyl ether, to give pale straw coloured needles of **6**·2MeCN.

^{19}F NMR (CD_3CN): δ -143.6 (4F, m, *o*-C_6F_4), -150.7 (4F, m, *m*-C_6F_4). $^{13}C\{^1H\}$ NMR (CD_3CN): δ 173.9 (s, C=O), 143.3 (dm, J_{CF} = 261 Hz, *o*-C_6F_4), 141.3 (dm, J_{CF} = 263 Hz, *m*-C_6F_4), 119.1 (s, *ipso*-C_6F_4). IR (powder): 1587 cm-^{1} ν(C=O). Anal. Found: C, 29.33; N, 4.32. Calcd for $C_{16}Ag_2F_8N_2O_4$: C, 29.46; N, 4.30 %.

*$(Ph_3P)Au[N(CO)_2C_6F_4]$ (**7a**)*

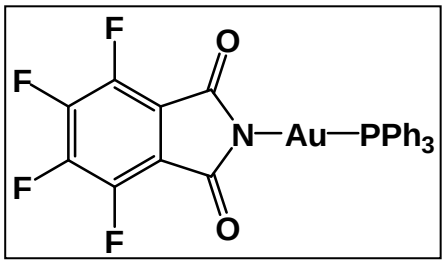

To a solution of **6** (0.502g, 1.55 mmol) in dry acetonitrile (50 mL) was added (triphenylphosphine)gold(I) chloride (0.768 g, 1.55 mmol). The reaction was stirred at room temperature for 30 min, before being filtered through Celite to give a clear yellow-green solution. The solvent was removed and the residue recrystallised from the minimum amount of hot toluene, to yield **7a** as colourless crystals (0.790 g, 1.19 mmol, 77 %).

^{1}H NMR ($CDCl_3$): δ 7.5 (15H, m, Ph). ^{19}F NMR ($CDCl_3$) δ -139.2 (2F, m, *o*-C_6F_4), -145.9 (2F, m, *m*-C_6F_4). ^{13}C{^{1}H} NMR ($CDCl_3$): δ 172.2 (s, C=O), 144.2 (dm, J_{CF} = 267 Hz, *o*-C_6F_4), 142.0 (dm, J_{CF} = 262 Hz, *m*-C_6F_4), 134.1 (s, *o*-Ph), 132.4 (s, *m*-Ph), 129.4 (s, *p*-Ph), 128.4, (d, J_{CP} = 63.1 Hz, *ipso*-Ph), 117.8 (s, *ipso*-C_6F_4). ^{31}P NMR ($CDCl_3$): δ 32.3 (s). IR (powder): 1678 cm^{-1} ν(C=O). Anal. Found: C, 46.13; H, 2.30; N, 2.10. Calcd for $C_{26}H_{15}AuF_4NO_2P$: C, 46.08; H, 2.23; N, 2.07 %.

*(Cy_3P)Au[N(CO)$_2$C$_6$F$_4$] (**7b**)*

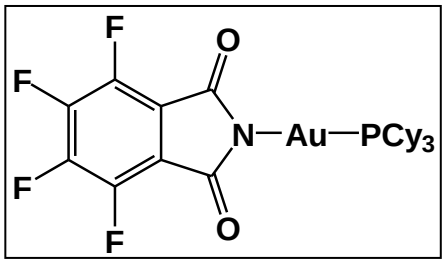

Using the procedure described for **7a**, the reaction yielded **7b** as colourless crystals (0.646 g, 0.82 mmol, 74 %).

^{1}H NMR ($CDCl_3$): δ 2.04 (12H, br., m, 1-Cy), 1.94 (12H, br., m, 2-Cy), 1.70 (3H, br., m, *ipso*-Cy), 1.42 (12H, br., m 3-Cy), 1.23 (6H, br., m, 4-Cy). ^{19}F NMR ($CDCl_3$) δ -139.7 (2F, m, *o*-C_6F_4), -146.4 (2F, m, *m*-C_6F_4). ^{13}C{^{1}H} NMR ($CDCl_3$): δ 172.5 (s, C=O), 143.9 (dm, J_{CF} = 266 Hz, *o*-C_6F_4), 141.8 (dm, J_{CF} = 258 Hz, *m*-C_6F_4), 117.1 (s, *ipso*-C_6F_4), 21.8-35.9 (8 signals, Cy). ^{31}P NMR ($CDCl_3$): δ 50.9 (s). IR (powder): 1679 cm^{-1} ν(C=O). Anal. Found: C, 50.25; H, 5.18; N, 1.71. Calcd for $C_{33}H_{41}AuF_4NO_2P$: C, 50.30; H, 5.25; N, 1.78 %.

*(tht)Au[N(CO)$_2$C$_6$F$_4$] (**8**)*

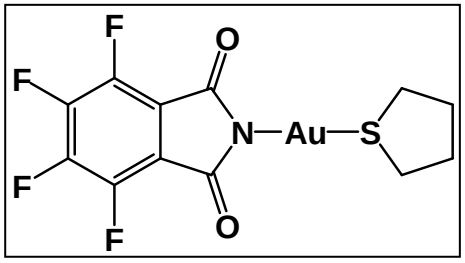

Using the procedure described for **7a**, **8** was obtained from (tht)AuCl as pale yellow crystals (283 mg, 0.56 mmol, 56 %).

^{1}H NMR ($CDCl_3$): δ 3.42 (4H, br. s, 1-tht), 2.21 (4H, br. s, 2-tht). ^{19}F NMR ($CDCl_3$): δ -138.8, (2F, m, *o*-C_6F_4), -145.9 (2F, m, *m*-C_6F_4). ^{13}C{^{1}H} NMR ($CDCl_3$): δ 170.9 (s, C=O), 144.4 (dm, J_{CF} = 271 Hz, *o*-C_6F_4), 141.7 (dm, J_{CF} = 266 Hz, *m*-C_6F_4), 120.2 (s, *ipso*-C_6F_4), 39.8 (s, 2-tht), 30.4 (s, 1-tht). IR (powder): 1678 cm^{-1} ν(C=O). Anal. Found: C, 28.74; H, 1.66; N, 2.85. Calcd for $C_{12}H_8AuF_4NO_2S$: C, 28.63; H, 1.60; N, 2.78 %.

*Ag[Au{N(CO)$_2$C$_6$F$_4$}$_2$](**9**)*

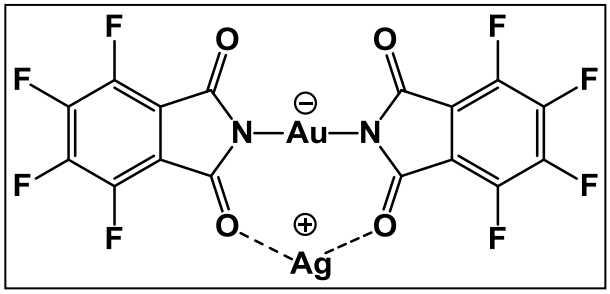

To a solution of **6** (0.810 g, 1.24 mmol) in acetonitrile (20 mL) was added AuCl (142 mg, 0.61 mmol). The mixture was stirred for 30 min. The resulting mixture was filtered through Celite to give a pale-brown solution. The solvent was removed and the residue was dried by evacuation to yield **9** as a dark brown powder (282.4 mg, 0.38 mmol, 63 %). For single crystal X-ray analysis, a hot concentrated acetonitrile solution was allowed to cool slowly, resulting in the formation of brown crystals of [(MeCN)$_2$Ag][Au{N(CO)$_2$C$_6$F$_4$}$_2$]·MeCN (**9**·3MeCN).

^{19}F NMR (CD$_3$CN) δ -143.0 (4F, m, *o*-C$_6$F$_4$), -149.7 (4F, m, *m*-C$_6$F$_4$). ^{13}C{^{1}H} NMR (CD$_3$CN): δ 171.7 (s, C=O), 143.8 (dm, J_{CF} = 266 Hz, *o*-C$_6$F$_4$), 141.9 (dm, J_{CF} = 256 Hz, m-C$_6$F$_4$). Further analysis was carried out after removing the solvent molecules in a vacuum; IR (powder): 1653 and 1620 cm^{-1} ν(C=O). Anal. Found: C, 26.01; N, 3.70. Calcd for C$_{16}$AgAuF$_8$N$_2$O$_4$: C, 25.92; N, 3.78 %.

Attempted Synthesis of [(MeCN)Au{N(CO)$_2$C$_6$F$_4$}]

The procedure described for **9** was used, except that a 1:1 stoichiometric ratio of **6** and AuCl was used. A pale yellow acetonitrile solution resulted. ^{19}F NMR (CDCl$_3$) δ -141.3, (2F, m, *o*-C$_6$F$_4$), -145.9 (2F, m, *m*-C$_6$F$_4$). IR (MeCN solution): 1676 cm^{-1} ν(C=O). Concentration of this solution and attempts to isolate the product resulted in decomposition to metallic gold.

*[Au(PPh$_3$)$_2$][N(CO{B(C$_6$F$_5$)$_3$})$_2$C$_6$F$_4$] (**10**)*

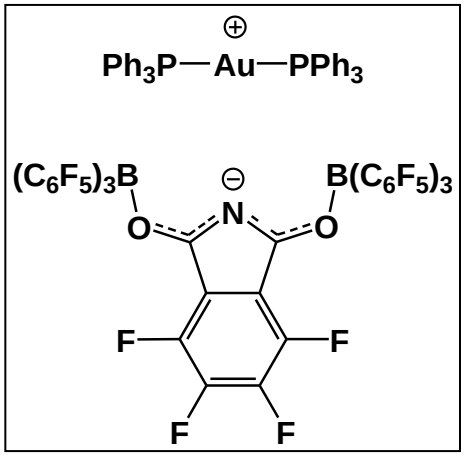

To a solution of **7a** (204 mg, 0.30 mmol) and triphenylphosphine (77 mg, 0.30 mmol) in dry diethyl ether (30 mL) was added at room temperature B(C$_6$F$_5$)$_3$·Et$_2$O (346 mg, 0.60 mmol). The mixture was stirred for 15 min, then the solvent was removed and the yellow solid residue recrystallised from a minimum amount of toluene layered with light petroleum. Yellow crystals of **10** were obtained (452 mg, 0.23 mmol, 78 %).

^{1}H NMR (CDCl$_3$): δ 7.48 (30H, m, Ph). ^{19}F NMR (CDCl$_3$) δ -115.9 (12F, t, J_{FF} = 22.4 Hz, *o*-C$_6$F$_5$), -133.5 (2F, br. s, *o*-C$_6$F$_4$), -141.0 (2F, br. s, *m*-C$_6$F$_4$), -158.2 (6F, t, J_{FF} = 22.4 Hz, *p*-C$_6$F$_5$), -162.3 (12F, m, *m*-C$_6$F$_5$). ^{31}P NMR (CDCl$_3$) 30.1 (s). ^{11}B NMR (CDCl$_3$): δ -2.7 (br.). IR (nujol mull): 1545 cm^{-1} ν(C=O).

*[Au(nbe)$_3$][N(CO{B(C$_6$F$_5$)$_3$})$_2$C$_6$F$_4$] (**11**)*

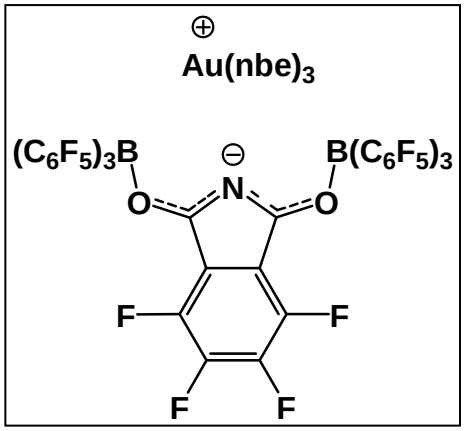

To a mixture of **8** (50 mg, 0.10 mmol) and norbornene (94 mg, 1.00 mmol) in dry toluene (10 mL) cooled to 0 °C was added tris(pentafluorophenyl)borane (130 mg, 0.25 mmol). The reaction was left to stir at 0 °C for 1 hour. The resulting solution was filtered and the solvent was removed *in vacuo* to leave a yellow solid. Recrystallisation in the minimum amount of dichloromethane at -30 °C gave **11** as yellow crystals in moderate yield (92 mg, 0.05 mmol, 54 %).

^{1}H NMR (CDCl$_3$): δ 0.94 (2H, d, J_{HH} = 9.7 Hz, nbe), 1.01 (2H, d, J_{HH} = 10.2 Hz, nbe), 1.23 (2H, dd, J_{HH} = 8.5, 2.0 Hz, nbe), 1.74 (2H, d, J_{HH} = 8.5 Hz, nbe), 3.02 (2H, s, nbe), 5.72 (2H, s, nbe). ^{19}F NMR (CDCl$_3$): δ -114.2 (12F, t, J_{FF} = 19.6 Hz, *o*-C$_6$F$_5$), -132.1 (2F, m, *o*-C$_6$F$_4$), -141.3 (2F, m, *o*-C$_6$F$_4$), -159.2 (6F, t, $J_{o\text{-}FF}$ = 19.6 Hz, *m*-C$_6$F$_5$), -165.4 (12F, m, *p*-C$_6$F$_5$). ^{11}B NMR (CDCl$_3$): δ 1.9 (br.).

[^{n}Bu$_4$N][Au(C$_6$F$_5$)$_2$]

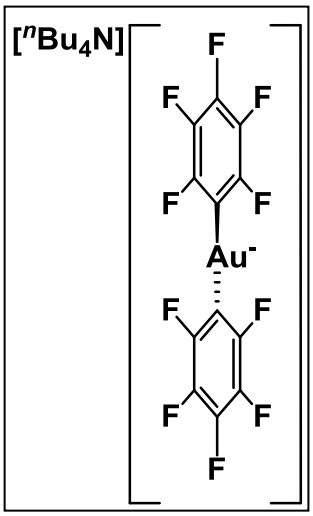

To a diethyl ether solution of (C$_6$F$_5$)MgBr (6.5 mL, 0.96 M, 6.24 mmol) at 0 °C was added (tht)AuCl (1.00 g, 3.12 mmol). After 1h of stirring, ^{n}Bu$_4$NCl (0.970 g, 3.49 mmol) was added and the reaction mixture was stirred at room temperature for 3 hours. The white solid formed was separated by filtration and washed with water (3 x 20 mL), diethyl ether (3 x 20 mL) and light petroleum (3 x 20 mL). The solid was dissolved in dichloromethane and concentrated under vacuum. Finally, the addition of light petroleum (20 mL) generated [^{n}Bu$_4$N][Au(C$_6$F$_5$)$_2$] as a white powder (1.68g, 2.17 mmol, 72%). Characterisation data compares to literature values.[218f]

*(C$_6$F$_5$)$_2$Au(SMe$_2$)(N{CO}$_2$C$_6$F$_4$) (**12**)*

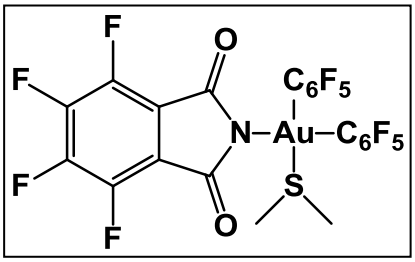

To a solution of [(C$_6$F$_5$)$_2$AuCl]$_2$ (102 mg, 0.092 mmol) and dimethyl sulfide (0.2 mL) in acetonitrile (10 mL), an addition of Ag$_2$[N(CO)$_2$C$_6$F$_4$]$_2$ (**6**, 58 mg, 0.090 mmol) was made and the reaction stirred under the exclusion of light for 1 hour. Evaporation of the solvent followed by redissolution in toluene, filtration through Celite and removal of solvent gave **12** as a yellow powder (118 mg, 0.146 mmol, 81 %). Recrystallisation in a reduced volume of toluene at 2 °C produces *cis*-**12** as yellow crystals.

<u>In CDCl$_3$:</u> *cis*:*trans* ratio was found to be 65:35.

***Cis*-12**: ^{1}H NMR (CDCl$_3$): δ 2.64 (br. s, SMe$_2^{cis}$ and SMe$_2^{trans}$). ^{19}F NMR (CDCl$_3$): δ -122.6 (4F, 2 × m, *o*-C$_6$F$_5$), -137.2 (2F, m, *o*-C$_6$F$_4$), -144.0 (2F, m, *m*-C$_6$F$_4$), -152.2 (1F, t, J_{FF} = 20.3 Hz, *p*-C$_6$F$_5$), -154.0 (1F, t, J_{FF} = 20.3 Hz, *p*-C$_6$F$_5$), -158.3 (2F, m, *m*-C$_6$F$_5$), -159.6 (2F, m, *m*-C$_6$F$_5$).

***Trans*-12**: ^{1}H NMR (CDCl$_3$): δ 2.64 (br. s, SMe$_2^{cis}$ and SMe$_2^{trans}$). ^{19}F NMR (CDCl$_3$): δ -122.0 (4F, m, *o*-C$_6$F$_5$), -138.8 (2F, m, *o*-C$_6$F$_4$), -145.6 (2F, m, *m*-C$_6$F$_4$), -156.4 (2F, t, J_{FF} = 19.8 Hz, *p*-C$_6$F$_5$), -161.4 (4F, m, *m*-C$_6$F$_5$)

Solid state: Isolated as ***cis*-12** only. IR (powder); 1690 cm^{-1} ν(C=O). Anal. found: C, 32.62; H, 0.73; N, 1.86. Calcd for $C_{22}H_6AuF_{14}NO_2S$: C, 32.55; H, 0.75; N, 1.73.

*$(C_6F_5)_2Au(PPh_3)(N\{CO\}_2C_6F_4)$ (**13**)*

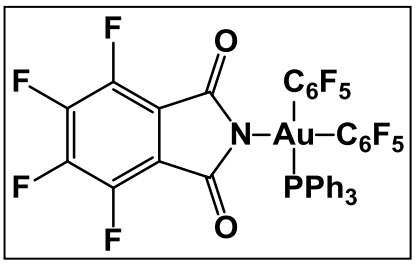

Method A: To a solution of $[(C_6F_5)_2AuCl]_2$ (126 mg, 0.111 mmol) and triphenylphosphine (63 mg, 0.240 mmol) in acetonitrile (10 mL) was added $Ag_2[N(CO)_2C_6F_4]_2$ (**6**, 73 mg, 0.112 mmol) and the reaction stirred under the exclusion of light for 1 hour. Evaporation of the solvent followed by redissolution in toluene, filtration through Celite and removal of solvent gave **13** as a yellow powder (185 mg, 0.183 mmol, 82 %). Recrystallisation in a reduced volume of toluene at 2 °C produces *cis*-**13** as yellow crystals.

Method B: A solution of **12** (60 mg, 0.073 mmol) in acetonitrile (10 mL) was dosed with triphenylphosphine (19 mg, 0.072 mmol) and stirred for 15 minutes before evaporation, redissolution in toluene, filtration through Celite and recrystallisation in a reduced volume of the solvent at 2 °C to give **13** as yellow crystals (31 mg, 0.031 mmol, 44 %).

In $CDCl_3$: *trans*-**13** was only observed. ^1H NMR ($CDCl_3$): δ 7.55 (3H, m, Ph), 7.41 (6H, m, Ph), 7.17 (6H, m, Ph). ^{19}F NMR ($CDCl_3$): δ -122.5 (4F, m, *o*-C_6F_5), -139.7 (2F, m, *o*-C_6F_4), -147.3 (2F, m, *m*-C_6F_4), -158.0 (1F, t, J_{FF} = 20.1 Hz, *p*-C_6F_5), -162.5 (2F, m, *m*-C_6F_5). $^{13}C\{^1H\}$ NMR ($CDCl_3$): δ 169.1 (s, C=O), 147.5 (m, *o*-C_6F_5), 145.5 (dm, J_{CF} = 272 Hz, *o*-C_6F_4), 144.0 (m, *m*-C_6F_5), 141.3 (dm, J_{CF} = 257 Hz, *m*-C_6F_4), 138.6 (m, *p*-C_6F_5), 133.5 (s, Ph), 131.0 (s, Ph), 129.2 (s, Ph), 117.5 (s, *ipso*-C_6F_4). ^{31}P NMR ($CDCl_3$, 121.5 MHz): δ 12.2 (s, PPh_3).

Solid state: found as *cis*-**13** only. IR(powder); 1694 cm^{-1} ν(C=O). Anal. found: C, 45.31; H, 1.56; N, 1.44. Calcd for $C_{38}H_{15}AuF_{14}NO_2P$: C, 45.10; H, 1.50; N, 1.39 %.

*[^{n}Bu$_4$N][(C$_6$F$_5$)$_2$Au(N{CO}$_2$C$_6$F$_4$)$_2$] (**14**)*

To a solution of **6** (45 mg, 0.069 mmol) in acetonitrile (10 mL) was added [^{n}Bu$_4$N][(C$_6$F$_5$)$_2$AuCl$_2$] (59 mg, 0.070 mmol). The mixture was stirred in the absence of light for 30 min. The resulting mixture was evaporated to dryness before redissolution in toluene (10 mL). The yellow solution was filtered through Celite and the filter bed washed with 5 mL toluene. The solvent was removed and the residue was dried. The reaction yielded **14** as a yellow powder (81 mg, 0.067 mmol, 96 %).

^{1}H NMR (CDCl$_3$): δ 3.27 (2H, m, ^{n}Bu$_4$N$^+$), 1.68 (2H, br. m, ^{n}Bu$_4$N$^+$), 1.41 (2H, m, ^{n}Bu$_4$N$^+$), 0.96 (3H, t, ^{n}Bu$_4$N$^+$). ^{19}F NMR (CDCl$_3$): δ -122.7 (4F, m, *o*-C$_6$F$_5$), -139.5 (4F, m, *o*-C$_6$F$_4$), -146.1 (4F, m, *m*-C$_6$F$_4$), -156.9 (2F, t, J_{FF} = 19.8 Hz, *p*-C$_6$F$_5$), -161.9 (4F, m, *m*-C$_6$F$_5$). ^{13}C{^{1}H} NMR (CDCl$_3$): δ 169.3 (s, C=O), 137.9-147.5 (br. m, *o*- and *m*-C$_6$F$_5$), 129.0 (s, *p*-C$_6$F$_5$), 128.2 (s, *m*-C$_6$F$_5$), 125.3 (s, *p*-C$_6$F$_5$), 117.4 (s, *ipso*-C$_6$F$_4$), 58.6 (s, ^{n}Bu$_4$N$^+$), 23.9 (s, ^{n}Bu$_4$N$^+$), 19.6 (s, ^{n}Bu$_4$N$^+$), 13.5 (s, ^{n}Bu$_4$N$^+$). IR (powder): 1695 cm^{-1} ν(C=O). Anal. Found: C, 43.91; H, 3.18; N, 3.87. Calcd for C$_{44}$H$_{36}$AuF$_{18}$N$_3$O$_4$: C, 43.66; H, 3.00; N, 3.47 %.

*Reactivity of [(2,4,6-C$_6$H$_2$Me$_3$)$_2$AuCl]$_2$ with **6***

(a) In the Presence of Tetrahydrothiophene

To a solution of [(2,4,6-C$_6$H$_2$Me$_3$)$_2$AuCl]$_2$ (104 mg, 0.111 mmol) and tetrahydrothiophene (0.2 mL) in acetonitrile (10 mL) an addition of **6** (79 mg, 0.121 mmol) was made and the reaction mixture was stirred under the exclusion of light for 1 hour. Evaporation of the solvent followed by redissolution in toluene, filtration through Celite and evaporation under reduced pressure produces **8** as a white powder (66 mg, 0.131 mmol, 59 %).

(b) In the Presence of Triphenylphosphine

Using the procedure described for the synthesis of **8** above, replacing tetrahydrothiophene with triphenylphosphine, the reaction yielded **7a** as a colourless powder (54 mg, 0.080 mmol, 71 %).

(c) In 1:2 Ratio

To a solution of $[(2,4,6\text{-}C_6H_2Me_3)_2AuCl]_2$ (59 mg, 0.063 mmol) in acetonitrile (10 mL) was added **6** (91 mg, 0.140 mmol). The mixture was stirred for 30 min. The resulting mixture was filtered through Celite to give a pale-brown solution. The solvent was removed and the residue was dried. The reaction yielded **9** as a dark brown powder (50 mg, 0.68 mmol, 55 %).

*$C_6F_4(CO)_2NI$ (**15**)*

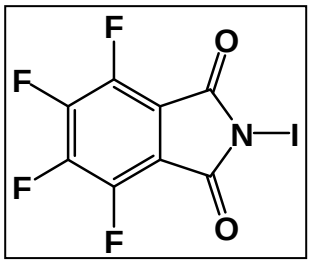

To a solution of iodine (0.76 g, 3.00 mmol) in dry 1,4-dioxane (10 mL) was added **6** (1.00 g, 1.53 mmol). The reaction was stirred in the dark for 10 min. After removal of the solvent under vacuum at 40°C, the residue was taken up in acetonitrile, the silver iodide filtered off and the orange filtrate concentrated *in vacuo* to give the *N*-iodo compound **15** as a yellow solid (0.84 g, 2.43 mmol, 81 %). Crystallisation from hot acetonitrile gave crystals of **15**·MeCN.

^{19}F NMR (CD_3CN): δ -139.4 (2F, m, *o*-C_6F_4), -146.5 (2F, m, *o*-C_6F_4). IR (nujol mull): 1702 cm^{-1} ν(C=O). Anal. Found: C, 27.89; N, 4.17. Calcd for $C_8F_4INO_2$: C, 27.83; N, 4.06 %.

Topic 2: Attempted Oxidation of Gold β-Diketiminates

*$[CH\{C(CF_3)N(3,5\text{-}CF_3C_6H_3)\}_2]K$ (**16a-K**)*

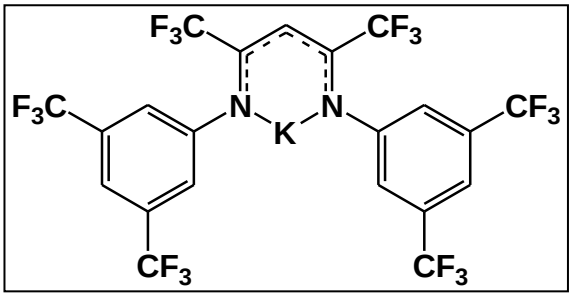

A suspension of KH (34 mg, 0.85 mmol) in diethyl ether (15 mL) was added to a solution of **16a-H** (0.486 g, 0.77 mmol) in diethyl ether (10 mL). The solution turned immediately from yellow to orange. The mixture was stirred for 5 h at room temperature and filtered. The solvent was removed under vacuum to leave **16a-K** as an orange solid (0.490 g, 0.81 mmol, 95 %).

^{1}H NMR ($(CD_3)_2CO$): δ 7.11 (2H, s, *p*-Ar^F), 6.20 (4H, s, *o*-Ar^F), 6.08 (1H, s, methine-CH), ^{19}F NMR ($(CD_3)_2CO$): δ -63.7 (12F, s, Ar-CF_3), -69.5 (6F, s, C-C*F*$_3$). Anal. Found: C, 37.79; H, 1.11; N, 4.28. Calcd for $C_{21}H_7F_{18}KN_2$: C, 37.72; H, 1.06; N, 4.19 %.

[CH{C(CF$_3$)N(3,5-CH$_3$C$_6$H$_3$)}$_2$]K ***(16b-K)***

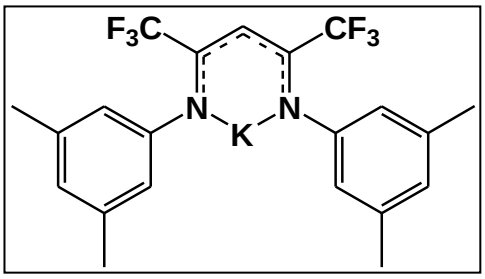

The synthesis was analogous to that of **16a-K**, giving **16b-K** as an orange solid (320 mg, 0.71 mmol, 93 %).

^{1}H NMR ($CDCl_3$): δ 6.80 (2H, s, *p*-Ar), 6.63 (4H, s, *o*-Ar), 5.81 (1H, s, methine-CH), 2.27 (12H, s, CH_3-Ar). ^{19}F NMR ($CDCl_3$): δ -62.8 (6F, s, C-CF_3). Anal. Found: C, 55.67; H, 4.35; N, 6.11. Calcd for $C_{21}H_{19}F_6KN_2$: C, 55.72; H, 4.23; N, 6.19 %.

[CH{C(CF$_3$)N(3,5-CH$_3$C$_6$H$_3$)}$_2$]Au(PPh$_3$) ***(17a)***

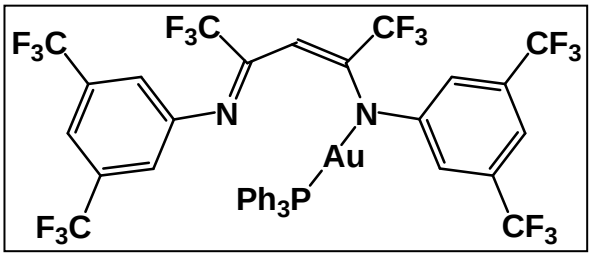

An orange-red solution of **16a-K** (0.31 g, 0.47 mmol) in dry THF (15 mL) was added by syringe to a colourless solution of (Ph_3P)AuCl (0.23 g, 0.47 mmol) in dry THF (20 mL) cooled on an ice bath. After 1 h at 0 ºC and 1h at room temperature the THF solvent was removed to leave an orange-red solid yield of **17a** (0.486 g, 0.45 mmol, 95 %). Recrystallisation from light petroleum at -28 °C gave orange crystals of **17a**, accompanied by a very small amount of yellow crystals of **16a-H**.

^{1}H NMR ($CDCl_3$): δ 7.51 (21H, m; 15H (PPh_3) and 6H (*o*-/*p*-Ar^F), 5.86 (s, 1H, methine-CH). ^{19}F NMR ($CDCl_3$, 20 °C): δ -63.0 (6F, br., N-Ar^F), -63.3 (6F, br., [Au]N-Ar^F), -66.2 (3F, br., N=C-C*F*$_3$), -72.0 (3F, br., [Au]N=C-C*F*$_3$). ^{13}C{^{1}H} NMR ($CDCl_3$): δ 152.7 (br. s), 148.6 (br. s) 133.8 (d, *J* = 13.6 Hz), 132.2 (s), 132.0 (q, *J* = 30.2 Hz), 129.4 (d, *J* = 12.1 Hz), 128.1 (d, *J* = 62.6 Hz), 125.0 (br. s), 121.2 (br. s), 120.4 (br. s), 118.7 (br. s), 114.1 (br. s), 93.6 (br. s). ^{31}P NMR ($CDCl_3$): δ 30.35 (s). Anal. Found: C, 42.92; H, 2.13; N, 2.48. Calcd for $C_{39}H_{22}AuF_{18}N_2P$: C, 43.01; H, 2.04; N, 2.57 %.

[CH{C(CH$_3$)N(3,5-CH$_3$C$_6$H$_3$)}$_2$]Au(PPh$_3$) ***(17b)***

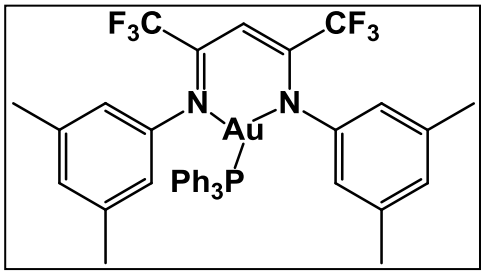

The reaction scheme based on the synthesis of **17a** was followed to produce, after crystallisation, yielded yellow crystals of **17b** (0.371 g, 0.43 mmol, 86 %).

^{1}H NMR (CDCl$_3$): δ 7.47 (15H, m, PPh$_3$), 6.53 (4H, s, *o*-Ar), 6.43 (2H, s, *p*-Ar), 5.51 (s, 1H, methine-CH), 2.07 (12H, s, Me). ^{19}F NMR (CDCl$_3$, 20°C): δ -66.1 (br., 3F, N=C-C*F$_3$*), -71.14 (br., 3F, [Au]N=C-C*F$_3$*). ^{13}C{^{1}H} NMR (CDCl$_3$): δ 142.6 (s), 148.6 (s) 138.4 (d, J = 13.6 Hz), 134.2 (s), 131.8 (s), 129.2 (br. s), 127.2 (s), 125.0 (br. s), 121.2 (br. s), 120.2 (br. s), 119.0 (br. s), 114.3 (br. s), 21.2 (s, Me). ^{31}P NMR (CDCl$_3$): δ 31.02 (s). Anal. Found: C, 53.52; H, 3.78; N, 3.33. Calcd for $C_{39}H_{34}AuF_6N_2P$: C, 53.66; H, 3.93; N, 3.21 %.

6.2.2 Benzylic C-H Activation of Electron-Rich Arenes by Gold(I)

General procedure for C-H activation reactions

(L)AuCl (L = Me$_2$S, or tetrahydrothiophene; 0.5 mmol) and an arene (hexamethylbenzene, pentamethylbenzene, 1,2,4,5-tetramethylbenzene or dimesitylmethane; 0.5 mmol) were dissolved in dichloromethane (15 mL). After cooling to the desired temperature (0 to 20 ˚C), the addition of the silver salt (AgSbF$_6$, AgBF$_4$, AgOTf or AgPF$_6$; 0.5 mmol) resulted in a grey precipitate. The mixture was stirred at RT for 1 – 3 h with the exclusion of light and filtered through a stainless steel cannula. The filtrate was reduced in volume to ~3 mL and diethyl ether was added (30 mL). A colourless solid precipitated which was filtered off, dried *in vacuo* and recrystallised from a minimum amount of dichloromethane (~2 mL) at -30 °C to isolate the products. Reaction conversions were determined by NMR spectroscopy.

Spectroscopic Data of Benzylsulfonium Salts

*[$Me_5C_6CH_2SMe_2$][SbF_6] (**18**)*

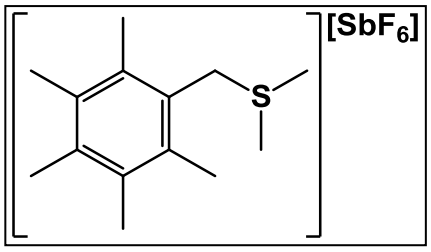

^{1}H NMR ($CDCl_3$): δ, 4.72 (2H, s, Ar$CH_2$$SMe_2$), 2.87 (6H, s, SMe_2), 2.31 (6H, s, *o*-Me), 2.24 (3H, s, *p*-Me), 2.21 (6H, s, *m*-Me). ^{13}C{^{1}H} NMR ($CDCl_3$): δ 140.9 (*Ar*CH_3), 138.2 (*Ar*CH_3), 137.3 (*Ar*CH_3), 47.1 (Ar$CH_2$$SMe_2$), 23.5 (S($CH_3$)$_2$), 19.8 (Ar$CH_3$), 19.5 (Ar$CH_3$), 19.0 (Ar$CH_3$). IR (powder): 659 cm^{-1} *v*(Sb-F).

*[$Me_5C_6CH_2$(tht)][SbF_6] (**20**)*

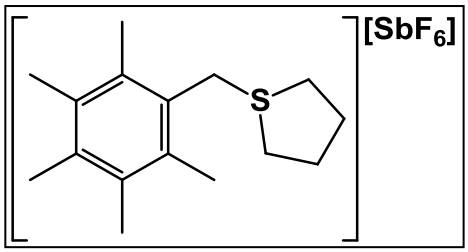

^{1}H NMR ($CDCl_3$): δ 4.60 (2H, s, ArCH_2(tht)), 3.47 (4H, br. m, 2,2'-(tht)), 2.29 (6H, s, *o*-Me), 2.28 (3H, s, *p*-Me), 2.20 (10H, br. m, 3,3'-(tht) and *m*-Me). ^{13}C{^{1}H} NMR ($CDCl_3$): δ 140.6 (*Ar*CH_3), 137.7 (*Ar*CH_3), 136.9 (*Ar*CH_3), 44.3 (ArCH_2(tht)), 37.8 (tht), 34.6 (tht), 19.6 (ArCH_3), 19.4 (ArCH_3), 18.8 (ArCH_3). IR (powder): 659 cm^{-1} *v*(Sb-F).

*[$Me_5C_6CH_2SMe_2$][BF_4] (**21**)*

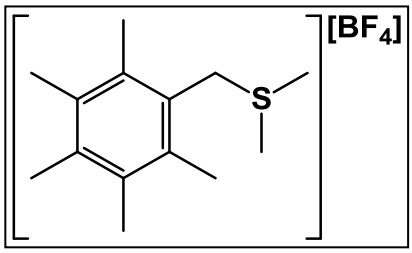

^{1}H NMR ($CDCl_3$): δ 4.77 (2H, s, Ar$CH_2$$SMe_2$), 2.92 (6H, s, SMe_2), 2.31 (6H, s, *o*-Me), 2.21 (3H, s, *p*-Me), 2.19 (6H, s, *m*-Me). ^{13}C{^{1}H} NMR ($CDCl_3$): δ 134.4 (*Ar*CH_3), 134.0 (*Ar*CH_3), 132.1 (*Ar*CH_3), 42.1 (Ar$CH_2$$SMe_2$), 42.1 (Ar$CH_2$($SMe_2$), 24.0 ($SMe_2$), 17.4 (Ar$CH_3$), 17.0 (Ar$CH_3$), 16.9 (Ar$CH_3$). ^{19}F NMR ($CDCl_3$): δ -153.7 ($^-BF_4$). ^{11}B NMR ($CDCl_3$): δ -0.97 ($^-BF_4$).

[Me$_5$C$_6$CH$_2$SMe$_2$][OTf] ***(22)***

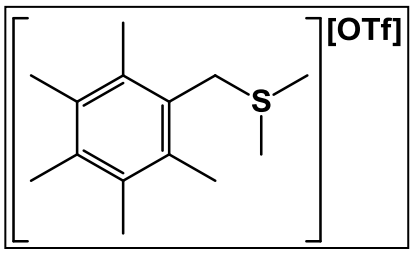

^{1}H NMR (CDCl$_3$): δ 4.79 (2H, s, ArC*H$_2$*SMe$_2$), 2.92 (6H, s, SMe$_2$), 2.31 (6H, s, *o*-Me), 2.24 (3H, s, *p*-Me), 2.20 (6H, s, *m*-Me). ^{13}C{^{1}H} NMR (CDCl$_3$): δ 140.7 (*Ar*CH$_3$), 137.7 (*Ar*CH$_3$), 136.6 (*Ar*CH$_3$), 44.9 (Ar*C*H$_2$SMe$_2$), 23.8 (S(*C*H$_3$)$_2$), 19.8 (Ar*C*H$_3$), 19.5 (Ar*C*H$_3$), 19.1 (Ar*C*H$_3$). ^{19}F NMR (CDCl$_3$): δ -78.2 ($^-$SO$_3$C*F$_3$*).

[Me$_5$C$_6$CH$_2$SMe$_2$][PF$_6$] ***(23)***

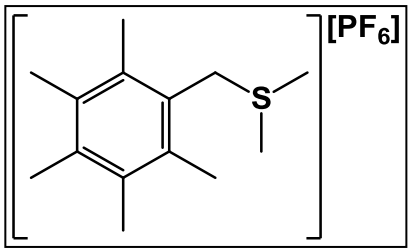

^{1}H NMR (CDCl$_3$): δ 4.79 (2H, s, ArC*H$_2$*SMe$_2$), 2.96 (6H, s, SMe$_2$), 2.32 (6H, s, *o*-Me), 2.21 (9H, m, *m*- and *p*-Me). ^{13}C{^{1}H} NMR (CDCl$_3$): δ 134.4 (*Ar*CH$_3$), 134.0 (*Ar*CH$_3$), 132.1 (*Ar*CH$_3$), 44.4 (Ar*C*H$_2$SMe$_2$), 23.1 (SMe$_2$), 17.3 (Ar*C*H$_3$), 17.1 (Ar*C*H$_3$), 16.8 (Ar*C*H$_3$). ^{19}F NMR (CDCl$_3$): δ -71.7 (d, J_{FP} = 714 Hz, $^-$PF$_6$). ^{31}P NMR (CDCl$_3$): δ -144.2 (s, J_{PF} = 714 Hz, $^-$PF$_6$).

[Me$_4$HC$_6$CH$_2$SMe$_2$][SbF$_6$] ***(24a-c)***

The products could not be separated and isomers were characterized from the mixture by ^{1}H NMR spectroscopy.

[o-Me$_4$HC$_6$CH$_2$SMe$_2$][SbF$_6$] ***(24a)***

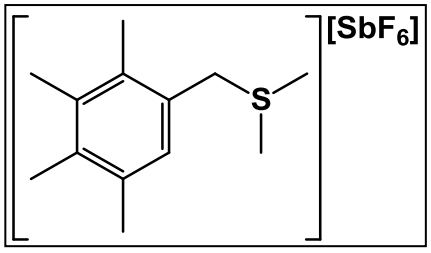

^{1}H NMR (CDCl$_3$): δ 6.99 (1H, s, Ar*H*), 4.50 (2H, s, ArC*H$_2$*SMe$_2$), 2.87 (6H, s, SMe$_2$), 2.44 (3H, s, *o*-Me).

[m-Me$_4$HC$_6$CH$_2$SMe$_2$][SbF$_6$] ***(24b)***

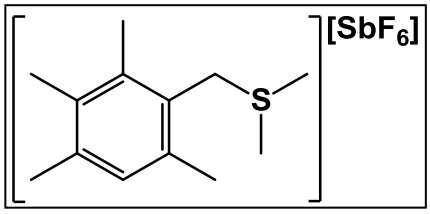

^{1}H NMR (CDCl$_3$): δ 6.82 (1H, s, Ar*H*), 4.64 (2H, s, ArC*H*$_2$SMe$_2$), 2.88 (6H, s, S(C*H*$_3$)$_2$), 2.55 (3H, s, *o*-Me).

[p-Me$_4$HC$_6$CH$_2$SMe$_2$][SbF$_6$] ***(24c)***

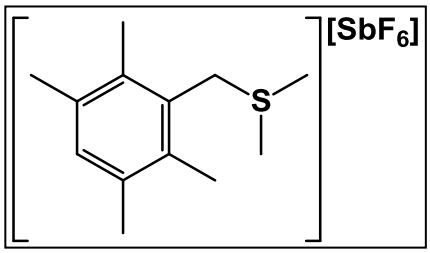

^{1}H NMR (CDCl$_3$): δ 6.92 (1H, s, Ar*H*), 4.72 (2H, s, ArC*H*$_2$SMe$_2$), 2.85 (6H, s, S(C*H*$_3$)$_2$), 2.48 (3H, s, *o*-Me).

[2,4,5-Me$_3$H$_2$C$_6$CH$_2$SMe$_2$][SbF$_6$] ***(25)***

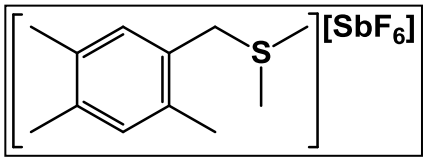

^{1}H NMR (CDCl$_3$): δ 7.09 (1H, s, *o*-H), 7.07 (1H, s, *m*-H), 4.46 (2H, s, ArC*H*$_2$SMe$_2$), 2.86 (6H, s, SMe$_2$), 2.32 (3H, s, *o*-Me), 2.20 (6H, s, *m*- and *p*-Me). ^{13}C{^{1}H} NMR (CDCl$_3$): δ 140.8 (*Ar*CH$_3$), 136.5 (*Ar*CH$_3$), 135.5 (*Ar*CH$_3$), 133.4 (*Ar*H), 133.1 (*Ar*H), 47.7 (Ar*C*H$_2$SMe$_2$), 23.9 (S(*C*H$_3$)$_2$), 19.8 (Ar*C*H$_3$), 19.3 (Ar*C*H$_3$), 18.9 (Ar*C*H$_3$). IR (powder): 658 cm^{-1} *ν*(Sb-F).

[2,4,6-Me$_3$H$_2$C$_6$CH$_2$SMe$_2$][SbF$_6$] ***(26)***

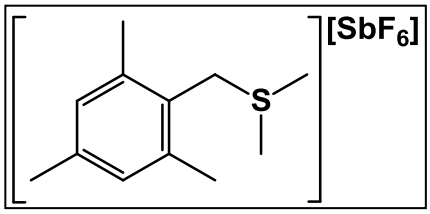

^{1}H NMR (CDCl$_3$): δ 6.90 (2H, s, *m*-H), 4.55 (2H, s, ArC*H*$_2$SMe$_2$), 2.89 (6H, s, S(C*H*$_3$)$_2$), 2.35 (6H, s, *o*-Me), 2.24 (3H, s, *p*-Me). ^{13}C{^{1}H} NMR (CDCl$_3$): δ 140.8 (*Ar*CH$_3$), 140.8 (*Ar*CH$_3$), 138.5 (*Ar*H), 130.6 (*Ar*H), 43.7 (Ar*C*H$_2$SMe$_2$), 24.5 (S(*C*H$_3$)$_2$), 21.1 (Ar*C*H$_3$), 20.2 (Ar*C*H$_3$). IR (powder): 659 cm^{-1} *ν*(Sb-F).

*[(2,4,6-$Me_3H_2C_6)_2CHSMe_2$][SbF_6] (**27**)*

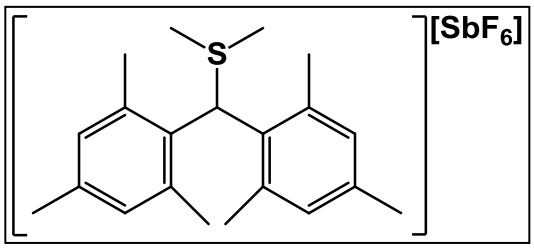

^{1}H NMR ($CDCl_3$): δ 6.92 (4H, s, *m*-H), 4.58 (1H, s, Ar_2CHSMe_2), 2.84 (6H, s, $S(CH_3)_2$), 2.33 (12H, s, *o*-Me), 2.25 (6H, s, *p*-Me).

Monitoring the 1,3,5-^{i}Pr$_3$C$_6$H$_3$ Reaction by NMR Spectroscopy

To a mixture of (Me_2S)AuCl (14 mg, 0.048 mmol) and 1,3,5-tri-*iso*-propylbenzene (10 mg, 0.49 mmol) in $CDCl_3$ in an NMR tube was added $AgSbF_6$ (14 mg, 0.048 mmol) in 0.3 mL $CDCl_3$. The sample was shaken thoroughly to initiate reaction and loaded in the NMR spectrometer to observe reaction progress.

Generation of a Cationic Benzyl Intermediate in the Presence of SMe_2

To a solution of 2,4,6-trimethylbenzyl chloride (101 mg, 0.60 mmol) and dimethylsulfide (0.1 mL) in dichloromethane (15 mL) was added $AgSbF_6$ (207 mg, 0.60 mmol). The mixture was stirred in the dark for 30 min. Filtration through Celite followed by evaporation of the solvent yielded [2,4,6-$C_6H_2Me_3CH_2SMe_2$][SbF_6] as a white powder (237 mg, 0.55 mmol, 92 %).

Competition Experiments

A Schlenk tube containing (Me_2S)AuCl (147 mg, 0.5 mmol) and the targeted arenes (C_6Me_6 vs. C_6Me_5H; C_6Me_6 vs. $C_6Me_4H_2$, 0.5 mmol each) in dichloromethane (15 mL) was cooled to the required temperature. $AgSbF_6$ (172 mg, 0.5 mmol) was added and the reaction was stirred for 1 h with exclusion of light. Analysis of an aliquot by ^{1}H NMR spectroscopy provided the conversion data.

Reaction Kinetics

(a) By ^{1}H NMR Spectroscopy

In an NMR tube (Me_2S)AuCl (0.024-0.133 mmol) was dissolved in a stock solution of the arene (C_6Me_6 or C_6Me_6-d^{18}) in chloroform-*d* (0.043-0.025 M, 0.3 mL) and warmed to the desired temperature (range 20 – 40 °C). The reaction was timed from the addition of a solution of $AgSbF_6$ in $CDCl_3$ (0.024-0.133 mmol, 0.3 mL). The sample was shaken thoroughly to initiate the reaction and loaded into the

NMR probe (pre-set to the desired temperature). Rates were determined from the growth of the signals for $[C_6Me_5CH_2SMe_2]^+$ (δ 4.75) and $[C_6(CD_3)_5CD_2S(CH_3)_2]^+$ (δ 2.87) for C_6Me_6 and $C_6(CD_3)_6$, respectively.

(b) By pH Measurements

A solution of $(Me_2S)AuCl$ (72 mg, 0.25 mmol), C_6Me_6 (40 mg, 0.25 mmol) and $AgSbF_6$ (86 mg, 0.25 mmol) in dichloromethane (50 mL) was stirred at the required temperature. At measured time intervals aliquots of 1 mL were taken, added to a vial containing 5 mL of distilled water and shaken thoroughly. The pH of the resulting aqueous phase was measured.

Spectroscopic Data of Gold Complexes Produced as By-products

$[(Me_2S)_2Au][SbF_6]$; ^{1}H NMR ($CDCl_3$): δ 2.82 (6H, s). $[(tht)_2Au][SbF_6]$; ^{1}H NMR ($CDCl_3$) δ 3.47 (8H, br. t), 2.21 (8H, br. t). $[(Me_2S)_2Au][BF_4]$; ^{1}H NMR ($CDCl_3$): δ 2.84 (6H, s). $[Au(2,4,6\text{-}C_6H_2Me_3)]_5$; ^{1}H NMR ($CDCl_3$, 263 K): δ 6.71 (10H, s), 2.57 (30H, br. s), 2.11 (15H, s).

6.2.3 General Chemistry of Gold(I) and Gold(III)

Topic 1: Zwitterionic Complexes of Gold(I)

*o-$(Ph_2P)C_6H_4SO_3K$ (**28-K**)*

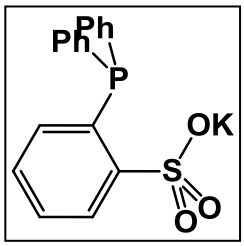

To a solution of *o*-$(PPh_2)C_6H_4SO_3H$ (**28-H**, 342 mg, 1.00 mmol) in CH_2Cl_2 (15 mL), an addition of potassium hydride (46 mg,1.15 mmol) was made, followed by stirring at 0 °C for one hour. The solution was filtered through Celite before evaporation of the filtrate by vacuum to give **28-K** as a white powder (341 mg, 0.90 mmol, 90 %). Characterisation data compares to literature values.[289]

*o-(Ph_2P)$C_6H_4SO_3Ag$ (**28-Ag**)*

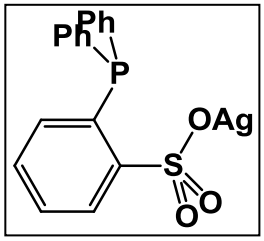

To a solution of *o*-(PPh_2)$C_6H_4SO_3H$ (**28-H**, 342 mg, 1.00 mmol) in CH_2Cl_2 (15 mL), an addition of silver oxide (120 mg, 0.52 mmol) was made, followed by stirring under exclusion of light for 2 hours. The solution was filtered through Celite before evaporation of the filtrate by vacuum to give **28-Ag** as a white powder (390 mg, 0.87 mmol, 87 %).

^{1}H NMR ($CDCl_3$): δ 8.25 (1H, s, 6-$ArSO_3$), 7.56-7.23 (12 H, m, Ph_2P and 4,5-$ArSO_3$), 6.97 (1H, m, 3-$ArSO_3$). ^{31}P NMR ($CDCl_3$): δ 8.6 (1P, s). ^{13}C{^{1}H} NMR ($CDCl_3$): 151.4 (s), 135.0 (s), 134.1 (s), 134.1 (s), 131.7 (s), 131.2 (s), 130.7 (s), 129.9 (s), 129.7 (s), 128.9 (s). Anal. Found: C, 48.00; H, 3.03. Calcd for $C_{18}H_{14}AgO_3PS$: C, 48.12; H, 3.14 %.

*o-(Ph_2PAuCl)$C_6H_4SO_3K$ (**29**)*

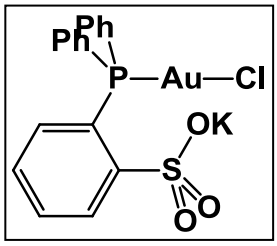

(tht)AuCl (170 mg, 0.53 mmol) and the potassium salt **28-K** (203 mg, 0.53 mmol) were dissolved in CH_2Cl_2 (10 mL) at 0 ˚C and the resulting solution stirred for 30 minutes. Reduction of volatiles to ca. 2 mL followed by addition of diethyl ether (10 mL) to the stirred concentrate liberates **29** as a white powder after filtration and drying under vacuum (288 mg, 0.47 mmol, 90 %).

^{1}H NMR ($CDCl_3$): δ 8.32 (1H, s, 6-$ArSO_3$), 7.48-7.16 (12 H, m, *Ph*$_2$P and 4,5-$ArSO_3$), 6.75 (1H, m, 3-$ArSO_3$). ^{31}P NMR ($CDCl_3$): δ 34.0 (1P, s). ^{13}C{^{1}H} NMR ($CDCl_3$): 153.1 (s), 134.2 (s), 134.1 (s), 132.3 (s), 131.2 (s), 130.4 (s), 129.8 (s), 129.0 (s). Anal. Found: C, 41.22; H, 4.60. Calcd for $C_{18}H_{14}AuClKO_3PS\cdot 2\ Et_2O$: C, 41.01; H, 4.50 %.

*[o-($Ph_2PAu(tht)$)$C_6H_4SO_3$] (**30a**)*

(tht)AuCl (167 mg, 0.52 mmol) and the silver salt **28-Ag** (235 mg, 0.52 mmol) were dissolved in CH_2Cl_2 (10 mL) at 0 ˚C and the resulting solution stirred for 30 minutes. Removal of the precipitate by filtration through Celite before

evaporation under reduced pressure gave **30a** as a white powder (305 mg, 0.49 mmol, 94 %).

^{1}H NMR ($CDCl_3$): δ 8.39 (1H, s, 6-$ArSO_3$), 7.53-7.24 (12 H, m, Ph_2P and 4,5-$ArSO_3$), 6.85 (1H, m, 3-$ArSO_3$), 3.45 (4H, br. s, tht), 2.19 (4H, br. s, tht). ^{31}P NMR ($CDCl_3$): δ 34.4 (1P, s). ^{13}C{^{1}H} NMR ($CDCl_3$): 152.0 (s), 134.7 (s), 134.2 (s), 134.1 (s), 132.1 (s), 131.3 (s), 130.6 (s), 130.2 (s), 129.7 (s), 129.0 (s), 38.5 (tht), 30.8 (tht). Anal. Found: C, 42.35; H, 3.78. Calcd for $C_{22}H_{22}AuO_3PS_2$: C, 42.17 H, 3.54 %.

*[o-($Ph_2PAu(SMe_2)$)$C_6H_4SO_3$] (**30b**)*

(Me_2S)AuCl (101 mg, 0.34 mmol) and the silver salt **28-Ag** (154 mg, 0.34 mmol) were dissolved in CH_2Cl_2 (10 mL) at 0 ˚C and the resulting solution stirred for 30 minutes. Removal of the precipitate by filtration through Celite before evaporation under reduced pressure gave **30b** as a white powder (186 mg, 0.31 mmol, 91 %).

^{1}H NMR ($CDCl_3$): δ 8.39 (1H, s, 6-$ArSO_3$), 7.54-7.23 (12 H, m, Ph_2P and 4,5-$ArSO_3$), 6.89 (1H, m, 3-$ArSO_3$), 2.73 (6H, s, Me_2S). ^{31}P NMR ($CDCl_3$): δ 34.3 (1P, s). ^{13}C{^{1}H} NMR ($CDCl_3$): 151.9 (s), 134.7 (s), 134.0 (s), 132.1 (s), 131.4 (s), 130.6 (s), 129.8 (s), 129.5 (s), 129.1 (s), 22.5 (SMe_2). Anal. Found: C, 39.83; H, 3.22. Calcd for $C_{20}H_{20}AuO_3PS_2$: C, 40.00; H, 3.36 %.

*[o-($Ph_2PAu(S^tBu_2)$)$C_6H_4SO_3$] (**30c**)*

($^{t}Bu_2S$)AuCl (42 mg, 0.11 mmol) and the silver salt **28-Ag** (50 mg, 0.11 mmol) were dissolved in CH_2Cl_2 (10 mL) at 0 ˚C and the resulting solution stirred for 1 hour. Removal of the precipitate by filtration through Celite before evaporation under reduced pressure gave **30c** as an off-white powder (59 mg, 0.08 mmol, 76 %).

^{1}H NMR ($CDCl_3$): δ 8.35 (1H, s, 6-$ArSO_3$), 7.70-7.25 (12 H, m, Ph_2P and 4,5-$ArSO_3$), 6.80 (1H, m, 3-$ArSO_3$), 1.67 (18H, br. s, $^{t}Bu_2S$). ^{31}P NMR ($CDCl_3$): δ 34.4 (1P, s).

Attempted synthesis of [2-(Ph_2PAu^+)$C_6H_4SO_3^-$]

AuCl (51 mg, 0.22 mmol) and the silver salt **28-Ag** (100 mg, 0.22 mmol) were dissolved in CH_2Cl_2 at 0 ˚C and the resulting solution stirred for 10 minutes. Removal of the precipitate by filtration through Celite before evaporation under reduced pressure gave [2-(Ph_2PAu^+)$C_6H_4SO_3^-$] as an unstable off-white powder (91 mg, 0.17 mmol, 76 %).

^{1}H NMR ($CDCl_3$): δ 8.22 (1H, s, 6-$ArSO_3$), 7.49-7.17 (12H, m, Ph_2P and 4,5-$ArSO_3$), 6.84 (1H, m, 3-$ArSO_3$). ^{31}P NMR ($CDCl_3$): δ 41.4 (1P, s).

Topic 2: Luminescent Studies and Anion Coordination of Unsupported Gold-Silver Tetrametallic Clusters

[Ph_4P][$Au(C_6F_5)_2$]

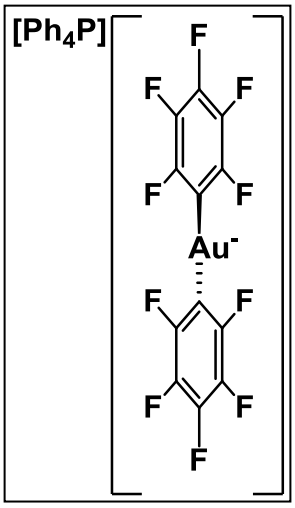

The compound was made following the procedure described for [^{n}Bu_4N][$(C_6F_5)_2Au$] on page 166, to give an off white powder of [Ph_4P][$(C_6F_5)_2Au$] (0.54 g, 0.62 mmol, 55 %).

^{1}H NMR ($CDCl_3$): δ 7.83 (4H, m, *Ph*$_4$P), 7.68 (8H, m, *Ph*$_4$P), 7.54 (4H, m, *Ph*$_4$P). ^{19}F NMR ($CDCl_3$): δ -114.9 (4F, d, J_{FF} = 22.6 Hz, *o*-C_6F_5), -162.4 (2F, t, J_{FF} = 19.8 Hz, *p*-C_6F_5), -163.8 (4F, m, *m*-C_6F_5). ^{31}P NMR ($CDCl_3$): δ 23.3 (s, Ph_4*P*).

*[({C_6F_5}$_2$Au)$_2$Ag$_2$(κ^1-NO$_3$)$_2$]$_n$ (**31a**) in Polymeric Form*

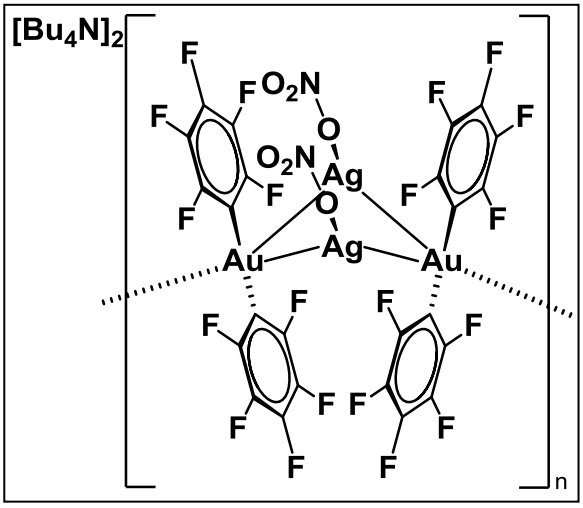

To a CH_2Cl_2/Et_2O solution (1:1, 4 mL) of [^{n}Bu$_4$N][(C$_6$F$_5$)$_2$Au] (78 mg, 0.101 mmol) was added $AgNO_3$ (17 mg, 0.100 mmol) in a 1 mL methanol solution. After 30 minutes stirring, the yellow solution was filtered, then stripped of its solvents by vacuum evaporation to give **31a** as an orange powder (94 mg, 0.45 mmol, 89 %). Recrystallisation of this cluster from a dichloromethane solution layered with light petroleum (1:1) at -30 °C gave a mixture of yellow platelets (**31a^1**) and orange needles (**31a^2**). Both crystals types were poorly resolved by X-ray crystallography experiments.

^{1}H NMR ($CDCl_3$): δ 3.14 (2H, m, ^{n}Bu$_4$N$^+$), 1.55 (2H, m, ^{n}Bu$_4$N$^+$), 1.36 (2H, m, ^{n}Bu$_4$N$^+$), 0.95 (3H, t, ^{n}Bu$_4$N$^+$). ^{19}F NMR ($CDCl_3$): δ -112.1 (8F, m, *o*-C$_6$F$_5$), -155.2 (4F, m, *p*-C$_6$F$_5$), -161.9 (8F, m, *m*-C$_6$F$_5$). IR (solid): ν(Au-C$_6$F$_5$) 1504, 964, 782; (^{n}Bu$_4$N) 2968, 2943, 2877, 877; (NO_3) 1298, 826 cm^{-1}. Anal. Found: C, 35.75; H, 3.75; N, 2.90. Calcd for $C_{56}H_{72}Ag_2Au_2F_{20}N_4O_6$: C, 35.63; H, 3.85; N, 2.97 %.

*[Ph$_4$P]$_{2n}$[({C_6F_5}$_2$Au)$_2$Ag$_2$(κ^2-NO$_3$)$_2$]$_n$ (**31b**) in Polymeric Form*

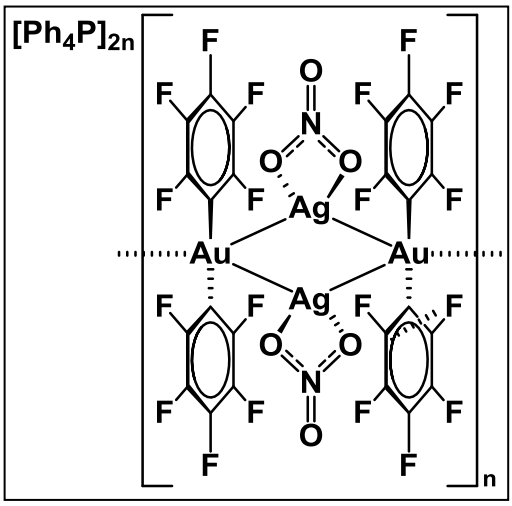

The synthetic procedure was the same as the preparation of **31a**, with [Ph$_4$P][(C$_6$F$_5$)$_2$Au] employed, yielding **31b** as a red powder (89 mg, 0.43 mmol, 92 %), Recrystallisation of **31b** from a dichloromethane solution layered with light petroleum (1:1) at -30 °C gave red needles suitable for X-ray crystallographic analysis.

^{1}H NMR ($CDCl_3$): δ 7.86 (4H, t, J_{HH} = 7.6 Hz, Ph$_4$P$^+$), 7.72 (8H, dt, J_{HH} = 7.6, 3.7 Hz, Ph$_4$P$^+$), 7.58 (8H, m, J_{HH} = 12.9, 7.6 Hz, Ph$_4$P$^+$). ^{19}F NMR ($CDCl_3$) δ

-112.5 (8F, m, *o*-C_6F_5), -155.9 (4F, m, *p*-C_6F_5), -162.5 (8F, m, *m*-C_6F_5). ^{31}P NMR ($CDCl_3$): δ 23.4 (1P, s). IR (solid): ν(Au-C_6F_5) 1500, 959, 784; (Ph_4P) 1590, 1439, 1105, 722, 685; (NO_3) 1296.7, 831 cm^{-1}. Anal. Found: C, 41.22; H, 1.88; N, 1.27. Calcd for $C_{72}H_{40}Ag_2Au_2F_{20}N_2O_6P_2$: C, 41.54; H, 1.94; N, 1.35 %.

*[^{n}Bu$_4$N]$_n$[({C$_6$F$_5$}$_2$Au)$_2$Ag$_2$(η^3-OAc^F)]$_n$ (**32a**) in Polymeric Form*

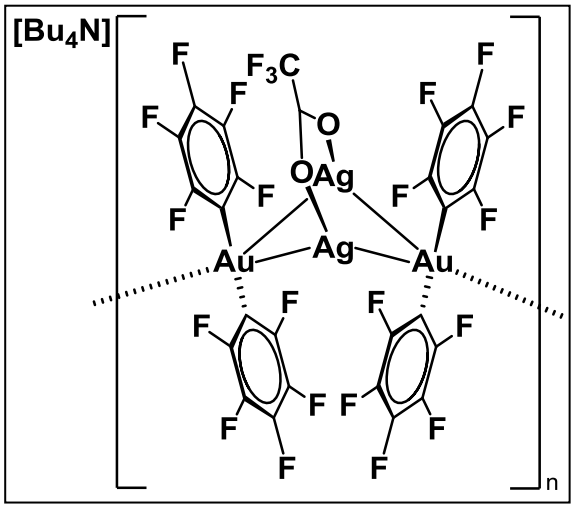

To a CH_2Cl_2/Et_2O solution (1:1, 4 mL) of [^{n}Bu$_4$N][(C_6F_5)$_2$Au] (82 mg, 0.106 mmol) was added AgO_2CCF_3 (20 mg, 0.100 mmol). A bright yellow solution formed immediately. After 30 minutes stirring, the solvent was removed under reduced pressure and the orange solids washed with Et_2O (2 x 5 mL) to give the crude product of **32a** as red solids (72 mg, 0.044 mmol, 88 %). Recrystallisation of this cluster from a dichloromethane solution layered with light petroleum (1:1) at -30 °C gave the pure cluster **32a** as red needles, which were poorly resolved by X-ray crystallography experiments.

^{1}H NMR ($CDCl_3$): δ 3.17 (2H, m, ^{n}Bu$_4$N$^+$), 1.55 (2H, m, ^{n}Bu$_4$N$^+$), 1.35 (2H, m, ^{n}Bu$_4$N$^+$), 0.94 (3H, t, ^{n}Bu$_4$N$^+$). ^{19}F NMR ($CDCl_3$) δ -73.5 (3F, s, $^-$O$_2$CC*F$_3$*), -111.3 (8F, m, *o*-C_6F_5), -154.3 (4F, m, *p*-C_6F_5), -161.4 (8F, m, *m*-C_6F_5). IR (solid): ν(Au-C_6F_5) 1503, 962, 781; (^{n}Bu$_4$N) 2970, 2920, 2880, 881; (OAc^F) 1661, 1193, 1140, 837, 780 cm^{-1}. Anal. Found: C, 31.06; H, 2.29; N, 0.97. Calcd for $C_{42}H_{36}Ag_2Au_2F_{23}NO_2$: C, 30.87; H, 2.12; N, 0.86 %.

*$[Ph_4P]_n[(\{C_6F_5\}_2Au)_2Ag_2(\eta^3\text{-}OAc^F)]_n$ (**32b**) in Polymeric Form*

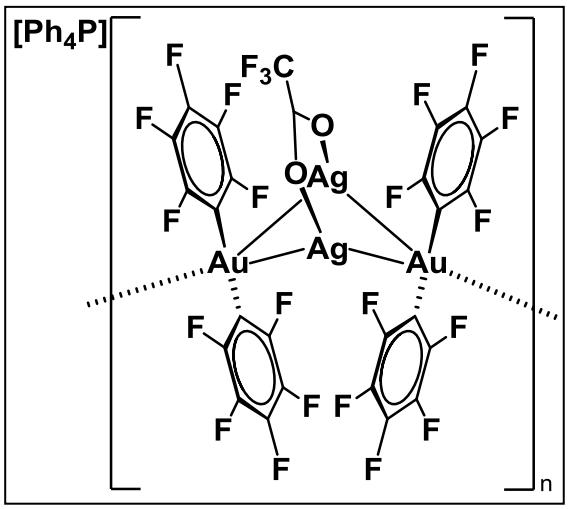

The synthetic procedure was analogous to that for **32a** when employing $[Ph_4P][(C_6F_5)_2Au]$, yielding crude **32b** as an orange-to-red powder (81 mg, 0.047 mmol, 85 %), Purification by recrystallisation **32a** from a dichloromethane solution layered with light petroleum (1:1) at -30 °C gave the pure product as orange/red needles, which were found to be polymorphic.

^{1}H NMR ($CDCl_3$): δ 7.89 (4H, m, Ph_4P^+), 7.76 (8H, m, Ph_4P^+), 7.59 (8H, m, Ph_4P^+). ^{19}F NMR ($CDCl_3$): δ -74.7 (3F, s, $^-O_2CCF_3$), -110.8 (8F, m, *o*-C_6F_5), -154.0 (4F, m, *p*-C_6F_5), -161.2 (8F, m, *m*-C_6F_5). ^{31}P NMR ($CDCl_3$): δ 23.6 (1P, s). IR (solid): ν(Au-C_6F_5) 1499, 953, 781; (Ph_4P) 1588, 1436, 1107, 721, 687; (OAc^F) 1661, 1195, 1136, 835, 781 cm^{-1}. Anal. Found: C, 34.88; H, 1.22. Calcd for $C_{50}H_{20}Ag_2Au_2F_{23}O_2P$: C, 34.69; H, 1.17 %.

*$[^nBu_4N]_n[(\{C_6F_5\}_2Au)_2Ag_2(\eta^3\text{-}SO_3CF_3)]_n$ (**33a**) in Polymeric Form*

To a CH_2Cl_2/Et_2O solution (1:1, 4 mL) of $[^nBu_4N][(C_6F_5)_2Au]$ (78 mg, 0.100 mmol) was added $AgOSO_2CF_3$ (26 mg, 0.100 mmol). A deep orange solid precipitate formed immediately over a 10 minute period. After 30 minutes stirring, the solids were filtered before evaporating to dryness to yield **33a** as a crude orange powder (138 mg, 0.044 mmol, 87 %). Recrystallisation of this cluster from a dichloromethane solution layered with light petroleum (1:1) at -30 °C gave the pure product as a mixture of green needles and orange/red blocks. These crystals decompose at room temperature after ~1 hour.

^{1}H NMR ($CDCl_3$): δ 3.17 (2H, m, $^nBu_4N^+$), 1.58 (2H, m, $^nBu_4N^+$), 1.34 (2H, m, $^nBu_4N^+$), 0.93 (3H, t, $^nBu_4N^+$). ^{19}F NMR ($CDCl_3$) δ -77.2 (3F, s, $^-OSO_2CF_3$) -109.9 (8F, m, *o*-C_6F_5), -151.3 (4F, m, *p*-C_6F_5), -161.0 (8F, m, *m*-C_6F_5). IR (solid): *ν*(Au-C_6F_5) 1503, 963, 783; ($^nBu_4N$) 2967, 2921, 2879, 882; (OTf) 1155 cm^{-1}.

*$[Ph_4P]_n[(\{C_6F_5\}_2Au)_2Ag_2(NO_3(\eta^3\text{-}SO_3CF_3)_n]_n$ (**33b**) in Polymeric Form*

The synthetic procedure was the same as that used the preparation of **33a**, with $[Ph_4P][(C_6F_5)_2Au]$ employed, yielding **33b** as an crude orange to red powder. (110 mg, 0.062 mmol, 88 %). Purification by recrystallisation from a dichloromethane solution layered with light petroleum (1:1) at -30 °C gave red blocks which break down after a short period of time at room temperature.

^{1}H NMR ($CDCl_3$): δ 7.78 (4H, m, Ph_4P^+), 7.75 (8H, m, Ph_4P^+), 7.60 (8H, m, Ph_4P^+). ^{19}F NMR ($CDCl_3$) δ -77.8 (3F, s, $^-OSO_2CF_3$) -109.8 (8F, m, *o*-C_6F_5), -151.5 (4F, m, *p*-C_6F_5), -160.5 (8F, m, *m*-C_6F_5). ^{31}P NMR ($CDCl_3$): δ 23.3 (1P, s). IR (solid): ν(Au-C_6F_5) 1508, 958, 788; (Ph_4P) 1585, 1439, 1108, 724, 687; (OTf) 1140 cm^{-1}.

*Isolation of the Dimeric/Oligomeric Forms of the Clusters **31a-33b***

The selected cluster was dissolved in dichloromethane (5 mL), before a drop wise addition of light petroleum (20 mL) to the stirred dichloromethane solution over a 5 minute period. The precipitate was filtered by cannula before washing with 5 mL light petroleum and drying under vacuum to give the clusters in its dimeric or oligomeric form in quantitative yields.

Topic 3: Studies into Au(III) Coordination Chemistry and Catalysis with Simple Arenes

Attempted Alkene Coordination with $[^nBu_4N][(C_6F_5)_2AuCl_2]$

(a) in Diethyl Ether

$AgSbF_6$ (128 mg, 0.37 mmol) was added to a solution of $[^nBu_4N][(C_6F_5)_2AuCl_2]$ (157 mg, 0.19 mmol) and norbornene (70 mg, 0.74 mmol) in diethyl ether (5 mL) and left to stir in the absence of light for 2 hours. Filtration through Celite gave a solution of $[(C_6F_5)_2Au(OEt_2)_2][SbF_6]$ only.[236]

(b) in Dichloromethane

To a solution of [^{n}Bu$_4$N][(C$_6$F$_5$)$_2$AuCl$_2$] (100 mg, 0.12 mmol) and norbornene (99 mg, 1.05 mmol) in dichloromethane (5 mL) was added AgSbF$_6$ (81 mg, 0.24 mmol) before stirring under the exclusion of light for 2 hours. Filtration through Celite before the addition of 40 mL light petroeum precipitates a white powder, which, when filtered, was found to be [Au(nbe)$_3$][SbF$_6$].[73] On inspection of the resulting filtrate, the observances of ^{19}F signals are seen corresponding to the diaryl, (C$_6$F$_5$)$_2$.

^{19}F NMR (CDCl$_3$) for (C$_6$F$_5$)$_2$: δ -143.4 (4F, m, *o*-C$_6$F$_5$), -158.8 (2F, t, J_{FF} 21.3 Hz, *p*-C$_6$F$_5$), -163.8 (4F m, *m*-C$_6$F$_5$).

Attempted Arene Coordination with [^{n}Bu$_4$N][(C$_6$F$_5$)$_2$AuCl$_2$].

AgSbF$_6$ (81 mg, 0.24 mmol) was added to a solution of [^{n}Bu$_4$N][(C$_6$F$_5$)$_2$AuCl$_2$] (101 mg, 0.12 mmol) and the arene (benzene, toluene, *o*-xylene, *p*-xylene, mesitylene, 1,2,4-trimethylbenzene, durene, pentamethylbenzene or hexamethylbenzene; 1.00 mmol) in dichloromethane (5 mL) before stirring under the exclusion of light for 2 hours.

For benzene, toluene, *o*-xylene and *p*-xylene, removal of solids by Celite filtration, followed by cooling to -30 ˚C and precipitation by addition of 40 mL diethyl ether gave white solids, which under a short time, turned purple. On inspection of the resulting filtrate, the observance of ^{19}F signals corresponding to the diaryl byproduct (C$_6$F$_5$)$_2$ were seen.

For mesitylene, 1,2,4-trimethylbenzene, durene, pentamethylbenzene and hexamethylbenzene, a gold film was formed with no evidence of gold within the solution.

General Procedure for the Screening of Hydroarylation Catalysed by Gold(III)

An NMR tube preloaded with pentamethylbenzene (296 mg, 2 mmol) and ethyl propiolate (0.2 mL, 2 mmol) was treated with a solution of the gold precatalyst [Ar$_2$AuCl]$_2$ (Ar = C$_6$F$_5$, 2,4,6-C$_6$H$_2$Me$_3$; 0.025 mmol), followed by the

chosen activator (0.05 mmol) in toluene-d^8 or $CDCl_3$ (0.6 mL). The reaction was agitated in exclusion of light and monitored by ^1H NMR spectroscopy until completion was observed.

6.2.4 Attempted Synthesis of an Oxidative Fluorinating Agent for Gold

NMR Reactions for $[R_2SF][FB(C_6F_5)_3]$ Synthesis

R = Me, Ph

In an NMR tube, $R_2S{\cdot}B(C_6F_5)_3$ (0.1 mmol respectively) was dissolved in 0.6 mL acetonitrile-d^3, before cooling the reaction vessel to -40 ˚C. An addition of xenon difluoride (17 mg, 0.1 mmol) was made before analysis by NMR spectroscopy at the selected temperature.

$[Me_2SF][FB(C_6F_5)_3]$ (**35**): ^{19}F NMR (CD_3CN -40 °C): δ -136.6 (6F, t, *o*-C_6F_5), -162.3 (3F, t, *p*- C_6F_5), -167.3 (6F, m, *m*- C_6F_5), -188.9 (1F, sept., Me_2S^+F), -190.3 (1F, br. s, $^-BF(C_6F_5)_3$).

$[Ph_2SF][FB(C_6F_5)_3]$ (**37**): ^{19}F NMR (CD_3CN, -20 °C): δ -136.5 (6F, t, *o*-C_6F_5), -162.4 (3F, t, *p*-C_6F_5), -167.3 (6F, m, *m*-C_6F_5), -190.3 (2F, br. m,, Ph_2S^+F and $^-BF(C_6F_5)_3$).

R = 4-NO_2-C_6H_4

In an NMR tube, $(4\text{-}NO_2\text{-}C_6H_4)_2S$ (19 µL, 0.1 mmol) in 0.6 mL acetonitrile-d_6, was cooled to -40 ˚C before the addition of xenon difluoride (17 mg, 0.1 mmol). After 5 minutes agitation, $B(C_6F_5)_3$ (51 mg, 0.1 mmol) was added and the reaction analysed by NMR spectroscopy at -40 °C, which found no evidence of the formation of $[(4\text{-}NO_2\text{-}C_6H_4)_2SF][FB(C_6F_5)_3]$, only its anticipated decomposition products.

NMR Reactions for the Attempted Fluorination of Diphenyl Ether

In an NMR tube, $B(C_6F_5)_3$ and diphenyl ether (0.1 mmol each) were dissolved in 0.6 mL acetonitrile-d^3, before cooling the reaction vessel to -40 ˚C. An

addition of xenon difluoride (17 mg, 0.1 mmol) was made before before analysis by NMR spectrometry at -40 °C. Upon slow warming to room temperature, ^{19}F signals were seen correlating to $[Xe(C_6F_5)][F_2B(C_6F_5)_2]$.[290]

NMR reactions for the production of $[Ph_3BiF]^+$ sources

Reactivity of Ph_3BiF_2 with $B(C_6F_5)_3$

In an NMR tube, Ph_3BiF_2 (48 mg, 0.1 mmol) in 0.6 mL acetonitrile-d^3 was cooled to -40 ˚C before the addition of xenon difluoride (17 mg, 0.1 mmol). After 5 minutes agitation, $B(C_6F_5)_3$ (51 mg, 0.1 mmol) was added and the reaction studied by NMR spectroscopy at -40 °C.

^{19}F NMR (CD_3CN, -40 °C): δ -133.7 to -134.9 (3 x *o*-C_6F_5), -155.8 to -158.0 (3 x *p*-C_6F_5), -162.1 to -164.0 (3 x *m*-C_6F_5), -175.3 (1F, s, Ph_3Bi^+F) -176.9 (1F, br. d, $^-BF(C_6F_5)_3$).

6.3 Crystallographic Data Tables

Data were processed and absorption corrections applied using the CrystalClear-SM.[291] The structure was determined by the direct methods routines in the SHELXS program[292] and refined by full-matrix least-squares methods, on F^2's, in SHELXL.[293] Scattering factors for neutral atoms were taken from reference 294. Computer programs used in this analysis have been noted above, and were run through WinGX on a Dell Precision 370 PC at the University of East Anglia.

Table 17. Crystal and structure refinement data for compounds **2**, **4** and **5**.

Compound	**2**	**4**	**5**
Elemental formula	$C_8HF_4NO_2$	$C_{11}H_9F_4NO_2Si$	$C_{11}H_9F_4NO_2Sn$
Formula weight	219.1	291.3	381.9
Crystal system	Monoclinic	Monoclinic	Monoclinic
Space group	$P2_1/c$	$P2_1/c$	$P2_1/c$
Unit cell dimensions: a (Å)	12.0520(5)	9.5135(8)	19.1926(6)
b	5.4998(2)	24.759(2)	6.6264(2)
c	11.4291(4)	10.7793(6)	20.1512(7)
α (°)	90	90	90
β	94.626(4)	91.391(6)	90.257(3)
γ	90	90	90
Volume (Å^3)	755.09(5)	2538.3(3)	2562.76(14)
No. of formula units, Z	4	8	8
Calculated density (Mg/m^3)	1.927	1.524	1.980
F(000)	432	1184	1472
Absorption coefficient μ (mm^{-1})	0.203	0.231	2.039
Crystal colour, shape	very pale yellow flat prism	colourless plate	colourless block
Crystal size (mm)	0.60 × 0.30 × 0.06	0.30 × 0.24 × 0.06	0.22 × 0.10 × 0.06
θ range (°)	3.4 to 25.0	3.1 to 20.0	3.4 to 30.0
Limiting indices	$-14 \leq h \leq 14$, $-6 \leq k \leq 6$, $-13 \leq l \leq 13$	$-9 \leq h \leq 9$, $-23 \leq k \leq 23$, $-10 \leq l \leq 10$	$-27 \leq h \leq 27$, $-9 \leq k \leq 9$, $-28 \leq l \leq 28$
Max. and min. transmission	1.069 and 0.926	1.029 and 0.967	1.112 and 0.873
Reflections collected (not including absences)	13776	27063	48849
No. of unique reflections, R_{int}	1334, 0.075	2357, 0.203	7468, 0.070
No. of 'observed' reflections ($I > 2\sigma_I$)	1181	1262	5577
Data / restraints / parameters	1334 / 0 / 140	2357 / 0 / 343	7468 / 0 / 349
Goodness-of-fit on F^2	1.129	0.869	0.912
Final R indices ('observed' data)	R_1 = 0.044, wR_2 = 0.097	R_1 = 0.052, wR_2 = 0.039	R_1 = 0.029, wR_2 = 0.056
Final R indices (all data)	R_1 = 0.056, wR_2 = 0.103	R_1 = 0.145, wR_2 = 0.049	R_1 = 0.050, wR_2 = 0.058
Largest diff. peak and hole (e Å^{-3})	0.24 and -0.23	0.20 and -0.19	0.82 and -0.80

Table 18. Crystal and structure refinement data for compounds **6**, **7a** and **7b**.

Compound	**6**·2 MeCN	**7a**	**7b**·0.5 C_7H_8
Elemental formula	$C_{20}Ag_2F_8N_2O_4$ ·$C_4H_6N_2$	$C_{26}H_{15}AuF_4NO_2P$	$C_{26}H_{33}AuF_4NO_2P$ ·0.5(C_7H_8)
Formula weight	734.0	677.3	741.5
Crystal system	Monoclinic	Monoclinic	Triclinic
Space group	$P2_1/c$	$P2_1/c$	$P\bar{1}$
Unit cell dimensions: a (Å)	7.93961(12)	13.79281(11)	11.3527(8)
b	26.9636(4)	12.00838(11)	11.7282(9)
c	10.48883(15)	28.1090(3)	11.9341 (9)
α (°)	90	90	74.895(6)
β	90	100.4139(10)	69.615(7)
γ	105.245(2)	90	72.833(6)
Volume (Å^3)	2166.43(5)	4578.99(7)	1400.86(18)
No. of formula units, Z	4	8	2
Calculated density (Mg/m^3)	2.250	1.965	1.758
F(000)	1408	2592	734
Absorption coefficient μ (mm^{-1})	1.915	6.553	5.363
Crystal colour, shape	colourless plate	colourless plate	colourless block, cut from prism
Crystal size (mm)	0.47 × 0.24 × 0.12	0.41 × 0.38 × 0.08	0.16 × 0.15 × 0.14
θ range (°)	3.3 to 27.5	3.3 to 30.0	3.4 to 30.0
Limiting indices	$-10 \le h \le 10$, $-35 \le k \le 35$, $-13 \le l \le 13$	$-19 \le h \le 19$, $-16 \le k \le 16$, $-39 \le l \le 39$	$-15 \le h \le 15$, $-16 \le k \le 16$, $-16 \le l \le 16$
Max. and min. transmission	1.038 and 0.978	1.325 and 0.497	1.159 and 0.796
Reflections collected (not including absences)	47568	117169	15566
No. of unique reflections, R_{int}	4974, 0.044	13315, 0.071	8119, 0.043
No. of 'observed' reflections ($I > 2\sigma_I$)	4481	11064	7071
Data / restraints / parameters	4974 / 0 / 367	13315 / 0 / 631	8119 / 0 / 362
Goodness-of-fit on F^2	1.181	1.214	1.051
Final R indices ('observed' data)	R_1 = 0.025, wR_2 = 0.050	R_1 = 0.052, wR_2 = 0.070	R_1 = 0.031, wR_2 = 0.079
Final R indices (all data)	R_1 = 0.031, wR_2 = 0.051	R_1 = 0.072, wR_2 = 0.074	R_1 = 0.038, wR_2 = 0.083
Largest diff. peak and hole (e Å^{-3})	0.65 and -0.53	1.80 and -2.43	2.79 and -3.68

Table 19. Crystal and structure refinement data for compounds **8**, **9** and **10**.

Compound	**8**·C_7H_8	**9**·3 MeCN	**10**
Elemental formula	$C_{12}H_8AuF_4NO_2S$ ·C_7H_8	$C_{16}AgAuF_8N_2O_4$ ·$C_6H_9N_3$	$C_{80}H_{30}AuB_2F_{34}NO_2$ ·*ca* 1.5 (C_4H_8O)
Formula weight	595.3	864.2	2071.73
Crystal system	Monoclinic	Triclinic	Monoclinic
Space group	$P2_1/c$	$P\bar{1}$	$P2_1/n$
Unit cell dimensions: *a* (Å)	11.8670(17)	8.24928(9)	15.4133(11)
b	23.7634(14)	9.49150(15)	32.505(2)
c	6.6297(5)	16.8812(3)	16.4236(12)
α (°)	90	94.1577(13)	90
β	90.071(9)	94.4125(11)	89.997(2)
γ	90	111.3597(12)	90
Volume (Å^3)	1869.6(3)	1220.12(3)	8228.3(10)
No. of formula units, *Z*	4	2	4
Calculated density (Mg/m^3)	2.115	2.352	1.672
F(000)	1136	812	4072
Absorption coefficient μ (mm^{-1})	8.034	6.911	1.956
Crystal colour, shape	colourless rod	colourless block	colourless block
Crystal size (mm)	0.50 × 0.04 × 0.03	0.28 × 0.18 × 0.16	0.14 × 0.09 × 0.05
θ range (°)	3.4 to 22.5	3.4 to 30.0	2.9 to 22.5
Limiting indices	$-12 \le h \le 12$, $-25 \le k \le 25$, $-7 \le l \le 7$	$-11 \le h \le 11$, $-13 \le k \le 13$, $-23 \le l \le 23$	$-16 \le h \le 16$, $-34 \le k \le 35$, $-17 \le l \le 17$
Max. and min. transmission	1.177 and 0.827	1.278 and 0.676	1.000 and 0.651
Reflections collected (not including absences)	18667	34701	37322
No. of unique reflections, R_{int}	2437, 0.119	7115, 0.041	10292, 0.075
No. of 'observed' reflections ($I > 2\sigma_I$)	1759	6535	8628
Data / restraints / parameters	2437 / 0 / 219	7115 / 12 / 390	10292 / 0 / 1145
Goodness-of-fit on F^2	1.043	1.042	1.036
Final *R* indices ('observed' data)	R_1 = 0.052, wR_2 = 0.091	R_1 = 0.017, wR_2 = 0.041	R_1 = 0.088, wR_2 = 0.179
Final *R* indices (all data)	R_1 = 0.082, wR_2 = 0.099	R_1 = 0.021, wR_2 = 0.042	R_1 = 0.111, wR_2 = 0.1924
Largest diff. peak and hole (e Å^{-3})	1.59 and -1.09	0.86 and -0.91	1.95 and -1.34

Table 20. Crystal and structure refinement data for compounds **12**, **13** and **15**.

Compound	**12**·0.5 C_7H_8	**13**·C_2H_3N	**15**·MeCN
Elemental formula	$C_{22}H_6AuF_{14}NO_2S$ ·$C_{3.5}H_4$	$C_{38}H_{15}AuF_{14}NO_2P$ ·C_2H_3N	$C_8F_4INO_2$ ·C_2H_3N
Formula weight	857.37	1052.50	386.0
Crystal system	Triclinic	Monoclinic	Monoclinic
Space group	$P\bar{1}$	$P2_{1/c}$	$P2_1/m$
Unit cell dimensions *a* (Å)	10.3418(2)	21.2988(6)	9.4073(7)
b	11.7842(3)	10.2608(2)	6.3030(5)
c	12.1670(4)	17.8953(5)	10.1518(10)
α (°)	68.659(3)	90	90
β	84.114(2)	112.092(3)	108.929(9)
γ	72.978(2)	90	90
Volume ($Å^3$)	1320.60(6)	3623.75(16)	569.39
No. of formula units, *Z*	2	4	2
Calculated density (Mg/m^3)	2.156	1.929	2.252
F(000)	814	2032	364
Absorption coefficient μ (mm^{-1})	5.776	4.217	2.865
Crystal colour, shape	Colourless block	Colourless block	colourless hexagonal plate
Crystal size (mm)	0.30 × 0.15 × 0.07	0.43 × 0.30 × 0.20	0.18 × 0.18 × 0.01
θ range (°)	3.6 to 28.2	3.5 to 28.3	3.6 to 25.0
Limiting indices	-13≤h≤13, -15≤k≤15, -16≤l≤16	-28≤h≤28, -13≤k≤13, -23≤l≤23	$-11 \le h \le 11$, $-7 \le k \le 7$, $-12 \le l \le 12$
Max. and min. transmission	0.688 and 0.276	0.486 and 0.264	1.054 and 0.962
Reflections collected (not including absences)	21341	58230	6985
No. of unique reflections, R_{int}	6555, 0.083	8993, 0.040	1103, 0.104
No. of 'observed' reflections ($I > 2\sigma_I$)	5323	8041	902
Data / restraints / parameters	6555 / 0 / 386	8993 / 0 / 231	1103 / 0 / 119
Goodness-of-fit on F^2	1.010	1.076	1.063
Final *R* indices ('observed' data)	R_1 = 0.045, wR_2 = 0.080	R_1 = 0.022, wR_2 = 0.046	R_1 = 0.057, wR_2 = 0.116
Final *R* indices (all data)	R_1 = 0.064, wR_2 = 0.085	R_1 = 0.028, wR_2 = 0.048	R_1 = 0.079, wR_2 = 0.123
Largest diff. peak and hole (e $Å^{-3}$)	2.02 and -1.12	0.77 and -1.00	2.45 and -1.04

Table 21. Crystal and structure refinement data for compounds **17a**, **17b** and **18**.

Compound	**17a**	**17b**	**18**·0.5 CH_2Cl_2
Elemental formula	$C_{39}H_{22}AuF_{18}N_2P$	$C_{39}H_{34}AuF_6N_2P$	$C_{14}H_{23}F_6SSb$ ·0.5(CH_2Cl_2)
Formula weight	1088.52	872.62	501.6
Crystal system	Monoclinic	Triclinic	Monoclinic
Space group	C2/c	$P\bar{1}$	$P2_1/c$
Unit cell dimensions: *a* (Å)	19.7418(5)	12.2054(4)	8.7669(4)
b	16.0248(4)	12.7181(4)	10.4373(5)
c	25.9858(9)	13.6002(4)	20.9854(11)
α (°)	90	101.607(2)	90
β	111.892(3)	111.625(2)	91.383(4)
γ	90	108.416(2)	90
Volume ($Å^3$)	7628.0(4)	1737.12(9)	1919.66(16)
No. of formula units, *Z*	8	2	4
Calculated density (Mg/m^3)	1.896	1.668	1.736
F(000)	4208	860	996
Absorption coefficient μ (mm^{-1})	4.021	4.344	1.734
Crystal colour, shape	Orange prism	Yellow plate	Colourless prism
Crystal size (mm)	0.26 × 0.19 × 0.10	0.10 × 0.04 × 0.01	0.33 × 0.23 × 0.14
θ range (°)	3.4 to 30.0	3.9 to 27.5	3.5 to 27.5
Limiting indices	$-27 \le h \le 27$, $-22 \le k \le 22$, $-36 \le l \le 36$	$-15 \le h \le 15$, $-16 \le k \le 16$, $-17 \le l \le 17$	$-11 \le h \le 11$, $-13 \le k \le 13$, $-27 \le l \le 27$
Max. and min. transmission	1.110 and 0.868	0.958 and 0.671	1.038 and 0.944
Reflections collected (not including absences)	76538	36687	32359
No. of unique reflections, R_{int}	11104, 0.101	7939, 0.087	4418, 0.051
No. of 'observed' reflections ($I > 2\sigma_I$)	7971	6531	3931
Data / restraints / parameters	11104 / 0 / 546	7939 / 0 / 446	4418 / 0 / 231
Goodness-of-fit on F^2	1.023	1.038	1.153
Final *R* indices ('observed' data)	R_1 = 0.046, wR_2 = 0.098	R_1 = 0.045, wR_2 = 0.084	R_1 = 0.035, wR_2 = 0.082
Final *R* indices (all data)	R_1 = 0.076, wR_2 = 0.105	R_1 = 0.066, wR_2 = 0.090	R_1 = 0.040, wR_2 = 0.083
Largest diff. peak and hole (e $Å^{-3}$)	1.92 and -1.62	0.92 and -1.75	1.30 and -1.30

Table 22. Crystal and structure refinement data for compounds **19**, **20** and **25**.

Compound	**19**	**20**·0.5 CH_2Cl_2	**25**
Elemental formula	$C_8H_{24}Au_2F_{12}S_4Sb_2$	$C_{16}H_{25}F_6SSb$ ·0.5(CH_2Cl_2)	$C_{12}H_{19}F_6SSb$
Formula weight	1113.9	527.6	431.1
Crystal system	Monoclinic	Triclinic	Monoclinic
Space group	I_2/a	P_{-1}	$P2_1/c$
Unit cell dimensions: *a* (Å)	44.765(3)	8.6200(3)	12.0274(2)
b	7.8085(3)	11.0278(3)	7.9197(7)
c	21.6181(13)	11.6892(4)	17.4074(9)
α (°)	90	66.587(3)	90
β	93.833(5)	88.441(2)	108.949(5)
γ	90	86.652(2)	90
Volume ($Å^3$)	7539.7(7)	1017.93(6)	1568.26(16)
No. of formula units, *Z*	12	2	4
Calculated density (Mg/m^3)	2.944	1.640	1.826
F(000)	6048	526	848
Absorption coefficient μ (mm^{-1})	14.180	1.640	1.941
Crystal colour, shape	Streaky colourless thin needle	Colourless plate	Pale brown flat prism
Crystal size (mm)	0.44 × 0.045 × 0.015	0.33 × 0.22 × 0.09	0.47 × 0.20 × 0.09
θ range (°)	3.4 to 22.5	3.5 to 30	3.6 to 27.5
Limiting indices	$-48 \le h \le 48$, $-8 \le k \le 8$, $-23 \le l \le 23$	$-12 \le h \le 12$, $-15 \le k \le 15$, $-16 \le l \le 16$	$-15 \le h \le 15$, $-10 \le k \le 10$, $-22 \le l \le 22$
Max. and min. transmission	1.074 and 0.893	1.067 and 0.920	1.109 and 0.893
Reflections collected (not including absences)	40013	20819	26713
No. of unique reflections, R_{int}	4922, 0.223	5928, 0.032	3598, 0.065
No. of 'observed' reflections ($I > 2\sigma_I$)	2952	5334	3079
Data / restraints / parameters	4922 / 0 / 319	5928 / 0 / 249	3598 / 0 / 239
Goodness-of-fit on F^2	1.013	1.054	1.066
Final *R* indices ('observed' data)	R_1 = 0.086, wR_2 = 0.132	R_1 = 0.021, wR_2 = 0.056	R_1 = 0.034, wR_2 = 0.080
Final *R* indices (all data)	R_1 = 0.154, wR_2 = 0.152	R_1 = 0.025, wR_2 = 0.057	R_1 = 0.042, wR_2 = 0.083
Largest diff. peak and hole (e $Å^{-3}$)	2.17 and -1.49	0.86 and -0.53	1.50 and -1.48

Table 23. Crystal and structure refinement data for compounds **26**, **29** and **31a**[1].

Compound	**26**·0.5 CH_2Cl_2	**29**·0.5 $CHCl_3$, 0.75 H_2O	**31a**[1]
Elemental formula	$C_{12}H_{19}F_6SSb$ ·0.5(CH_2Cl_2)	$C_{18.5}H_{14.5}AuCl_{2.5}K$ $O_{3.75}PS$	$C_{112}H_{144}Ag_4Au_4F_{40}$ N_8O_{12}
Formula weight	473.5	684.52	3773.7
Crystal system	Monoclinic	Triclinic	Monoclinic
Space group	C2/c	P-1	P2/c
Unit cell dimensions: *a* (Å)	25.5825(4)	9.638(3)	18.488(11)
b	8.66762(11)	12.896(4)	16.062(13)
c	16.1148(3)	18.060(6)	23.785(14)
α (°)	90	78.697(11)	90
β	94.2792(14)	88.390(15)	108.99(7)
γ	90	85.950(16)	90
Volume ($Å^3$)	3563.32(13)	2195.5(12)	6679(6)
No. of formula units, *Z*	8	4	2
Calculated density (Mg/m^3)	1.765	2.071	1.877
F(000)	1864	1308	3664
Absorption coefficient μ (mm^{-1})	1.862	7.384	5.062
Crystal colour, shape	Colourless block	Colourless block	Yellow plate
Crystal size (mm)	0.33 × 0.27 × 0.17	0.10 × 0.08 × 0.01	0.11 × 0.08 × 0.01
θ range (°)	3.5 to 30	3.1 to 27.5	3.5 to 20.0
Limiting indices	-35≤h≤35, -12≤k≤12, -22≤l≤22	-12≤h≤9, -16≤k≤16, -23≤l≤22	-17≤h≤17, -15≤k≤15, -22≤l≤22
Max. and min. transmission	1.016 and 0.982	1.000 and 0.749	1.000 and 0.286
Reflections collected (not including absences)	33679	20803	45005
No. of unique reflections, R_{int}	5186, 0.039	9893, 0.072	6222
No. of 'observed' reflections ($I > 2\sigma_I$)	4353	7979	4085
Data / restraints / parameters	5186 / 0 / 216	9893 / 0 / 235	6222 / 0 / 527
Goodness-of-fit on F^2	1.017	1.101	1.042
Final *R* indices ('observed' data)	R_1 = 0.022, wR_2 = 0.056	R_1 = 0.086, wR_2 = 0.186	R_1 = 0.118, wR_2 = 0.229
Final *R* indices (all data)	R_1 = 0.030, wR_2 = 0.057	R_1 = 0.105, wR_2 = 0.200	R_1 = 0.176, wR_2 = 0.249
Largest diff. peak and hole (e $Å^{-3}$)	0.59 and – 0.63	3.78 and -4.63	3.21 and -2.06

Table 24. Crystal and structure refinement data for compounds **31a**[2], **31b** and **32a**.

Compound	**31a**[2]	**31b**·CH_2Cl_2	**32a**·*ca* 1.25 CH_2Cl_2
Elemental formula	$C_{152}H_{180}Ag_6Au_6F_{60}N_{11}O_{18}$	$C_{72}H_{40}Ag_2Au_2F_{20}N_2O_6P_2 \cdot CH_2Cl_2$	$C_{42}H_{36}Ag_2Au_2F_{23}NO_2$. *ca* 1.25 CH_2Cl_2
Formula weight	5418.09	2165.60	1739.55
Crystal system	Orthorhombic	Orthorhombic	Orthorhombic
Space group	Pcnb	$P2_12_12_1$	Fddd
Unit cell dimensions: *a* (Å)	18.733(13)	14.713(3)	21.737(3)
b	27.930(18)	17.364(4)	43.490(9)
c	35.35(2)	27.669(6)	44.520(9)
α (°)	90	90	90
β	90	90	90
γ	90	90	90
Volume ($Å^3$)	18493(18)	7069(3)	42087(13)
No. of formula units, *Z*	4	4	32
Calculated density (Mg/m^3)	1.946	2.035	2.196
F(000)	10436	4152	26320
Absorption coefficient μ (mm^{-1})	5.478	4.913	6.539
Crystal colour, shape	Orange needle	Red needle	Red needle
Crystal size (mm)	0.32 × 0.02 × 0.01	0.15 × 0.02 × 0.01	0.21 × 0.02 × 0.02
θ range (°)	2.2 to 20.0	2.9 to 27.5	2.5 to 25.0
Limiting indices	$-18 \le h \le 17$, $-26 \le k \le 26$, $-34 \le l \le 34$	$-19 \le h \le 19$, $-21 \le k \le 22$, $-35 \le l \le 19$	$-25 \le h \le 19$, $-51 \le k \le 51$, $-52 \le l \le 52$
Max. and min. transmission	1.000 and 0.704	1.000 and 0.661	1.000 and 0.645
Reflections collected (not including absences)	48132	41437	95596
No. of unique reflections, R_{int}	8496, 0.115	16009, 0.045	9265, 0.086
No. of 'observed' reflections ($I > 2\sigma_I$)	6938	5334	9044
Data / restraints / parameters	8496 / 2 / 750	16009 / 0 / 982	9265 / 0 / 692
Goodness-of-fit on F^2	1.270	0.985	1.332
Final *R* indices ('observed' data)	R_1 = 0.113, wR_2 = 0.174	R_1 = 0.047, wR_2 = 0.067	R_1 = 0.079, wR_2 = 0.151
Final *R* indices (all data)	R_1 = 0.137, wR_2 = 0.183	R_1 = 0.057, wR_2 = 0.071	R_1 = 0.081, wR_2 = 0.152
Largest diff. peak and hole (e $Å^{-3}$)	0.75 and -0.64	1.23 and -1.69	1.15 and -1.03

7 - References

1. A. Laguna (Ed.), *Modern Supramolecular Gold Chemistry: Gold-Metal Interactions and Applications*, Wiley-VCH, Weinheim, 2008.
2. D. R. Lide (Ed.), *CRC Handbook of Chemistry and Physics: 89th Edition*, CRC Press, Florida, 2008.
3. D. J. Gorin and D. F. Toste, *Nature* 2007, **446**, 395.
4. This increase of 1st ionisation potential commonly observed with most period 6 heavy elements, as the post-lanthanide elements contain a large number of protons in their atomic nuclei; an increase of nuclear charge is felt accompanied by poor shielding from the filled 4*f* subshell. The combination of these effects results in the increased affinity of valences electrons in the 5*d* or 6*s* subshell.
5. P. Schwerdtfeger, *Heteroatom Chem.* 2002, **13**, 578.
6. J. A. McCleverty and T. J. Mayer (Eds.) *Comprehensive Coordination Chemistry II; Volume 6: Transition Metal Groups 9-12*, Elsevier Science, Oxford, 2004.
7. R. Usón and A. Laguna, *Coord. Chem. Rev.* 1986, **70**, 1.
8. D. M. P. Mingos and R. H. Crabtree, *Comprehensive Organometallic Chemistry III: From Fundamentals to Applications*, Elsevier Science, Oxford, 2007.
9. A. Laguna and M. Laguna, *Coord. Chem. Rev.* 1999, **193-5**, 837.
10. Examples are noted in S. A. Cotton, *Chemistry of Precious Metals*, Chapman & Hall, London, 1997.
11. A. A. Mohamed, *Coord. Chem. Rev.* 2010, **254**, 1918.
12. M. A. Carvajal, J. J. Novoa and S. Alvarez, *J. Am. Chem. Soc.* 2004, **126**, 1465.
13. H. Schmidbaur, *Gold Bull.* 1990, **23**, 11.
14. P. Schwerdtfeger, P. D. W. Boyd, A. K. Burrell, W. T. Robinson and M. J. Taylor, *Inorg. Chem.* 1990, **29**, 3593.
15. P. Pyykkö, *Chem. Rev.* 1988, **88**, 563.
16. P. Pyykkö and J. P. Desclaux, *Acc. Chem. Res.* 1979, **12**, 276.
17. K. S. Pitzer, *Acc. Chem. Res.* 1979, **12**, 271.
18. H. Schmidbaur and A. Schier, *Chem. Soc. Rev.* 2012, **41**, 370.
19. A. Leyva-Pérez and A. Corma, *Angew. Chem., Int. Ed.* 2012, **51**, 614.
20. N. Bartlett, *Gold Bull.* 1998, **31**, 22.
21. P. Schwerdtfeger, M. Dolg, W. H. E. Schwarz, G. A. Bowmaker and P. D. W. Boyd, *J. Chem. Phys.* 1989, **91**, 1762.
22. A. Codina, E. J. Fernández, P. G. Jones, A. Laguna, J. M. López-de-Luzuriaga, M. Monge, M. E. Olmos, J. Pérez and M. A. Rodríguez, *J. Am. Chem. Soc.* 2002, **124**, 6781.
23. J. P. Desclaux, *Atom. Data Nucl. Data Tables* 1973, **12**, 311.

24. N. D. Shapiro and D. F. Toste, *Synlett* 2010, **2010**, 675.

25. Complexes containing Au···Group 9 metal contacts: M. J. Calhorda, C. Ceamanos, O. Crespo, M. C. Gimeno, A. Laguna, C. Larraz, P. D. Vaz and M. D. Villacampa, *Inorg. Chem.* 2010, **49**, 8255.

26. Complexes containing Au···Group 10 metal contacts: (a) M. H. Pérez-Temprano, J. A. Casares, Á. R. de Lera, R. Álvarez and P. Espinet, *Angew. Chem., Int. Ed.* 2012, **51**, 4917; (b) V. Phillips, K. J. Willard, J. A. Golen, C. J. Moore, A. L. Rheingold, and L. H. Doerrer, *Inorg. Chem.* 2010, **49**, 9265; (c) Q.-J. Pan, Y.-R. Guo and H.-X. Zhang, *Organometallics* 2010, **29**, 3261; (d) V. Phillips, F. G. Baddour, T. Lasanta, J. M. López-de-Luzuriaga, J. W. Bacon, J. A. Golen, A. L. Rheingold, L. H. Doerrer, *Inorg. Chim. Acta* 2010, **364**, 195; (e) J. Vicente, P. González-Herrero and M. Pérez-Cadenas, *Inorg. Chem.* 2007, **46**, 4718; (f) R. Hayoun, D. K. Zhong, A. L. Rheingold and L. H. Doerrer, *Inorg. Chem.* 2006, **45**, 6120; see also reference 32.

27. Recent examples of complexes containing Au···Group 11 metal contacts: (a) I. O. Koshevoy, Y.-C. Chang, A. J. Karttunen, M. Haukka, T. Pakkanen, and P.-T. Chou, *J. Am. Chem. Soc.* 2012, **134**, 6564; (b) A. C. Jahnke, K. Pröpper, C. Bronner, J. Teichgräber, S. Dechert, M. John, O. S. Wenger, and F. Meyer, *J. Am. Chem. Soc.* 2012, **134**, 2938; (c) V. Vreshch, W. Shen, B. Nohra, S.-K. Yip, V. W.-W. Yam, C. Lescop and R. Réau, *Chem. Eur. J.* 2012, **18**, 466; (d) A. Ilie, C. I. Raţ, S. Scheutzow, C. Kiske, K. Lux, T. M. Klapötke, C. Silvestru and K. Karaghiosoff, *Inorg. Chem.* 2011, **50**, 2675; (e) E. J. Fernández, C. Hardacre, A. Laguna, M. C. Lagunas, J. M. López-de-Luzuriaga, M. Monge, M. Montiel, M. E. Olmos, R. C. Puelles and E. Sánchez-Forcada, *Chem. Eur. J.* 2009, **15**, 6222; (f) O. Crespo, M. C. Gimeno, A. Laguna, C. Larraz and M. D. Villacampa, *Chem. Eur. J.* 2007, **13**, 235; see also reference 25.

28. Complexes containing Au···Group 12 metal contacts; See reference 27c.

29. Complexes containing Au···*p*-block heavy element contacts: (a) C. Tschersich, C. Limberg, S. Roggan, C. Herwig, N. Ernsting, S. Kovalenko and S. Mebs, *Angew. Chem., Int. Ed.* 2012, **51**, 4989; (b) J. M. López-de-Luzuriaga, M. Monge, M. E. Olmos, M. Rodríguez-Castillo, A. Laguna and F. Mendizabal, *Theor. Chem. Acc.* 2011, **129**, 593; (c) E. J. Fernández, A. Laguna, J. López-de-Luzuriaga, M. Monge and F. Mendizabal, *J. Mol. Struct.-Theochem.* 2008, **851**, 121.

30. (a) M. Rodríguez-Castillo, M. Monge, J. M. López-de-Luzuriaga, M. E. Olmos, A. Laguna and F. Mendizabal, *Comp. Theor. Chem.* 2011, **965**, 163; (b) J. Muňiz, L. E. Sansores, A. Rojano, A. Martínez and R. Salcedo, *J. Mol. Struct.-Theochem.* 2009, **901**, 232; (c) B. Assadollahzadeh and P. Schwerdtfeger, *Chem. Phys. Lett.* 2008, **462**, 222; (d) E. J. Fernández, A. Laguna, J. M. López-de-Luzuriaga, M. Monge, M. E. Olmos, and R. C. Puelles, *J. Phys, Chem. B* 2005, **109**, 20652; see also reference 29b.

31. L. H. Doerrer, *Dalton Trans.* 2010, **39**, 3543.

32. P. Pyykkö, *Annu. Rev. Phys. Chem.* 2012, **63**, 45.

33. Modified from Reference 31.

34. See references cited in 18 and 35.

35. H. Schmidbaur and A. Schier, *Chem. Soc. Rev.* 2008, **37**, 1931.

36. N. Runeberg, M. Schütz and H.-J. Werner, *J. Chem. Phys.* 1999, **110**, 7210.

37. H. de la Riva, A. Pintado-Alba, M. Nieuwenhuyzen, C. Hardacre and M. C. Lagunas, *Chem. Commun.* 2005, 4970.

38. M. A. Bennett, S. K. Bhargava, N. Mirzadeh, S. H. Privér, J. Wagler and A. C. Willis, *Dalton Trans.* 2009, 7537.

39. Details of applications of these lattices are cited in: L. H. Doerrer, *Comment. Inorg. Chem.* 2008, **29**, 93.

40. K.-L. Cheung, S.-K. Yip and V. W.-W. Yam, *J. Organomet. Chem.* 2004, **689**, 4451.

41. E. J. Fernández, A. Laguna and J. M. López-de-Luzuriaga, *Dalton Trans.* 2007, **36**, 1969.

42. (a) M. A. Malwitz, S. H. Lim, R. L. White,-Morris, D. M. Pham, M. M. Olmstead and A. L. Balch, *J. Am. Chem. Soc.* 2012, 134, 10885; (b) L. Rodríguez, M. Ferrer, R. Crehuet, J. Anglada and J. C. Lima, *Inorg. Chem.* 2012, **51**, 7636; (c) S. Han, Y. Y. Yoon, O.-S. Jung and Y.-A Lee, *Chem. Commun.* 2011, **47**, 10689; (d) T. K.-M. Lee, N. Zhu and V. W.-W. Yam, *J. Am. Chem. Soc.* 2010, **132**, 17646; (e) M. Saitoh, A. L. Balch, J. Yuasa and T. Kawai, *Inorg. Chem.* 2010, **49**, 7129; (f) O. Crespo, M. C. Gimeno, A. Laguna, M. Kulcsar and C. Silvestru, *Inorg. Chem.* 2009, **48**, 4134; (g) M. C. Gimeno and A. Laguna, *Chem. Soc. Rev.* 2008, **37**, 1952.

43. (a) K. M.-C. Wong, L.-L. Hung, W. H. Lam, N. Zhu and V. W.-W. Yam, *J. Am. Chem. Soc.* 2007, **129**, 4350; (b) V. W.-W. Yam, K. M.-C. Wong, L.-L. Hung and N-Zhu, *Angew. Chem., Int. Ed.* 2005, **44**, 3107; (c) K. M.-C. Wong, X. Zhu, L.-L. Hung, N. Zhu, V. W.-W. Yam and H.-S. Kwok, *Chem. Commun.* 2005, 2906.

44. Reviews for organic transformations mediated by gold catalysis: (a) H. A. Wegner and M. Auzias, *Angew. Chem., Int. Ed.* 2011, **50**, 8236; (b) S. P. Nolan, *Acc. Chem. Res.* 2011, **44**, 91; (c) T. de Haro and C. Nevado, *Synthesis* 2011, 2530; (d) M. Rudolph and A. S. K. Hashmi, *Chem. Commun.* 2011, **47**, 6536; (e) T. C. Boorman and I. Larrosa, *Chem. Soc. Rev.* 2011, **40**, 1910; (f) H. G. Raubenheimer and H. Schmidbaur, *S. Afr. J. Sci.* 2011, **107**, no page number given; (g) M. S. Dudnik, N. Chernyak and V. Gevorgyan, *Aldrichchim. Acta* 2010, **43**, 37; (h) A. S. K. Hashmi and M. Bührle, *Aldrichchim. Acta* 2010, **43**, 27; (i) C.-J. Li, *Acc. Chem. Res.* 2010, **43**, 581; (j) A. S. K. Hashmi, *Angew. Chem., Int. Ed.* 2010, **49**, 5762; (k) S. Díez-González, N. Marion and S. P. Nolan, *Chem. Rev.* 2009, **109**, 3612; (l) E. Soriano and J. Marco-Contelles, *Acc. Chem. Res.* 2009, **42**, 1026; (m) A. Arcadi, *Chem. Rev.* 2008, **108**, 3266; (n) Z. Li, C. Brouwer and C. He, *Chem. Rev.* 2008, **108**, 3239; (o) H. C. Shen, *Tetrahedron* 2008, **64**, 7847; (p) H. C. Shen, *Tetrahedron* 2008, **64**, 3885; (q) R. Skouta and C.-J. Li, *Tetrahedron* 2008, **64**, 4917; (r) A. Fürstner and P. W.

Davies, *Angew. Chem., Int. Ed.* 2007, **46**, 3410; (s) A. S. K. Hashmi, *Catal. Today* 2007, **122**, 211; see also reference 24.

45. (a) L. Jašíková and J. Roithová, *Organometallics* 2012, **31**, 1935; (b) T. J. Brown and R. A. Widenhoefer, *J. Organomet. Chem.* 2011, **696**, 1216; (c) M. García-Mota, N. Cabello, F. Maseras, A. M. Echavarren, J. Pérez-Ramírez and N. Lopez, *ChemPhysChem* 2008, **9**, 1624.

46. For Au-alkyne calculations: (a) H. V. R. Dias and J. Wu, *Eur. J. Inorg. Chem.* 2008, **2008**, 509; (b) A. S. K. Hashmi, *Gold Bull.* 2003, **36**, 3.

47. Bond dissociation enthalpies of $M^+(C_2H_4)$, where M – Cu, Ag, Au: (a) K. L. Stringer, M. Citir and R. B. Metz, *J. Phys. Chem. A* 2004, **108**, 6996; (b) M. R. Sievers, L. M. Jarvis and P. B. Armentrout, *J. Am. Chem. Soc.* 1998, **120**, 1891; (c) D. Schröder, H. Schwarz, J. Hrušák and P. Pyykkö, *Inorg. Chem.* 1998, **37**, 624; (d) R. H. Hertwig, W. Koch, D. Schröder, H. Schwarz, J. Hrušák and P. Schwerdtfeger, *J. Phys. Chem.* 1996, **100**, 12253; (e) D. Schröder, J. Hrušák, H. Hertwig, W. Koch, P. Schwerdtfeger and H. Schwarz, *Organometallics* 1995, **14**, 312; (f) B. C. Guo and A. W. Castleman Jr., *Chem. Phys. Lett.* 1991, **181**, 16.

48. M. S. Nechaev, V. M. Rayón and G. Frenking, *J. Phys. Chem. A* 2004, **108**, 3134.

49. M. J. S. Dewar, *Bull. Soc. Chim. Fr.* 1951, C71.

50. For Au-ethylene calculations: (a) A. S. K. Hashmi, *Gold Bull.* 2004, **37**, 51; (b) J. Chatt and L. A. Duncanson, *J. Chem. Soc.* 1953, 2939.

51. J. J. BelBruno, *Surf. Sci.* 2005, **577**, 167.

52. T. N. Hooper, C. P. Butts, M. Green, M. F. Haddow, J. E. McGrady and C. A. Russell, *Chem. Eur. J.* 2009, **15**, 12196.

53. (a) W. C. Zeise, *Ann. Phys. Chem.* 1831, **21**, 497; (b) W. C. Zeise, *Poggendorf's Ann. Phys.* 1827, **9**, 632.

54. M. Black, R. H. B. Mais and P. G. Owston, *Acta Cryst. B* 1969, **B25**, 1753.

55. (a) H. Coutelle and R. Hüttel, *J. Organomet. Chem.* 1978, **153**, 359; (b) P. Tauchner and R. Hüttel, *Chem. Ber.* 1974, **107**, 3761; (c) R. Hüttel and H. Forkl, *Chem. Ber.* 1972, **105**, 2913; (d) R. Hüttel and H. Forkl, *Chem. Ber.* 1972, **105**, 1664; (e) R. Hüttel, P. Tauchner and H. Forkl, *Chem. Ber.* 1972, **105**, 1; (f) P. Tauchner and R. Hüttel, *Tetrahedron Lett.* 1972, **46**, 4733; (g) R. Hüttel, H. Reinheimer and K. Nowak, *Chem. Ber.* 1968, **101**, 3761; (h) R. Hüttel, H. Reinheimer, K. Nowak and H. Dietl *Tetrahedron Lett.* 1967, 1019; (i) R. Hüttel and H. Reinheimer, *Chem. Ber.* 1966, **99**, 2778; (j) R. Hüttel, H. Reinheimer and H. Dietl, *Chem. Ber.* 1966, **99**, 462.

56. H. Schmidbaur and A. Schier, *Organometallics* 2010, **29**, 2.

57. D. B. Dell'Amico, F. Calderazzo, R. Dantona, J. Strähle and H. Weiss, *Organometallics* 1987, **6**, 1207.

58. (a) H. V. R. Dias and J. Wu, *Organometallics* 2012, **31**, 1511; (b) H. V. R. Dias and J. Wu, *Angew. Chem., Int. Ed.* 2007, **46**, 7814.

59. J. A. Flores and H. V. R. Dias, *Inorg. Chem.* 2008, **47**, 4448.

60. E. Herrero-Gómez, C. Nieto-Oberhuber, S. López, J. Benet-Buchholz and A. M. Echavarren, *Angew. Chem., Int. Ed.* 2006, **45**, 5455.

61. (a) J. L. Zhang, G.-C. Yang and C. He, *J. Am. Chem. Soc.* 2006, **128**, 1798; (b) C. Brouwer and C. He, *Angew. Chem., Int. Ed.*2006, **45**, 1744; (c) R.-V. Nguyen, X. Yao and C.-J. Li, *Org. Lett.* 2006, **8**, 2397; (d) X. Yao and C.-J. Li, *J. Am. Chem. Soc.* 2004, **126**, 6884.

62. C. M. Grisé, E. M. Rodrigue and L. Barriault, *Tetrahedron* 2008, **64**, 797.

63. (a) M. A. Cinellu, G. Minghetti, F. Cocco, S. Stoccoro, A. Zucca, M. Manassero and M. Arca, *Dalton. Trans.* 2006, 5073; (b) M. A. Cinellu, G. Minghetti, S. Stoccoro, A. Zucca and M. Manassero, *Angew. Chem., Int. Ed.* 2005, **44**, 6892; (c) M. A. Cinellu, G. Minghetti, S. Stoccoro, A. Zucca and M. Manassero, *Chem. Commun.* 2004, 1618.

64. T. J. Brown, M. G. Dickens and R. A. Widenhoefer, *J. Am. Chem. Soc.* 2009, **131**, 6350.

65. T. N. Hooper, M. Green, J. E. McGrady, J. R. Patel and C. A. Russell, *Chem. Commun.* 2009, 3877.

66. H. Clavier and S. P. Nolan, *Chem. Commun.* 2010, **46**, 841.

67. A. El-Hellani, C. Bour and V. Gandon, *Adv. Synth. Catal*. 2011, **353**, 1865.

68. (a) A. S. Rajashekharayya, S. K. Patra, M. Green and C. A. Russell, *Chem. Commun.* 2012, **48**, 1060; (b) A. S. Rajashekharayya, T. N. Hooper, C. P. Butts, M. Green, J. E. McGrady and C. A. Russell, *Angew. Chem., Int. Ed.* 2011, **50**, 7592.

69. D. Zuccaccia, L. Belpassi, F. Tarantelli and A. Macchioni, *J. Am. Chem. Soc.* 2009, **131**, 3170.

70. (a) R. E. M. Brooner and R. A. Widenhoefer, *Organometallics* 2012, **31**, 768; (b) I. Krossing, *Angew. Chem., Int. Ed.* 2011, **50**, 11576.

71. H. V. R. Dias, M. Fianchini, T. R. Cundari and C. F. Campana, *Angew. Chem., Int. Ed.* 2008, **47**, 556.

72. (a) M. Green, J. A. K. Howard, J. L. Spencer and F. G. A. Stone, *J. Chem. Soc, Dalton Trans.* 1977, 271; (b) M. Green, J. A. K. Howard, J. L. Spencer and F. G. A. Stone, *J. Chem. Soc, Chem. Commun.* 1975, 449.

73. M. Fianchini, H. Dai and H. V. R. Dias, *Chem. Commun.* 2009, 6373.

74. A. Das, C. Dash, M. Yousufuddin, M. A. Celik, G. Frenking and H. V. R. Dias, *Angew. Chem., Int. Ed.* 2012, **51**, 3940.

75. J. Wu, P. Kroll and H. V. R. Dias, *Inorg. Chem.* 2009, **48**, 423.

76. H. V. R. Dias, J. A. Flores, J. Wu and P. Kroll, *J. Am. Chem. Soc.* 2009, **131**, 11249.

77. S. Flügge, A. Anoop, R. Goddard, W. Thiel and A. Fürstner, *Chem. Eur. J.* 2009, **15**, 8558.

78. T. N. Hooper, M. Green and C. A. Russell, *Chem. Commun.* 2010, **46**, 2313.

79. D. Zuccaccia, L. Belpassi, L. Rocchigiani, F. Tarantelli and A. Macchioni, *Inorg. Chem.* 2010, **49**, 3080.

80. T. J. Brown and R. A. Widenhoefer, *Organometallics* 2011, **30**, 6003.

81. A. Himmelspach, M. Finze and S. Raub, *Angew. Chem., Int. Ed.* 2011, **50**, 2628.

82. V. Lavallo, G. D. Frey, S. Kousar, B. Donnadieu and G. Bertrand, *Proc. Natl. Acad. Sci. USA* 2007, **104**, 13569.

83. R. Casado, M. Contel, M. Laguna, P. Romero and S. Sanz, *J. Am. Chem. Soc.* 2003, **125**, 11925.

84. A. S. K. Hashmi and G. J. Hutchings, *Angew. Chem., Int. Ed.* 2006, **45**, 7896.

85. A. Fürstner, *Chem. Soc. Rev.* 2009, **38**, 3208.

86. (a) R. R. Schmidt, *Angew. Chem., Int. Ed.* 1973, **12**, 212; (b) B. Rao and L. Weiler, *Tetrahedron Lett.* 1971, **12**, 927.

87. H. Schmidbaur and A. Schier, *Z. Naturforsch. B* 2011, **66b**, 329.

88. D. Wang, R. Cai, S. Sharma, J. Jirak, S. K. Thummanapelli, N. G. Akhmedov, H. Zhang, X. Liu, J. L. Petersen and X. Shi, *J. Am. Chem. Soc.* 2012, **134**, 9012.

89. M. T. Reetz and K. Sommer, *Eur. J. Org. Chem.* 2003, **18**, 3465.

90. E. J. Fernández, A. Laguna and J. M. López-de-Luzuriaga, *Dalton Trans.* 2007, 1969.

91. E. Jiménez-Núňez and A. M. Echavarren, *Chem. Rev.* 2008, **108**, 3326.

92. N. Mézailles, L. Ricard and F. Gagosz, *Org. Lett.* 2005, **7**, 4133.

93. (a) M. Raducan, C. Rodríguez-Escrich, X. C. Cambiero, E. C. Escudero-Adán, M. A. Pericàs and A. M. Echavarren, *Chem. Commun.* 2011, **47**, 4893; (b) C. Gronnier, Y. Odabachian and F. Gagosz, *Chem. Commun.* 2011, **47**, 218.

94. A. S. K. Hashmi and L. Lothschütz, *ChemCatChem* 2010, **2**, 133.

95. L. Ricard and F. Gagosz, *Organometallics* 2007, **26**, 4704.

96. (a) B. K. Corkey and F. D. Toste, *J. Am. Chem. Soc.* 2005, **127,** 17168; (b) J. J. Kennedy-Smith, S. T. Staben and F. D. Toste, *J. Am. Chem. Soc.* 2004, **126**, 4526.

97. M. Preisenberger, A. Shier and H. Schmidbaur, *J. Chem. Soc., Dalton. Trans.* 1999, 1645.

98. P. Römbke, A. Schier and H. Schmidbaur, *Z. Naturforsch. B* 2002, **57b**, 605.

99. P. G. Jones, *Acta. Crystallogr. C* 1984, **C40**, 1320.

100. A. N. Nesmeyanov, E. G. Perevalova, Y. T. Struchkov, M. Y. Antipin, K. I. Grandberg and V. P. Dyadhenko, *J. Organomet. Chem.* 1980, **201**, 343.

101. (a) B. D. Sherry, L. Maus, B. N. Laforteza and F. D. Toste, *J. Am. Chem. Soc.* 2006, **128**, 8132; (b) B. D. Sherry and F. D. Toste, *J. Am. Chem. Soc.* 2004, **126**, 15978.

102. X. Yao and C.-J. Li, *Org. Lett.* 2006, **8**, 1953.

103. C. Nieto-Oberhuber, M. P. Muňoz, E. Buñuel, C. Nevado, D. J. Cardenas and A. M. Echavarren, *Angew. Chem., Int. Ed.* 2004, **43**, 2402.

104. (a) Z.-Y. Han, H. Xiao, X.-H. Chen and L.-Z. Gong, *J. Am. Chem. Soc.* 2009, **131**, 9182; (b) A. S. K. Hashmi and M. C. Blanco, *Eur. J. Org. Chem.* 2006, **2006**, 4340; (c) E. Mizushima, K. Sato, T. Hayashi and M. Tanaka, *Angew. Chem., Int. Ed.* 2002, **41**, 4563; (d) J. H. Teles, S. Brode and M. Chabanas, *Angew. Chem., Int. Ed.*1998, **37**, 1415.

105. A. Pradal, P. Y. Toullec and V. Michelet, *Org. Lett.* 2011, **13**, 6086.

106. Y. Fuchita, Y. Utsunomiya and M. Yasutake, *J. Chem. Soc., Dalton Trans.* 2001, 2330.

107. See the review articles in reference 44 for more details.

108. First evidence of gold-carbenoid intermediates: (a) M. R. Luzung, J. P Markham and F. D. Toste, *J. Am. Chem. Soc.* 2004, **126**, 10858; (b) V. Mamane, T. Gress, H. Krause and A. Fürstner, *J. Am. Chem. Soc.* 2004, **126**, 8654; see also reference 103.

109. Recent evidence of gold-carbenoid intermediates: (a) A. El-Hellani, C. Bour and V. Gandon, *Adv. Synth. Catal.* 2011, **353**, 1865; (b) C. R. Solorio-Alvarado and A. M. Echavarren, *J. Am. Chem. Soc.* 2010, **132**, 11881; (c) D. Benitez, N. D. Shapiro, E. Tkatchouk, Y. Wang, W. A. Goddard III and F. D. Toste, *Nature Chemistry* 2009, **1**, 482; (d) G. Seidel, R. Mynott and A. Fürstner, *Angew. Chem., Int. Ed.* 2009, **48**, 2510; (e) R. Sanz, D. Miguel and F. Rodríguez, *Angew. Chem., Int. Ed.* 2008, **120**, 7464; (f) L. Peng, X. Zhang, S. Zhang and J. Wang, *J. Org. Chem.* 2007, **72**, 1192; (g) S. López, E. Herrero-Gómez, P. Pérez-Galán, C. Nieto-Oberhuber and A. M. Echavarren, *Angew. Chem., Int. Ed.* 2006, **45**, 6029; (h) C. Nieto-Oberhuber, S. López, E. Jiménez-Núňez and A. M. Echavarren, *Chem. Eur. J.* 2006, **12**, 5916.

110. C. Nevado and A. M. Echavarren, *Synthesis* 2005, 167.

111. Z. Shi and C. He, *J. Org. Chem.* 2004, **69**, 3669.

112. S. R. Patrick, I. I. F. Boogaerts, S. Gaillard, M. Z. Slawin and S. P. Nolan, *Beilstein J. Org. Chem.* 2011, **7**, 892.

113. (a) P. Lu, T. C. Boorman, A. M. Z. Slawin and I. Larrosa, *J. Am. Chem. Soc.* 2010, **132**, 5580; (b) S. Gaillard, A. M. Z. Slawin and S. P. Nolan, *Dalton Trans.* 2009, 6967.

114. (a) M. S. Kharasch and H. S. Isbell, *J. Am. Chem. Soc.* 1931, **53**, 3053; (b) M. S. Kharasch and H. S. Isbell, *J. Am. Chem. Soc.* 1931, **53**, 2701.

115. K. S. Liddle and C. Parkin, *J. Chem. Soc., Chem. Commun.* 1972, 26.

116. P. W. J. de Graaf, J. Boerasma and G. J. M. van der Kerk, *J. Organomet. Chem.* 1976, **105**, 399.

117. (a) A. M. Tyabji and C. S. Gibson, *J. Chem. Soc.* 1952, 450; (b) W. J. Pope, *Brit. Pat. Appl.* 1929, **338506**.

118. F. Muggia, *Gynecol. Oncol.* 2009, **112**, 275.

119. M. A. Fuertes, J. Castilla, C. Alonso and J. M. Pérez, *Curr. Med. Chem.* 2003, **10**, 257.

120. A short review of the therapeutic applications of gold; C.-M. Che and W.-Y. Sun, *Chem. Commun.* 2011, **47**, 9554 and references 1-24 within.

121. N. A. Malik, P. J. Sadler, S. Neidle and G. L. Taylor, *J. Chem. Soc., Chem. Commun.* 1978, 711.

122. B. M. Sutton, E. McGusty, D. T. Walz and M. J. DiMartino, *J. Med. Chem.* 1972, **15**, 1095.

123. S. J. Berners-Price, M. J. DiMartino, D. T. Hill, R. Kuroda, M. A. Mazid and P. J. Sadler, *Inorg. Chem.* 1985, **24**, 3425.

124. P. Lange, A. Schier, J. Riede and H. Schmidbaur, *Z. Naturforsch. B* 1994, **49**, 643.

125. D. M. L. Goodgame, C. A. O'Mahoney, S. D. Plank and D. J. Williams, *Polyhedron* 1993, **12**, 2705.

126. A. V. Churakov, L. G. Kuz'mina, J. A. K. Howard and K. I. Grandberg, *Acta Crystallogr. C* 1998, **C54**, 54.

127. D. Koch, K. Sünkel and W. Beck, *Z. Naturforsch. B* 1999, **54b**, 96.

128. G. L. Wegner, A. Jockisch, A. Schier and H. Schmidbaur, *Z. Naturforsch. B* 2000, **55**, 347.

129. S. Friedrichs and P. G. Jones, *Acta Crystallogr. C* 2000, **C56**, 56.

130. A selection of references since early 2011 which employ phosphinegold(I) catalysts: (a) M. Raducan, M. Moreno, C. Bour and A. M. Echavarren, *Chem. Commun.* 2012, **48**, 52; (b) S. Cai, Z. Liu, W. Zhang, X. Zhao and D. Z. Wang, *Angew. Chem., Int. Ed.* 2011, **50**, 11133; (c) Y. Park, S. Y. Kim, J. H. Park, J. Cho, Y. K. Kang and Y. K. Chung, *Chem. Commun.* 2011, **47**, 5190; (d) S. Ngwerume and J. E. Camp, *Chem. Commun.* 2011, **47**, 1857; (e) P. W. Davies, A. Cremonesi and N. Martin, *Chem. Commun.* 2011, **47**, 379; (f) B.-L. Lu and M. Shi, *Chem. Eur. J.* 2011, **17**, 9070; (g) A. S. K. Hashmi, A. M. Schuster, S. Litters, F. Rominger and M. Pernpointner, *Chem. Eur. J.* 2011, **17**, 5661; (h) X. Du, S. Yang, J. Yang and Y. Liu, *Chem. Eur. J.* 2011, **17**, 4981; (i) H. Gao, X. Wu and J. Zhang, *Chem. Eur. J.* 2011, **17**, 2838; (j) T. Wang and J. Zhang, *Chem. Eur. J.* 2011, **17**, 86.

131. A selection of references since early 2011 which uses $(R_3P)AuN(Tf)_2$ as the active catalyst in organic transformations: (a) L. Ye, Y. Wang, D. H. Aue and L. Zhang, *J. Am. Chem. Soc.* 2012, **134**, 31; (b) A. Pradal, Q. Chen, P. Faudot dit Bel, P. Y. Toullec and V. Michelet, *Synlett* 2012, **2012**, 74; (c) W. He, C. Li and L. Zhang, *J. Am. Chem. Soc.* 2011, **133**, 8482; (d) B. Lu, Y. Luo, L. Liu, L. Ye, Y. Wang and L. Zhang, *Angew. Chem., Int. Ed.* 2011, **50**, 8358; (e) Q. Zhang, J. Sun, Y. Zhu, F. Zhang and B. Yu, *Angew. Chem., Int. Ed.* 2011, **50**, 4933; (f) T. Matsuda, Y. Yamaguchi, M. Shigeno, S. Sato and M. Masahiro, *Chem. Commun.* 2011, **47**, 8697; (g) N. Kern, A. Blanc, J.-M. Weibel and P. Pale, *Chem. Commun.* 2011, **47**, 6665; (h) T. De Haro and C. Nevado, *Chem. Commun.* 2011, **47**, 248; (i) D. A. Capretto, C. Brouwer, C. B. Poor and C. He, *Org. Lett.* 2011, **13**, 5842; (j) J. Qian, Y. Liu, J. Zhu, B. Jiang and Z. Xu, *Org. Lett.* 2011, **13**, 4220; (k) C. C. J. Loh, J. Badorrek, G. Raabe and D. Enders, *Chem. Eur. J.* 2011, **17**, 13409; (l) X. Xie, X. Du, Y. Chen and Y. Liu, *J. Org. Chem.* 2011, **76**, 9175; (m) M. N. Pennell, T. D. Sheppard, M. G.

Unthank, P. Turner and T. D. Sheppard, *J. Org. Chem.* 2011, **76**, 1479; (n) I. N. Lykakis, C. Efe, C. Gryparis and M. Stratakis, *Eur. J. Org. Chem.* 2011, **2011**, 2334.

132. (a) C. Wölper, S. R. Piňol, S. D. Ibáňez, M. Freytag, P. G. Jones and A. Blaschette, *Z. Anorg. Allg. Chem.* 2008, **634**, 1506; (b) P. G. Jones, A. Blaschette, J. Lautner and C. Thöne, *Z. Anorg. Allg. Chem.* 1997, **623**, 775.
133. (a) S. P. Fricker, *Metal Based Drugs* 1999, **6**, 291; (b) R. V. Parish, *Metal Based Drugs* 1999, **6**, 271.
134. K. J. Kilpin, W. Henderson and B. K. Nicholson, *Polyhedron* 2007, **26**, 204.
135. V. J. Scott, J. A. Labinger and J. E. Bercaw, *Organometallics* 2010, **29**, 4090.
136. F. Y. Mo, J. M. Yan, D. Qiu, F. Li, Y. Zhang and J. B. Wang, *Angew. Chem., Int. Ed.* 2010, **49**, 2028.
137. K. Oyaizu, Y. Ohtani, A. Shiozawa, K. Sugawara, T. Saito and M. Yuasa, *Inorg. Chem.* 2005, **44**, 6915.
138. B. Gething, C. R. Patrick and J. C. Tatlow, *J. Chem. Soc.* 1961, 1574.
139. J. F. Tannaci, M. Noji, J. McBee, and T. D. Tilley, *J. Org. Chem.* 2007, **72**, 5567.
140. A. L. Baumstark, M. Dotrong, M. G. Oakley, R. R. Stark and D. W. Boykin, *J. Org. Chem.* 1987, **52**, 3640.
141. R. Usón, A. Laguna and J. Vicente, *J. Organomet. Chem.* 1977, **131**, 471.
142. W. E. Piers and T. Chivers, *Chem. Soc. Rev.* 1997, **26**, 345.
143. A. A. Mohamed, H. E. Abdou and J. P. Fackler Jr., *Coord. Chem. Rev.* 2010, **254**, 1253.
144. P. H. M. Budzelaar, A. B. Van Oort and A. G. Orpen, *Eur. J. Inorg. Chem.* 1998, **1998**, 1485.
145. Reviews on known *β*-diketiminatometal complexes: (a) Y.-C. Tsai, *Coord. Chem. Rev.* 2012, **256**, 722. (b) L. Bourget-Merle, M. F. Lappert and J. R. Severn, *Chem. Rev.* 2002, **102**, 3031.
146. H. V. R. Dias and J. A. Flores, *Inorg. Chem.* 2007, **46**, 5841.
147. C. Shimokawa and S. Itoh, *Inorg. Chem.* 2005, **44**, 3010.
148. H. A. Chiong and O. Daugulis, *Organometallics* 2006, **25**, 4054.
149. B. Guan, D. Xing, G. Cai, X. Wan, N. Yu, Z. Fang, L. Yang and Z. Shi, *J. Am. Chem. Soc.* 2005, **127**, 18004.
150. A. Venugopal, M. K. Ghosh, H. Jürgens, K. W. Törnroos, O. Swang, M. Tilset and R. H. Heyn, *Organometallics* 2010, **29**, 2248.
151. J. D. Farwell, P. B. Hitchcock, M. F. Lappert and A. V. Protchenko, *J. Organomet. Chem.* 2007, **692**, 4953.
152. (a) A. S. Borovik, *Chem. Soc. Rev.* 2011, **40**, 1870; (b) A. Gunay and K. H. Theopold, *Chem. Rev.* 2010, **110**, 1060.

153. D. M. P. Mingos, P. Day and J. P. Dahl (Eds.), *Molecular Electronic Structures of Transition Metal Complexes I: Structure and Bonding*, Springer-Verlag, Berlin, 2012.

154. (a) H. W. Roesky, L. Haiduc and N. S. Hosmane, *Chem. Rev.* 2003, **103**, 2579; (b) E. A. Carter and W. A. Goddard III, *J. Phys. Chem.* 1988, **92**, 2109; (c) J. M. Mayer, *Comments Inorg. Chem.* 1988, **8**, 125.

155. K. P. O'Halloran, C. Zhao, N. S. Ando, A. J. Schultz, T. F. Koetzle, P. M. B. Piccoli, B. Hedman, K. O. Hodgson, E. Bobyr, M. L. Kirk, S. Knottenbelt, E. C. Depperman, B. Stein, T. M. Anderson, R. Cao, Y. V. Geletti, K. I. Hardcastle, D. G. Musaev, W. A. Neiwert, X. Fang, K. Morokuma, S. Wu, P. Kögerler and C. L. Hill, *Inorg. Chem.* 2012, **51**, 7025.

156. M. Bardají, P. Uznanski, C. Amiens, B. Chaudret and A. Laguna, *Chem. Commun.* 2002, 598.

157. (a) E. C. Tyo, A. W. Castleman Jr., D. Schröder, P. Milko, J. Roithova, J. M. Ortega, M. A. Cinellu, F. Cocco and G. Minghetti, *J. Am. Chem. Soc.* 2009, **131**, 13009; (b) M. A. Cinellu, G. Minghetti, M. V. Pinna, S. Stoccoro, A. Zucca and M. Manassero, *Chem. Commun.* 1998, 2397; (c) M. A. Cinellu, G. Minghetti, M. V. Pinna, S. Stoccoro, A. Zucca, M. Manassero and M. Sansoni, *J. Chem. Soc., Dalton Trans.* 1998, 4119; (d) J. Vicente, M. D. Bermúdez, F. J. Carrión and P. G. Jones, *J. Organomet. Chem.* 1996, **508**, 53.

158. R. Cao, T. M. Anderson, P. M. B. Piccoli, A. J. Schultz, T. F. Koetzle, Y. V. Geletii, E. Slonkina, B. Hedman, K. O. Hodgson, K. I. Hardcastle, X. Fang, M. L. Kirk, S. Knottenbelt, P. Kögerler, D. G. Musaev, K. Morokuma, M. Takahashi and C. L. Hill, *J. Am. Chem. Soc.* 2007, **129**, 11118.

159. (a) Y. Wang, H. Ji, S. Lan and L. Zhang, *Angew. Chem., Int. Ed.* 2012, **51**, 1915; (b) S. Vasu, H.-H. Hung, S. Bhunia, S. A. Gawade, A. Das and R.-S. Liu, *Angew. Chem., Int. Ed.* 2011, **50**, 6911.

160. L. T. Bell, G. C. Lloyd-Jones and C. A. Russell, *Chem. Eur. J.* 2012, **18**, 2931.

161. D. S. Laitar, C. J. N. Mathison, W. M. Davis and J. P. Sadighi, *Inorg. Chem.* 2003, **42**, 7354.

162. Structural information of **16a-H** can be found in N. Carrera, N. Savjani, J. Simpson, D. L. Hughes and M. Bochmann, *Dalton Trans.*, 2011, **40**, 1016.

163. For a discussion of C-H···F-N bonding criteria see for example: A. J. Mountford, D. L. Hughes and S. J. Lancaster, *Chem. Commun.* 2003, 2148.

164. D. Phillips, O. Zava, R. Scopilitti, A. A. Nazarov and P. J. Dyson, *Organometallics* 2010, **29**, 417.

165. S. Hong, L. M. R. Hill, A. K. Gupta, B. D. Naab, J. B. Gilroy, R. G. Hicks, C. J. Cramer and W. B. Tolman, *Inorg. Chem.* 2009, **48**, 4514.

166. P. F. Barron, L. M. Engelhardt, P. C. Healy, J. Oddy and A. H. White, *Aust. J. Chem.* 1987, **40**, 1545.

167. X. Zhang, H. Liu, X. Hu, G. Tang, Y. Zhao and J. Zhu, *Org. Lett.* 2011, **13**, 3478.

168. T. Brasey, A. Buryak, R. Scopelliti and K. Severin, *Eur. J. Inorg. Chem.* 2004, **2004**, 964.

169. Y. Sarazin, D. L. Hughes, N. Kaltsoyannis, J. A. Wright and M. Bochmann, *J. Am. Chem. Soc.* 2007, **129**, 881.

170. Y. Sarazin, N. Kaltsoyannis, J. A. Wright and M. Bochmann, *Organometallics* 2007, **26**, 1811.

171. P. A. Dean, D. G. Ibbott and J. B. Stothers, *J. Chem. Soc., Chem. Commun.* 1973, 626.

172. L. C. Damude, P. A. W. Dean, M. D. Sefcik and J. Schaefer, *J. Organomet. Chem.* 1982, **226**, 105.

173. A. S. Borovik, S. G. Bott and A. R. Barron, *J. Am. Chem. Soc.* 2001, **123**, 11219.

174. J. A. Labinger and J. E. Bercaw, *Nature* 2002, **417**, 507.

175. (a) S. S. Stahl, J. A. Labinger and J. E. Bercaw, *Angew. Chem., Int. Ed.* 1998, **37**, 2180; (b) A. E. Shilov and G. B. Shul'pin, *Chem. Rev.* 1997, **97**, 2879; (c) R. H. Crabtree, *Chem. Rev.* 1995, **95**, 987; (d) B. A. Arndtsen, R. G. Bergman, T. A. Mobley and T. H Peterson, *Acc. Chem. Res.* 1995, **28**, 154.

176. R. Jazzar, J. Hitce, A. Renaudat, J. Sofack-Kreutzer and O. Baudoin, *Chem. Eur. J.* 2010, **16**, 2654.

177. L. Johansson, O. B. Ryan, C. Rømming and M. Tilset, *J. Am. Chem. Soc.* 2001, **123**, 6579.

178. A. S. McCall, H. Wang, J. M. Desper and S. Kraft, *J. Am. Chem. Soc.* 2011, **133**, 1832.

179. References 1-3 in J. T. Groves and P. Viski, *J. Am. Chem. Soc.* 1989, **111**, 8537.

180. References 9-17 in J. T. Groves and P. Viski, *J. Am. Chem. Soc.* 1989, **111**, 8537.

181. J. T. Groves and P. Viski, *J. Am. Chem. Soc.* 1989, **111**, 8537.

182. G. C. Hsu, W. P. Kosar and W. D. Jones, *Organometallics* 1994, **13**, 385.

183. (a) J. P. Collman and R. Boulatov, *Inorg. Chem.* 2001, **40**, 2461; (b) K. J. Del Rossi and B. B. Wayland, *J. Am. Chem. Soc.* 1985, **107**, 7941.

184. J. Zhu, X. Bu, P. Feng and G. D. Stucky, *J. Am. Chem. Soc.* 2000, **122**, 11563.

185. S. Shimada, A. S. Batsanov, J. A. K. Howard and T. B. Marder, *Angew. Chem., Int. Ed.* 2001, **40**, 2168.

186. A. G. Wong-Foy, G. Bhalla, X. Y. Liu and R. A. Periana, *J. Am. Chem. Soc.* 2003, **125**, 14292.

187. A. M. Voutchkova and R. H. Crabtree, *J. Mol. Catal A: Chem.* 2009, **312**, 1.

188. H. A. Zhong, J. A. Labinger and J. E. Bercaw, *J. Am. Chem. Soc.* 2002, **124** (7), 1378.

189. S.-B. Zhao, D. Song, W.-L. Jia and S. Wang, *Organometallics* 2005, **24**, 3290.

190. A. Miyashita, M. Hotta and Y. Saida, *J. Organomet. Chem.* 1994, **473**, 353.

191. A. N. Vedernikov, S. V. Borisoglebski, A. B. Solomonov and B. N. Solomonov, *Mendeleev Commun*. 2000, **10** (1), 20.

192. (a) R. H. Crabtree (Ed.), *Energy Production and Storage: Inorganic Chemical Strategies for a Warming World*, Wiley-VCH, Weinheim, 2010; (b) G. S. Chen, J. A. Labinger and J. E. Bercaw, *Organometallics* 2009, **28**, 4899; (c) J. A. Labinger, A. M. Herring and J. E. Bercaw, *J. Am. Chem. Soc.* 1990, **112**, 5628.

193. As indicated by the formation of Au(0) in this reaction, Au(III) is reduced under these conditions and therefore exhibits the same reaction pattern as outlined for Au(I) precursors.

194. (a) J.-J. Li, R. Giri and J.-Q. Yu, *Tetrahedron* 2008, **64**, 6979; (b) W. D. Jones, *Acc. Chem. Res.* 2003, **36**, 140.

195. (a) N. F. Gol'dshleger, V. V. Es'kova, A. E. Shilov, A and A. Shteinmann, *Zh. Fiz. Khim. (Engl. Transl.)* 1972, **46**, 785; (b) N. F. Gol'dshleger, M. B. Tyabin, A. E. Shilov and A. A. Shteinman, *Zh. Fiz. Khim. (Engl. Transl.)* 1969, **43**, 1222.

196. M. Lin, C. Shen, E. A. Garcia-Zayas and A. Sen, *J. Am. Chem. Soc.* 2001, **123**, 1000.

197. (a) P. B. Merkel, P. Luo, J. P. Dinnocenzo and S. Farid, *J. Org. Chem.* 2009, **74**, 5163; (b) C. Amatore and C. Lefrou, *J. Electroanal. Chem.* 1992, **325**, 239.

198. A report probing the electron transfer processes from benzyl-radicals to C_6Et_6 and 1,3,5-$C_6H_3(^tBu)_3$ found steric crowding hindered electron transfer; P. Luo, J. P. Dinnocenzo, P. B. Merkel, R. H. Young and S. Farid, *J. Org. Chem.* 2012, **77**, 1632.

199. (a) R. Usón, A. Laguna, E. J. Fernández, M. E. Ruiz-Romero, P. G. Jones and J. Lautner, *J. Chem. Soc., Dalton Trans.* 1989, 2127; (b) S. Gambarotta, C. Floriani, A. Chiesi-Villa and C. Guastini, *J. Chem. Soc., Chem. Commun.* 1983, 1304.

200. H. Salem, Y. Ben-David, L. J. W. Shimon and D. Milstein, *Organometallics* 2006, **25**, 2292.

201. M. E. van der Boom, S.-Y. Liou, L. J. W. Shimon, Y. Ben-David and D. Milstein, *Inorg. Chim. Acta* 2004, **357**, 4015.

202. M. E. van der Boom, H.-B. Kraatz, L. Hassner, Y. Ben-David and D. Milstein, *Organometallics* 1999, **18**, 3873.

203. M. E. van der Boom, S.-Y. Liou, Y. Ben-David, M. Gozin and D. Milstein, *J. Am. Chem. Soc.* 1998, **120**, 13415.

204. R. Chauvin, *Eur. J. Inorg. Chem.* 2000, **2000**, 577.

205. M. Stradiotto, K. D. Hesp and R. J. Lundgren, *Angew. Chem. Int. Ed.* 2010, **49**, 494.

206. J.-Q. Zhou and H. Alper, *Organometallics* 1994, **13**, 1586.

207. D. Cauzzi, M. Delferro, C. Graiff, R. Pattacini, G. Predieri and A. Tiripicchio, *Coord. Chem. Rev.* 2010, **254**, 753.

208. References 1-5 in M. Sircoglou, N. Saffon, Y. Coppel, G. Bouhadir, L. Maron and D. Bourissou, *Angew. Chem. Int. Ed.* 2009, **48**, 3454.

209. (a) P. Gualco, T.-P. Lin, M. Sircoglou, M. Mercy, S. Ladeira, G. Bouhadir, L. M. Pérez, A. Amgoune, L. Maron, F. Gabbaï and D. Bourissou, *Angew. Chem. Int. Ed.* 2009, **48**, 9892;

(b) M. Sircoglou, S. Bontemps, M. Mercy, N. Saffon, M. Takahashi, G. Bouhadir, L. Maron and D. Bourissou, *Angew. Chem. Int. Ed.* 2007, **46**, 8583.

210. M. Sircoglou, G. Bouhadir, N. Saffon, K. Miqueu and D. Bourissou, *Organometallics* 2008, **27**, 1675.

211. M. Sircoglou, N. Saffon, Y. Coppel, G. Bouhadir, L. Maron and D. Bourissou, *Angew. Chem. Int. Ed.* 2009, **48**, 3454..

212. B. M. Wile, R. J. Burford, R. McDonald, M. J. Ferguson and M. Stradiotto, *Organometallics* 2006, **25**, 1028.

213. Nickel-catalysed: (a) S. L. Scott and M. A. C. Campos, *U.S Pat. Appl.* 2009, **US 2009/0326174 A1**; (b) S. Noda, T. Kochi and K. Nozaki, *Organometallics* 2009, **28**, 656; (c) R. J. Nowack, A. K. Hearley and B. Rieger, *Z. Anorg. Allg. Chem.* 2005, **631**, 2775.

214. Ru-catalysed: (a) L. Piche, J.-C. Daigle, and J. P. Claverie, *Chem. Commun.* 2011, **47**, 7836; (b) Z. Sahli, B. Sundararaju, M. Achard and C. Bruneau, *Org. Lett.* 2011, **13**, 3964; (c) B. Sundararaju, M. Achard, B. Demerseman, L. Toupet, G. V. M. Sharma and C. Bruneau, *Angew. Chem. Int. Ed.* 2010, **49**, 2782; (d) B. Sundararaju, Z. Tang, M. Achard, G. V. M. Sharma, L. Toupet and C. Bruneau, *Adv. Synth. Catal.* 2010, **352**, 3141.

215. Pd-catalysed: (a) J.-C. Daigle, L. Piche, A. Arnold and J. P. Claverie, *ACS Macro Lett.* 2012, **1**, 343; (b) T. M. J. Anselment, C. E. Anderson, B. Rieger, M. B. Boeddinghaus and T. F. Fässler, *Dalton Trans.* 2011, **40**, 8304; (c) J.-C. Daigle, L. Piche and J. P. Claverie, *Macromolecules* 2011, **44**, 1760; (d) Z. Shen and R. F. Jordan, *J. Am. Chem. Soc.* 2010, **132**, 52; (e) L. Piche, J.-C. Daigle, R. Poli and J. P. Claverie, *Eur. J. Inorg. Chem.* 2010, **2010**, 4595; (f) W. Weng, Z. Shen and R. F. Jordan, *J. Am. Chem. Soc.* 2007, **129**, 15450; (g) T. Kochi, A. Nakamura, H. Ida and K. Nozaki, *J. Am. Chem. Soc.* 2007, **129**, 7770; (h) T. Kochi, K. Yoshimura and K. Nozaki, *Dalton Trans.* 2006, **35**, 25; (i) A. K. Hearley, R. J. Nowack and B. Rieger, *Organometallics*, 2005, **24**, 2755; (j) T. Schultz and A. Pfaltz, *Synthesis* 2005, **6**, 1005; (k) S. Noda, A. Nakamura, T. Kochi, L. W. Chung, K. Morokuma and K. Nozaki, *J. Am. Chem. Soc.* 2009, **131**, 14088.

216. Group 11 gold-heterometallic clusters containing metallophilic interactions supported by alkynyl ligands: (a) J. R. Shakirova, E. V. Grachova, V. V. Gurzhiy, I. O. Koshevoy, A. S. Melnikov, O. V. Sizova, S. P. Tunik and A. Laguna, *Dalton Trans.* 2012, **41**, 2941; (b) I. O. Koshevoy, C.-L. Lin, A. J. Karttunen, M. Haukka, C.-W. Shih, P.-T. Chou, S. P. Tunik and T. A. Pakkanen, *Chem. Comm.* 2011, **47**, 5533; (c) I. O. Koshevoy, C.-L. Lin, A. J. Karttunen, J. Jänis, M. Haukka, S. P. Tunik, P.-T. Chou, and T. A. Pakkanen, *Inorg. Chem.* 2011, **50**, 2395; (d) I. O. Koshevoy, C.-L. Lin, A. J. Karttunen, J. Jänis, M. Haukka, S. P. Tunik, P.-T. Chou and T. A. Pakkanen, *Chem. Eur. J.* 2011, **17**, 11456; (e) I. O. Koshevoy, A. J. Karttunen, J. R. Shakirova, A. S. Melnikov, M. Haukka, S. P. Tunik and T. A. Pakkanen, *Angew. Chem., Int. Ed.* 2010, **49**, 8864; (f) I. O. Koshevoy, Y.-C. Lin, Y.-C. Chen, A. J. Karttunen, M. Haukka, P.-T. Chou, S. P. Tunik and T. A. Pakkanen, *Chem.*

Comm. 2010, **46**, 1440; (g) I. O. Koshevoy, A. J. Karttunen, S. P. Tunik, J. Jänis, M. Haukka, A. S. Melnikov, P. Y. Serdobintsev and T. A. Pakkanen, *Dalton Trans.* 2010, **39**, 2676; (h) I. O. Koshevoy, P. V. Ostrova, A. J. Karttunen, A. S. Melnikov, M. A. Khodorkovskiy, M. Haukka, J. Jänis, S. P. Tunik and T. A. Pakkanen, *Dalton Trans.* 2010, **39**, 9022; (i) I. O. Koshevoy, Y.-C. Lin, A. J. Karttunen, M. Haukka, P.-T. Chou, S. P. Tunik and T. A. Pakkanen, *Chem. Comm.* 2009, 2860; (j) I. O. Koshevoy, A. J. Karttunen, S. P. Tunik, M. Haukka, S. I. Selivanov, A. S. Melnikov, P. Y. Serdobintsev and T. A. Pakkanen, *Organometallics* 2009, **28**, 1369; (k) I. O. Koshevoy, E. Gutierrez-Puebla, P. Lahuerta, A. Monge, M. A. Ubeda and M. Sanaú, *Dalton Trans.* 2009, 8392; (l) Y.-C. Lin, P.-T. Chou, I. O. Koshevoy and T. A. Pakkanen, *J. Phys. Chem. A* 2009, **113**, 9270; (m) I. O. Koshevoy, Y.-C. Lin, A. J. Karttunen, P.-T. Chou, P. Vainiotalo, S. P. Tunik, M. Haukka and T. A. Pakkanen, *Inorg. Chem.* 2009, **48**, 2094; (n) I. O. Koshevoy, L. Koskinen, M. Haukka, S. P. Tunik, P. Y. Serdobintsev, A. S. Melnikov and T. A. Pakkanen, *Angew. Chem., Int. Ed.* 2008, **47**, 3942; (o) I. O. Koshevoy, A. J. Karttunen, S. P. Tunik, M. Haukka, S. I. Selivanov, A. S. Melnikov, P. Y. Serdobintsev, M. A. Khodorkovskiy and T. A. Pakkanen, *Inorg. Chem.* 2008, **47**, 9478.

217. Group 11 gold-heterometallic clusters containing metallophilic interactions supported by chelating *N*-substituted-phosphine ligands: (a) O. Crespo, M. C. Gimeno, A. Laguna, F. J. Lahoz and C. Larraz, *Inorg. Chem.* 2011, **50**, 9533; (b) I. O. Koshevoy, J. R. Shakirova, A. S. Melnikov, M. Haukka, S. P. Tunik and T. A. Pakkanen, *Dalton Trans.* 2011, **40**, 7927; (c) J.-H. Jia and Q.-M. Wang, *J. Am. Chem. Soc.* 2009, **131**, 16634; (d) O. Crespo, E. J. Fernández, M. Gil, M. C. Gimeno, P. G. Jones, A. Laguna, J. M. López-de-Luzuriaga and M. E. Olmos, *Dalton. Trans.* 2002, 1319; (e) L. Hao, M. A. Mansour, R. J. Lachicotte, H. J. Gysling and R. Eisenberg, *Inorg. Chem.* 2000, **39**, 5520; see also references 25 and 27f.

218. Group 11 gold-heterometallic clusters with unsupported metallophilic interactions: (a) J. M. López-de-Luzuriaga, M. Monge, M. E. Olmos, D. Pascual and M. Rodríguez-Castillo, *Organometallics* 2012, **31**, 3720; (b) J. M. López-de-Luzuriaga, M. Monge, M. E. Olmos, D. Pascual and M. Rodríguez-Castillo, *Inorg. Chem.* 2011, **50**, 6910; (c) E. J. Fernández, A. Laguna, J. M. López-de-Luzuriaga, M. Monge, M. Montiel, M. E. Olmos and M. Rodríguez-Castillo, *Dalton Trans.* 2009, 7509; (d) E. J. Fernández, J. M. López-de-Luzuriaga, M. Monge, M. E. Olmos, R. C. Puelles, A. Laguna, A. A. Mohamed and J. P. Fackler Jr., *Inorg. Chem.* 2008, **47**, 8069; (e) E. J. Fernández, P. G. Jones, A. Laguna, J. M. López-de-Luzuriaga, M. Monge, M. E. Olmos and R. C. Puelles, *Organometallics* 2007, **26**, 5931; (f) E. J. Fernández, A. Laguna, J. M. López-de-Luzuriaga, M. Montiel, M. E. Olmos, J. Perez and R. C. Puelles, *Organometallics* 2006, **25**, 4307; (g) E. J. Fernández, A. Laguna, J. M. López-de-Luzuriaga, M. Monge, M. Montiel, M. E. Olmos and M. Rodríguez-Castillo, *Organometallics* 2006, **25**, 3639; (h) E. J. Fernández, A. Laguna, J. M. López-de-Luzuriaga, M. Monge, P. Pyykkö and N. Runeberg, *Eur. J. Inorg. Chem.* 2002, **2002**, 750; see also reference 27e.

219. A. K. Ghosh and V. J. Catalano, *Eur. J. Inorg. Chem.* 2009, **2009**, 1832.

220. R. Usón, A. Laguna, M. Laguna and A. Usón, *Organometallics* 1987, **6**, 1778.

221. R. Usón, Antonio Laguna, M. Laguna, P. G. Jones and G. M. Sheldrick, *J. Chem. Soc., Chem. Commun.* 1981, 1097.

222. (a) A. Luquin, C. Elosúa, E. Vergara, J. Estella, E. Cerrada, C. Bariáin, I. R. Matías, J. Garrido and M. Laguna, *Gold Bull.* 2007, **40**, 225; (b) D. B. Leznoff and J. Lefebvre, *Gold Bull.* 2005, **38**, 47.

223. R. Usón, A. Laguna, M. Laguna, B. R. Manzano, P. G. Jones and G. M. Sheldrick, J. Chem. Soc., *Dalton Trans.* 1984, 285.

224. T. Lasanta, M. E. Olmos, A. Laguna, J. M. López-de-Luzuriaga and P. Naumov, *J. Am. Chem. Soc.* 2011, **133**, 16358.

225. A. Laguna, T. Lasanta, J. M. López-de-Luzuriaga, M. Monge, P. Naumov and M. E. Olmos, *J. Am. Chem. Soc.* 2010, **132**, 456.

226. R. Usón, A. Laguna, M. Laguna, B. R. Manzano and A. Tapia, *Inorg. Chim. Acta* 1985, **101**, 151.

227. E. J. Fernandez, A. Laguna, J. M. López-de-Luzuriaga, M. Monge, M. Montiel and M. E. Olmos, *Inorg. Chem.* 2005, **44**, 1163.

228. L. Wilkinson, MChem. dissertation, 2011.

229. The chelation of the trifluoroacetate anion is similar to that seen in $[(tht)Au(C_6F_5)][Ag_2(CF_3CO_2)_2]_n$; see reference 218e.

230. This poor resolution of fluorescence excitation signals in solution has precedence with **CI·NCMe** in acetonitrile; see reference 218f.

231. A common assignment is made in reference 218f.

232. Examples of gold thiolates containing bridging phosphines in the presence and absence of aurophilic interactions affecting the emission output; X. He and V. W.-W. Yam, *Coord. Chem. Rev.* 2011, **255**, 2111.

233. E. J. Fernández, A. Laguna and M. E. Olmos, *Coord. Chem. Rev.* 2008, **252**, 1630.

234. The UV-vis data of $[Ph_4P]Cl$ in ethanol show absorption signals at 262, 269 and 276 nm; K. Ohkubo and T. Yamabe, *J. Org. Chem.* 1971, **36**, 3149.

235. The UV-vis data of free AgOTf (0.04 M) in THF gives and absorption signal at 305 nm; M. E. Woodhouse, F. D. Lewis and T. J. Marks, *J. Am. Chem. Soc.* 1982, **104**, 5586.

236. R. Usón, A. Laguna and M. L. Arrese, *Synth. React. Inorg. Met.-Org. Chem.* 1984, **14**, 557.

237. See citations in reference 56.

238. It is noteworthy that in this situation, the hydroarylation of electron-deficient alkynes was not catalyzed by strong Brønsted acids; see reference 111.

239. M. K. Ghosh, M. Tilset, A. Venugopal, R. H. Heyn and O. Swang, *J. Phys. Chem. A* 2010, **114**, 8135.

240. M. Fianchini, H. Dai and H. V. R. Dias, *Chem. Commun.* 2009, 6373.

241. At the time of experimentation, this salt was incorrectly defined as '$[Et_3Si][B(C_6F_5)_4]$'; the discovery of its true form was only published in 2011; M. Nava and C. A. Reed, *Organometallics* 2011, **30**, 4798.

242. A number of peaks are observed in the ^{19}F NMR spectrum, believed to be for $(C_6F_5)_2$, C_6F_5-C_6Me_5 and the coupling product of C_6F_5 + $HC{\equiv}CCO_2Et$, but no definitive assignments can be made at this point.

243. (a) G. A. Nifontova and I. P. Lavrentiev, *Transition Met. Chem.* 1993, **18**, 27; (b) G, A, Nifontova, O. N. Krasochka, I.P Lavrentiev, D. D. Makitova, L. O. Atovmyan and M. L. Khidekel, *Izv. Akad. Nauk. SSSR, Ser. Khim.* 1988, 450.

244. The halosulfonium halides can be isolated and used as an oxidising reagent, or produced *in situ* from a mixture of DMSO and HCl/HBr; (a) P. G. Gassman, J. J. Roos and S. J. Lee, *J. Org. Chem.* 1984, **49**, 717; (b) Y. L. Chow and B. H. Bakker, *Can. J. Chem.* 1982, **60**, 2268; (c) R. M. Munavu, *J. Org. Chem.* 1980, **45**, 3341; (d) J. R. Gouvreau, S. Poignant and G. J. Martin, *Tetrahedron Lett.* 1980, **21**, 1319.

245. A. M. Forster and A. J. Downs, *J. Chem. Soc., Dalton Trans.* 1984, 2827.

246. R. Minkwitz and A. Werner, *Z. Naturforsch. B* 1988, **43**, 403.

247. F. Mohr, *Gold Bull.* 2004, **37**, 164.

248. (a) C. J. Evans and M. C. L. Gerry, *J. Am. Chem. Soc.* 2000, **122**, 1560; (b) S. A. Brewer, A. K. Brisdon, J. H. Holloway and E. G. Hope, *Polyhedron* 1994, **13**, 749; (c) A. K. Brisdon, J. H. Holloway, E. G. Hope, W. Levason, J. S. Ogden and A. K. Saad, *J. Chem. Soc., Dalton Trans.* 1992, 139; (d) E. W. Kaiser, J. S. Muenter, W. Klemperer, W. E. Falconer and W. A. Sunder, *J. Chem. Phys.* 1970, **53**, 1411.

249. D. Kurzydlowski and W. Grochala, *Chem. Commun.* 2008, 1073.

250. D. S. Laitar, P. Müller, T. G. Gray and J. P. Sadighi, *Organometallics* 2005, **24**, 4503.

251. N. P. Mankad and F. D. Toste, *Chem. Sci.* 2012, **3**, 72.

252. (a) S. A. Cooke and M. C. L. Gerry, *J. Am. Chem. Soc.* 2004, **126**, 17000; (b) D. Bellert and W. H. Breckenbridge, *Chem. Rev.* 2002, **102**, 1595.

253. (a) T. Drews, S. Seidel and K. Seppelt, *Angew. Chem., Int. Ed.* 2002, **41**, 454; (b) I. C. Hwang and K. Seppelt, *Z. Anorg. Allg. Chem.* 2002, **628**, 765; (c) R. Küster and K. Seppelt, *Z. Anorg. Allg. Chem.* 2000, **626**, 236; (d) S. H. Elder, G. M. Lucier, F. J. Hollander and N. Bartlett, *J. Am. Chem. Soc.* 1997, **119**, 1020.

254. D. Y. Melgarejo, G. M. Chiarella, J. P. Fackler Jr., L. M. Perez, A. Rodrigue-Witchel and C. Reber, *Inorg. Chem.* 2011, **50**, 4238.

255. A. G. Sharpe, *J. Chem. Soc.* 1949, 2901.

256. A. A. Woolf, *J. Chem. Soc.* 1954, 4694.

257. F. W. B. Einstein, P. R. Rao, J. Trotter and N. Bartlett, *J. Chem. Soc. A* 1967, 478.

258. (a) R. Schmidt and B. G. Muller, *Z. Anorg. Allg. Chem.* 1999, **625**, 602; (b) R. Fischer and B. G. Muller, *Z. Anorg. Allg. Chem.* 1997, **623**, 1729; (c) H. Bialowons and B. G. Muller, *Z. Anorg. Allg. Chem.* 1997, **623**, 1719; (d) H. Bialowons and B. G. Muller, *Z. Anorg. Allg. Chem.* 1997, **623**, 434; (e) O. Graudejus and B. G. Muller, *Z. Anorg. Allg. Chem.* 1996, **622**, 1076; (f) U. Engelmann and B. G. Muller, *Z. Anorg. Allg. Chem.* 1993, **619**, 1661; (g) U. Engelmann and B. G. Muller, *Z. Anorg. Allg. Chem.* 1992, **618**, 43; (h) U. Engelmann and B. G. Muller, *Z. Anorg. Allg. Chem.* 1991, **598/599**, 103; (i) K. Lutar, A. Jesih, I. Leban, B. Zemva and N. Bartlett, *Inorg. Chem.* 1989, **28**, 3467; (j) B. G. Muller, *Angew. Chem. Int. Ed.* 1987, **26**, 688; (k) B. G. Muller, *Z. Anorg. Allg. Chem.* 1987, **555**, 57; (l) R. Hoppe and R. Homann, *Z. Anorg. Allg. Chem.* 1970, **379**, 193; (m) A. J. Edwards and R. G. Jones, *J. Chem. Soc. A* 1969, 1936; (n) R. D. Peacock, *Chem. Ind.* 1959, 904; (o) R. Hoppe and W. Klemm, *Z. Anorg. Allg. Chem.* 1952, **268**, 365.

259. N. P. Mankad and F. D. Toste, *J. Am. Chem. Soc.* 2010, **132**, 12859.

260. I. C. Hwang and K. Seppelt, *Angew. Chem., Int. Ed.* 2001, **40**, 3690.

261. (a) J. F. Lehmann and G. J. Schrobilgen, J. *Fluorine Chem.* 2003, **119**, 109; (b) M. J. Vasile, T. J. Richardson, F. A. Stevie and W. E. Falconer, *J. Chem. Soc., Dalton Trans.* 1976, 351; (c) V. B. Sokolov, V. N. Prusakov, A. V. Ryzhkov, Y. V. Drobyshevskii and S. S. Khoroshev, Dokl. *Akad. Nauk SSSR* 1976, **229**, 884; (d) N. Bartlett and K. Leary, *Rev. Chim. Min.* 1976, **13**, 82; (e) J. H. Holloway and G. J. Schroblingen, *J. Chem. Soc., Chem. Commun.* 1975, 623; (f) K. Leary, A. Zalkin and N. Bartlett, *Inorg. Chem.* 1974, **13**, 775; (g) K. Leary, A. Zalkin and N. Bartlett, *J. Chem. Soc., Chem. Commun.* 1973, 131; (h) G. Kaindl, K. Leary and N. Bartlett, *J. Chem. Phys.* 1973, **59**, 5050; (i) K. Leary and N. Bartlett, *J. Chem. Soc., Chem. Commun.* 1972, 903.

262. This reaction product was also seen upon heating of $[Me_2SF][HF_2]$; see reference 245.

263. The ^{19}F NMR spectrum match that documented in H. J. Frohn, S. Jakobs and G. Henkel, *Angew. Chem. Int. Ed.* 1989, **28**, 1506.

264. D. H. R. Barton, J.-P. Finet, W. B. Motherwell and C. Pichon, *Tetrahedron* 1986, **42**, 5627.

265. F. Challenger and J. F. Wilkinson, *J. Chem. Soc., Trans.* 1922, **121**, 91.

266. E. Nield, R. Stephens and J. C. Tatlow, *J. Chem. Soc.* 1959, 166.

267. M. Laguna and D. Villacampa, *Inorg. Chem.* 1998, **37**, 133.

268. J. J. Eisch, J. E. Galle and S. Kozima, *J. Am. Chem. Soc.* 1986, **108**, 379.

269. I. R. Whittall, M. G. Humphrey, M. Samoc, B. Luther-Davies and D. C. R. Hockless, *J. Organomet. Chem.* 1997, **544**, 189.

270. H. Schmidbaur and K. C. Dash, *Chem. Ber.* 1972, **105**, 3662.

271. S. M. Aucott, P. Bhattacharyya, H. L. Milton, A. M. Z. Slawin and D. Woollins, *New J. Chem.* 2003, **27**, 1466.

272. J. Vicente, P. González-Herrero, Y. Garciá-Sánchez, P. G. Jones and M. Bardají, *Inorg. Chem.* 2004, **43**, 7516.
273. P. Braunstein and R. J. H. Clark, *J. Chem. Soc., Dalton Trans.* 1973, 1845.
274. M. Contel, A. J. Edwards, J. Garrido, M. B. Hursthouse, M. Laguna and R. Terroba, *J. Organomet. Chem.* 2000, **607**, 129.
275. D. Alberti and K.-R. Pörschke, *Organometallics* 2004, **23** 1459.
276. V. J. Scott, R. Çelenligil-Çetin and O. V. Ozerov, *J. Am. Chem. Soc.* 2005, **127**, 2852.
277. N. Yanagihara, T. Gotoh and T. Ogura, *Polyhedron* 1996, **15**, 4349.
278. H. M. R. Hoffmann, *J. Chem. Soc.* 1965, 6748.
279. H. M .R. Hoffmann, D. R. Joy and A. K. Suter, *J. Chem. Soc. B* 1968, 57.
280. R. Hara and G. H. Cady, *J. Am. Chem. Soc.* 1954, **76**, 4285.
281. T. Gramstad and R. H. Haszeldine, *J. Chem. Soc.* 1957, 4069.
282. W. Kelm and W. Preetz, *Z. Anorg. Allg. Chem.* 1989, **568**, 117.
283. K. Rousseau, G. C. Farrington and D. Dolphin, *J. Org. Chem.* 1972, **37**, 3968.
284. J.-A. MacPhee and J.-E. Dubois, *Tetrahedron* 1980, **36**, 775.
285. E. H. Amonoo-Neizer, R. A. Shaw, D. O. Skovlin, B. C. Smith, J. W. Rosenthal and W. L. Jolly, *Inorg. Synth.* 1966, **8**, 19.
286. P. Dauban, L. Sanière, A. Tarrade and R. H. Dodd, *J. Am. Chem. Soc.* 2001, **123**, 7707.
287. N. W. Alcock, W. D. Harrison and C. Howes, *J. Chem. Soc., Dalton Trans.* 1984, 1709.
288. D. H. R. Barton, N. Y. Bhatnagar, J.-P. Finet and W. B. Motherwell, *Tetrahedron* 1986, **42**, 3111.
289. M. Canipelle, L. Caron, C. Christine, S. Tilloy and E. Monflier, *Carb. Res.* 2002, **337**, 281.
290. H. J. Frohn, S. Jakobs and G. Henkel, *Angew. Chem., Int. Ed.* 1989, **28**, 1506.
291. CrystalClear-SM Expert 2.0 r11: An Integrated Program for the Collection and Processing of Area Detector Data, Rigaku Corporation, 2011.
292. G. M. Sheldrick, SHELX-97 – Programs for crystal structure determination (SHELXS) and refinement (SHELXL), *Acta Crystallogr. A* 2008, **64**, 112.
293. *'International Tables for X-ray Crystallography: C'*, Kluwer Academic Publishers, Dordrecht, 1992, pages 193, 219 and 500.
294. L. J. Farrugia, *J. Appl. Crystallogr.* 1999, **32**, 837.